The application of electrocoagulation process for wastewater treatment and for the separation and purification of biological media

Nidal Fayad

N° d'ordre : D. U : 2830
E D S P I C : 806

UNIVERSITE CLERMONT AUVERGNE

ECOLE DOCTORALE
SCIENCES POUR L'INGENIEUR DE CLERMONT-FERRAND

T h è s e

Présentée par

NIDAL FAYAD

pour obtenir le grade de

DOCTEUR D'UNIVERSITÉ

SPECIALITE : GENIE DES PROCEDES

Mise en œuvre du procédé d'électrocoagulation pour le traitement des eaux usées et pour la séparation et la purification de milieux biologiques

Soutenue publiquement le 19 juillet 2017 devant le jury :

Mme GENESTE Florence, DR CNRS, Université de Rennes 1	Président
M. TAHA Samir, Professeur, Université Libanaise, Liban	Rapporteur
Mme. POCHAT-BOHATIER Céline, MCF HDR, IEM, Université de Montpellier	Rapporteur
M. VIAL Christophe, Professeur, UCA, Institut Pascal, Clermont-Ferrand	Directeur de thèse
M. AUDONNET Fabrice, MCF HDR, UCA, Institut Pascal, Clermont-Ferrand	Directeur de thèse

N° d'ordre: D. U: 2830
E D S P I C: 806

UNIVERSITE CLERMONT AUVERGNE

ECOLE DOCTORALE
SCIENCES POUR L'INGENIEUR DE CLERMONT-FERRAND

Thesis

Defended by

Nidal FAYAD

To obtain the degree of

DOCTOR OF PHILOSOPHY

SPECIALITY: PROCESS ENGINEERING

The application of electrocoagulation process for wastewater treatment and for the separation and purification of biological media

Defended publicly on July 19, 2017

Members of the defense jury:

President:
Mrs. GENESTE Florence, CNRS Research Director, Rennes 1 University
Reviewers:
Mr. TAHA Samir, Professor, Lebanese University, Lebanon
Mrs. POCHAT-BOHATIER Céline, Associate professor, IEM, Montpellier Universit
Thesis director:
Mr. VIAL Christophe, Professor, UCA, Institut Pascal, Clermont-Ferrand
Thesis co-director:
Mr. AUDONNET Fabrice, Associate professor, UCA, Institut Pascal, Clermont-Ferrand

ACKNOWLEDGMENTS

Undertaking this PhD has been a truly life-changing experience for me and it would not have been possible to do without the help of **God** who provided me with strength and patience.

I deeply thank Prof. Gilles DUSSAP, the Head of the GePEB research group for giving me the opportunity to do my research work in the laboratory.

I would like to express my sincere gratitude to my thesis director, Prof. Christophe VIAL, for his continuous support, patience, kindness, modesty, motivation and immense knowledge. His guidance helped me enormously throughout the three years of this thesis. I could not have imagined having a better director and mentor for my PhD study.

My sincere thanks also go to Dr. Fabrice AUDONNET, my co-supervisor, who was always there whenever I needed help and support. I deeply appreciate his insightful comments and encouragement.

I would also like to thank the members of my thesis jury: Mr. Samir TAHA, Professor at the Lebanese University, Director of the LBA3B laboratory and Head of M2R Applied Biotechnology in the Lebanese University, and Mrs. Céline Pochat-Bohatier, Doctor at Montepellier 2 University, Responsible for the 4th year in the Science and Technology Department of the Food Industries and responsible of four Engineering Units in Process Engineering, for dedicating their time to assess my work and for accepting to be its reporters. I equally thank Mrs. Florence Geneste, Professor and CNRS Director of research at Rennes 1 University France for being the president of the jury.

I would like to thank my family: my mother, my brother, my step-father, my mother-in-law, my father-in-law and my brothers-in-law and their wives for supporting me spiritually throughout the thesis. Without their support, this thesis would not have been accomplished.

I dedicate this thesis to the innocent soul and memory of my brother-in-law Mohammad YEHYA who inspired me through the tough times of this work.

This last word of acknowledgment is to my wonderful wife, Tania YEHYA, who is the best thing happened to me, and for my daughter, my world, Anna-Bella, for being the greatest motivation to finish this work.

TABLE OF CONTENTS

INTRODUCTION

Electrocoagulation (EC) is an electrochemical technique commonly used in the treatment of water and industrial effluents, since it is capable of simultaneously eliminating very wide variety of pollutants. These include, among others, refractory organics, colloidal particles, suspended particles, turbidity, color or even ions (heavy metals, nitrates...). It combines in fact a very wide variety of remediation mechanisms, such as coagulation, precipitation and adsorption, but also electro-reduction and electro-oxidation. The pollutants are generally recovered in the solid phase by sedimentation, but they can also be separated by flotation thanks to hydrogen gas generated at the cathode.

Although EC has been widely and successfully employed for the treatment of water and wastewater, it was not widely invested for recovering or separating valuable molecules and biomolecules that exist in water. Consequently, the objective of this work, on the one hand, is to employ EC as a conventional wastewater treatment technique for the elimination of biological pollution from water and, on the other hand, to develop an original variant of EC which aims to separate and purify biological media.

The impact of EC, as an alternative treatment method, for whey proteins removal first is investigated. These proteins, as the other components of dairy wastewater, are usually treated by aerobic and anaerobic biological processes. However, aerobic processes are highly energy intensive and anaerobic ones often reflect very poor nutrient removal. Moreover, the application of EC as an original separation method is extended to the purification of volatile fatty acids issued from acidogenic fermentation to replace conventional expensive methods in order to use them as precursors in biobased chemistry. This thesis also proposes EC as an alternative harvesting process of the two microalgae species (*Chlorella vulgaris* and *Chlamydomonas reinhardtii*) from their culture media. Microalgae recovery necessitates the development of new methods as EC, since currently used methods (mainly centrifugation, flocculation and filtration) exhibit many drawbacks, such as high cost, fouling and the possibility of additional contamination.

Consequently, this Ph.D. thesis comprises six chapters. Chapter 1 is a submitted literature review about the use of EC as a water treatment process. This review summarizes the theory of EC, its history and its advantages and drawbacks, particularly for colloid removal. Then, it

presents recent works carried out on using EC alone and EC coupled to other treatment methods aiming at treating wastewater.

Chapter 2 is a submitted literature review on the recovery of microalgae and plant extracts using EC. Contrary to chapter 1 in which water preservation was the only objective, the aim in this chapter mainly involves the valorization of the products collected by the flocs. This review summarizes studies carried out on microalgae recovery by EC and discusses the influence of operating parameters on the efficiency of the process. Then, electrical energy consumption and metal content in the effluent and biomass are discussed. Finally, works performed on the purification of plant extracts using EC are summarized.

Chapter 3 is an article, published in Desalination and Water Treatment journal, that describes the elimination of whey proteins from water by EC. This article details the principles of experimental techniques used in this work along with the experimental setup available for whey proteins removal. The influence of the main operating parameters on the efficiency of the process is discussed. Then, the cost of the whole process is analyzed. Moreover, the mechanisms responsible for whey proteins removal are explained along with analyzing the solid and liquid phases. Finally, a model on whey proteins removal is developed.

Chapter 4 is an article, published in Separation and Purification Technology journal, that describes the separation and purification of volatile fatty acids, which are widely used in the industries of food, pharmaceuticals, petrochemicals, cosmetics and tanning, in adigestate from acidogenic fermentation using EC. In this work, the influences of the main parameters on the efficiency of the process are investigated. In addition, a clear cost analysis of the whole process is also discussed.

Chapter 5 is a submitted article that describes the recovery of the microalgae species *Chlamydomonas reinhardtii* by electro-coagulation-flocculation (ECF) in batch. In this work, response surface methodology (RSM) is used to investigate the effect of the most influential variables on the efficiency of the process. Moreover, cost analysis of the process is carried out. Then, two models for predicting recovery efficiency and ECF operating cost are developed in addition to discussing the kinetics and mechanisms of recovery. Finally, ECF is compared to chemical flocculation with chitosan.

Chapter 6 is an article, published in Algal Reasearch journal, about harvesting the microalgae species *Chlorella vulgaris* by discontinuous electro-coagulation-flocculation (ECF). In this

paper, the effects of the main operating parameters on the process effectiveness are explained along with discussing the mechanisms of recovery. Then, electrical energy consumption and ECF effect on lipid and pigment content are presented. Finally, aluminum accumulation during ECF is analyzed.

Finally, chapter 7 is a submitted article that describes the recovery of the microalgae species *Chlorella vulgaris* by continuous ECF. This article employs response surface methodology (RSM) to evaluate the influence of current density and inlet flow rate (retention time) on the recovery efficiency of *Chlorella vulgaris*. A model for predicting microalgae recovery is developed. Moreover, recovery kinetics during the transient phase is studied. Finally, comparison of ECF performance in continuous mode with and without polarity exchange (PE) to ECF performance in batch mode is carried out.

CHAPTER 1: THE USE OF ELECTROCOAGULATION FOR WATER AND WASTEWATER TREATMENT

This review article is submitted to the Journal of Environmental Management. Consequently, this chapter follows the guidelines of this journal.

Nidal Fayad, Tania Yehya, Fabrice Audonnet, Christophe Vial.

ABSTRACT

Electrocoagulation (EC) is an efficient non-specific electrochemical technique that has been successfully employed for the treatment of different types of wastewater. This technique uses direct currentbetween metal electrodes immersed in wastewater, which causes the dissolution of electrodes into the effluent. The metal ions, at suitable pH, generate a wide range of coagulated species and metal hydroxides that destabilize and aggregate particles or precipitate and adsorb the dissolved pollutants. This process is able to remove more than 99 % of some heavy metal cations, and seems also to be able to electrocute microorganisms in the water. It is also capable of precipitating charged colloids and removing significant amounts of other ions, colloids and emulsions. The aim of this review is to explain the theory of EC, discuss the factors that affect its efficiency, explain how EC cost is estimated, and finally review recent studies on EC application and EC coupling with other wastewater treatment methods.

1. INTRODUCTION

Since the beginning of the 21st century, the world is facing a huge water shortage crisis resulting from urbanization, continuous population growth, land use change, industrialization, food production practices, increased living standards and poor water use practices and lack of efficient wastewater management strategies. Therefore, it is of utmost importance to develop efficient and cost effective technologies for wastewater management. These technologies should be considered as part of an integrated, full life cycle, ecosystem-based management system that operates across all three dimensions of sustainable development (social, economic and environmental), geographical borders, and includes both fresh and marine water [1].

One of the emerging technologies that proved its efficiency in treating different types of wastewater is electrocoagulation (EC). EC, which is an advanced, economic, electro-chemical

process that simultaneously removes heavy metals, suspended solids, emulsified organics and many other contaminants from water using electricity. It is an alternative treatment process to the more traditional chemical and biological processes familiar to wastewater treatment professionals.

The purpose of this review is to summarize the principle of EC before explaining the main mechanisms of de-pollution, depict the history of EC in addition to its advantages and drawbacks, discuss the factors that affect its efficiency, explain how EC cost is estimated, and finally review recent studies on EC application and EC coupling with other wastewater treatment methods.

2. THEORY OF EC

EC which combines coagulation, flotation and electrochemistry is a process of destabilizing suspended, emulsified or dissolved contaminants in an aqueous medium by introducing an electric current into the medium [2]. In its simplest form, an EC reactor is composed of an electrolytic cell with one anode and one cathode metal electrodes immersed in the solution to be treated and connected externally to a direct current power supply, as shown in **Figure 1**.

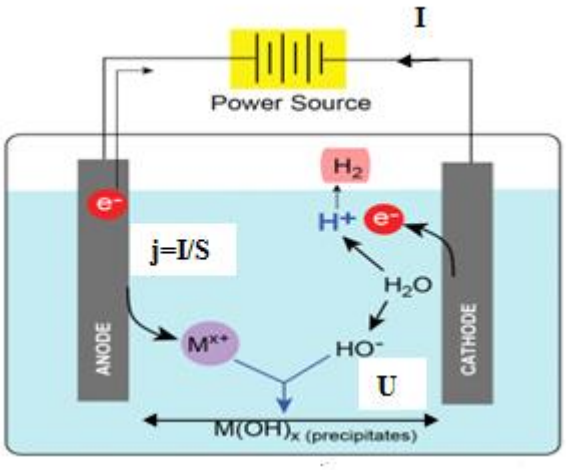

Figure 1. Simple EC cell, where M is metal, x is the oxidation state of the metal, I is current, U is cell potential, j is current density, and S is the surface area of the anode.

During EC, the coagulating ions are generated continuously by electrochemical dissolution of the sacrificial anode. These ions spontaneously undergo hydrolysis in water forming various coagulant species including metallic hydroxide precipitates (eliminate contaminants by adsorption/settling) and various other ions metal species [3].

The dissociation of the ions from the anode follows Faraday's law (eq. 1):

$m = I\ t\ M/z\ F$ (eq. 1)

where I is the current (A), t is the time of operation (s), M is the molecular weight of the anode material (g/mol), F is Faraday's constant (96,485 C/mol), z is the number of electrons involved in the reaction and m is the mass of anode dissolved (g).

The destabilization mechanisms of contaminants, particulate suspension and emulsion breaking are summarized as follows:

1. Compression of the diffuse double layer around the charged species by the ions generated by the oxidation of the sacrificial anode;
2. Charge neutralization of the ions existing in wastewater by the counter ions generated by the electrochemical dissolution of the sacrificial electrode. These counter ions decrease the electrostatic interparticle repulsion to the extent that the van der Waals attraction predominates, thus causing coagulation. A zero net charge results in the process;
3. Floc formation as a result of coagulation creates a blanket of sludge that entraps and bridges colloidal particles still remaining in the solution. The hydroxides, oxyhydroxides and solid oxides give active surfaces for the adsorption of the polluting species [4].

In most cases, the electrodes are made up of aluminum or iron due to various advantages that these materials offer, such as: their availability and low price, their non-toxicity, as iron and aluminum hydroxides formed by precipitation are relatively non-toxic, and their high valence that leads to an efficient pollutant removal [3].

Iron and aluminum cations dissolve from the anodes according to eqs. (2) and (3) [5,6]:

$Fe_{(s)} \rightarrow Fe^{n+}_{(aq)} + ne^-$ (eq. 2)

$Al_{(s)} \rightarrow Al^{3+}_{(aq)} + 3e^-$ (eq. 3)

During EC, iron dissolves either into a divalent Fe(II) or a trivalent Fe(III) form in the aqueous medium depending on the pH of the solution and the potential E as illustrated in the E-pH diagram for iron. Fe(II) may further oxidize to Fe(III) [eq. (4)] under appropriate oxidation-reduction potential and pH conditions [6].

$4Fe^{2+}_{(aq)} + 10H_2O + O_2 \rightarrow 4Fe(OH)_{3(s)} + 8H^+$ (eq. 4)

On the other hand, aluminum dissolves only into a trivalent form Al(III).

The E-pH (Pourbaix) diagrams of iron and aluminum (**Figures 2** and **3**) allow the prediction of the stable compounds of each at different conditions [2], having in mind that these diagrams describe only thermodynamic equilibria, which may differ in real situations when kinetically-controlled conditions prevail. Pourbaix proposed three possible states of a metallic material [7]:

Immunity region: In the conditions of potential and pH of that region a metal is considered totally immune from corrosion attack and safe to use.

Passive region: In this region, the metal tends to become coated with an oxide or hydroxide that may form on the metal either as a compact and adherent film practically preventing all direct contact between the metal itself and the environment, or as a porous deposit which only partially prevents contact between the metal and the environment.

Corrosion region: Thermodynamic calculations indicate that, in such region of an E-pH diagram, a metal is stable as an ionic (soluble) product and therefore susceptible to corrosion attack. Experience is required to find out the kinetics, the extent and form of the corrosion attack that may take place in the corrosion region(s) of a Pourbaix diagram.

Figure 2A illustrates the E-pH diagram for a soluble Fe species at a concentration of 1 M. The diagram depicts that the aqueous chemistry of iron is dominated by two oxidation states II and III. The reduction of $Fe^{3+}_{(aq)}$ to $Fe^{2+}_{(aq)}$ always takes place at a potential value of +0.77 V, as indicated by the upper horizontal line in the left-hand corner of the diagram. The lower horizontal line defines the reduction of $Fe^{2+}_{(aq)}$ to $Fe_{(s)}$ which occurs at a potential of −0.45 V. As indicated on the diagram, the $Fe^{3+}_{(aq)}$ and $Fe^{2+}_{(aq)}$ ions might precipitate from the solution in the presence of OH^-. Precipitation of the $Fe^{2+}_{(aq)}$ ion occurs at a pH of 6.0 with the formation of $Fe(OH)_{2(s)}$, while the$Fe^{3+}_{(aq)}$ ion precipitates as the oxyhydroxide, $FeO(OH)_{(s)}$, at pH value of 1.3. The reduction of $Fe(OH)_{2(s)}$ to Fe is defined by the inclined line running from E=−0.45 V (pH = 6.0) to E=−0.99 V (pH = 15.0). The oxyhydroxide species, FeO(OH), is reduced to $Fe^{2+}_{(aq)}$ at pH values below 6.0, as demonstrated by the inclined line running from E=−0.06 V (pH = 6.0) to E=−0.77V (pH 1.3) or to $Fe(OH)_{2(s)}$ at pH values higher than 6.0 as depicted by the inclined line running from E=−0.06 V (pH = 6.0) to E=−0.59 V (pH = 15.0).

The generalized algebraic equations that define the lines separating the predominance regions for Fe for various iron concentration of soluble species are summarized in **Table 1**. With the equations in **Table 1**, the species conversion lines have been determined for soluble Fe species concentrations of $10^{-4.0}$, $10^{-8.0}$, $10^{-12.0}$ and $10^{-16.0}$ M. These data have been combined into a single plot as shown in **Figure 2B.** This figure shows that the predominance zones of the $Fe^{2+}_{(aq)}$ and $Fe^{3+}_{(aq)}$species increase and the predominance regions for $Fe(OH)_{2(s)}$ and $FeO(OH)_{(s)}$decrease as the soluble species concentration decreases [8, 9].

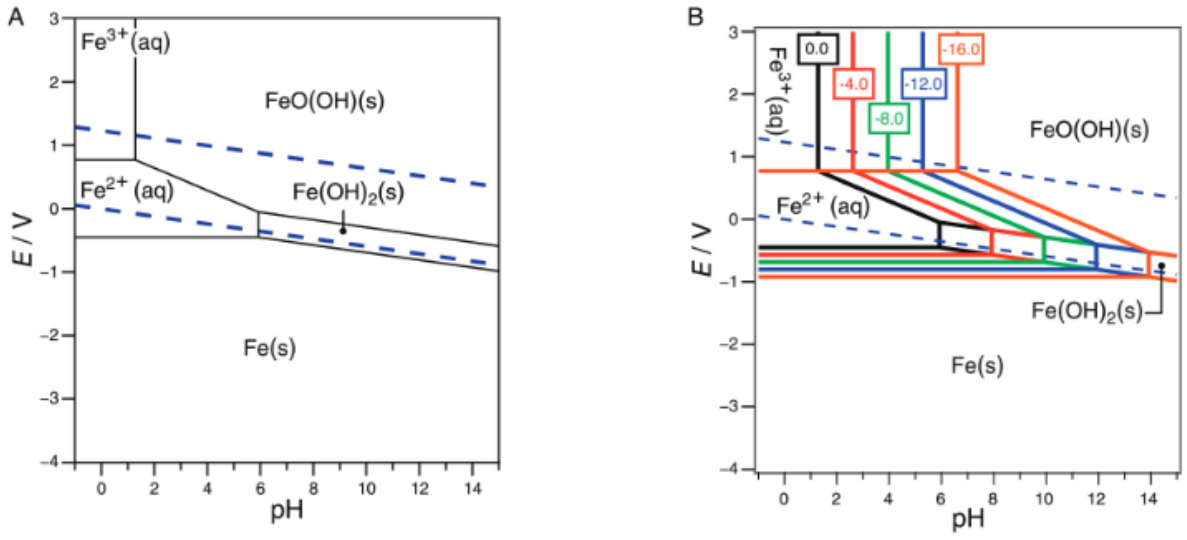

Figure 2. E-pH diagrams for Fe at soluble species concentration of A) $10^{0.0}$ M and B) $10^{0.0}$, $10^{-4.0}$, $10^{-8.0}$, $10^{-12.0}$ and $10^{-16.0}$ M (298 K).

Table 1. Species, chemical reactions and algebraic equations considered in the construction of the Fe E−pH diagram at 298 K [10].

Couple	Chemical reaction	Algebraic equation (concentrations in M)
Fe^{2+}/Fe^{3+}	$Fe^{3+} + e^- \rightarrow Fe^{2+}$	E = 0.77 V
Fe^{2+}/Fe	$Fe^{2+} + 2e^- \rightarrow Fe$	$E= -0.45 +0.030 \log[Fe^{2+}]$ V
$FeO(OH)/Fe^{2+}$	$FeO(OH) + e^- + 3H^+ \rightarrow Fe^{2+} + 2HOH$	$E= 1.00 - 0.177\ pH - 0.059 \log[Fe^{2+}]$ V
$FeO(OH)/Fe(OH)_2$	$FeO(OH) + e^- + H^+ \rightarrow Fe(OH)_2$	E= 0.30−0.059 pH V
$Fe(OH)_2/Fe$	$Fe(OH)_2 + 2e^- + 2H^+ \rightarrow Fe + 2HOH$	E=−0.10 −0.059 pH V
$FeO(OH)/Fe^{3+}$	$FeO(OH) + 3H^+ \rightarrow Fe^{3+} + 2HOH$	$3\ pH = 3.9 - \log[Fe^{3+}]$

The E−pH diagram for a soluble Al species concentration of 1 M is shown in **Figure 3A**. This figure depicts that aluminum hydroxide $Al(OH)_{3(s)}$, which exists in the solution between pH values of 3.4 and 12.4 if the potential is sufficiently high, dissolves in acidic medium forming $Al^{3+}_{(aq)}$, as indicated by the vertical line at a pH value of 3.4, and dissolves in alkaline medium to produce $Al(OH)_4^-{}_{(aq)}$, as indicated by the vertical line at a pH value of 12.4. The reduction of each of the three Al(III) species to $Al_{(s)}$ is signaled by a specific line in the lower half of **Figure 3A**: the horizontal line at −1.68 V running from pH −1.0 to 3.4 for the reduction of $Al^{3+}_{(aq)}$, the sloped line running from pH = 3.4 (E=−1.68 V) to 12.4 (E=−2.20 V) for the reduction of $Al(OH)_{3(s)}$ and the sloped line running from pH = 12.4 (E=−2.20 V) to 15 (E=−2.42 V) for the

reduction of $Al(OH)_4^-$. The algebraic equations that define the lines separating the predominance regions for summarized in **Table 2**.

Using the equations in **Table 2**, the species conversion lines have been determined for soluble Al species concentrations of $10^{-2.0}$, $10^{-4.0}$, $10^{-6.0}$ and $10^{-6.8}$ M. These data have been combined into a single plot as seen in **Figure 3B**. In this figure, it is demonstrated that as the soluble species concentration declines the predominance regions of both $Al^{3+}_{(aq)}$ and $Al(OH)_4^-{}_{(aq)}$ ions increase until the predominance zone of the $Al(OH)_{3(s)}$ disappears completely at a soluble species concentration of $10^{-6.8}$ M. This behavior of Al(III) species could be derived by setting the last two equations in **Table 2** equal to each other and solving for the Al(III) species concentration. It is also worth noting that for $Al^{3+}_{(aq)}$ ion concentrations less than $10^{-6.8}$ M, the addition of hydroxides does not lead to the precipitation of $Al(OH)_{3(s)}$ but to the direct conversion to $Al(OH)_4^-{}_{(aq)}$ [8].

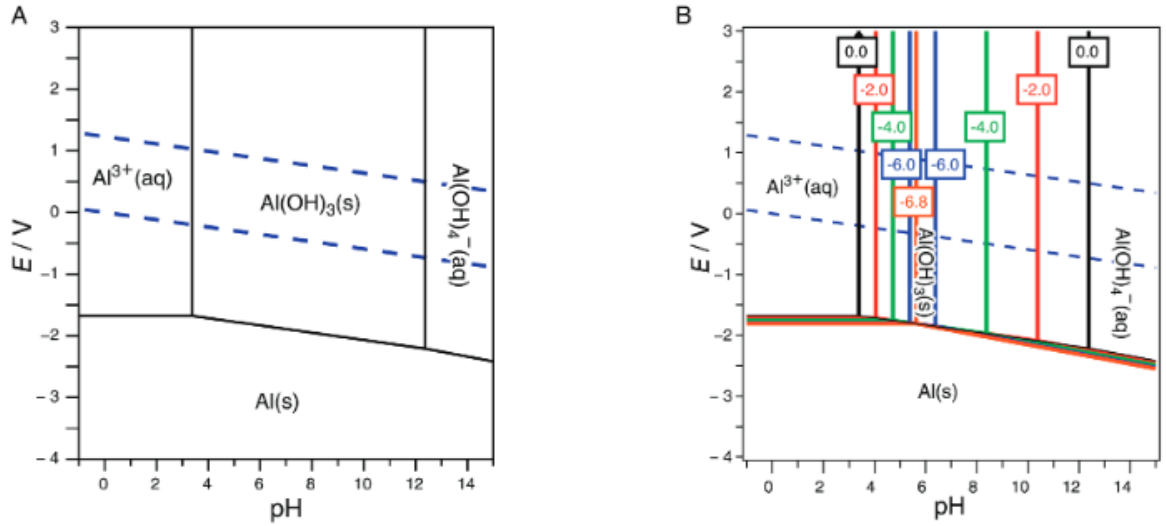

Figure 3. E-pH diagrams for Al at soluble species concentration of A) $10^{0.0}$ M and B) $10^{0.0}$, $10^{-2.0}$, $10^{-4.0}$, $10^{-6.0}$ and $10^{-6.8}$ M (298 K).

Table 2. Species, chemical reactions and algebraic equations considered in the construction of the Al E−pH diagram (298 K) [10].

Couple	Chemical reaction	Algebraic equation(concentrations in M)
Al^{3+}/Al	$Al^{3+} + 3e^- \rightarrow Al$	$E=-1.68 + 0.020 \log[Al^{3+}]$ V

$Al(OH)_3/Al$	$Al(OH)_3 + 3e^- + 3H^+ \rightarrow Al + 3HOH$	$E = -1.47 - 0.059\ pH\ V$
$Al(OH)_4^-/Al$	$Al(OH)_4^- + 3e^- + 4H^+ \rightarrow Al + 4HOH$	$E = -1.23 - 0.079\ pH + 0.020\log[Al(OH)_4^-]\ V$
$Al(OH)_3/Al^{3+}$	$Al(OH)_3 + 3H^+ \rightarrow Al^{3+} + 3HOH$	$3\ pH = 10.2 - \log[Al^{3+}]$
$Al(OH)_4^-/Al(OH)_3$	$Al(OH)_4^- + H^+ \rightarrow Al(OH)_3 + HOH$	$pH = 12.4 + \log[Al(OH)_4^-]$

It is possible that other reactions take place in the EC cell that are considered as secondary reactions [11, 12]. These reactions include:

-The evolution of hydrogen gas bubbles at the cathode (eq. 5 - eq.7).

- Metal ions reduction on the cathode.

$$2H_2O + 2e^- \rightarrow H_{2(g)} + 2OH^- \quad \text{(eq. 5)}$$

$$2H^+ + 2e^- \rightarrow H_{2(g)} \quad \text{(eq. 6)}$$

$$2Al_{(s)} + 6H_2O + 2OH^-_{(aq)} \rightarrow 2\,[Al(OH)_4]^-_{(aq)} + 3H_{2(g)} \quad \text{(eq. 7)}$$

- The increase of pH due to the formation of hydroxyl ions or the consumption of hydronium ions/protons (eq. 5, eq. 6).

Sometimes, the experimental anode dissolution does not match the theoretical one calculated by Faraday's law (eq. 1), which indicates that other electrochemical parasitic reactions might be occurring at the anode. In this case, the faradaic yield of metal dissolution (ϕ) [(eq. 8)] is not equal to 1.

$$\phi = \text{Experimental anode mass loss / Theoretical anode mass loss} \quad \text{(eq. 8)}$$

Several authors suggested that oxygen gas evolution on the anode might take place at alkaline pH values and high anodic potential (eq. 9) which may be the cause of the mismatch between theoretical and experimental anodic dissolution [4, 13, 14].

$$2H_2O \rightarrow O_2 + 4H^+ + 4e^- \quad \text{(eq. 9)}$$

3. MECHANISMS OF POLLUTANTS REMOVAL BY EC

Different mechanisms are involved in the removal of the various types of contaminants that exist in water and wastewater which include oxidation, reduction, coagulation, adsorption, precipitation, flotation and others. As pollutants in raw water and wastewater are mostly colloidal particles, their removal is mainly accomplished by destabilization and adsorption, which are discussed in the next two subsections.

3.1. DESTABILIZATION OF COLLOIDAL PARTICLES

Colloidal particles stability is usually explained by the presence of repulsive electrical charges on the surface of particles and stability could be estimated by considering the attraction forces between the particles. When repulsive forces dominate, the system will remain in the dispersed state. However, when the attraction forces become dominant, the particles will coagulate/flocculate and consequently the suspensions will be destabilized. Particles with the same charge repel each other, so if destabilization is aimed, this repulsion should be reduced [15]. Colloids are microscopic particles that are extremely small in size (1–1000 nm), having a very small mass to surface area ratio. Since their surface area is large compared to their mass and size, the gravitational forces of colloids are often neglected as compared to the surface phenomena predominating when studying colloidal suspension. The suspension and stability of colloidal particles in water is attributed to the fact that they carry similar charges, usually negatively charged, so they repel each other and remain suspended. In order to neutralize the charge, counter charged particles are employed to attach to the surface of the colloids forming an electric double layer as illustrated in **Figure 4**.

The electric double layer **(Figure 4)** is comprised of an inner layer (Stern layer), where oppositely charged ions are tightly bound to the surface of colloidal particles and an outer layer, where the ions move freely due to diffusion (ion diffuse layer or slipping plane). The interface of the inner and outer layers is known as the shear surface which defines the outer boundary of the Stern layer [13].

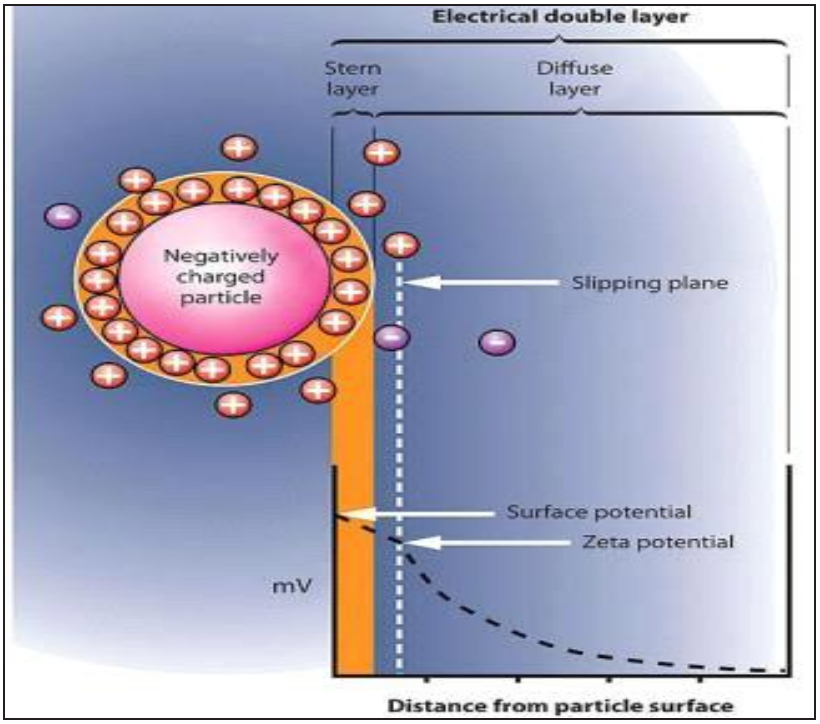

Figure 4. Schematic representation of the electrical double layer.

The maximum potential at the surface of colloidal particle is known as the Nernst potential. This potential decreases across the Stern layer due to the presence of oppositely charged particles resulting in what is called the zeta potential measured at the shear surface [16]. Zeta potential (which is close to the surface potential) is the main parameter able to estimate the stability of a colloidal system, as it represents the electrical charge difference between the first and second layer and indicates the extent of repulsion between colloidal particles. The higher the absolute value of zeta potential, the greater the magnitude of repulsion between particles and consequently the more stable is the colloidal system. In general, colloidal particles in suspensions with zeta potential values more positive than +30 mV or more negative than -30 mV are deemed stable [17].

DLVO (Derjaguin-Landau-Verwey-Overbeek) theory is able to describe the stability of colloidal particles [18-20]. Simply, DLVO theory describes the combined effects of the attractive van der Waals forces and the repulsive electrostatic forces, with Brownian motion of particles also being taken into consideration. In essence, as two charged surfaces approach each other, the double layers overlap and, as the electrical potentials are approximately additive, the net potential operating between the two surfaces increases and the repulsive energy resulting from overlap is exponentially related to the distance separating the particles. According to DLVO theory, the repulsive energy prevents the surfaces from adhering; if the surfaces collide

with enough energy to overcome this energy barrier, then the surfaces will adhere due to van der Waals attractive forces. Thus, a colloidal system is said to be stable if repulsive forces are stronger than the attractive ones [21]. In essence, the stability of a given colloidal system is governed by the net interaction energy (V_T) between two charged surfaces. This net interaction energy of two particles is given by the sum of Van der Waals attraction energy (V_A) and electrostatic repulsion energy (V_R) [4, 15,16]. The total interaction energy between two charged surfaces as a function of distance is shown qualitatively in **Figure 5**.

In EC, colloidal destabilization is the key process for pollution removal, first because it is able to promote the removal of suspended or emulsified materials, but also because it promotes the removal of precipitated hydroxides, not only from the sacrificial anode, but also from heavy metals together with the soluble compounds entrapped or adsorbed in these precipitates. Then, particles can settle, as in chemical coagulation, but the presence of microbubbles released by water reduction at the cathode also leads to flotation of colloidal species, which explains that EC is sometimes confounded with electroflotation (EF).

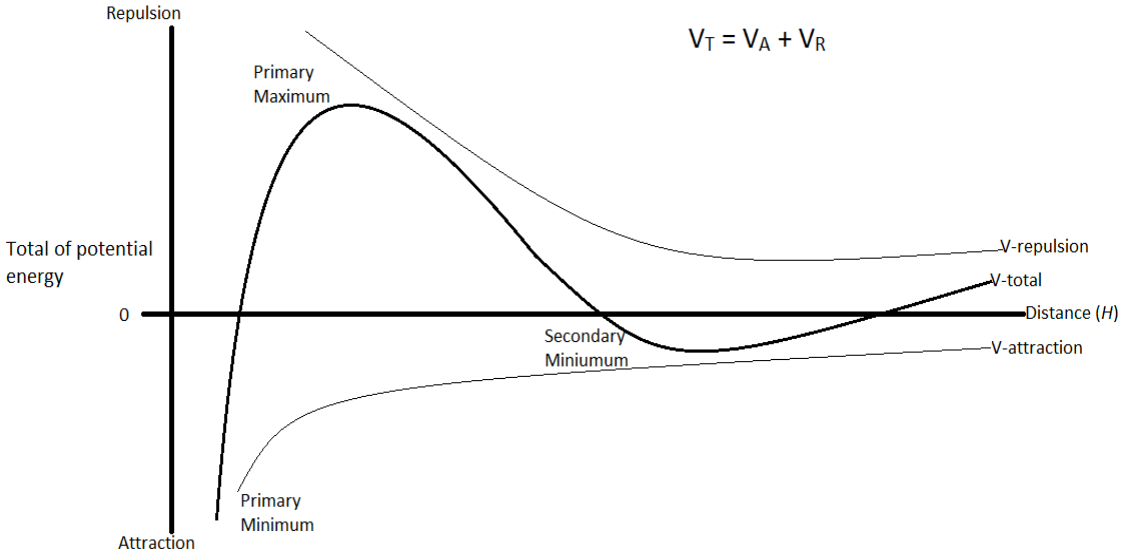

Figure 5. Typical evolution of the total interaction energy (V_T) between two charged surfaces as a function of distance, where V_A and V_E represent the Van der Waals attraction energy and electrostatic repulsive energy, respectively.

3.2. ADSORPTION

Adsorption is a surface phenomenon with common mechanism for the removal of organic and inorganic pollutants. Adsorption of soluble pollutants on metal hydroxides is, therefore, the

second key process for pollution removal. When an adsorbable solute in the solution comes into contact with a porous solid, solid–liquid intermolecular attraction forces cause the deposition of some solute molecules at the solid surface. The retained solute (on the solid surface) in the adsorption process is the adsorbate, whereas, the solid on which it is retained is the adsorbent. This creation of an adsorbed phase having a composition different from that of the bulk fluid phase forms the basis of separation by adsorption. The atoms on the surface of the adsorbent are not completely surrounded by other adsorbent atoms and therefore can attract adsorbates. The exact nature of the bonding depends on the details of the species involved, but the adsorption process is generally classified as physisorption (characteristic of weak Van der Waals forces) or chemisorption (characteristic of covalent bonding). It might also occur due to electrostatic attraction.

With the progress of adsorption, an equilibrium of solute adsorption between the solution and adsorbent is reached (where the adsorption of solute from the bulk onto the adsorbent is at its minimum). The amount of adsorbed solute (q_e, mmol/g) at equilibrium is determined according to the following equation in a batch system (eq. 10):

$$q_e = V(C_0\text{-}C_e) / M \qquad \text{(eq. 10)}$$

where V is the solution volume (L), M is the mass of monolithic adsorbents (g), and C_0 and C_e are the initial and equilibrium adsorbate concentrations, respectively [22].

During electrocoagulation, the contaminants are adsorbed at the surface of the metal hydroxides being continuously produced. In order to identify the adsorption mechanism, it is important to establish the most suitable correlation for the equilibrium curves. Langmuir and Freundlich adsorption isotherms are the most commonly applied to establish the relationship between the amount of pollutant adsorbed onto the metal hydroxides and its equilibrium concentration in the solution.

The Langmuir isotherm model represents chemisorption at a set of well-defined localized adsorption sites with the same adsorption energy, independent of the surface coverage and without any interaction between adjacent adsorbed molecules. This model assumes a monolayer deposition on a surface with a finite number of identical sites. The Langmuir equation is valid for a homogeneous surface [23]. The linearized form of Langmuir adsorption isotherm model is represented in eq. (11):

$$C_e/q_e = 1/q_m b + C_e/Q_m \qquad \text{(eq. 11)}$$

where q_e (mg/g) is the amount adsorbed at equilibrium, C_e (mg/L) is the equilibrium concentration, q_m is the Langmuir constant representing maximum monolayer adsorption capacity and b is the Langmuir constant related to energy of adsorption.

According to eq.(10), if adsorption obeys the Langmuir equation, a plot of C_e/q_e versus C_e should be a straight line with a slope of $1/q_m$ and intercept $1/q_m b$. This important characteristic of the Langmuir isotherm can be expressed in terms of a dimensionless factor, R_L (eq. 12) [24] which is defined as:

$R_L = 1/1+bC_0$ (eq. 12)

where R_L is the equilibrium constant which indicates the type of adsorption, as either unfavorable (R_L>1), linear (R_L = 1), favorable (0<R_L<1) or irreversible (R_L = 0), b is the Langmuir constant and C_0 is the initial pollutant concentration.

The Freundlich isotherm model applies to adsorption on heterogeneous surfaces with interaction between the adsorbed molecules, and is not restricted to the formation of a monolayer. This model assumes that as the adsorbate concentration increases, the concentration of adsorbate on the adsorbent surface also increases and, correspondingly, the sorption energy exponentially decreases on completion of the sorption sitesin the adsorbent [25]. The well-known expression for the Freundlich model is given in eq. (13):

$\log q_e = \log K_f + 1/\text{n} \log C_e$ (eq. 13)

where q_e is the amount adsorbed at equilibrium (mg/g), K_f is the Freundlich constant, 1/n is the heterogeneity factor which is related to the capacity and intensity of the adsorption, and C_e is the equilibrium concentration (mg/L). The values of K_f and 1/n can be obtained from the slope and intercept of the plot of $\log q_e$ against $\log C_e$.

4. HISTORY OF EC

The first document on the use of EC for the treatment of effluents is a US patent filed in 1880 [26]. In the same year, a sewage treatment plant was built on the basis of this patent, in Salford (UK) to treat polluted urban waters [27]. In 1909, a new patent on this process was filed, where the anodes were made from iron and aluminum plates [28]. By the 1930s, all electrolytic sludge treatment plants had been abandoned due to high operating costs and the ready availability of mass-produced alternatives for chemical coagulant dosing [29].

In 1946, the process was studied more precisely with a reactor equipped with aluminum electrodes. While comparing the physicochemical coagulation process and the electrochemical

process, it was observed that the coagulation phenomenon was faster with the electrochemical method. Based on these results, an economic comparison of the two methods was performed in 1947. It was found that for small sized installations, EC is more competitive than conventional processes [30].

In 1963, magnesium electrodes and sea water were used to disinfect wastewater by EC. The drawn conclusion was that the chloride ions in sea water were oxidized at the anode into hypochlorous ions. The colloidal particles were adsorbed on the precipitate of $Mg(OH)_2$, the hydrogen bubbles formed by reduction of water at the cathode participated in electroflotation of adsorbed particles [31]. It was only until the 1970s and 1980s that research on the application of EC for the treatment of various types of wastewater has generated significant interest. The industrial development of EC process was, however, hampered by the cost deemed too high and by the competition of chemical treatment processes, without ruling out its use [27]. EC started to regain importance in the late twentieth century with the progress of the electrochemical processes and with the development of strict regulations on discharges [32]. Meanwhile, the demand for quality drinking water quality is globally increasing and environmental regulations regarding wastewater discharge are becoming increasingly stringent. Therefore, it has become necessary to develop more effective treatment methods for water purification and/or enhance the operation of current methods. This and eco-friendliness have led to increasing global interest in EC as a research subject [33].

5. ADVANTAGES AND DRAWBACKS OF EC

As any process, EC has its advantages and drawbacks [34]. These are summarized in **Table 3**.

Table 3. Advantages and drawbacks of EC.

Advantages of EC	Drawbacks of EC
Requires simple equipment and is easy to operate	Gelatinous hydroxides may solubilize
EC cell has no moving parts and requires little maintenance as the electrolytic processes are controlled electrically	Sacrificial anodes, which are oxidized should be replaced regularly
The treated solutions give palatable, pleasant, clear, colorless and odorless water	Electricity is not always easily available and it is expensive in some regions
The formed sludge is mainly composed of metallic oxides/hydroxides, so it is readily settable and easy to de-water	Passivation decreases EC efficiency

The formed flocs are much larger than those produced by chemical coagulation, contain less bound water and are acid-resistant and more stable	Wastewater conductivity must be high to prevent the ohmic drop
Does not require the use of chemicals, so there will be less risk of secondary pollution, contrary to chemical coagulation, where chemical substances are added at high concentrations	
The gas bubbles generated during electrolysis result in the flotation of the pollutants, and consequently their separation is facilitated	
It is possible to use EC with the help of other renewable sources of energy such as solar or wind energy in rural areas where power is not easily available	

It is clear from the previous table that EC advantages are much more that its drawbacks, which may also be controlled or reduced. Consequently, EC is a recommended, efficient and environment friendly choice for industrial, commercial and municipal wastewater treatment.

6. FACTORS INFLUENCING THE EFFICIENCY OF EC

Different parameters affect the efficiency of EC and its ability to remove pollutants from wastewater; the most important parameters are discussed in this section.

6.1. ELECTRODE ARRANGEMENT

There are several ways in which the electrodes can be arranged in the EC system. In monopolar-parallel (MP-P) configuration **(Figure 6a)**, all the anodes are connected to each other and to the external DC power supply, and the same type of connection is applied to cathode electrodes, which corresponds to identical cells working in parallel at the same cell potential. In this configuration, the current is divided between the electrodes resulting in a lower potential difference if compared to the series configuration.

In monopolar-series (MP-S) connection **(Figure 6b)**, the two outermost electrodes are connected to the external circuit forming the anode and cathode, while each pair of the inner electrodes are connected to each other without an interconnection to the outer electrodes. In this connection type, the cell potential is additive, resulting in a higher potential difference. The inner electrodes could be made of similar or different material, so as to decrease the consumption of the anode and passivation of the cathode.

The third option is the bipolar-series (BP-S) configuration **(Figure 6c)**. In this type of connection, the outermost electrodes are directly connected to the external power supply, while the inner ones are not connected at all, which constitutes the simplest connection for EC maintenance. As current passes through the main electrodes, the adjacent sides of inner electrodes get polarized and will carry a charge opposite to the charge of the nearby electrode. In such configuration, the two outermost electrodes are monopolar whereas the inner sacrificial electrodes are bipolar [35, 36].

Several studies have tested the influence of the electrode arrangement on pollutant removal efficiency and cost. Demirci et al. found that all connection types showed similar results in reducing color and turbidity, while MP-P was preferred as a low-cost connection mode due to the lower cell potential [35]. Kobya et al. also found that MP-P is the most economic connection configuration [37]. Monopolar configuration has been reported to be better in the treatment of laundry wastewater [38] and oily water [39].

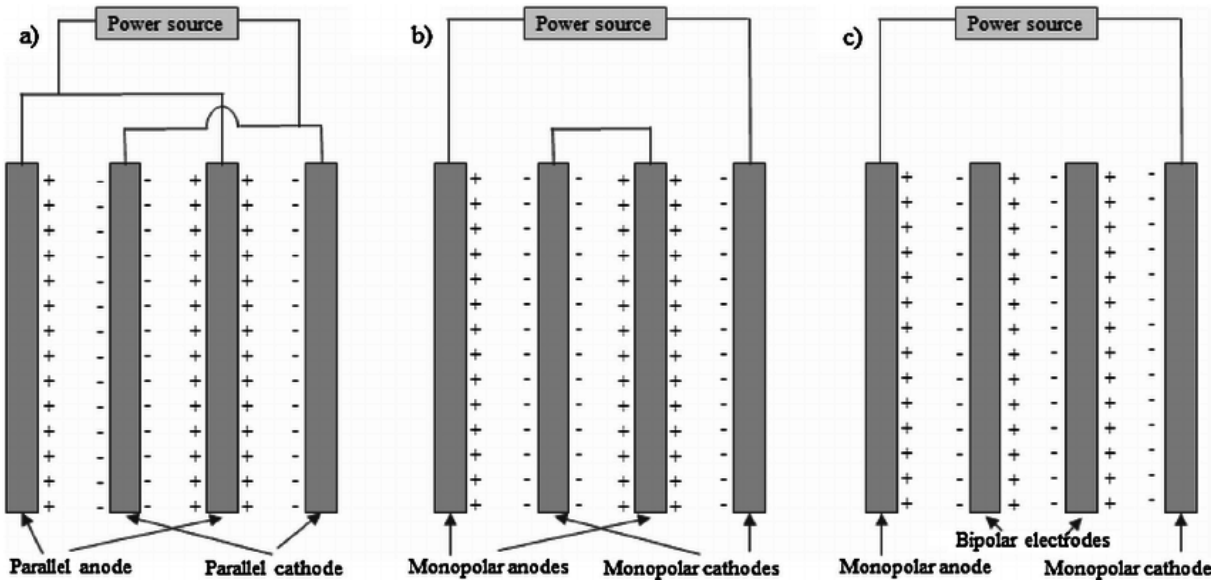

Figure 6. Different EC system electrode connections. a) monopolar-parallel (MP-P) configuration, b) monopolar- series (MP-S) configuration, c) bipolar- series (BP-S) configuration.

6.2. BATCH *VS.* CONTINUOUS OPERATION MODES

EC for water and wastewater treatment has been studied in the batch and continuous modes (**Figure 7**). Batch systems, in which the output depends on the operating time, are more suited for research. The parametric optimization in the batch processes serves as guidelines to operate

in the continuous mode, in which the outcome is not time dependent, but determined by the inlet flow rate and space time. Continuous systems, which are inherently dynamic in application and operate under steady state conditions, especially at fixed pollutant concentration and inlet flow rate, are better at the industrial scale for large volumes of effluent. The continuous mode of operation is preferred, as it can be more controlled than the batch mode of operation. Moreover, continuous operations yield more predictable behavior and a better opportunity to maintain a steady-state process, while consuming less energy in shorter time [40-42].

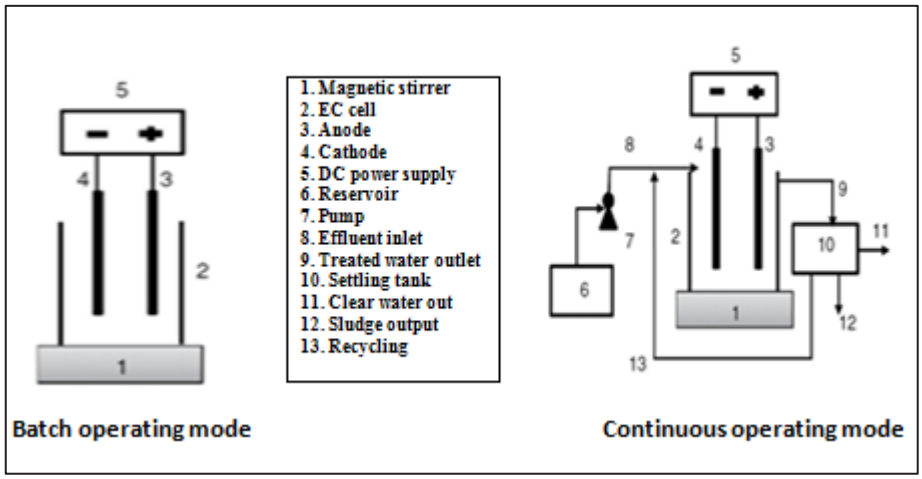

Figure 7. Schemes of batch and continuous modes of operation.

6.3. SHAPE OF THE ELECTRODE

Very few studies exist in the literature on the effect of the shape of the electrode on the removal efficiency of pollutants, as in most of the works plane electrodes are used. The shape of the electrode affects the surface-area-to-volume ratio (S/V), which in its turn affects the performance of EC. Usually, increasing this ratio increases pollutants removal efficiency. Khandegar and Saroha showed in their study an increase in the color removal efficiency using the punched electrode compared with the plane electrode [36]. In another study, Kobya et al. who compared the effect of iron (Fe) ball and plate anodes on arsenic removal depicted a removal efficiency of 99.3% and operating cost of 1.55 $\$/m^3$ at 20 min with Fe ball electrodes and 96.9% and 0.101 $\$/m^3$ at 6 min with for Fe plate electrodes, respectively [43]. Even though complex electrode geometry is sometimes proposed in industrial units, planar electrodes make maintenance easier for sacrificial anodes.

6.4. ELECTRODE MATERIAL

Electrode material is one of the most important factors in EC [44]. In most literature studies on electrocoagulation, both electrodes are made of the same material. Various metals such as aluminum, iron, zinc, stainless steel, graphite, magnesium and titanium have been used as electrode material in electrocoagulation [45-48]. Polyvalent metal electrodes such as aluminum and iron are usually used to benefit from the coagulating properties of multivalent ions [49]. It is worth noting that iron is cheaper than aluminum and not toxic as the latter.

In addition to these traditional materials, dimensionally stable anodes are sometimes used in combination with sacrificial anodes, such as tin dioxide (SnO_2), lead dioxide (PbO_2), graphite (C), nickel (Ni) and boron-doped diamond (BDD) electrodes, so as to enhance flotation. These electrodes are more chemically resistant. Graphite and PbO_2 are the most common insoluble anodes used in EC [50]. These anodes are advantageous, as they are cheap and readily available. However, their utilization is restricted by their high oxygen evolution over-potential and, for some of them, their low durability [51]. Titanium/lead dioxide (Ti/PbO_2) or titanium/ silicon dioxide (Ti/SiO_2) anodes are also used and are preferred to the expensive iridium oxide (IrOx) and titanium/iridium oxide (Ti/IrOx) – tantalum pentoxide (Ta_2O_5), as they are more efficient in oxidizing toxic compounds [52].

In their study, Dia et al. found that aluminum and iron have similar performance for organic compounds removal [53]. In another study, Llano et al. who presented an integrated electro-disinfection/EC (ED–EC) process for urban wastewater reuse that employs iron bipolar electrodes, showed that the efficiency of the process depends mainly on the anodic material and is not affected by the material of the bipolar electrode. In contrast, the removal of turbidity is more efficient when iron is used as a bipolar electrode, especially at low current densities, due to the formation of a passive layer on the aluminum that hinders the dissolution of the bipolar electrode [54].

6.5. INTER-ELECTRODE DISTANCE

Inter-electrode distance (d) is another significant parameter that affects the removal efficiency of pollutants during EC, as the electrostatic field relies on the distance between the anode and cathode. As the inter-electrode distance increases, ohmic drop (IR) increases, as described by eq. (14):

$$IR = \frac{I.d}{A.\kappa} \qquad \text{(eq. 14)}$$

where I is the current (A), d is the inter-electrode distance (m), A is the active anode surface (m^2), κ is the specific conductivity (S/m).

At high inter-electrode distances, removal efficiency decreases due to reduced rate of mass transfer and due to elevated ohmic drop which reduces the anodic oxidation [55]. Atashzaban et al. reported that the removal efficiency of COD and TS decreased with increasing electrode distance from 1 to 3 cm [56]. In another study, it was shown that COD removal efficiency decreased from 83.3 to 48.3% as inter-electrode distance increased from 0.8 to 2.0 cm when using Al electrodes, while it decreased from 90.5 to 48.3% with the same variation in the inter-electrode using Fe electrodes [57]. Moreover, the inter-electrode distance also has an important effect on the cell voltage *U* according to eq. (15):

$$U = E_A + \eta_A - E_C + \eta_C + \mathrm{IR} \qquad \text{(eq. 15)}$$

where E_A and E_C are the reversible anodic and cathodic potentials, respectively, and η_A and η_C are the corresponding overpotentials, respectively. The last term is related to the electrolyte IR drop. This effect on cell voltage affects the electrical energy consumed (*E*) during EC, according to eq. (16):

$$E = \int UI \cdot dt \qquad \text{(eq. 16)}$$

Martínez-Villafane et al. depicted the influence of inter-electrode distance on energy consumption in EC, as they showed that that electrical energy consumption increased from0.061 to 0.184 kWh/m^3 with increasing the inter-electrode from 0.3 to 0.9 cm [58].

Finally, no general conclusion can be drawn from the choice of electrode material, as this is strongly dependent on water quality and on economic criteria.

6.6. TEMPERATURE

The influence of temperature on the removal efficiency of pollutants by EC is not widely reported in the literature, even though this technology has been used for more than 100 years. In the EC process, the temperature cannot, in general, be controlled, as it can vary with place and seasons, but the influence of temperature is of high interest. In a study conducted by Chou et al., the influence of temperature on the removal efficiency of indium ions from aqueous medium by EC with iron electrodes was investigated in the range of 288 K to 318 K. It was found that, after 50 min of electrolysis, the indium ion removal efficiency reached 80.9%, 90.4%, 92.7%, and 94.1% for temperatures of 288, 298, 308 and 318 K, respectively [59]. This

result is explained by the fact that higher temperatures led to greater mobility and more frequent collisions of generated species, resulting in an increased reaction rate of the metal hydroxides with pollutants [60]. However, there was no significant increase in the indium ion removal efficiency after 50 min of electrolysis when the temperature was above 298 K [59]. This is due to the increase of precipitates solubility [61]. In their study, they also showed that when the solution temperature was increased from 298 to 308 and 318 K, the specific energy consumption increased from 0.085 to 0.091 and 0.095 kWh/kg, respectively.

6.7. INITIAL POLLUTANT CONCENTRATION

The initial pollutant concentration, as temperature, varies with locations and seasons, and its influence is also a function of the type of pollutant (soluble or not, inorganic or organic…). However, the pollutant removal efficiency usually decreases with the increase in the initial concentration of the pollutant at a constant current density. This is because the amount of metal hydroxide flocs produced is insufficient to coagulate the high amount of pollutant molecules at higher initial pollutant concentrations [62]. At elevated pollutant initial concentration, current density does not usually have any significant effect on removal efficiency, especially at the early stages of EC [63]. Modirshahla et al. reported that the removal efficiency of 4-nitrophenol decreased from 99.9 to 88.7% as its initial concentration increases from 15 to 35 mg/L [64], which is the most common trend reported in the literature, whatever the pollutant considered.

6.8. TYPE OF POWER SUPPLY

EC may be operated in Direct Current (DC) or Alternating Current (AC) mode. In DC mode, the electric charge (current) only flows in one direction, however in AC mode, current changes direction periodically. DC mode is reported more than AC mode in the literature and 50-60 Hz sinusoidal voltage is usually poorly efficient, but square waves with low frequency are more interesting. DC causes oxidation/consumption of the anode and formation of an oxide layer on the cathode (cathode passivation) [65]. Passivation results in an increase in passive over potential, which leads to higher energy consumption; this passive layer also results in a decreased current flow between the two electrodes, especially at long operating time, and thus decreases EC efficiency [2]. Some studies reported that passivation could be prevented when a sufficient amount of chloride ions (initially present or added) which breakdown the passive layer or by using AC mode which prevents passivation when Al or Fe electrodes are used [65]. Vasudevan et al. who investigated the effects of AC and DC modes on the removal efficiency

of cadmium from water using aluminum alloy as anode and cathode, obtained a removal efficiency of 97.5 and 96.2% with an energy consumption of 0.454 and 1.002 kWh/m^3 at a current density of 0.2 A/dm^2 and pH of 7.0 using AC and DC, respectively [66]. So, AC can prevent passivation and improve EC performance, provided anode and cathode are of the same material. However, even for square waves, no general study on the influence of the frequency of polarity exchange is available up to now.

6.9. CURRENT DENSITY

Current density, $j=I/A$ (A/m^2) is a result of dividing electric current I by the effective area of the anode. It is the key parameter in EC, as it determines the coagulant dosage rate, bubble production rate, size and growth of the flocs, which can influence the efficiency of the process [58]. In practice, j is more robust than current I for scale-up purpose. Thus, it is the most studied parameter in the literature, where it is usually imposed (galvanostatic mode), rather than voltage (potentiometric mode) as along with time; so, it determines charge loading according to eq. (17)

$$I=jA=dq/dt \quad \text{(eq. 17)}$$

where I is current (A), q charge loading (C), A the electrode surface area (m^2), and t operating time (s). As current density rises, the rate of anodic dissolution increases. This leads to an increase in metal hydroxide flocs resulting in the increase of pollutant removal efficiency. However, increasing current density above the optimum value does not further enhance removal efficiency or sometimes it results in reducing pollutant removal efficiency due to parasitic reactions which result in oxygen production [67].

Ulu et al. reported that the removal efficiency of humic acid increased from 81.6 to 87.6% as current density increased from 0.42 to1.2 mA/cm^2 [68]. In another study, the removal efficiency of sulfides increased from 60 to 84% with the increase of current density from 10.6 to 21.2 mA/cm^2 [69]. Similar results were demonstrated by Maha Lakshmi et al., as increasing current density from 10 to 20 mA/cm^2 increased COD removal efficiency from 87% to 90%, however further increase of current density till 40 mA/cm^2 decreased removal efficiency from 90% to 81% [67]. Den et al. who used EC for bio-treated distillery wastewater treatment using Al-Al electrode pair reported an average percentage removal of COD, nitrate, and phosphate of 50%, 26% and 61%, respectively with the highest tested current density of 35.92 A/m^2, flow rate of 0.4 L/min and initial pH of 3 [70]. Current also has an impact on electrical energy consumption as shown by eq. (16). In one study, it was reported that increasing current density from 20 to

50 A/m^2 at 12.8 m^2/m^3 surface area to volume ratio increased power consumption from 0.0015 to 0.0067 kWh [71].

6.10. INITIAL pH

Solution pH is a main operating factor in EC, as it has a significant influence on the conductivity of the solution, dissolution of the electrodes, speciation of hydroxides, and zeta-potential of colloidal particles. However, it is complicated to establish a clear relationship between the pH of the solution and pollutant removal efficiency as pH changes during EC [72].

Al and Fe electrodes behave differently during EC. Different species are formed in the solution at different pH values. In highly basic solutions, $Al(OH)_4^-$ and $Fe(OH)_4^-$ ions are formed (even though **Figure 2** and **Figure 3** have shown that the formation of $Al(OH)_4^-$anions is more likely to occur than that of $Fe(OH)_4^-$). These ions are considered weak coagulants compared to Fe(III). Fe(III) is efficient in a wider pH range than Al(III) and works also in slightly basic solutions. At acidic pH, the dissolution of the iron electrodes is significant even without electricity [73]. Morgan and Lahav depicted the strong dependence of the reaction rate of Fe^{2+} oxidation to Fe^{3+} (eq. 18) on pH and oxygen saturation conditions in non-electrochemical processes [74]. Under alkaline conditions, the Fe^{2+} ions will immediately oxidize to Fe^{3+} (pH 7.6–14). At more acidic pH values, the rates will be much lower and below pH 4, oxidation becomes negligible.

$$4Fe^{2+} + O_2 + 2H_2O \rightarrow 4Fe^{3+} + 4OH^- \quad \text{(eq. 18)}$$

While reaction (eq.18) is not directly connected to the electrochemical process, it is influenced by the oxygen saturation level in the solution and, thus, by the importance of the oxygen-evolution and the redox potential of the solution. Both the oxygen state and the redox potential can change as a result of EC. Therefore, it is important to understand whether different iron-oxidation rates occur in electrochemical and non-electrochemical reactions.

Mouedhen et al. reported a sharp increase in the released amount of aluminum in the pH range 2–3. Beyond pH 3, the variation of the amount of dissolved aluminum was insignificant. In their study, the amount of aluminum generated during electrolysis always exceeded that theoretical calculated from Faraday's law. When aluminum is used in EC and the initial pH is acidic, final pH value rises and when initial pH is alkaline, final pH drops. In highly acidic or alkaline solutions, the pH remains constant. This invariability is attributed to the limited effects of phenomena allowing pH changes. For electrolyte at pH 9, the invariability of pH is due to the fact that alkalizing phenomena offset the acidifying ones [14]. Chemical dissolution of

aluminum cathodes, which increases the faradaic yield, takes place because pH increases to a level where aluminate is formed. The acidic bulk solution inhibits this reaction because the generated hydroxyl ions are consumed by the acid in the solution [75].

6.11. ELECTROLYSIS TIME

The efficiency of EC is strongly influenced by the operating time in the batch mode and space time in the continuous mode, deduced from the cell volume to volumetric flow rate ratio. The amount of coagulant produced during EC is directly proportional to the electric charge added per unit of volume [76]. It is possible to calculate the amount of produced coagulant using Faraday's law (eq. 1) when current and operating time are known Even though, complete pollutant removal is never achieved, the pollutant removal efficiency increases as electrolysis time increases. However, beyond the optimum electrolysis time, the pollutant removal efficiency remains constant and does not increase with a further increase in the electrolysis time. This is because, sufficient amount of flocs is available for the removal of the pollutant [77, 78]. As a conclusion, as for current density, electrolysis time is a key parameter in the design and the scale-up of an EC cell.

6.12. ELECTROLYTES AND WATER CONDUCTIVITY

As shown previously by eq. (14), water conductivity has an influence on ohmic drop and consequently on removal efficiency and energy consumption during EC. Increasing solution's conductivity increases current density at constant applied voltage, or decreases the cell voltage and thus power consumption at constant current density [79]. The conductivity of the solution relies mainly on the nature and concentration of the electrolytes. In the literature, many types of electrolytes have been studied, such as NaCl, $BaCl_2$, KCl, Na_2SO_4, and KI. NaCl is often added in to increase the ionic strength of the solution [51, 80], but this is not representative of real water and wastewater in which mixtures of various ionic species are involved. For example, Kobya et al. reported that removal efficiencies during EC remained unchanged with iron and aluminum in the conductivity range of 1000–4000 μS/cm. The COD removal efficiency with aluminum electrodes was slightly reduced, whereas with iron electrodes, it was slightly enhanced with increasing conductivity. For both electrodes, the energy consumption decreased with increasing wastewater conductivity [81].

In fact, electrolytes have three types of effects: they change water conductivity, but also the ionic strength (which modifies water and ion activities), and they may finally have specific

effects, *e.g.* by inducing or inhibiting secondary reactions. The concentration of specific anions in the solution influences the stability of the passive layer of an electrode. CO_3^{2-} and SO_4^{2-} ions lead to the deposition of Ca^{2+} and Mg^{2+} ions and the formation of an oxide layer which inhibits metal dissolution from the electrodes and thus causes a reduction in faradaic yield [29, 82]. Chlorides, on the other hand, induce the breakdown of the passive layer by pitting corrosion [83, 84]. The ratio of $[Cl^-]/[SO_4^{2-}]$ should be 0.1 or higher to ensure the breakdown of the passive film [85]. Some salts can precipitate on the cathodes if the concentration of the salt in water is sufficiently high [86]. Another study which investigated the effect of co-existing ions during EC using aluminum electrodes reported that the existence of sulfate ions inhibited the localized corrosion of aluminum electrodes, leading to lower defluorination efficiency because of lower current efficiency. However, the presence of chloride or nitrate ions prevented the inhibition caused by sulfate ions. It was also demonstrated that chloride ions were more efficient than nitrates [87]. In another study, Na_2SO_4 was found less efficient than NaCl as a supporting electrolyte for the removal of humic substances, oil-in-water emulsions, and fluoride. However, for unskimmed milk sample and cutting oil emulsion, sulfate anions were found to be quite harmful both for electrical consumption and EC efficiency [82].

As a conclusion, while conductivity is the main parameter studied in the literature, EC is also affected by the type of anions involved, which is a key problem when for the design and the scale-up of EC when large variability of water composition is possible.

7. EC COST ANALYSIS

The economic aspect of any process determines its practical applicability. Thus, EC should be cost effective to be applied without obstacles. The costs in EC include, the cost of energy consumption, the cost of electrode material consumed and the cost of any external chemical added (for increasing the solution conductivity or modifying the pH of the solution), as well as the costs of labor, maintenance, sludge dewatering and disposal. The latter costs items are largely independent of the type of the electrode material and are rarely taken into consideration in the literature when estimating EC costs.

Overall EC cost is usually evaluated as follows (eq. 19):

$$\text{EC Cost } (\$/m^3) = aEEC + bEMC + cCC \quad \text{(eq. 19)}$$

The electrical energy consumption (EEC) is calculated in terms of kWh per m^3 of treated effluent using eq. (20):

$$\text{EEC (kWh/m}^3) = \frac{\text{U.I.t}}{\text{V}} \quad \text{(eq. 20)}$$

where U is the cell voltage (V), I the current (A), t the electrolysis time (h) and V the volume (L) of effluent to be treated in the batch mode.

In parallel, electrode material consumed [(EMC) (kg/m^3)] at the same time t considered for EEC above is calculated theoretically by Faraday's law. Finally, CC is chemicals consumed (for pH and conductivity adjustment) and expressed in kg/m^3.

Thakur and Mondal studied the simultaneous arsenic and fluoride removal from synthetic and real groundwater by EC. In their study, an operating cost of 0.357 US \$/m^3 treated water was needed for removal efficiency of 98.51% arsenic and 88.33% fluoride [88]. This cost is more economic than the cost of using reverse osmosis (0.4-0.59 US \$/m^3) or activated alumina (0.41-0.54 US \$/m^3) for the removal of arsenic and fluoride from water [89]. In another study, Hashim et al. found that a minimum operating cost of 0.22 US \$/m^3 is required to reduce iron concentration in drinking water from 20 to 0.3 mg/L within 20 min of electrolysis [90]. This cost is very economic when comparing it to other treatment methods used to remove iron from drinking water, such as oxidation/filtration method which costs 4.05 US \$/m^3 [91]. Elazzouzi et al. who studied pollutants removal from urban wastewater found that EC required 0.9 \$/kg COD removed and 0.35 \$/kg P removed [92].

Akbal et al. compared the operating cost of EC using Al and Fe electrodes to chemical coagulation using $Al_2(SO_4)_3$. The operating cost was 0.590 US \$/m^3 and 0.970 US \$/m^3 with Fe and Al electrodes, respectively, while it increased to 1.176 US \$/m^3 with $Al_2(SO_4)_3$ [93].

8. EC APPLICATIONS

EC has been widely used for the treatment of different types of wastewater such as tannery and textile industry wastewater, paper industry wastewater, refinery wastewater, food industry wastewater, etc. Literature reports a lot of studies on the use of EC for wastewater treatment and many reviews on EC applications are available. **Table 4** summarizes some of the most recent of these studies, which are complementary to older ones already reviewed [94-103].

Table 4. Recent EC studies. COD: Chemical oxygen demand, CODs: Soluble chemical oxygen demand, BOD5: 5-day biochemical oxygen demand, TSS: Total suspended solids, TPh: Total phenolic.

Effluent	Current density (mA/cm^2)	Operating or retention time (min)	Initial pH	Inter-electrode distance(cm)	Anode-Cathode	Mode of operation	Removal efficiency (%)	Ref
Groundwater	1	95	7	1	Al-Al	Batch	Arsenic (98.51), Fluoride (83.33)	88
Drinking water	1.5	20	6	0.5	Al-Al	Batch	Iron (99.6)	90
Urban wastewater	20	30	7.4	3	Al-Al	Batch	COD (85), BOD_5 (84), TSS (94), N (63), NO_3 (73) and P (99)	92
Drinking water	2	55	7	0.5	Al-Al	Batch	Nitrate (85)	104
Synthetic lead solution	1.13	10	7	1	Zn-Zn	Batch	Lead ions (99.9)	105
Drinking water	2	25	6	0.5	Al-Al	Batch	Fluoride (98)	106
Textile wastewater	4	10	4.57	1	Al-Al	Batch	COD (97.1), Phenol (99.99)	107
Synthetic bilge water	/	120	7	1	Al-Al	Batch	COD_s (85)	108
Synthetic acetamiprid solution	5	60	7.77	/	Al-Al	Batch	Acetamiprid (97.6)	109
Synthetic arsenic solution	0.54	30	4	0 .5	Fe-Fe	Batch	Arsenic (99.5)	110
Synthetic phenol solution	25	180	3.2	1	Zn-SS	Batch	TPh content (84.2), COD (40.3)	111
Rice grain based distillery effluent	8.93	115	3.5	2	Cu-Cu	Batch	COD (80), color (65)	112
Cheese whey wastewater	60	20	5	1	Fe-Fe	Continuous	COD (86.4)	113
Strained yogurt wastewater	30	90	4.53	1	Fe-Fe	Batch	COD (84)	114
Dyehouse wastewater	6.5	35	5.5	2	Al-Al	Continuous	COD (85)	115
Dyehouse wastewater	6.5	350	5.5	2	Fe-Fe	Continuous	COD (77)	115
Anaerobically treated municipal wastewater	2	5	7.5	1.5	Al-Al	Continuous	Total coliform (99.81), faecal coliform (99.86)	116
Can manufacturing wastewater	2	40	3	1.3	Al-Al	Batch	COD (72)	117
Synthetic glyphosate solution	6	60	6.7	6	Cu-Cu	Batch	Glyphosate (46.69)	118

Table 4 clearly demonstrates the ability of EC to treat various types of water and wastewater. However, EC has a limited ability to remove some substances, such as ammonium ions and it is unable to eliminate

very soluble molecules such as, glucose, and lactose and volatile fatty acids (not mentioned in the table). Concerning the pollutants removable by EC, optimization is required in many cases to improve the removal efficiency of these pollutants. Moreover, more studies in the continuous mode should be carried out, as the clear majority of works in the literature are carried out in the batch mode, which is an obstacle in the way of scale-up. In addition to that, the EC modeling approaches in the literature are insufficient, as only few authors took it to the next step and established models for design and scale-up of the EC cells as a function of operating parameters. Such models could make easier to predict the performance of EC reactors before designing them and provide us with a better understanding of the design aspects allowing EC technology to progress beyond the current state of empiricism that prevails in the design of EC cells.

9. COUPLING OF EC WITH OTHER TREATMENT METHODS

EC may be coupled with other treatment methods in a hybrid process to increase the removal efficiency of pollutants. The most recent studies on hybrid processes involving EC with other treatment methods are summarized in **Table 5**. As seen in **Table 5**, coupling conventional EC to other wastewater treatment techniques could achieve very high removal efficiencies. This is not the only advantage of coupling, as it also reduces power consumption and operating time, which makes it much better than conventional EC. However, increased equipment cost and scale-up remain the major challenges of these hybrid technologies for the coming years, although the very positive results obtained at the lab and bench scales make them very promising.

Table 5. Recent studies of EC coupled with other treatment methods. COD: Chemical oxygen demand, BOD: Biochemical oxygen demand, TOC: Total organic carbon, TPH: Total petroleum hydrocarbon.

Combination	Effluent treated	Removal efficiency (%)	Reference
EC + Biofiltration	Landfill leachate	NH_4 (94), BOD (96), refractory COD (53), Color (85)	119
EC + Adsorption (banana peel)	Synthetic methylene blue solution	Methylene blue (99)	120
EC + fixed film biological process	Oil refinery wastewater	Total petroleum hydrocarbon TPH (98), COD (>95)	121
EC + Photoelectro-Fenton processe + UVA light irradiation	Synthetic Tartrazine solution	Color (100)	122
EC/EF + Removal by Graphene-containing ceramic composite tubular membrane	Synthetic phthalates and pharmaceuticals solution	Butyl phthalate and Di(2-ethylhexyl) phthalate (99), Cephalexin, Sulfamethoxazole and Caffeine (32–97)	123
EC + photocatalytic process	Lithographic wastewater	TOC (74.43)	124

EC + Advanced oxidation process	Distillery industrial effluent	COD and color (100)	125
EC + photochemical oxidation	Synthetic hydroquinone solution	Hydroquinone (91.5)	126
EC + Dynamic membrane	Oily wastewater	Effluent oil (65), Permeate oil (98.5)	127
EC + Ozonation	Distillery industry wastewater	Color (10), COD (95)	128
EC + Electrooxidation	Industrial park wastewater	TOC (70.26), COD (99.7), Color (100), Turbidity (95)	129
EC + Electro-flotation	Synthetic Doxycycline solution	Doxycycline (99)	130
EC + H2O2 intermittent addition	Synthetic perfluorooctanoic acid solution	Perfluorooctanoic acid (99)	131
EC + anodic oxidation	Arsenic contaminated groundwater	Arsenic (100)	132

10. CONCLUSION

The rapid industrialization and urbanization are causing high levels of water pollution, which in its turn reduces available clean water worldwide. Consequently, wastewater should be treated to face the shortage of clean water. The choice of an effluent treatment technique is governed by various parameters, such as the type of pollutants, their concentration, the volume to be treated and toxicity to microbes. EC is an effective technique for the treatment of various kinds of wastewater, due to several advantages including environmental capability, versatility, energy efficiency, safety and cost effectiveness. EC is characterized by easy operation, simple equipment, short operating time and reduced amount of sludge which retains less water and sediments rapidly.

However, pollution removal in EC results from the combination of complex mechanisms (colloidal destabilization, adsorption…) which depend not only on the key operating parameters (current, electrolysis time), but also are also sensitive to water properties (pH, ionic composition…) and also to electrode passivation that may increases the operating cost of EC over time. As a consequence, even if the potential applications of EC alone or in a hybrid process are numerous and attractive in the literature, EC remains disregarded in comparison to other treatment processes because no design and scale-up rules are clearly established. In addition, most of literature deals with experiments at the laboratory scale using synthetic solutions; so, more studies should be performed at pilot plant scale and in the continuous mode using real industrial effluents, which means that more research is still required to optimize pollutant removal efficiency.

REFERENCES

1. Corcoran, E., Nellemann, C., Baker, E., Bos, R., Osborn, D., Savelli, H (eds)., 2010 Sick Water? The central role of wastewater management in sustainable development. A Rapid Response Assessment. United Nations Environment Programme, UN-HABITAT, GRID-Arendal.

2. Ahmad, H., Lafi, W.K., Abushgair, K., Assbeihat, J.M., 2016. Comparison of coagulation, electrocoagulation and biological techniques for the municipal wastewater treatment. International Journal of Applied Engineering Research 11, 11014–11024.

3. Hakizimana, J.N., Gourich, B., Chafi, M., Stiriba, Y., Vial, C., Drogui, P., Naja, J., 2017. electrocoagulation process in water treatment: A review of elecrocoagulation modeling approaches. Desalination 404, 1–21.

4. Mollah, M.Y.A., Morkovsky, P., Gomes, J.A.G., Kesmez, M., Parga, J., Cocke, D.L., 2004a. Fundamentals, present and future perspectives of electrocoagulation. Journal of Hazardous Materials 114, 199–210.

5. Barrera-Díaz, C.E., Lugo-Lugo, V., Bilyeu, B., 2012. A review of chemical, electrochemical and biological methods for aqueous Cr(VI) reduction. Journal of Hazardous Materials 223–224, 1–12.

6. Chaturvedi, S.I., 2013. Electrocoagulation: A novel waste water treatment method. International Journal of Modern Engineering Research 3, 93–100.

7. http://corrosion-doctors.org/Corrosion-Thermodynamics.

8. Pesterfield, L.L., Maddox, J.B., Crocker, M.S., Schweitzer, G.K., 2012. Pourbaix (E–pH-M) diagrams in three dimensions. Journal of Chemical Educaion 89, 891–899.

9. Duan, J., Gregory, J., 2003. Coagulation by hydrolysing metal salts. Advances in Colloid and Interface Science 100–102, 475–502.

10. The Aqueous Chemistry of the Elements, 2010. Journal of The American Chemical Society 132, 4501–4501.

11. Ukiwe, L.N., Ibeneme, S.I., Duru, C.E., Okolue, B.N., Onyedika, G.O., Nweze, C.A., 2014. Chemical and electrocoagulation techniques in coagulation-floccculation in water and wastewater treatment-Review. International Journal of Research and Reviews in Applied Sciences 181, 285–294.

12. Khaled, B., Wided, B., Béchir, H., Elimame, E., Mouna, L., Zied, T., 2015. Investigation of electrocoagulation reactor design parameters effect on the removal of cadmium from synthetic and phosphate industrial wastewater. Arabian Journal of Chemistry. In Press, Corrected Proof.

13. Vepsäläinen, M., 2012. EC in the treatment of industrial waters and wastewaters. PhD Dissertation, Mikkeli university, Mikkeli, Finland.

14. Mouedhen, G., Feki, M., Wery, M.D.P., Ayedi, H.F., 2008. Behavior of aluminum electrodes in electrocoagulationprocess. Journal of Hazardous Materials 150, 124–135.

15. Moussa, D.T., El-Naas, M.H., Nasser, M., Al-Marri, M.J., 2017. A comprehensive review of electrocoagulation for water treatment: Potentials and challenges. Journal of Environmental Management 186 (pt 1), 24–41.

16. Ghernaout, D., Naceur, M.W., Ghernaout, B., 2011a. A review of electrocoagulation as a promising coagulation process for improved organic and inorganic matters removal by electrophoresis and electroflotation. Desalination and Water Treatment 28, 287–320.

17. Duman, O., Tunç, S., 2009. Electrokinetic and rheological properties of Na-bentonite in some electrolyte solutions. Microporous and Mesoporous Materials 117, 331–338.

18. Nasser, M.S., James, A.E., 2006. The effect of polyacrylamide charge density and molecular weight on the flocculation and sedimentation behaviour of kaolinite suspensions. Separation and Purification Technology 52, 241–252.

19. Nasser, M.S., James, A.E., 2007. Numerical simulation of the continuous thickening of flocculated kaolinite suspensions. International Journal of Mineral Processing, Special Issue To Honor The Late Professor R. Peter King 84, 144–156.

20. Tadros, T.F., 1986. Prevention of formation of dilatant sediments in suspension concentrates. Colloids and Surfaces 18, 427–438.

21. Liang, Y., Hilal, N., Langston, P., Starov, V., 2007. Interaction forces between colloidal particles in liquid: Theory and experiment. Advances in Colloid and Interface Science, Surface forces: wetting phenomena, membrane separation, rheology. Topical issue in honour of Victor Starov 134–135, 151–166.

22. Rashed, M.N., 2013. Adsorption technique for the removal of organic pollutants from water and wastewater. doi:10.5772/54048.

23. Demiral, H., I. Demiral, F. Tumsek and B. Karacbacakoglu., 2008. Adsorption of chromium (VI) from aqueous solution by activated carbon derived from olive baggase and applicability of different adsorption models. ChemicalEngineering Journal 144, 188.

24. Krishna, R.H., Swamy, A., 2012. Physico-chemical key parameters, Langmuir and Freundlich isotherm and Lagergren rate constant studies on the removal of divalent nickel from the aqueous solutions onto powder of calcined brick. International Journal of Engineering Research and Development 4, 29–38.

25. Vijayakumar, G., Tamilarasan, R., Dharmendirakumar, M., 2012.Adsorption, kinetic, equilibrium and thermodynamic studies on the removal of basic dye Rhodamine-B from aqueous solution by the use of natural adsorbent perlite.Journal ofMaterials and Environmental Science 3, 157–170.

26. Picard T., 2000. Contribution à l'étude des réactions aux électrodes en vue de l'application à l'électrocoagulation.PhD Dissertation, Université de Limoges, Limoges, France.

27. Zodi, S., 2012. Étude de l'épuration d'effluents de composition complexe par électrocoagulation et des couplages intervenants entre le traitement électrochimique et l'étape de séparation: application à l'industrie textile et papetière. PhD Dissertation, Université de Lorraine, Nancy, France.

28. Holt P.K., 2002. Electrocoagulation: unraveling and synthesizing themechanisms behind a water treatment process. PhD Dissertation, Université de Sydney, Sydney, Australia.

29. Holt, P.K., Barton, G.W., Mitchell, C.A., 2005. The future for electrocoagulation as a localised water treatment technology. Chemosphere 59, 355–367.

30. Bennajah,M., 2007. Traitement des rejets industriels liquide par électrocoagulation/électroflotation en réacteur airlift. PhD Dissertation, Polytechnique de Toulouse, Toulouse, France.

31. Bensaid, J., 2009.Contribution à la dépollution des eaux usées par électrocoagulation et par adsorption sur des hydroxydes d'aluminium, Thèse de doctorat d'état, Université Mohammed V – Agdal, Maroc.

32. El Nemr, Ahmad., 2011. Non-conventional textile waste water treatment, National Institute of Oceanography and Fisheries, Alexandria, Egypt.

33. Khemis, M., 2005. Etude théorique et expérimentale du procédé d'électrocoagulation:application au traitement des effluents liquides hautement chargés en impuretés organiques et minérales.PhD dissertation, Université de Nancy, Nancy,France.

34. Mollah, M.Y.A., Schennach, R., Parga, J.R., Cocke, D.L., 2001. Electrocoagulation (EC)–science and applications. Journal of Hazardous Materials 84, 29–41.

35. Demirci, Y., Pekel, L.C., Alpbaz, M., 2015. Investigation of different electrode connections in electrocoagulation of textile wastewater treatment. International Journal of Electrochemical Science 10, 2685–2693.

36. Khandegar, V., Saroha, A.K., 2013a. Electrocoagulation for the treatment of textile industry effluent–A review. Journal of Environmental Management 128, 949–963.

37. Kobya, M., Ulu, F., Gebologlu, U., Demirbas, E., Oncel, M.S., 2011. Treatment of potable water containing low concentration of arsenic with electrocoagulation: Different connection modes and Fe–Al electrodes. Separation and Purification Technology 77, 283–293.

38. Wang, C.-T., Chou, W.-L., Kuo, Y.-M., 2009. Removal of COD from laundry wastewater by electrocoagulation/electroflotation. Journal of Hazardous Materials 164, 81–86.

39. Asselin, M., Drogui, P., Brar, S.K., Benmoussa, H., Blais, J.-F., 2008. Organics removal in oily bilgewater by electrocoagulation process. Journal of Hazardous Materials 151, 446–455.

40. Emamjomeh, M.M., Sivakumar, M., 2009. Fluoride removal by a continuous flow electrocoagulation reactor. Journal of Environmental Management 90, 1204–1212.

41. Merzouk, B., Gourich, B., Sekki, A., Madani, K., Vial, C., Barkaoui, M., 2009. Studies on the decolorization of textile dye wastewater by continuous electrocoagulation process. Chemical Engineering Journal 149, 207–214.

42. Sandoval, M.A., Fuentes, R., Nava, J.L., Rodríguez, I., 2014. Fluoride removal from drinking water by electrocoagulation in a continuous filter press reactor coupled to a flocculator and clarifier. Separation and Purification Technology 134, 163–170.

43. Kobya, M., Ozyonar, F., Demirbas, E., Sik, E., Oncel, M.S., 2015. Arsenic removal from groundwater of Sivas-Şarkişla Plain, Turkey by electrocoagulation process: Comparing with iron plate and ball electrodes. Journal of Environmental Chemical Engineering 3, 1096–1106.

44. Heffron, J., Marhefke, M., Mayer, B.K., 2016. Removal of trace metal contaminants from potable water by electrocoagulation. Scientific Reports 6, 28478.

45. Akyol, A., 2012.Treatment of paint manufacturing wastewater by electrocoagulation. Desalination 285, 91-99.

46. Bouhezila, F., Hariti, M., Lounici, H., Mameri, N., 2011.Treatment of the OUED SMAR town landfill leachate by an electrochemical reactor. Desalination 280, 347–353.

47. Bayramoglu, M., Kobya, M., Eyvaz, M., Senturk, E., 2006.Technical and economic analysis of electrocoagulation for the treatment of poultry slaughterhouse wastewater. Separation and Purification Technology 51, 404–408.

48. Yuksel, E., Eyvaz, M., Gurbulak, E., 2013.Electrochemical treatment of colour index reactive orange 84 and textile wastewater by using stainless steel and iron electrodes; Environmental Progress and Sustainable Energy 32, 60–68.

49. Pearse, M.J., 2003. Historical use and future development of chemicals for solid–liquid separation in the mineral processing industry. Minerals Engineering 16, 103–108.

50. Burns, S.E., Yiacoumi, S., Tsouris, C., 1997. Microbubble generation for environmental and industrial separations. Separation and Purification Technology 11, 221–232.

51. Sahu, O., Mazumdar, B., Chaudhari, P.K., 2014. Treatment of wastewater by electrocoagulation: a review. Environmental Science and Pollution Research 21, 2397–2413.

52. Polcaro, A.M., Palmas, S., Renoldi, F., Mascia, M., 1999. On the performance of Ti/SnO2 and Ti/PbO2nodesin electrochemical degradation of 2-chlorophenolfor wastewater treatment. Journal of Applied Electrochemistry 29, 147–151.

53. Dia, O., Drogui, P., Buelna, G., Dubé, R., Ihsen, B.S., 2017. Electrocoagulation of bio-filtrated landfill leachate: Fractionation of organic matter and influence of anode materials. Chemosphere 168, 1136–1141.

54. Llanos, J., Cotillas, S., Cañizares, P., Rodrigo, M.A., 2014. Effect of bipolar electrode material on the reclamation of urban wastewater by an integrated electrodisinfection/EC process. Water Research 53, 329–338.

55. Nasrullaha, M., Singhb, L., Wahida, Z.A., 2012. Treatment of sewage by electrocoagulation and the effect of high current density.Energy and Environmental Engineering Journal 1, 27–31.

56. Atashzaban, Z., Seidmohammadi, A., Nematollahi, D., Azarian, G., Shayesteh, O.H., Rahmani, A.R., 2016. The efficiency of electrocoagulation and electroflotation processes for removal of polyvinyl acetate from synthetic effluent. Avicenna Journal of Environmental Health Engineering 3, e7469.

57. Ghalwa, N.M.A., Saqer, A.M., Farhat, N.B., 2016. Removal of reactive red 24 dye by clean electrocoagulation process using iron and aluminum electrodes. Journal of Applied Chemical Research 10, 117–132.

58. Martínez-Villafañe, J.F., Montero-Ocampo, C., García-Lara, A.M., 2009. Energy and electrode consumption analysis of electrocoagulation for the removal of arsenic from underground water. Journal of Hazardous Materials. 172, 1617–1622.

59. Chou, W.-L., Huang, Y.-H., 2009. Electrochemical removal of indium ions from aqueous solution using iron electrodes. Journal of Hazardous Materials 172, 46–53.

60. El-Ashtoukhy, E.-S., Amin, N.K., Abdelwahab, O., 2009. Treatment of paper mill effluents in a batch-stirred electrochemical tank reactor. Chemical Engineering Journal 146, 205–210.

61. Golder, A.K., Samanta, A.N., Ray, S., 2006. Removal of phosphate from aqueous solutions using calcined metal hydroxides sludge waste generated from electrocoagulation. Separation and Purification Technology 52, 102–109.

62. Dalvand, A., Gholami, M., Joneidi, A., Mahmoodi, N.M., 2011. Dye removal, energy consumption and operating cost of electrocoagulation of textile wastewater as a clean process. Clean–Soil, Air, Water 39, 665–672.

63. Ajeel, M.A., Aroua, M.K., Daud, W.M.A.W., 2015. p-Benzoquinone anodic degradation by carbon black diamond composite electrodes. Electrochimica Acta 169, 46–51.

64. Modirshahla, N., Behnajady, M.A., Mohammadi-Aghdam, S., 2008. Investigation of the effect of different electrodes and their connections on the removal efficiency of 4-nitrophenol from aqueous solution by electrocoagulation. Journal of Hazardous. Materials 154, 778–786.

65. Yang, Z., Xu, H., Zeng, G., Luo, Y., Yang, X., Huang, J., Wang, L., Song, P., 2015. The behavior of dissolution/passivation and the transformation of passive films during electrocoagulation: influences of initial pH, Cr (VI) concentration, and alternating pulsed current. Electrochimica Acta 153, 149–158.

66. Vasudevan, S., Lakshmi, J., Sozhan, G., 2011. Effects of alternating and direct current in electrocoagulation process on the removal of cadmium from water. Journal of Hazardous Materials 192, 26–34.

67. Maha Lakshmi, P., Sivashanmugam, P., 2013. Treatment of oil tanning effluent by electrocoagulation: Influence of ultrasound and hybrid electrode on COD removal. Separation and Purification Technology 116, 378–384.

68. Ulu, F., Barışçı, S., Kobya, M., Särkkä, H., Sillanpää, M., 2014. Removal of humic substances by electrocoagulation (EC) process and characterization of floc size growth mechanism under optimum conditions. Separation and Purification Technology 133, 246–253.

69. Ben Hariz, I., Halleb, A., Adhoum, N., Monser, L., 2013. Treatment of petroleum refinery sulfidic spent caustic wastes by electrocoagulation. Separation and Purification Technology 107, 150–157.

70. Den, C., Belo, L.P., Mission, E.G., Hinode, H., Abella, L.C., Gaspillo, P.-A, D., 2016. Experimental investigations of the effects of current density during the electrocoagulation of bio-treated distillery

wastewater using aluminum-aluminum electrode pair. DLSU Research De La Salle University, Manila, Philippines.

71. Han, Z., Wang, L., Duan, L., Zhu, S., Ye, Z., Yu, H., 2015. The electrocoagulation pretreatment of biogas digestion slurry from swine farm prior to nanofiltration concentration. Separation and Purification Technology 156, Part 2, 817–826.

72. Mansoorian, H.J., Mahvi, A.H., Jafari, A.J., 2014. Removal of lead and zinc from battery industry wastewater using electrocoagulation process: Influence of direct and alternating current by using iron and stainless steel rod electrodes. Separation and Purification Technology 135, 165–175.

73. Ben Sasson, M., Calmano, W., Adin, A., 2009. Iron-oxidation processes in an electroflocculation (electrocoagulation) cell. Journal of Hazardous Materials 171, 704–709.

74. Morgan, B., Lahav, O., 2007. The effect of pH on the kinetics of spontaneous Fe (II) oxidation by O_2 in aqueous solution–basic principles and a simple heuristic description. Chemosphere 68, 2080–2084.

75. Picard, T., Cathalifaud-Feuillade, G., Mazet, M., Vandensteendam, C., 2000. Cathodic dissolution in the EC process using aluminium electrodes. Journal of Environmental Monitoring 2, 77–80.

76. Abdel-Gawad, S.A., Baraka, A.M., Omran, K.A., Mokhtar, M.M., 2012. Removal of some pesticides from the simulated waste water by electrocoagulation method using iron electrodes. International Journal of Electrochemical Science 7, 6654–6665.

77. Choudhary, A., Mathur, S., 2016. Performance Evaluation of non rotating and rotating anode reactor in electro coagulation process, in: International Conference on Advanced Material Technologies (ICAMT).Dadi Institute of Engineering and Technology (DIET), Visakhapatnam, Andhra Pradesh, India.

78. Bazrafshan, E., Mohammadi, L., Ansari-Moghaddam, A., Mahvi, A.H., 2015. Heavy metals removal from aqueous environments by electrocoagulation process–a systematic review. Journal of Environmental Health Science and Engineering 13, 74.

79. Nandi, B.K., Patel, S., 2013. Effects of operational parameters on the removal of brilliant greendye from aqueous solutions by EC. Arabian Journal of Chemistry, In Press, Corrected Proof.

80. Aoudj, S., Khelifa, A., Drouiche, N., 2017. Removal of fluoride, SDS, ammonia and turbidityfrom semiconductor wastewater by combined electrocoagulation–electroflotation. Chemospher 180, 379–387.

81. Kobya, M., Can, O.T., Bayramoglu, M., 2003. Treatment of textile wastewaters by electrocoagulation using iron and aluminum electrodes. Journal of Hazardous Materials 100, 163–178.

82. Ghernaout, D., Ghernaout, B., 2011b. On the controversial effect of sodium sulphate as supporting electrolyte on electrocoagulation process: A review. Desalination and Water Treatment 27, 243–254.

83. Khandegar, V., Saroha, A.K., 2013b. Electrochemical treatment of effluent from small-scale dyeing unit. Indian Chemical Engineer 55, 112–120.

84. Khandegar, V., Saroha, A.K., 2013c. Electrochemical treatment of textile effluent containing acid red 131 dye. Journal of Hazardous, Toxic,and Radioactive Waste18, 38–44

85. Naje, A.S., Chelliapan, S., Zakaria, Z., Ajeel, M.A., Alaba, P.A., 2016a. A review of electrocoagulation technology for the treatment of textile wastewater. Reviews in Chemical Engineering. doi: 10.1515/revce-2016-0019.

86. Hasson, D., Lumelsky, V., Greenberg, G., Pinhas, Y., Semiat, R., 2008. Development of the electrochemical scale removal technique for desalination applications. Desalination 230, 329–342.

87. Hu, C.Y., Lo, S.L., Kuan, W.H., 2003. Effects of co-existing anions on fluoride removal in electrocoagulation (EC) process using aluminum electrodes. Water Research 37, 4513–4523.

88. Thakur, L.S., Mondal, P., 2017. Simultaneous arsenic and fluoride removal from synthetic and real groundwater by electrocoagulation process: Parametric and cost evaluation. Journal of Environmental Management 190, 102–112.

89. Piñón-Miramontes, M., Bautista-Margulis, R.G., Pérez-Hernández, A., 2003. Removal of arsenic and fluoride from drinking water with cake alum and a polymeric anionic flocculent. Fluoride 36,122–128.

90. Hashim, K.S., Shaw, A., Al Khaddar, R., Pedrola, M.O., Phipps, D., 2017a. Iron removal, energy consumption and operating cost of electrocoagulation of drinking water using a new flow column reactor. Journal of Environmental Management 189, 98–108.

91. Chaturvedi, S., Dave, P.N., 2012. Removal of iron for safe drinking water. Desalination 303, 1–11.

92. Elazzouzi, M., Haboubi, K., Elyoubi, M.S., 2017. Electrocoagulaion flocculation as a low-cost process for pollutants removal from urban wastewater. Chemical Engineering Research and Design 117, 614–626.

93. Akbal, F., Camcı, S., 2010. Comparison of electrocoagulation and chemical coagulation for heavy metal removal. Chemical Engineering Technolnology 33, 1655–1664.

94. Bayramoglu, M., Kobya, M., Can, O.T., Sozbir, M., 2004. Operating cost analysis of electrocoagulation of textile dye wastewater. Separation and Purification Technology 37, 117–125.

95. Chen, X., Chen, G., Yue, P.L., 2000. Separation of pollutants from restaurant wastewater by electrocoagulation. Separation and Purification Technology 19, 65–76.

96. Emamjomeh, M.M., Sivakumar, M., 2009. Denitrification using a monopolar electrocoagulation/flotation (ECF) process. Journal of Environmental Management. 91, 516–522.

97. Emamjomeh, M.M., Sivakumar, M., 2006. An empirical model for defluoridation by batch monopolar electrocoagulation/flotation (ECF) process. Journal of Hazardous Materials 131, 118–125.

98. Holt, P.K., Barton, G.W., Wark, M., Mitchell, C.A., 2002. A quantitative comparison between chemical dosing and electrocoagulation. Colloids and Surfaces A: Physicochemical and Engineering Aspects 211, 233–248.

99. Koparal, A.S., Öğütveren, Ü.B., 2002. Removal of nitrate from water by electroreduction and electrocoagulation. Journal of Hazardous Materials 89, 83–94.

100. Lai, C.L., Lin, S.H., 2004. Treatment of chemical mechanical polishing wastewater by electrocoagulation: system performances and sludge settling characteristics. Chemosphere 54, 235–242.

101. Mollah, M.Y.A., Pathak, S.R., Patil, P.K., Vayuvegula, M., Agrawal, T.S., Gomes, J.A.G., Kesmez, M., Cocke, D.L., 2004b. Treatment of orange II azo-dye by electrocoagulation (EC) technique in a continuous flow cell using sacrificial iron electrodes. Journal of Hazardous Materials 109, 165–171.

102. Yavuz, Y., 2007. EC and EF processes for the treatment of alcohol distillery wastewater. Separation and Purification Technology 53, 135–140.

103. Yilmaz, A.E., Boncukcuoğlu, R., Kocakerim, M.M., Keskinler, B., 2005. The investigation of parameters affecting boron removal by electrocoagulation method. Journal of Hazardous Materials 125, 160–165.

104. Hashim, K.S., Shaw, A., Al Khaddar, R., Pedrola, M.O., Phipps, D., 2017b. Energy efficient electrocoagulation using a new flow column reactor to remove nitrate from drinking water–Experimental, statistical, and economic approach. Journal of Environmental Management 196, 224–233.

105. Hashim, K.S., Shaw, A., Al Khaddar, R., Pedrola, M.O., Phipps, D., 2017c. Defluoridation of drinking water using a new flow column-electrocoagulation reactor (FCER)-Experimental, statistical, and economic approach. Journal of Environmental Management 197, 80–88.

106. Hussin, F., Abnisa, F., Issabayeva, G., Aroua, M.K., 2017. Removal of lead by solar-photovoltaic electrocoagulation using novel perforated zinc electrode. Journal of Cleaner Production 147, 206–216.

107. Naje, A.S., Chelliapan, S., Zakaria, Z., Abbas, S.A., 2016b. Electrocoagulation using a rotated anode: A novel reactor design for textile wastewater treatment. Journal of Environmental Management 176, 34–44.

108. Aswathy, P., Gandhimathi, R., Ramesh, S.T., Nidheesh, P.V., 2016. Removal of organics from bilge water by batch electrocoagulation process. Separation and Purification Technology 159, 108–115.

109. John, S., Soloman, P.A., Fasnabi, P.A., 2016. Study on removal of Acetamiprid from wastewater by electrocoagulation. Procedia Technology 24, 619–630.

110. Can, B.Z., Boncukcuoglu, R., Yilmaz, A.E., Fil, B.A., 2014. Effect of some operational parameters on the arsenic removal by electrocoagulation using iron electrodes. Journal of Environmental Health Science and Engineering 12, 95.

111. Fajardo, A.S., Rodrigues, R.F., Martins, R.C., Castro, L.M., Quinta-Ferreira, R.M., 2015.Phenolic wastewaters treatment by electrocoagulation process using Zn anode. Chemical Engineering Journal 275, 331–341.

112. Prajapati, A.K., Chaudhari, P.K., Pal, D., Chandrakar, A., Choudhary, R., 2016. Electroocagulation treatment of rice grain based distillery effluent using copper electrode. Journal of Water Process Engineering 11, 1–7.

113. Un, U.T., Kandemir, A., Erginel, N., Ocal, S.E., 2014. Continuous EC of cheese whey wastewater: an application of response surface methodology. Journal of Environmental Management 146, 245–250.

114.Un, U.T., Ozel, E., 2013. Electrocoagulation of yogurt industry wastewater and the production of ceramic pigments from the sludge. Separation and Purification Technology 120, 386–391.

115. Kobya, M., Gengec, E., Demirbas, E., 2016. Operating parameters and costs assessments of a real dyehouse wastewater effluent treated by a continuous electrocoagulation process. Chemical Engineering and Processing: Process Intensification 101, 87–100.

116. Makwana, A.R., Ahammed, M.M., 2016. Continuous electrocoagulation process for the post-treatment of anaerobically treated municipal wastewater. Process Safety and Environmental Protection 102, 724–733.

117. Kobya, M., Demirbas, E., 2015. Evaluations of operating parameters on treatment of can manufacturing wastewater by electrocoagulation. Journal of Water Process Engineering 8, 64–74.

118. Danial, R., Abdullah, L.C., Sobri, S., 2017. Potential of copper electrodes in electrocoagulation process for glyphosate herbicide removal, in: MATEC Web of Conferences. EDP Sciences, p. 06019.

119. Oumar, D., Patrick, D., Gerardo, B., Rino, D., Ihsen, B.S., 2016. Coupling biofiltration process and electrocoagulation using magnesium-based anode for the treatment of landfill leachate. Journal of Environmental Management 181, 477–483.

120. Carvalho, H.P. de, Huang, J., Zhao, M., Liu, G., Dong, L., Liu, X., 2015. Improvement of Methylene Blue removal by electrocoagulation/banana peel adsorption coupling in a batch system. Alexandria Engineering Journal 54, 777–786.

121. Pérez, L.S., Rodriguez, O.M., Reyna, S., Sánchez-Salas, J.L., Lozada, J.D., Quiroz, M.A., Bandala, E.R., 2016. Oil refinery wastewater treatment using coupled electrocoagulation and fixed film biological processes. Physics and Chemistry of the Earth, Parts A/B/C 91, 53–60.

122. Thiam, A., Zhou, M., Brillas, E., Sirés, I., 2014. Two-step mineralization of Tartrazine solutions: study of parameters and by-products during the coupling of electrocoagulation with electrochemical advanced oxidation processes. Applied Catalysis B: Environmental 150, 116–125.

123. Yang, G.C., Chen, Y.-C., Yang, H.-X., Yen, C.-H., 2016. Performance and mechanisms for the removal of phthalates and pharmaceuticals from aqueous solution by graphene-containing ceramic composite tubular membrane coupled with the simultaneous electrocoagulation and electrofiltration process. Chemosphere 155, 274–282.

124. Suárez-Escobar, A., Pataquiva-Mateus, A., López-Vasquez, A., 2016. Electrocoagulation–photocatalytic process for the treatment of lithographic wastewater. Optimization using response surface methodology (RSM) and kinetic study. Catalysis Today 266, 120–125.

125. Aziz, A.R.A., Asaithambi, P., Daud, W.M.A.B.W., 2016. Combination of electrocoagulation with advanced oxidation processes for the treatment of distillery industrial effluent. Process Safety and Environmental Protection 99, 227–235.

126. Akyol, A., Can, O.T., Bayramoglu, M., 2015. Treatment of hydroquinone by photochemical oxidation and electrocoagulation combined process. Journal of Water Process Engineering 8, 45–54.

127. Yang, T., Qiao, B., Li, G.-C., Yang, Q.-Y., 2015. Improving performance of dynamic membrane assisted by electrocoagulation for treatment of oily wastewater: Effect of electrolytic conditions. Desalination 363, 134–143.

128. Asaithambi, P., Aziz, A.R.A., Daud, W.M.A.B.W., 2016. Integrated ozone–electrocoagulation process for the removal of pollutant from industrial effluent: Optimization through response surface methodology. Chemical Engineering and Processing: Process Intensification 105, 92–102.

129. García-García, A., Martínez-Miranda, V., Martínez-Cienfuegos, I.G., Almazán-Sánchez, P.T., Castañeda-Juárez, M., Linares-Hernández, I., 2015. Industrial wastewater treatment by electrocoagulation–electrooxidation processes powered by solar cells. Fuel 149, 46–54.

130. Zaidi, S., Chaabane, T., Sivasankar, V., Darchen, A., Maachi, R., Msagati, T.A.M., Prabhakaran, M., 2016. Performance efficiency of electro-coagulation coupled electro-flotation process (EC-EF) versus adsorption process in doxycycline removal from aqueous solutions. Process Safety and Environmental Protection 102, 450–461.

131. Yang, B., Han, Y., Deng, Y., Li, Y., Zhuo, Q., Wu, J., 2016. Highly efficient removal of perfluorooctanoic acid from aqueous solution by H2O2-enhanced electrocoagulation-electroflotation technique. Emerging Contaminants 2, 49–55.

132. Zhang, P., Tong, M., Yuan, S., Liao, P., 2014. Transformation and removal of arsenic in groundwater by sequential anodic oxidation and EC. Journal of Contaminant Hydrology 164, 299–307.

CHAPTER 2: THE USE OF ELECTROCOAGULATION FOR THE RECOVERY OF MICROALGAE AND PLANT EXTRACTS

This review article is submitted to the Journal of Applied Phycology. Consequently, this chapter follows the guidelines of this journal.

Nidal Fayad, Tania Yehya, Fabrice Audonnet, Christophe Vial.

ABSTRACT

This paper aims to review the recent published literature related to the use of electrocoagulation (EC) and relevant electrochemical methods for the recovery of microalgae and some plant extracts. The review presents works carried out for the recovery of various microalgal species. It also focuses on the influence of the main operating parameters on the process efficiency, details energy consumption in different studies and discusses biomass and effluent pollution by metals (Al and Fe). Moreover, works performed for the recovery of plant extracts by electrocoagulation are reviewed.

Keywords: electrocoagulation, recovery, plant extracts, microalgae

1. INTRODUCTION

Electrocoagulation (EC) is a non-specific electrochemical technique usually used for treating contaminated water using electricity instead of expensive chemical reagents (Naje and Abbas 2013). It has been successfully applied for treating potable water (Mameri et al. 2015), electroplating wastewater (Adhoum et al. 2004; Kobya et al. 2016), laundry wastewater (Janpoor et al. 2011), restaurant wastewater (Chen et al. 2000), poultry slaughterhouse wastewater (Bayar 2011), dyes (Mbacké 2016) and textile industry effluent (Naje et al. 2016). EC exhibits many advantages over conventional chemical and physicochemical treatments such as easy automation, low waste production, little maintenance requirements and operation possibility at mild conditions (room temperature and atmospheric pressure) (Cotillas et al. 2014).

Although EC has been successfully used for water and wastewater treatment, it was not widely employed as a separation technique for the recovery of valuable biomolecules, such as microalgae and plant extracts. Microalgae have been intensively researched due to their ability to produce biofuels (Ma et al. 2015) and their superiority over 1st generation energy crops in terms of energy potential, as shown in **Table 1**. Microalgae are usually recovered using a two-step concentration process: thickening and dewatering **(Figure 1)**. These 2 stages consist of various biological, chemical and physical methods and

are essential to obtain a thick algal slurry from the initial microalgal suspension and to facilitate further downstream processes (Barros et al. 2015). The main methods usually used for thickening and dewatering of microalgae are flocculation (Molina et al. 2003; Pérez et al. 2017), centrifugation (Heasman et al. 2000; Dassey and Theegala 2013) and filtration (Zhao et al. 2017). Although these processes have several advantages, they also have many drawbacks **(Table 2)** which necessitate the development of alternative microalgal recovery techniques, such as dissolved air flotation, fluidic oscillation, EC and others. When EC is employed for microalgae harvesting, the microalgal cells may be recovered by flotation thanks to the hydrogen gas produced at the cathode, neutralization of these negatively charged cells by the produced cations which increases their zeta potential and, thus, the cells come close to each forming aggregates, adsorption onto the produced flocs or by sweeping flocculation by these flocs.

On the other hand, plant extracts which are used in food, pharmaceuticals and cosmetics (Kammerer et al. 2011) are usually recovered either by solvent extraction where costly and sometimes also toxic organic solvents are used (Chairungsi et al. 2006), or by chromatography which uses the same kinds of organic solvents and in which unrecoverable adsorbents are left over (Jumptong et al. 2006). Accordingly, employing EC for harvesting plant extracts could be a successful replacement for the conventional methods used.

In the first part of this review, works carried out by using EC and other electrochemical techniques for the recovery of microalgae are presented. Moreover, the effects of operating parameters, electrical energy consumption and metal (aluminum and iron) content in effluent and biomass are discussed. In the second part, this review highlights studies performed for the recovery and purification of plant extracts using EC.

Table 1. Analysis of the composition and energy potential of terrestrial, 1st generation energy crops, versus microalgae (http://cellana.com/algae-oil/).

Oil source	Biomass (Mt/ha/yr)	Oil content (% dry mass)	Biodiesel (Mt/ha/yr)	Energy content (boe/1000 ha/day)
Microalgae	**140-225**	**35-65**	**50-100**	**1150-2000**
Soya	1-2.5	20	0.2-0.5	3-8
Rapeseed	3	40	1.2	22
Jatropha	7.5-10	30-50	2.2-5.3	40-100
Palm oil	19	20	3.7	63
Mt: metric tons, ha: hectare, yr: year, boe: barrel of oil equivalents				

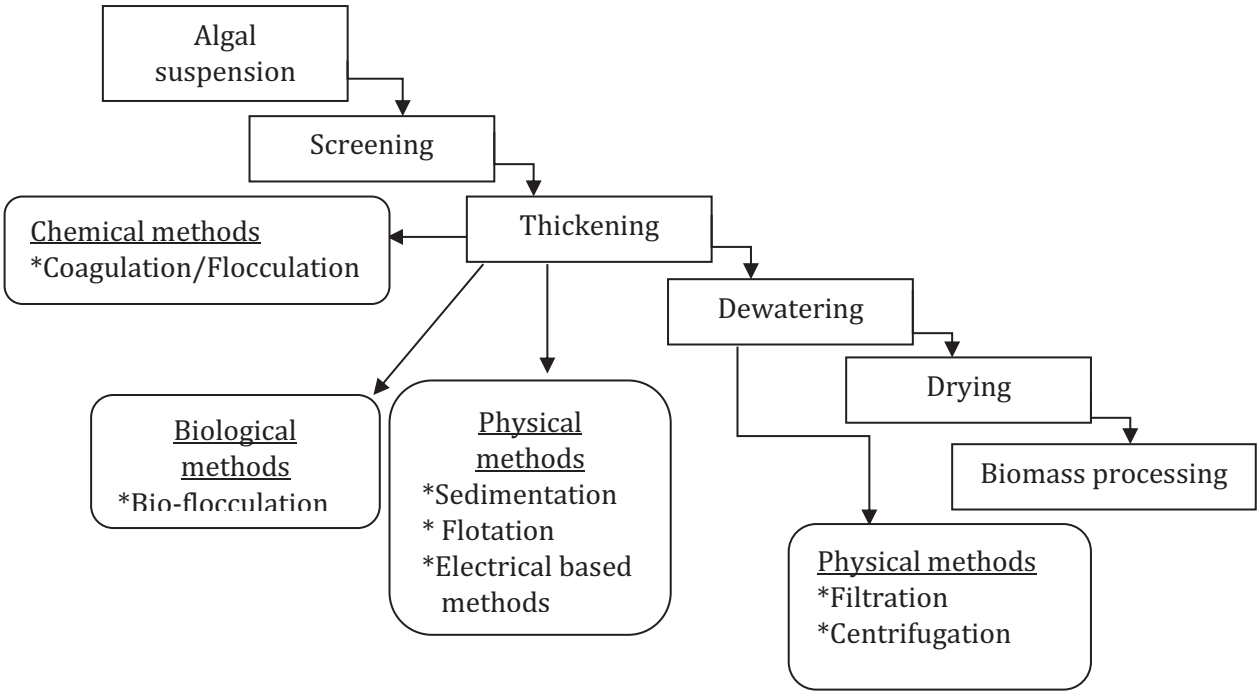

Figure 1. Diagram of microalgae harvesting and drying techniques (Barros et al. 2015).

Table 2. Drawbacks of microalgae harvesting methods.

Harvesting method	Disadvantages	Reference
Chemical flocculation	Chemical contamination Highly dependent on pH Flocculants may be microalgal species Specific Produces large amount of sludge that is difficult to dehydrate	Zhang et al. 2014; Ahmad et al. 2014
Bio-flocculation	High energy input is required	Lam et al. 2012a,b
Centrifugation	High capital and operational costs Cell damage	Christenson and Sims 2011
Filtration	Fouling Slow process Appropriate for large algal cells	Mata et al. 2010
Cross flow membrane filtration	Membrane fouling and clogging	Elcik and Cakmakci 2016; Castrillo et al. 2013
Submerged membrane filtration	Scale-up problems	Bilad et al. 2012
Coagulation-membrane filtration	Coagulants might neutralize or increase membrane surface charge	Lee et al. 2012a,b

2. ELECTROCOAGULATION PROCESS

The electrocoagulation process involves both chemical and physical mechanisms working simultaneously to separate suspended materials from their medium. By using electrolysis, coagulants can be formed via the in-situ dissolution of cations from the reactive sacrificial anode. The charged cations contribute to charge neutralization and destabilize the negatively charged microalgae cells, allowing aggregation and floc formation to occur. The reduction reaction at the cathode generates hydrogen bubbles which enable the resulting flocs to be carried to the surface and form a concentrated layer (Uduman et al. 2010). The commonly used electrode materials are aluminum, iron, stainless steel, mild steel and graphite as they are cheap, readily available and very effective. When aluminum and iron, the most common, are used as anode material, metal ions are released and many ionic monomeric hydrolysis species are formed, depending on the solution's pH. The reactions that take place when using Al and Fe electrodes during EC are summarized in **Table 3** (Khandegar and Saroha 2013).

Table 3. Reactions at Al and Fe electrodes during EC.

	Anode – Oxidation	**Cathode – Reduction**
Al	$Al(s) \rightarrow Al_{(aq)}^{3+} + 3e^-$ (1)	$3H_2O + 3e^- \rightarrow 3/2H_{2(g)} + 3OH^-$ (2)
Overall reaction	$Al^{3+} \rightarrow Al(OH)_n^{(3-n)} \rightarrow Al_2(OH)_2^{4+} \rightarrow Al_3(OH)_4^{5+} \rightarrow Al_{13}$ complex $\rightarrow Al(OH)_3$ (3)	
Fe	$Fe(s) \rightarrow Fe_{(aq)}^{2+} + 2e^-$ (4) $Fe(s) \rightarrow Fe_{(aq)}^{3+} + 3e^-$ (5)	$2H_2O + 2e^- \rightarrow H_{2(g)} + 2OH^-$ (6) $3H_2O + 3e^- \rightarrow 3/2H_{2(g)} + 3OH^-$ (7)
Overall reaction	$Fe_{(aq)}^{2+} + 2OH^- \rightarrow Fe(OH)_{2(s)}$ (8) $Fe_{(aq)}^{3+} + 3OH^- \rightarrow Fe(OH)_{3(s)}$ (9)	

The different steps that occur during EC are as follows (Zodi 2012):

a) Coagulants formation by sacrificial metal electrolytic oxidation;

b) Destabilization of contaminants, suspended solids and breakage of emulsions. This step includes compression of the diffuse double layer around the charged species by the interaction of ions generated by oxidation of the sacrificial anode, charge neutralization (resulting in a zero-net charge) of the ionic species present in the media by counter ions produced by the electrochemical dissolution of the sacrificial anode and floc formation as a result of particle bridging;

c) Aggregation of destabilized phases to form flocs.

Other electrolytic methods may be used for the recovery of microalgae such as, electroflocculation and electroflotation. Electroflocculation is a process by which negatively charged algal cells are attracted to the anode and are electrically neutralized there upon contact. In this process, the anode is both electrically and chemically inert. Neutralized algae come together or self-flocculate to form large aggregates.

Electrocoagulation is differentiated from electroflocculation by the oxidative dissolution of a sacrificial anode, which provides a source of polyvalent metal cations that form large flocs and entrap the algal cells. Both processes can use electrolysis to produce hydrogen gas at the cathode and oxygen gas at the anode. Electroflotation may be a part of EC, *i.e.* it occurs when gas bubbles attach to algal flocs and rise them to the water surface or it might be used as a separate process using non-sacrificial electrodes as titanium. In this case, the aim is to produce gas bubbles that will attach and carry the microalgal cells to the water surface.

3. INFLUENCE OF OPERATING PARAMETERS ON MICROALGAE RECOVERY

Various parameters, such as initial pH, current density, initial concentration, salinity, agitation, electrode material and inter-electrode distance affect recovery efficiency of microalgae. Accordingly, many studies are reported in the literature on these parameters and their effect on recovery efficiency. These parameters are discussed in the following part.

3.1. EFFECT OF INITIAL pH (pH_i)

It is well known that pH is an essential parameter in EC (Mouedhen et al. 2008; Atashzaban et al. 2016), as it determines the speciation of hydroxides in the solution. The net charge of hydroxides is positive at acidic pH and negative at alkaline pH (Duan and Gregory 2003).

Concerning microalgal removal efficiency, Gao et al. (2010) found that electrocoagulation-flotation (ECF) with aluminum electrodes exhibited a higher removal efficiency under the pH_i of 4–7 when compared to that under 7–10. These results were consistent with those of Vandamme et al. (2011) who reported that for harvesting the freshwater microalgal species *Chlorella vulgaris* and the marine species *Phaeodactylum tricornutum* using aluminum electrodes, the efficiency of the process decreased with increasing pH. This pH influence was more pronounced with *Phaeodactylum tricornutum* than with *Chlorella vulgaris*. These results are explained by the fact that under alkaline conditions, the formation of the negatively charged aluminum hydroxide $Al(OH)^-_4$ is promoted. This species does not react with the negatively charged microalgal cells. However, under acidic conditions, the formation of positively charged monomeric aluminum hydroxides, or polymeric aluminum hydroxide cations is favored (Mollah et al. 2001). These aluminum species react with the negatively charged surface of the microalgal cells and are able to destabilize the microalgal suspension by charge neutralization. Under these conditions, coagulation–flocculation of microalgal cells is probably mostly due to sweeping coagulation–flocculation by the insoluble aluminum hydroxide $Al(OH)_3$ (Vandamme et al. 2011).

In another study performed by Golzary et al. (2015), results depicted that a decrease of pH from 6 to 5 or an increase from 8 to 9 led to 4% and 2% decrease in microalgae harvesting efficiency, respectively at a constant time and current density. However, with any given combination of time and current density, pH 6 provided the highest recovery efficiency. Kim et al. (2012b) investigated the influence of three pH_i values (4, 6 and 8) on microalgae recovery efficiency, it was revealed that pH_i 8 yielded the highest mean recovery efficiency within the first 5 minutes of operation. However, after 5 minutes, the mean recovery efficiency converged on a value of 93% at all tested pH_i values. It was also found that the amount of settled microalgal flocs declined as pH increased.

On the contrary, Uduman et al. (2010) who worked on the recovery of the two marine microalgae species, *Chlorococcum sp.* and *Tetraselmis sp.* neglected the effect of pH on microalgae recovery efficiency. This result may be linked to the high salinity of water. Finally, this highlights that the influence of pH_i is far from being understood and strongly depends on the culture media.

3.2. EFFECT OF CURRENT DENSITY

Current density determines the coagulant dosage rate, bubble production rate, size and growth of the flocs, which have immense effects on the effectiveness of EC (Katal and Pahlavanzadeh 2011), and thus is one of the crucial factors in electrochemical processes. Optimal recovery higher than 80% of the fresh water species *Chlorella vulgaris* was obtained with EC at a run time of 30 min and current density 3 mA/cm^2 (Vandamme et al. 2011). A more efficient recovery efficiency of the microalgae *Desmodesmus subspicatus* of 95.4% was obtained by electroflotation with aluminum electrodes at a shorter run time of only 20 minutes and with a current of 3 A (Baierle et al. 2015). Even a higher harvesting efficiency of 96% was obtained with a continuous electrolytic microalgae (CEM) harvest system where the run time needed was shortened with the increase of current (15 min at 0.25 A, 10 min at 0.5 A and 5 min at 0.75 A), with no increase in recovery efficiency beyond 96% for longer times at all three currents used (Kim et al. 2012a).

However, a better performance at higher current density was reported by Golzary et al. (2015). For instance, when current density increased from 6.59 mA/cm^2 to 23.41 mA/cm^2, microalgae recovery efficiency increased from 65% to approximately 91%. Similar results were reported by Gao et al. (2010) who found that the higher the current density was, the faster the electrocoagulation-flotation treatment for algae removal was. For example, 25 min was demonstrated to be enough for complete removal at the current density of 5 mA/cm^2; while 45 min was needed at 1 mA/cm^2. The higher efficiency and faster microalgae harvesting at higher current densities could be explained according to Faraday's law:

$$W = ItM/nF \quad (10)$$

where W is the dissolved electrode mass in grams, I the electric current in ampere, t the electrolysis time in seconds, M the molecular weight of a given metal in grams per mole, n the number of electrons exchanged in the electrode surface and F Faraday's constant (F = 96,487 C/mol).

Based on Faraday's law, electric current density has a direct effect on the anode dissolution rate, which has a significant effect on EC process performance. As the electric current density increases the amount of coagulant ions and, consequently, microalgae recovery rate increases. On the other hand, current density determines the speed and the amount of hydrogen gas produced. The higher the hydrogen production rate and, the greater the amount of algal cells rise to the water surface, and thus recovered. As a conclusion, current emerges as the key operating parameter of the EC harvesting process.

3.3. EFFECT OF INITIAL CONCENTRATION

It is significant to assess the influence of microalgal initial concentration, as this concentration varies with species and culture media. Usually, recovery efficiency decreases with the increase in initial concentrationat constant current, as metallic cations will not be enough for harvesting all the microalgal cells. Zhang et al. (2014) reported that the microalgal recovery efficiency decreased significantly from 98.7% to 4.49% when the cell density increased from 0.24 g/L to 1.10 g/L. Similar results were reported by Gao at al. (2010). In practice, due to their culture condition, microalgae concentration often remains below 1 g/L. This is favorable to EC in terms of harvesting efficiency, but not in terms of the cost of algal lipid (Coons et al. 2014).

3.4. EFFECT OF SALINITY

Salinity of the solution has a direct effect on its conductivity, which is a key parameter in electrolysis process, as it affects the microalgae harvesting efficiency and EC operating cost. This effect originates from the influence of conductivity on ohmic drop, as shown in the following equation:

$$IR = I.d/A.\kappa \quad (11)$$

where I is the current (A), d is the inter-electrode distance (m), A is the active anode surface (m^2), κ is the specific conductivity (S/m). The solution must have some minimum conductivity for the flow of the electric current (Khadengar and Saroha 2013). Current density increases as conductivity of the solution increases at constant cell voltage or cell voltage decreases at constant current density (Kashefialasl et al. 2006). In a study conducted by Uduman et al. (2011), it was found that the percentage of microalgal recovery decreased as the salinity of the microalgae culture decreased. Similar results were reported by Lal and Das (2016), who found that increasing NaCl concentration from 0.5 g/L to 1 g/L reduced the

time required to attain more than 95% recovery efficiency, from 30 min to 15 min. As a result, the performance of the EC harvesting process strongly depends on the culture medium, which means that the composition of culture media must be optimized not only for enhancing microalgae productivity, but also microalgae harvesting.

3.5. EFFECT OF AGITATION

Agitation helps to maintain uniform conditions and to avoid the formation of concentration gradient in the electrolysis cell. Moreover, agitation in the electrolysis cell enhances momentum and species transport, in particular for the generated ions (Modirshahla et al. 2008). With respect to microalgae recovery, agitation improves the recovery efficiency by enhancing contact rates between the coagulants and the microalgal cells (Mollah et al. 2004). Several studies reported on the influence of agitation during EC. For instance, Ilhan et al. (2008) reported that mechanical mixing interfered with the formation of microalgal flocs, and hence increased electricity consumption. Kim et al. (2012b) noted that mechanical mixing of the solution affects the CEM harvest system operated with PE (polarity exchange) at two currents: 0.25 and 0.5 A. Their results indicated that recovery efficiency was 7% greater at 0.25 A with mechanical mixing. In contrast, there was no noticeable effect of mechanical mixing on the mean recovery efficiency at 0.5 A.

Maleki et al. (2014) noted in a series of experiments at current 1 A, inter-electrode distance 1 cm and operating time of 20 minutes, that by increasing agitation speed from 0 to 200 rpm, the microalgae harvesting efficiency increased from 91% to 97%. However, further increase in the speed till 400 rpm decreased recovery efficiency from 97% to 94%. In another series of experiments conducted by the same authors at current 0.3 A and operating time of 5 minutes, results depicted that increasing stirring speed from 0 to 200 rpm increased recovery efficiency from 49% to 55%, but further increase in the speed till 400 rpm decreased recovery efficiency to 52%. It can be concluded that up to 200 rpm stirring speed, mixing enabled clotted material to come closer to each other slowly and create larger particles, that could easily float or sediment; however, when increasing speed to 400 rpm, coagulated material was either not able to flocculate the microalgae or was broken after formation.

A better recovery efficiency was demonstrated by Vandamme et al. (2011), where the increase in stirring speed from 0 to 60 and 150 rpm, reduced the time required to achieve destabilization of the microalgal suspension by almost a factor of two. However, at the maximum stirring speed of 200 rpm, the time required to achieve destabilization increased again. This highest stirring rate probably caused break-up of microalgal flocs due to the high shear forces applied, resulting in a longer time needed to achieve a similar recovery efficiency.

However, the main weakness of all these works is that agitation conditions are never related to the EC cell geometry and to dimensionless parameters, such as the Reynolds number, which reduces their interest for scale-up purpose.

3.6. EFFECT OF ELECTRODE MATERIAL

Electrical-based methods are strongly influenced by the electrode material. Aluminum and iron are the most commonly used metals in such type of process (Zayed and Bellakhal 2009; Llanos et al. 2014). In most research studies, aluminum electrodes were more efficient than iron ones in term of harvesting efficiency. The lower efficiency of the iron electrodes is probably due to the lower current efficiency generated by iron electrodes when compared to aluminum electrodes (Cañizares et al. 2006). Moreover, iron hydroxides are relatively inefficient coagulants compared to aluminum hydroxides (Emamjomeh and Sivakumar 2009). **Table 5** summarizes some of the works which compare the efficiency of Al and Fe electrodes. These works are presented in chronological order by the date of their publication (from the oldest to the newest).

Table 5. Comparison of aluminum and iron efficiency during EC applied to microalgae harvesting under the same experimental conditions.

Electrode material	Recovery efficiency (%)	Reference
Al	100	Gao et al. 2010
Fe	78.9	
Al	~ 80	Vandamme et al. 2011
Fe	~ 0	
Al	91-97	Maleki et al. 2014
Fe	70-86	
Al	95.4	Baierle et al. 2015
Fe	64.7	

The electrode material also has a significant effect on the time needed to reach the highest recovery efficiency. In a study conducted by Bleeke et al. (2015), a time duration of 7.3 min, 9.0 min, 14.2 min, 14.6 min, 30.9 min and 46.9 min was required to reach 90% recovery efficiency with magnesium, aluminum, zinc, copper, brass and iron, respectively. Kim et al. compared the efficiency of two electrode pairs (1) aluminum and dimensionally stable anode (Al–DSA), and (2) Al–platinum (Al–Pt). Their results demonstrated that the pair Al–DSA exhibited better performance than Al–Pt, as it led to less cell damage and was less expensive (Kim et al. 2012a). However, even the cost of many DSA electrodes does not comply with the economic constraints of microalgae harvesting in comparison to Al or Fe electrodes.

3.7. EFFECT OF INTER-ELECTRODE DISTANCE (d)

The inter-electrode distance is another variable which may have an influence on the efficiency of EC, as it affects the ohmic drop as shown previously by equation 11. When the distance increases, the faradaic yield, which is the result of dividing the experimental anode mass loss over the theoretical mass loss, decreases. Consequently, the amount of metal getting dissolved into the solution is reduced (Attour et al. 2014). Consequently, the microalgal recovery efficiency decreases at higher inter-electrode distance. Another possible explanation for the higher recovery efficiency at lower inter-electrode distance is that low inter-electrode distances result in an electric field with high potential gradient and low resistance to motion of ions. This results in a faster formation of aluminum hydroxide species and in faster collision of precipitate particles with microalgal cells and H_2 bubbles (Hakizimana et al. 2016).

Some data are available in the literature on the effect of inter-electrode distance on microalgae harvesting efficiency using different electrochemical methods. However, due to the absence of a common tested microalgal species and cell concentration, it is complicated to make a strict and clear comparison among these results. Literature data can be summarized as follows. Concerning harvesting efficiency, Valero et al. (2015) who evaluated the biomass separation of the microalgal species *Desmodesmus subspicatus* by electroflotation with a spiral-shaped electrode using aluminum or iron tubes, found that inter-electrode distance of 5.5 cm was 2.61% more effective than the inter-electrode distance of 7 cm, and 3.15% than 11 cm distance. A similar result was reported by Maleki et al. (2014) who found that the electrode gap has positive linear effect and negative quadratic effects on the recovery efficiency. When ECF was conducted with aluminum electrodes, stirring speed of 200 rpm, current intensity of 1 A and ECF time of 20 minutes, increasing electrode gap from 1 to 2 cm decreased the recovery efficiency from 97% to 95% and with increasing electrode gap to 3 cm, the recovery efficiency was reduced to 85%. When ECF was carried out at current intensity of 300 mA, while fixing the other conditions (aluminum electrodes, stirring speed of 200 rpm and ECF time of 20 minutes), it was observed that by increasing the electrode gap from 1 to 2 cm, the recovery efficiency has decreased from 92% to 89%, and with increasing the inter-electrode distance to 3 cm, the recovery efficiency has decreased to 79%.

In practice, it emerges that there is, probably, an optimum distance between electrodes to maximize microalgae harvesting. However, this distance must also account for hydrodynamics and the ease of maintenance when sacrificial electrodes must be changed, even though these aspects are seldom accounted for in the literature.

4. ELECTROCHEMICAL STUDIES FOR MICROALGAE RECOVERY

Various environment friendly electrical approaches and methods combinations are employed for microalgae harvesting (Uduman et al. 2010). The two most used techniques for harvesting both freshwater and marine microalgae are electroflocculation and electrocoagulation processes. **Table 4** summarizes works carried out on microalgae recovery using electrical-based methods, in the chronological order of their publishing date (from the oldest to the newest). In the works summarized in this table, the tested parameters are as follows: Initial pH (pH_i), initial concentration (C_i), volume (V), current (I), current density (J), U (voltage), frequency (F), height of the culture column (H), stirring speed (SS), inter-electrode distance (d), temperature (T), optical density (OD), time (t), and electrode material (Al – Aluminum, Fe – Iron, C – Carbon, Ni – Nickel, Pt – Platinum, Pb – Lead, Mg – Magnesium, DSE – Dimensionally stable electrode).

As seen in **Table 4**, electrochemical methods were successfully used for harvesting different microalgal species; however, there is a lack of common reliable operating conditions, which is an obstacle in the way of scale-up. Moreover, most of the studies are, unfortunately, carried out in the batch mode, which raises the question about their benefit. In conclusion, despite the high potential of EC for microalgae harvesting that emerges from **Table 4**, industrial application remains in the future because the design and scale-up methodology for continuous EC harvesting process is still to be established.

Table 4. Summary of works carried out on microalgae recovery using electrical based methods.

Microalgae or Effluent	Process	Electrode Material	Experimental set-up	R (%)	Ref
Coelosphaerium sp., Aphanizomenon sp., Closterium sp., Pediastrum sp., Cryptomonas sp., Staurastrum sp., Asterionella sp., Cyclotella sp., Melosira sp.	Electrolytic flocculation in batch	Pb-Al	pH_i 8; V = 100 L; C_i = 2.7 - 36.1 mg/L; I = 4 A; U = 85 V; d = 18.5 cm	>90	Poelman et al. 1997
Botryococcus brauni	Electroflocculation in batch integrated with dispersed-air flotation	Al	pH_i 11; V = 0.6 L; C_i = 1.6 g/L; I = 0.101 A; U = 60 V; d = 10 cm; t = min	98.9	Xu et al. 2010
Microcystis aeruginosa	Electrocoagulation flotation in batch	Al	pH_i 4 - 7; V = 1 L; $C_i = 0.55\times10^9$-1.55×10^9 cells/mL; J = 1 mA/cm^2; SS = 200 rpm; T = 18 - 36 °C	100	Gao et al. 2010
Chlorococcum sp. (Chlor) and Tetraselmis sp. (Tetr)	Electrocoagulation in batch	Stainless steel	pH_i 9.1 and 8.3 for *Chlor* and *Tetr*, respectively; V = 0.3 L; C_i = 0.6 g/L and 0.3 g/L for *Chlor* and *Tetr*, respectively; U = 10 V; d = 4.8 cm; t = 15 min	*Chlor* 98 *Tetr* 99	Uduman et al. 2011
Chlorella vulgaris	Electro-coagulation-flocculation in batch	Al	pH_i 8; V = 1 L; C_i = 0.3 - 0.6 g/L; J = 3 mA/cm^2; no stirring; t = 20 min	92	Vandamme et al. 2011
Phaeodactylum tricornutum	Electro-coagulation-flocculation in batch	Al	pH_i 8; V = 1 L; C_i = 0.3 - 0.6 g/L; J = 3 mA/cm^2; no stirring	72	Vandamme et al. 2011
Nannochloris oculata	Continuous microalgae recovery using electrolysis	Al-Pt	pH_i 8.3; C_i = 1g/L; I = 0.25 A; SS = 150 rpm; T = 25 ± 1°C; t = 15 min	>99	Kim et al. 2012a
Nannochloris oculata	Continuous microalgae recovery using electrolysis	Al-DSE	pH_i 8.3; C_i = 1g/L; I = 0.25 A; SS = 150 rpm; T = 25°C ± 1°C; t = 10 min	99.9	Kim et al. 2012a
Nannochloris oculata	Continuous microalgae recovery using electrolysis with polarity exchange	Al-DSE	pH_i 8; C_i = 1g/L; I = 0.25 A; SS = 150 rpm; T = 25°C; t = 15 min	95.8	Kim et al. 2012b
Tetraselmis sp.	Electroflocculation in batch	Al	pH_i 8.4; $C_i = 149.5\times10^4$ cells/mL; I = 9.9 A; U = 5.3V; SS = 20 rad/s; T = 22°C; t = 0.5 min	92	Lee et al. 2013
Tetraselmis sp.	Electroflocculation in batch	Al	pH_i 8.4; $C_i = 135.5\times10^4$ cells/mL; I = 9.9 A; U = 5.2 V; SS = 20 rad/s; T = 22°C; t = 1 min	95	Lee et al. 2013
Chlorella vulgaris	Electrocoagulation in batch	Al	V = 0.5 L; C_i = 2.5 g/L; J = 33.3 mA/cm^2; SS = 150 rpm; d = 1 cm; t = 30 min	88.7	Matos et al. 2013b
Dunaliella Salina		Al	$C_i = OD_{680}$ of 0.333; V = 300 mL; J = 90 A/m^2;	97.44	Zenouzi et al. 2013

	Electroflocculation in batch		SS = 100 rpm ; d = 1 cm; t = 3 min		
Desmodesmus subspicatus	Electroflotation in batch	Al	pH_i 5.70 ± 0.15; $C_i = 1.84\times10^7$cells/mL; J = 5.6 mA/cm^2; t = 15 - 20 min	66-95.4	Baierle et al. 2015
Desmodesmus subspicatus	Electroflotation in batch	Fe	pH_i 5.70 ± 0.15; $C_i = 1.84\times10^7$cells/mL; J = 5.6 mA/cm^2; t = 15 - 20 min	64.7-89.3	Baierle et al. 2015
Dunaliella Salina	Electro-coagulation-flocculation in batch	Al	I = 999 mA; SS = 222 rpm; d = 1.39 cm; t = 20 min	98.06	Maleki et al. 2014
Chlorella vulgaris	Electro-coagulation-flotation in batch	Al	pH_i 8; V = 0.65 L; C_i = 0.48 g/L; J = 2.08 mA/cm^2; SS = 50 rpm; d = 2 cm; t = 20 min	99.2	Zhang et al. 2014
Chlorella, Chloroccum, Chlamydomonas	Electroflocculation in batch	Al	pH_i 6.5; V = 0.2 L; C_i = 0.4 g/L; U = 5 V; d = 3 cm; t = 30 min	>90	Udhaya et al. 2014
Pond wastewater from Fortaleza, Ceará, Brazil	Electroflotation in batch	Non sacrificial steel	V = 2.9 L (reactor 1) and 40 L (reactor 2); F = 1.56 kHz; d = 0 .5 cm; t = 140 min	99	de Carvalho Neto et al. 2014
Scenedesmus sp. (24%) *Kirchneriella sp.* (1%) *Microcystis sp.* (75%)	Electroflocculation in batch	Fe	$C_i = 10^6$ cells/mL; U = 10 V; H = 4 cm; d = 5.5 cm; T = 22°C; t = 1 min	95	Valero et al. 2015
Chlorella sp.	Electro-coagulation–flotation in batch	Al	pH_i 6; V = 1.28 L; C_i = 0.82 mg/L; J = 1.6 mA/cm^2; d = 1 cm; t = 17.65 min	96.8	Golzary et al. 2015
Scenedesmus obliquus	Electrochemical harvesting in batch	Non-sacrificial carbon	pH_i 9; V = 0.9 L; C_i = 2.4 g/L; I = 1.5 A; U = 4.6 V; [NaCl] = 6 g/L; d = 3 cm; t = 60 min	83	Misra et al. 2015
Scenedesmus acuminatus	Electroflocculation in batch	Mg	pH_i 7-8; V = 0.09 L; $C_i = 1\times10^7$ cells/mL; U = 40 V; SS = 100 rpm; d= 2.5 cm; t = 7.3 min	90	Bleeke et al. 2015
Ankistrodesmus falcatus	Electrochemical harvesting in batch	C	pH_i 8; V = 1 L; C_i = 2.88 g/L; I = 1 A; d = 3 cm; t = 30 min	91	Guldhe et al. 2016
Nannochloropsis sp.	Continuous electro-coagulation–flocculation	Ni	pH_i 7.5; C_i = OD of 1.4; U = 7 V; d = 0.635 cm; Flow rate = 0.4 L/min; t = 30 min	92	Shuman et al. 2016
Chlorella (Chlor), Synechocystis (Synec)	Electroflocculation in batch	Stainless steel	pH_i 6 – 7; V = 0.4 L; C_i = 1.5 g/L; J = 1.66 mA/cm^2; U = 12 V; SS = 150 rpm; [NaCl] = 1 g/L; d = 4 cm; t = 15 min	*Chlor* 95-98 *Synec* 96	Lal and Das 2016

5. EFFECT OF ELECTROCHEMICAL METHODS ON MICROALGAL LIPID CONTENT

To be deemed successful, any employed microlalgal harvesting technique must not affect the lipid content and should not hamper the extraction techniques that follow the recovery. Also, it should not significantly modify the lipid profile, for example by oxidizing unsaturated fatty acids. The studies which investigated the lipid profile after microalgae harvesting are rare in the literature. Misra et al. (2015) who investigated the harvesting of *Chlorella sorokiniana* and *Scenedesmus obliquus,* reported that ECF did not affect lipid content in both microalgal species. In their work, the lipid content after ECF, was kept at 12% and 15% dry cell weight for *C. sorokiniana* and *S. obliquus*, respectively. As a result, more work is needed to confirm that EC does not impair the lipid profile and, consequently, the quality of algal biofuel, even though the electric field in EC should not be intense enough to affect intracellular materials.

6. ENERGY CONSUMPTION

Energy consumption during the recovery of microalgae is an essential element that determines the future applicability of the process involved in microalgae harvesting. In current microalgal production systems for high value applications, centrifugation is the most commonly used technology for harvesting microalgae (Vandamme et al. 2011), where the electrical energy consumption of conventional centrifugation has been estimated at 8 kWh/m^3 of microalgal suspension (Danquah et al. 2009). At the same time, it is worth noting that harvesting microalgae by electrochemical based methods were found to consume less energy than centrifugation. **Table 6** compares the energy expenditure of different methods used for microalgae harvesting to electrochemical methods. The works in this table are depicted in chronological order by the date of publication (from the oldest to the newest).

Coons et al. (2014) reported that the operating cost for microalgal recovery under continuous flow conditions by electrochemical methods is a function of the ratio of electric current to algal water flow rate (I/Q) and on the initial biomass concentration, as shown in **Figure 2**. The I/Q parameter in the continuous mode corresponds to the q/V parameter in the batch mode where q=It is charge loading, V the volume of the EC cell and t the electrolysis time. **Figure 2** shows a large discrepancy in the I/Q values, from 10 to 400 Ah/m^3, which cannot be explained only by differences in microalgae species and concentrations, which confirms that the design of EC cells for microalgae harvesting is far from being mature.

Table 6. Energy expenditure of different methods used for microalgae harvesting

Harvesting Process	Energy expenditure (kWh/m^3)	Reference
Electrolytic flocculation	0.3	Poelman et al. 1997
Filtration (pressurized)	0.88	Semerjian and Ayoub 2003
Centrifugation	8	Molina et al. 2003
Gravity sedimentation	0.1	Shelef et al. 1984
Vaccum filtration	5.9	Molina et al. 2003
Filtration	0.4	Semerjian and Ayoub 2003
Electroflotation	5	Azarian et al. 2007
Polymer flocculation	14.81	Danquah et al. 2009
Tangential flow filtration	2.06	Danquah et al. 2009
Electrocoagulation-flotation	0.4	Gao et al. 2010
Electrocoagulation	1.3 -5.5	Uduman et al. 2011
Electroflocculation	0.621	Zenouzi et al. 2013
Electroflocculation-flotation	0.16	Lee et al. 2013
Electrocoagulation	0.06 - 1	Matos et al. 2013b
Electrocoagulation-flotation	0.022 - 0.134	Golzary et al. 2015
Electrochemical harvesting	9.2	Misra et al. 2015
Electrochemical harvesting	7.9	Guldhe et al. 2016
Electrocoagulation-flocculation	0.08 - 6.43	Shuman et al. 2016

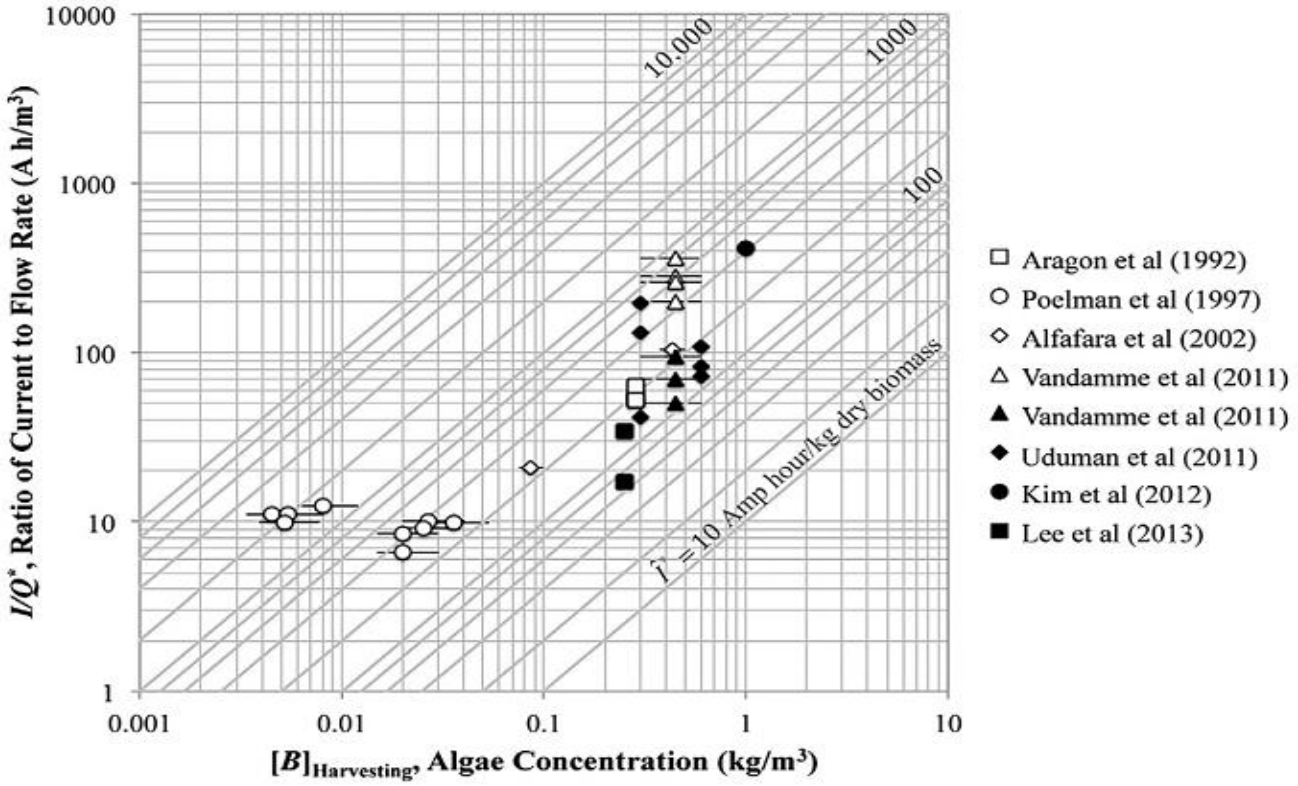

Figure 2. A survey of conditions applied for the removal of algae from water using electrolytic separation technologies. Open and closed symbols represent freshwater and marine species of algae, respectively.

In practice, many other parameters can explain these discrepancies. Different studies in the literature investigated the influence of electrode material and changing the range of tested variables on the energy expenditure of EC and other electrochemical methods used for microalgae harvesting. First, a study conducted on harvesting the freshwater microalgae (*Chlorella vulgaris*) and the marine microalgae (*Phaeodactylum tricornutum*) by electro-coagulation-flocculation, reported that the minimal electrical energy consumption per unit of microalgal biomass recovered was much lower when lower current densities were used. For *Chlorella vulgaris*, 0.59 kWh/m^3 recovered microalgae was consumed at a current density of 1.5 mA/cm^2, while 4.27 kWh/m^3 recovered microalgae was consumed at 6 mA/cm^2. For *Phaeodactylum tricornutum*, the difference was smaller, with 0.09 kWh/m^3 recovered microalgae consumed at 0.6 mA/cm^2, and 0.18 kWh/m^3 recovered microalgae was consumed at 3 mA/cm^2 (Vandamme et al. 2011). Similar results were obtained with Gao et al. (2010), where energy consumption increased dramatically from 0.20 to 2.28 kWh/m^3 as current density varied from 0.5 to 5.0 mA/cm^2. The results of Guldhe et al. (2016) who harvested microalgae electrochemically using non-sacrificial carbon electrodes followed the same trend, as increasing current from 0.5 to 1.5 A increased energy consumption from 2.42 to 10.43 kWh/m^3.

Similarly, the influence of water properties could also explain these discrepancies. Concerning the influence of pH on energy consumption during EC for microalgae recovery, a study carried out by Gao et al. (2010) showed that when initial pH (pH_i) varied in the range of 4–7, the energy consumption was constant at the level of about 0.3 kWh/m^3. However, as the pH_i further increased from 7 to 9, the electrolysis time required for complete microalgal removal increased from 45 to 75 min correspondingly, which led to an increase of energy consumption from 0.3 to 0.53 kWh/m^3. On the other hand, a similar energy consumption was noted for pH_i values of 9 and 10 (0.53 kWh/m^3 *vs.* 0.60 kWh/m^3), mainly due to the same electrolysis time of 75 min required for complete microalgae removal. In another study on the effect of pH on energy expenditure, Zhang et al. (2014) who investigated the influence of pH_i in the range of 5-9, reported that the lowest energy consumed (0.15 kWh/m^3) was achieved at pH_i 5. When testing the effect of salt addition on energy consumption during the electrochemical recovery of microalgae, Misra et al. (2015) concluded that adding 6 g/L of NaCl when working at current 1.5 A decreased energy consumption from 21.29 to 8.12 kWh/m^3.

Concerning the influence of inter-electrode distance d on energy expenditure, Zenouzi et al. (2013) who harvested the microalgae *Dunaliella Salina* found that energy expenditure increased from 0.13 to 0.23 kWh/m^3 upon increasing the inter-electrode distance from 1 to 4 cm. In another work, Lee et al. (2013) who tested the influence of inter-electrode distance in the range of 5 – 30 cm, reported that the energy consumption was approximately flat up to a d value of 15 cm followed by a steady increase.

Other works depicted that the electrode material had a strong influence on energy consumption. Zenouzi et al. (2013) reported that when switching from Fe to Al electrodes, the energy expenditure decreased from 0.765 to 0.621 kWh/m^3. Another study on the effect of electrode material on the energy consumption using electrolysis with polarity exchange for the continuous recovery of the microalgae *Nannochloris oculata,* found that energy consumption was 1.19 kWh/m^3 when the electrode pair Aluminum-Platinum (Al-Pt) was tested; however, this energy expenditure was higher (1.23 kWh/m^3) with the electrode pair Aluminum-Dimensionally stable anode (Al-DSA) (Kim et al. 2012a).

Another author suggested that combining different recovery methods could lower the energy consumption. In fact, combining electroflocculation with mixing and settling, in harvesting the microalgae *Tetraselmis sp.* lowered energy consumption from 0.16 kWh/m^3, which was obtained with electroflocculation followed by flotation to 0.09 kWh/m^3 (Lee et al. 2013).

Finally, it appears that for minimizing energy consumption and assessing the economic viability the EC harvesting process, only an optimization procedure involving all these parameters for a defined culture medium and microalgae concentration range seems possible at the moment.

7. RECOVERY OF PLANT EXTRACTS USING ELECTROCOAGULATION

The recovery of plant extracts is usually carried out by a complicated procedure using expensive solvents. Over the past years, EC was used, alone or coupled to other techniques, as an alternative method for plant extracts recovery. As for microalgae, this constitutes a rather original use of EC that was designed, first, to remove pollutants from water and not to harvest or recover molecules and products of interest. In these studies, EC was first applied to plant extracts, and then, it was usually followed by more steps which included extraction using solvents to obtain the pure form of the targeted biomolecule. **Table 7** summarizes most of these studies. The main points of the works are reported in the table in the chronological order of their publication (from the oldest to the newest).

Table 7. Electrocoagulation studies for the recovery of plant extracts. Al – aluminum, Fe – iron, d – inter-electrode distance, NaCl – Sodium chloride, DC – direct current, t – electrolysis time, V – treated solution volume.

Treated solution	Experimental conditions and procedure	Result	Reference
Aqueous bark extracts of five plants: *Lithocarpus elegans, Quercus kerrii, Quercus brandisiana, Quercus kingiana and Castanopsis armata*	EC : Al, t = 60 min, d = 3 cm, V = 800 mL, DC current (2.0 A, 16 V), 1.6 g NaCl After EC, the mixture was filtered and dried, dissolved in acid and then extracted with alcohol which was finally evaporated	- Recovery between 59% and 95% of the crude extract - An enrichment between 0% and 48% of the phenolic substances in the recovery extract (exposed to EC) compared to the crude extract - The recovery extracts, except that of *Castanopsis armata* showed more activity than the crude extracts - Poor correlation between the degree of tannin enrichment and antioxidant activity increases - In the case of *Castanopsis armata*, the recovery extract contained equal amount of tannin as the crude extract (73%); the antioxidant activity of the former decreased 44% compared to that of the latter	Chowwanapoonpohn et al. 2003
Aqueous alcoholic synthetic solutions of tannin and morin (aqueous ethanol concentrations used were 25%, 50%, 75% or 85% v/v)	EC: Al, t =120 min, d = 3 cm, V = 250 mL, DC current (0.3 A), 0.5 g NaCl	-At a concentration of 0.1% tannin in 85% ethanol, the solution was almost completely detannized within 15 minutes - At a concentration of 1.0% tannin, complete detannization needed 80 minutes - In the case of morin: as the water in the solvent decreased (or the alcohol increased), coagulation efficiency decreased proportionally	Chairungsi et al. 2006a
Aqueous β-carotene alcoholic synthetic solution Crude chlorophyll extract from *Spinach oleracea* (extracted with 75 or 85% ethanol)	EC: Al or Fe, t = 120 min, d = 1.5 cm, V = 200 mL, DC current (0.9 A, 16.9-31.6 V), 0.2 g NaCl	- β-carotene was hardly affected by EC with both Al and Fe electrodes - In the case of chlorophyll, coagulation was less efficient as the water content in the solvent decreased	Chairungsi et al. 2006a
Alcoholic synthetic solutions of the following quinones: alizarin, purpurin, chrysazin, emodin, anthrarufin and plumbagin	EC: Al, V = 250 mL, t = 120 min, d = 3 cm, DC current (0.3 A, 24-31 V), 0.5 g NaCl	- The two most rapidly and completely coagulated quinones were alizarin and purpurin - Chrysazin and emodin were coagulated less completely and more slowly than the first two ones - Anthrarufin and plumbagin which were barely coagulated	Chairungsi et al. 2006b

Aqueous alcoholic extract of the roots of *Plumbago rosea*	EC: Al, t = 120 min, d = 3 cm, DC current (2.0 A, 12 V), 0.2% NaCl After EC, the mixture was filtered and re-electrolyzed, refiltered, distilled and extracted	- 0.49 g of pure plumbagin were obtained (0.54 % yield) - The obtained plumbagin was identical to authentic plumbagin	Chairungsi et al. 2006b
Aqueous alcoholic extract of the roots of *Morinda angustifolia*	EC: Al, t = 30 min, d = 1.5 cm, DC current (1.7 A, 30V), 0.1% NaCl After EC, the mixture was filtered and dissolved in acid and then extracted with alcohol which was finally evaporated	- 2.72 g of morindone were obtained - The obained morindone was identical to authentic morindone	Chairungsi et al. 2006b
Aqueous alcoholic extract of seedlac	EC: Al, t = 60 min, d = 3 cm, DC current (0.3 A, 22-27 V), 0.2% NaCl After EC, the mixture was filtered and the filtrate was evaporated. The residue was dissolved in ethanol followed by filtration and evaporation.	- 0.37 g of erythrolaccin were obtained - The obtained erythrolaccin was not identical to the authentic erythrolaccin	Chairungsi et al. 2006b
Aqueous alcoholic extracts of the leaves of the following plants *Stevia rebaudiana (stevia), Cassia siamea, Solanum laciniatum, Andrographis paniculata and Centella asiatica*	EC: Al or Fe, t =120-150 min, d = 1.5 cm, V = 200 mL, DC current (0.9 A, 16.9-31.6 V), 0.1% NaCl. After EC, the mixture was filtered to afford a colorless solution.	- Dechlorophyllation by EC was more efficient than the conventional solvent fractionation - Solasodine was obtained at a yield of 1% - The yield of bioactive lactone in the crude extract was 38% - Asiaticoside was obtained at a 4% yield in the crude extract	Jumpatong et al. 2006
Synthetic solutions of the following alkaloids: caffeine, capsaisin, reserpine, ajmaline and arecoline	EC: Al, t = 120 min, d = 3 cm, V = 200 mL, DC current (0.2-2.6 A, 19-31 V), 0.4 g NaCl	The alkaloids remained in the electrolyzed solution.	Phutthawong et al. 2007
Aqueous alcoholic extracts of dry tea leaves, dry tobacco leaves, dry black pepper fruits, areca nuts, fruits of *Capsicum frutescens* and roots of *Rauvolfia serpentina*	EC: Al or Fe, t = 30 – 150 min, d = 1.5 – 3 cm, DC current (up to 8 A and 31 V), 0.2% NaCl After EC, the mixture was filtered followed by evaporating the solvent and dissolving it in a little non-aqueous solvent	- Caffeine was extracted from tea in a purer form but in lower yield (0.4 vs. 0.7%), than that obtained by a classical laboratory procedure. - Capsaicin and dihydrocapsaicin were isolated from red chili at a yield of 0.4%. - Resperine and ajmaline were isolated from the roots of *Rauvolfia serpentina* at a yield of 0.1% and 0.8%, respectively.	Phutthawong et al. 2007

It is also worth noting that in some cases, flocs formed a gel at the end of EC, which was used for subsequent extraction steps. An example is applying the adsorption step onto aluminum hydroxide gel produced by EC as a clarification stage in downstream processing of tobacco leaf extracts (Phutthawong

et al. 2007). Results have shown high removal efficiencies of chlorophyll and phenolic compounds from extracts while losing only a small fraction of proteins. But the process was most efficient in removing proteins with acidic isoelectric point (pI below 6.03), independently of EC pH. In addition to that, the removal efficiencies of proteins with acidic pI were higher at lower EC pH, whereas the removal efficiency of basic proteins was higher at higher EC pH.

In general, EC has demonstrated its capability to contribute to the recovery of various plant extracts. However, the studies which employ EC for harvesting plant extracts are still very rare in the literature, with no studies in the continuous mode. Consequently, and as EC use for plant extracts recovery is still at the preliminary stage, much work is required to fill this gap, eventhough EC has already shown the potential to replace or assist the expensive conventional methods used for the recovery of plant extracts, as a preliminary purification step.

8. ALUMINUM AND IRON CONTENT OF EFFLUENT AND BIOMASS

8.1. ALUMINUM AND IRON EFFECT ON HUMAN HEALTH

Although EC is a successful and reliable technique for harvesting biomolecules, metal contamination which results primarily from the oxidation of the anode, should not be ignored. In fact, aluminum and iron affect human negatively. Starting with aluminum, an association was discovered between the presence of aluminum (Al^{3+}) in scalp hair samples and Alzheimer's disease in patients (Arain et al. 2015). Other research studies (Kruger and Parsons 2007; Sang et al. 2008) have indicated that these metal ions accumulate in the bone and brain, leading to encephalopathy, weakening neurological development and causing renal osteodystrophy, which is thought to be at the origin of Parkinson's disease. Moreover, oral introduction of small doses of aluminum sulfates to rats stimulated defects in learning and memory (Bondy 2010). The Environmental Protection Agency (EPA) recommends a Secondary Maximum Contaminant Level (SMCL) of 0.05–0.2 mg/L for aluminum in drinking water. The Food and Drug Administration (FDA) set a limit for bottled water of 0.2 mg/L.

Regarding iron, estimates of the minimum daily requirement for iron depend on age, sex, physiological status, and iron bioavailability and range from about 10 to 50 mg/day (Gassmann 1991). The average lethal dose of iron is 200–250 mg/kg of body weight, but death has occurred following the ingestion of doses as low as 40 mg/kg of body weight (U.S. NRC, 1979).

In addition, it must be reminded that the higher limit of dissolved iron ions concentration permitted in water class 1 (water suitable for primary contact in recreation, the protection of aquatic communities,

aquaculture and fishing activities; supplies for human consumption after conventional or advanced treatments; irrigation of vegetables, irrigation of parks, gardens, sports fields and places of leisure, in direct contact with the public) is 0.3 mg/L. Accordingly, attention should be paid when conducting experiments with iron electrodes on the final quality of water effluents and on the amount of metal released with the biomolecules or in the microalgae.

8.2. ALUMINUM IN THE EFFLUENT AND BIOMASS

In this section, all the data concern, actually, the concentration of aluminum after EC for the recovery of microalgae, as no data could be found in literature on aluminum content when the recovery of plant extracts was involved.

In fact, there is no simple way to limit aluminum concentration in EC effluents. In Baierle et al. (2015), aluminum content in the effluent was higher than the value recommended for effluent emission in superficial water (10 mg/L) in the state of Rio Grande do Sul in Brazil. At low current values, there was no sufficient destabilization of the suspended particles, but at the same time, electrode dissolution continued and the concentration of Al ions in the liquid medium increased. As current increased, the dissolved ions attached to the microalgal cells and destabilized the suspension. Consequently, the concentration of metals in the effluent decreased. However, when all the biomass had been destabilized, the particle aggregation decreases and the ion concentration in the process water increased again. Vandamme et al. (2011) reported that aluminum concentration in both the effluent and biomass increased with time and current density. In the experiment with the fresh water microalgal species *Chlorella vulgaris*, aluminum concentration in the effluent was relatively high, *i.e.* about 2.1 and 2.7 mg/L at current density 1.5 and 3.0 mA/cm^2, respectively, after 30 minutes of electrolysis time. It was noted that aluminum concentration continued to increase after reaching the maximal harvesting efficiency, which is attributed to continued precipitation of aluminum hydroxides. On the other hand, with the marine microalgal species *Phaeodactylum tricornutum*, the Al concentration in the effluent was much lower (about 0.25 mg/L at both current densities 0.6 and 1.5 mA/cm^2). This concentration stabilized when the maximal recovery efficiency was reached. This difference in aluminum concentration in the effluent between the marine (*Phaeodactylum tricornutum)* and freshwater (*Chlorella vulgaris*) species is linked to different chemical composition of freshwater and seawater medium. In fact, the seawater medium contains high concentrations of sulfate anions, which facilitate precipitation of aluminum hydroxides (Matos et al. 2013a). This explains the low residual aluminum concentrations in the effluent in the experiments with *Phaeodactylum tricornutum*.

Concerning aluminum content in biomass when harvesting *Chlorella vulgaris*, it was observed that the percentage of aluminum in the biomass increased from 1.5 to 3.1% as current density increased from 1.5 to 3.0 mA/cm^2. In the case of *Phaeodactylum tricornutum*, aluminum percentage in biomass increased from 1.25 to 2% as current density increased from 0.6 to 1.5 mA/cm^2 (Vandamme et al. 2011). These percentages are considered high, as the percentage of aluminum in the biomass should not exceed 1% (w/w) in order not to hamper further processes. In another study conducted by Matos et al. (2013a) who worked on harvesting the microalgal species *Nannochloropsis* by EC, the amount of aluminum in the recovered microalgal biomass increased from 0.56% to 1.39% when using current densities of 3.3 mA/cm^2 and 8.3 mA/cm^2. Kim et al. (2012a) introduced a Continuous Electrolytic Microalgae (CEM) harvest system with Polarity Exchange (PE). This PE results in two separate phases, one dissolving and the other stable, during the CEM harvest: *i.e.*, a first phase (P1) in which flocs of microalgal cells are formed by means of the destabilization of negatively charged microalgae mediated by metal ions liberated from the dissolving electrode, and a second phase (P2) in which the generation of metal ions is terminated and bubbles generated from both electrodes cause the generated flocs to float. In their work, these authors found that as the recovery time increased, the residual Al concentration in the harvest and cultivation chambers increased with both electrode pairs (Al–DSA and Al–Pt). However, the content of Al, especially in the cultivation chamber, was lower with Al–DSA, which allows increased cell viability for microalgae cultivation using recycled medium. It was also reported that during the CEM harvest of microalgae with PE (polarity exchange), Al ions were mainly released in the P1 phase. Thus, the concentration of residual Al in the cultivation chamber and harvest chamber was reduced as the duration of P1 was decreased. When the P1:P2 ratio was 1:1.5 for 5 minutes operating time, Al accumulation was 57% lower, and cell viability did not change. P1:P2 ratio of 1:1.2 at 10 min resulted in similar results (Al accumulation was 48% lower) and cell viability increased by 19%. In another study, residual Al concentration in the harvest chamber was lower at high pH and the rate of Al accumulation in the cultivation tank was higher at lower pH (Kim et al. 2012b). This result is consistent with the results of Mouedhen et al. (2008) who found that, at identical current, more Al was dissolved from the electrodes at a lower pH, resulting in an increase in residual Al concentration. In the same work, mechanical mixing at 0.25 A lowered the residual Al concentration in the harvest chamber by 13%, as mixing allows more contact between Al and the microalgae. Without mechanical mixing at 0.5 A, the amount of settled Al was 31% and 8% lower in the harvest chamber and cultivation tank, respectively, because of poor contact between Al and microalgae (Kim et al. 2012b).

As a conclusion, if there are strategies that permit to reduce the amount of Al in the effluents and the biomass harvested, this constitutes an actual concern that has not been enough considered in the literature on EC harvesting technology.

8.3. IRON IN THE EFFLUENT AND BIOMASS

As for aluminum, the data available on iron content are only for the use of EC for microalgae recovery. Baierle et al. (2015) showed that when working at current of 1 A, iron concentration in the effluent was 4.8, 4.9 and 0.77 mg/L at 10, 15 and 20 minutes operating time, respectively. At current of 2 A, iron concentration was 0.17, 0.83 and 0.37 mg/L at 10, 15 and 20 minutes of operating time, respectively. At the highest current of 3 A, iron concentration was 0.87, 1.90, 0.15 and 0.41 mg/L at 10, 15, 20 and 30 minutes of operating time, respectively. Thus, at all experimental conditions, the iron concentration in the effluent was lower than the discharge limit set by the Brazilian legislation on effluent discharges (15 mg/L, and by the state of Rio Grande do Sul, 10 mg/L).

Concerning iron concentration in biomass, it was 33.7, 22.72 and 22.49 mg/g at 10, 15 and 20 minutes of operating time, respectively, at current of 1 A. When current was increased to 2 A, iron biomass concentration was 14.19, 46.29 and 32.44 mg/g at 10, 15 and 20 minutes of operating time respectively. Further increase in the current till 3 A resulted in iron biomass concentration of 38.49, 28.27 and 26.71 mg/g at 10, 15 and 20 minutes of operating time, respectively. It seems that iron concentration resulting from EC in this study is acceptable and does not affect the quality of water and biomass.

If iron has been less considered than aluminum in the literature, the reason seems to be less critical in the effluents. In the biomass, the amount of iron may be higher than 1% (w/w), even though it is unclear whether this can have an impact on downstream processes.

9. CONCLUSION

Electrocoagulation (EC) is an electrochemical technique widely and successfully used for wastewater treatment; however, it was not much employed to recover valuable biomolecules. This paper reviewed the successful use of electrocoagulation and other electrochemical techniques for the recovery of microalgae and plant extracts. In addition to that, this review discussed the influence of various operating parameters (initial pH, current density, initial microalgae concentration, salinity, agitation, electrode material and inter-electrode distance) on the process efficiency for harvesting microalgae. Moreover, electric energy consumption of EC during microalgae recovery, the influence of EC on microalgal lipid content and effluent and biomass metal contamination by EC were presented. In this review,

electrocoagulation was demonstrated to be successful technique for microalgae and plant extracts recovery. However, further research is required on this process, to improve the extraction of biomolecules and microalgae harvesting, particularly in the continuous mode, with less metal pollution (Al and Fe). Moreover, a compromise between energy consumption and recovery efficiency should be achieved to make the process economically feasible. At the moment, algal lipids are still far from industrialization, but it is hopeful that enhancing harvesting technology will contribute to improve the economic viability of 3rd generation biofuels.

REFERENCES

Adhoum N, Monser L, Bellakhal N, Belgaied J-E (2004) Treatment of electroplating wastewater containing Cu^{2+}, Zn^{2+} and Cr(VI) by electrocoagulation. Journal of Hazardous Materials 112:207–213.

Ahmad AL, Mat Yasin NH, Derek CJC, Lim JK (2014) Comparison of harvesting methods for microalgae *Chlorella sp*. and its potential use as a biodiesel feedstock. Environmental Technology 35:2244–2253.

Aragón AB, Padilla RB, Ros de Ursinos JAF (1992) Experimental study of the recovery of algae cultured in effluents from the anaerobic biological treatment of urban wastewaters. Resources, Conservation and Recycling 6:293–302.

Arain MS, Arain SA, Kazi TG, Afridi HI, Ali J, Naeemullah, Arain SS, Brahman KD, Mughal MA (2015) Temperature controlled ionic liquid-based dispersive micro-extraction using two ligands, for determination of aluminium in scalp hair samples of Alzheimer's patients: a multivariate study. Spectrochimica Acta Part A: Molecular and Biomolecular Spectroscopy 137:877–885.

Atashzaban Z, Seidmohammadi A, Nematollahi D, Azarian G, Shayesteh OH, Rahmani AR (2016) The efficiency of electrocoagulation and electroflotation processes for removal of polyvinyl acetate from synthetic effluent. Avicenna Journal of Environmental Health Engineering. 3:e7469.

Attour A, Touati M, Tlili M, Ben Amor M, Lapicque F, Leclerc J-P (2014) Influence of operating parameters on phosphate removal from water by electrocoagulation using aluminum electrodes. Separation and Purification Technology 123:124–129.

Azarian GH, Mesdaghinia AR, Vaezi F, Nabizadeh R, Nematollahi D (2007) Algae removal by electro-coagulation process, application for treatment of the effluent from an industrial wastewater treatment plant. Iranian Journal of Public Health 36:57–64.

Baierle F, John DK, Souza MP, Bjerk TR, Moraes MSA, Hoeltz M, Rohlfes ALB, Camargo ME, Corbellini VA, Schneider RCS (2015) Biomass from microalgae separation by electroflotation with iron and aluminum spiral electrodes. Chemical Engineering Journal 267:274–281.

Barros AI, Gonçalves AL, Simões M, Pires JCM (2015) Harvesting techniques applied to microalgae: A review. Renewable and Sustainable Energy Reviews 41:1489–1500.

Bayar S, Yıldız YŞ, Yılmaz AE, İrdemez Ş (2011) The effect of stirring speed and current density on removal efficiency of poultry slaughterhouse wastewater by electrocoagulation method. Desalination 280:103–107.

Bilad MR, Vandamme D, Foubert I, Muylaert K, Vankelecom IFJ (2012) Harvesting microalgal biomass using submerged microfiltration membranes. Bioresource Technology 111:343–352.

Bleeke F, Quante G, Winckelmann D, Klöck G (2015) Effect of voltage and electrode material on electroflocculation of *Scenedesmus acuminatus*. Bioresources and Bioprocessing 2:36.

Bondy SC (2010) The neurotoxicity of environmental aluminum is still an issue. Neurotoxicology 31:575–581.

Cañizares P, Martínez F, Jiménez C, Lobato J, Rodrigo MA (2006) Coagulation and electrocoagulation of wastes polluted with dyes. Environmental Science and Technology 40:6418–6424.

Castrillo M, Lucas-Salas LM, Rodríguez-Gil C, Martínez D (2013) High pH-induced flocculation-sedimentation and effect of supernatant reuse on growth rate and lipid productivity of *Scenedesmus obliquus* and *Chlorella vulgaris*. Bioresource Technology 128:324–329.

Chairungsi N, Jumpatong K, Phutdhawong W, Buddhasukh D (2006a) Solvent effects in electrocoagulation of selected plant pigments and tannin. Molecules 11:309–317.

Chairungsi N, Jumpatong K, Suebsakwong P, Sengprasha W, Phutdhawong W, Buddhasukh D (2006b) Electrocoagulation of quinone pigments. Molecules 11:514–522.

Chen X, Chen G, Yue PL (2000) Separation of pollutants from restaurant wastewater by electrocoagulation. Separation and Purification Technology 19:65–76.

Chowwanapoonpohn S, Chewchanwuttiwong S, Garson MJ, Buddhasukh D (2003) Electrocoagulation and recovery of tannins from tree barks. Journal of Applied Electrochemistry 33:647–650.

Christenson L, Sims R (2011) Production and harvesting of microalgae for wastewater treatment, biofuels, and bioproducts. Biotechnology Advances 29:686–702.

Coons JE, Kalb DM, Dale T, Marrone BL (2014) Getting to low-cost algal biofuels: A monograph on conventional and cutting-edge harvesting and extraction technologies. Algal Research 6, Part B:250–270.

Cotillas S, Llanos J, Miranda OG, Diaz-Trujillo GC, Cañizares P, Rodrigo MA (2014) Coupling UV irradiation and electrocoagulation for reclamation of urban wastewater. Electrochimica Acta 140:396–403.

Danquah MK, Ang L, Uduman N, Moheimani N, Forde GM (2009) Dewatering of microalgal culture for biodiesel production: exploring polymer flocculation and tangential flow filtration. Journal of Chemical Technology and Biotechnology 84:1078–1083.

Dassey AJ, Theegala CS (2013) Harvesting economics and strategies using centrifugation for cost effective separation of microalgae cells for biodiesel applications. Bioresource Technology 128:241–245.

de Carvalho Neto RG, do Nascimento JG, Costa MC, Lopes AC, Abdala Neto EF, Filho CR, Dos Santos AB (2014) Microalgae harvesting and cell disruption: a preliminary evaluation of the technology electroflotation by alternating current. Water Science and Technology 70:315–320.

Duan J, Gregory J (2003) Coagulation by hydrolysing metal salts. Advances in Colloid and Interface Science 100–102:475–502.

Elcik H, Cakmakci M (2017) Harvesting microalgal biomass using crossflow membrane filtration: critical flux, filtration performance, and fouling characterization. Environmental Technology 38: 1585 – 1596.

Emamjomeh MM, Sivakumar M (2009) Fluoride removal by a continuous flow electrocoagulation reactor. Journal of Environmental Management 90:1204–1212.

Gao S, Yang J, Tian J, Ma F, Du M (2010) Electrocoagulation–flotation process for algae removal. Journal of Hazardous Materials 177:336–343.

Gassmann B (1991) Requirements of Vitamin A, Iron, Folate and Vitamin B12. Report of Joint FAO/WHO Expert Consultation. 107 Seiten, 5 Abb., 24 Tab. Food and Agriculture Organization of the United Nations; Rome 1988. Nahrung 35:20–20.

Golzary A, Imanian S, Abdoli MA (2015) A cost-effective strategy for marine microalgae separation by electrocoagulation–flotation process aimed at bio-crude oil production: Optimization and evaluation study. Separation and Purification Technology 147:156–165.

Gregory J, Duan J (2009) Hydrolyzing metal salts as coagulants. Pure and Applied Chemistry 73:2017–2026.

Guldhe A, Misra R, Singh P (2016) An innovative electrochemical process to alleviate the challenges for harvesting of small size microalgae by using non-sacrificial carbon electrodes. Algal Research 19:292–298.

Hakizimana JN, Gourich B, Vial C (2016) Assessment of hardness, microorganism and organic matter removal from seawater by electrocoagulation as a pretreatment of desalination by reverse osmosis. Desalination 393:90–101.

Heasman M, Diemar J, O'connor W (2000) Development of extended shelf-life microalgae concentrate diets harvested by centrifugation for bivalve molluscs – a summary. Aquaculture Research 31:637–659.

Ilhan F, Kurt U, Apaydin O, Gonullu MT (2008) Treatment of leachate by electrocoagulation using aluminum and iron electrodes. Journal of Hazardous Materials 154:381–389.

Janpoor F, Torabian A, Khatibikamal V (2011) Treatment of laundry wastewater by electrocoagulation. Journal of Chemical Technology and Biotechnology 86:1113–1120.

Jumpatong K, Phutdhawong W, Buddhasukh D (2006) Dechlorophyllation by electrocoagulation. Molecules 11:156–162.

Kammerer J, Schweizer C, Carle R, Kammerer DR (2011) Recovery and fractionation of major apple and grape polyphenols from model solutions and crude plant extracts using ion exchange and adsorbent resins. International Journal of Food Science & Technology 46:1755–1767.

Kashefialasl M, Khosravi M, Marandi R, Seyyedi K (2005) Treatment of dye solution containing colored index acid yellow 36 by electrocoagulation using iron electrodes. International Journal of Environmental Science and Technology 2:365–371.

Katal R, Pahlavanzadeh H (2011) Influence of different combinations of aluminum and iron electrode on electrocoagulation efficiency: Application to the treatment of paper mill wastewater. Desalination 265:199–205.

Khandegar V, Saroha AK (2013) Electrocoagulation for the treatment of textile industry effluent – A review. Journal of Environmental Management 128:949–963.

Kim J, Ryu B-G, Kim B-K (2012a) Continuous microalgae recovery using electrolysis with polarity exchange. Bioresource Technology 111:268–275.

Kim J, Ryu B-G, Kim K (2012b) Continuous microalgae recovery using electrolysis: effect of different electrode pairs and timing of polarity exchange. Bioresource Technology 123:164–170.

Kobya M, Demirbas E, Ozyonar F (2016) Treatments of alkaline non-cyanide, alkaline cyanide and acidic zinc electroplating wastewaters by electrocoagulation. Process Safety and Environmental Protection 105:373–385.

Kruger PC, Parsons PJ (2007) Determination of serum aluminum by electrothermal atomic absorption spectrometry: A comparison between Zeeman and continuum background correction systems. Spectrochimica Acta Part B: Atomic Spectroscopy 62:288–296.

Lal A, Das D (2016) Biomass production and identification of suitable harvesting technique for Chlorella sp. MJ 11/11 and Synechocystis PCC 6803. 3 Biotech 6:41.

Lam MK, Lee KT (2012a) Microalgae biofuels: A critical review of issues, problems and the way forward. Biotechnology Advances 30:673–690.

Lam MK, Lee KT (2012b) Immobilization as a feasible method to simplify the separation of microalgae from water for biodiesel production. Chemical Engineering Journal 191:263–268.

Lee AK, Lewis DM, Ashman PJ (2013) Harvesting of marine microalgae by electroflocculation: The energetics, plant design, and economics. Applied Energy 108:45–53.

Lee D-J, Liao G-Y, Chang Y-R, Chang J-S (2012a) Coagulation-membrane filtration of *Chlorella vulgaris*. Bioresource Technology 108:184–189.

Lee D-J, Liao G-Y, Chang Y-R, Chang J-S (2012b) Chitosan coagulation–membrane filtration of Chlorella vulgaris. International Journal of Hydrogen Energy 37:15643–15647.

Llanos J, Cotillas S, Cañizares P, Rodrigo MA (2014) Effect of bipolar electrode material on the reclamation of urban wastewater by an integrated electrodisinfection/electrocoagulation process. Water Research 53: 329–338.

Ma NL, Teh KY, Lam SS (2015) Optimization of cell disruption methods for efficient recovery of bioactive metabolites via NMR of three freshwater microalgae (*chlorophyta*). Bioresource Technology 190:536–542.

Maleki HM-G, Almassi M, Hejazi MA, Minaei S (2014) Harvesting of microalgae by electro-coagulation-flocculation for biodiesel production: An investigation of the effect of operational parameters and forecast model using response surface methodology. International Journal of Biosciences 4: 258–269.

Mameri N, Yeddou AR, Lounici H (1998) Defluoridation of septentrional Sahara water of north Africa by electrocoagulation process using bipolar aluminium electrodes. Water Research 32:1604–1612.

Mata TM, Martins AA, Caetano NS (2010) Microalgae for biodiesel production and other applications: A review. Renewable and Sustainable Energy Reviews 14:217–232.

Matos CT, Santos M, Nobre BP, Gouveia L (2013a) *Nannochloropsis sp*. biomass recovery by electrocoagulation for biodiesel and pigment production. Bioresource Technology 134:219–226.

Matos CT, Santos M, Nobre BP, Gouveia L (2013b) Microalgae biomass harvesting by electrocoagulation. EfS2013 Conference - Energy for sustainability: Sustainable cities: Designing for people and the planet, Coimbra, Portugal, 1–6.

Mbacké MK, Kane C, Diallo NO (2016) Electrocoagulation process applied on pollutants treatment-experimental optimization and fundamental investigation of the crystal violet dye removal. Journal of Environmental Chemical Engineering 4:4001–4011.

Misra R, Guldhe A, Singh P (2015) Evaluation of operating conditions for sustainable harvesting of microalgal biomass applying electrochemical method using non sacrificial electrodes. Bioresource Technology 176:1–7.

Modirshahla N, Behnajady MA, Mohammadi-Aghdam S (2008) Investigation of the effect of different electrodes and their connections on the removal efficiency of 4-nitrophenol from aqueous solution by electrocoagulation. Journal of Hazardous Materials 154:778–786.

Molina Grima E, Belarbi E-H, Acién Fernández F (2003) Recovery of microalgal biomass and metabolites: process options and economics. Biotechnology Advances 20:491–515.

Mollah MYA, Morkovsky P, Gomes JAG (2004) Fundamentals, present and future perspectives of electrocoagulation. Journal of Hazardous Materials 114:199–210.

Mollah MYA, Schennach R, Parga JR, Cocke DL (2001) Electrocoagulation (EC) – science and applications. Journal of Hazardous Materials 84:29–41.

Mouedhen G, Feki M, Wery MDP, Ayedi HF (2008) Behavior of aluminum electrodes in electrocoagulation process. Journal of Hazardous Materials 150:124–135.

Naje AS, Abbas SA (2013) Electrocoagulation technology in wastewater treatment: A review of methods and applications. Civil and Environmental Research 3: ISSN 2224-5790 (Paper) ISSN 2225-0514 (Online).

Naje AS, Chelliapan S, Zakaria Z, Abbas SA (2016) Electrocoagulation using a rotated anode: A novel reactor design for textile wastewater treatment. Journal of Environmental Management 176:34–44.

Pérez L, Salgueiro JL, Maceiras R (2017) An effective method for harvesting of marine microalgae: pH induced flocculation. Biomass and Bioenergy 97:20–26.

Phutthawong N, Jampatong K, Chairungsi N, Wangkarn S, and Buddhasu D (2007) Application of electrocoagulation to the isolation of alkaloids. Chiang Mai Journal of Science 34:127–133.

Poelman E, De Pauw N, Jeurissen B (1997) Potential of electrolytic flocculation for recovery of micro-algae. Resources, Conservation and Recycling 19:1–10.

Robić G, Miranda EA (2010) Modeling of protein and phenolic compound removal from aqueous solutions by electrocoagulation. Biotechnology Progress 26:186–191.

Sang H, Liang P, Du D (2008) Determination of trace aluminum in biological and water samples by cloud point extraction preconcentration and graphite furnace atomic absorption spectrometry detection. Journal of Hazardous Materials 154:1127–1132.

Semerjian L, Ayoub GM (2003) High-pH–magnesium coagulation–flocculation in wastewater treatment. Advances in Environmental Research 7:389–403.

Shelef G (1984) Microalgae harvesting and processing: A literature review a subcontract report. Technion Research and Development Foundation. 65 pages.

Shuman TR, Mason G, Reeve D, Schacht A, Goodrich A, Napan K, Quinn J (2016) Low-energy input continuous flow rapid pre-concentration of microalgae through electro-coagulation-flocculation. Chemical Engineering Journal 297:97–105.

Udhaya R, Bruno BL, Sandhya S (2014) Evaluation of chemical flocculation-electroflocculation for harvesting of halotolerant microalgae. International Journal of Environmental Sciences 4:899–905.

Uduman N, Bourniquel V, Danquah MK, Hoadley AFA (2011) A parametric study of electrocoagulation as a recovery process of marine microalgae for biodiesel production. Chemical Engineering Journal 174:249–257.

Uduman N, Qi Y, Danquah MK, Forde GM, Hoadley A (2010) Dewatering of microalgal cultures: A major bottleneck to algae-based fuels. Journal of Renewable and Sustainable Energy 2:01270–15.

(U.S.) NRC (1979) The National Research Council in 1979: Current Issues and Studies. Washington: National Academy Sciences.

Valero E, Álvarez X, Cancela Á, Sánchez Á (2015) Harvesting green algae from eutrophic reservoir by electroflocculation and post-use for biodiesel production. Bioresource Technology 187:255–262.

Vandamme D, Pontes SCV, Goiris K (2011) Evaluation of electrocoagulation-flocculation for harvesting marine and freshwater microalgae. Biotechnology and Bioengineering 108:2320–2329.

Xu L, Wang F, Li H-Z (2010) Development of an efficient electroflocculation technology integrated with dispersed-air flotation for harvesting microalgae. Journal of Chemical Technology and Biotechnology 85:1504–1507.

Zaied M, Bellakhal N (2009) Electrocoagulation treatment of black liquor from paper industry. Journal of Hazardous Materials 163:995–1000.

Zenouzi A, Ghobadian B, Hejazi MA, Rahnemoon P (2013) Harvesting of microalgae *Dunaliella salina* using electroflocculation. Journal of Agricultural Science and Technology 15:879–887.

Zhang D, Yu Y, Li C (2014) Factors affecting microalgae harvesting efficiencies using electrocoagulation-flotation for lipid extraction. RSC Advances 5:5795–5800.

Zhang X, Zhang X, Rong J, Chen H, He C, Wang Q (2014) Current status and outlook in the application of microalgae in biodiesel production and environmental protection. Frontiers in Energy Research 2: 1–15.

Zhao F, Chu H, Yu Z (2017) The filtration and fouling performance of membranes with different pore sizes in algae harvesting. Science of the Total Environnent 587–588:87–93.

Zodi S (2012) Étude de l'épuration d'effluents de composition complexe par électrocoagulation et des couplages intervenants entre le traitement électrochimique et l'étape de séparation : application à l'industrie textile et papetière. PhD Thesis, Université de Lorraine (Nancy, France).

CHAPTER 3: ELIMINATION OF WHEY PROTEINS BY ELECTROCOAGULATION: INVESTIGATION OF SOME KEY OPERATIONAL PARAMETERS AND MODELING

This article is published online on March 2017 in Desalination and Water Treatment. Consequently, this chapter follows the guidelines of this journal.

Nidal Fayad, Tania Yehya, Fabrice Audonnet, Christophe Vial.

Elimination of whey proteins by electrocoagulation: Investigation of some key operational parameters and modeling, volume 68, pages 143-152.

ABSTRACT

Whey proteins removal from water by electrocoagulation (EC), a non-specific electrochemical technology was investigated for the first time. Experiments were carried out in synthetic wastewater in batch mode using aluminum electrodes. The respective influences of initial pH (pH_i), initial whey proteins concentration, applied current and electrolyte concentration were investigated. Results showed that the best (100%) and fastest removal of whey proteins was observed at pH_i 4, current 4.5 A, and electrolyte concentration of 6.25 g/L. The mechanism responsible for whey proteins elimination was found to be adsorption onto the flocs. Adsorption of whey proteins on flocs forming during EC at all tested currents (78.0 mg N/g solid, 61.57 mg N/g solid, and 53.18 mg N/g solid at current of 1.5 A, 3.0 A, and 4.5 A, respectively) was shown to be more efficient than adsorption of these whey proteins on preformed flocs (27.78 mg N/g solid) at the same initial concentration of 0.75 g/L. A model able to describe quantitatively protein removal was established. Experiments also showed that EC cost increased with increasing pH_i, current and electrolyte concentration. They demonstrate that EC is a promising technology for the elimination of whey proteins from dairy effluents.

Keywords: Whey proteins, electrocoagulation, wastewater treatment, adsorption

1. INTRODUCTION

The increasing scarcity of clean water sets the need for appropriate management of available water resources. Regions suffering from a lack of water urgently need integrated environmental protection and resource conservation technologies in order to enable effective management of the available water resources [1]. As a solution for water scarcity, wastewater which has been altered by human activity, whether domestic, industrial or agricultural, must necessarily be treated, with the aim to preserve the resource, while promoting cost and energy savings.

The treatment of industrial wastewater is a difficult task as this exhibits large variations of flow rate and composition, high concentrations of organic matter and salts, and the presence of poorly biodegradable organic compounds or substances [2]. From these wastewaters, those from agro-industries are characterized by a high chemical oxygen demand (COD) due to their high organic content. The dairy industry which generates a huge quantity of wastewater is particularly concerned: approximately 0.2 L to 10 L of waste per liter of processed milk [3]. These wastewaters contain whey that is the liquid phase recovered from the curds formed during cheese production. This liquid represents 80–90% of the total volume of milk used in the cheese-making process. Whey can be processed and reused for animal feed or for human consumption [4]. Whey proteins which constitute about 10% of the total dry solids in whey and 15–20% of total milk proteins contribute to the increase of COD constitute. These whey proteins are globular proteins with molar mass ranging from 14 to 1,000 kg/mol and are composed of 60% β-lactoglobulin (β-Lg), 22% α-lactalbumin (α-La), 9% immunoglobulins (Ig) and 5.5% bovine serum albumin (BSA). [5]. In small dairies producing cheese, whey reuse is not practicable and whey is, therefore, discharged as waste along with the rest of wastewater.

Actually, the disposal of whey produced during cheese production has always been a major problem because of its organic material content [6]. Dairy wastewaters are usually treated

using biological methods, such as activated sludge process, aerated lagoons, aerobic bioreactor, trickling filters, sequencing batch reactor (SBR), upflow anaerobic sludge blanket (UASB) reactor, upflow anaerobic filters and biocoagulation. On the one hand, aerobic biological processes are highly energy intensive, whereas anaerobic treatment of dairy wastewater reflects a very poor nutrient removal, so that effluents treated by anaerobic biological processes need additional treatment [7]. In the last decades, it has been revealed that electrocoagulation (EC) is an attractive and appropriate method for the management of various kinds of wastewater due to various benefits, including environmental compatibility, versatility, energy efficiency, safety, selectivity, susceptibility to automation and cost efficiency [8]. Electrocoagulation which is a non-specific electrochemical technique has been proposed as a promising alternative to chemical coagulation for removing various pollutants from freshwaters and wastewaters. It is based upon the production of soluble metal cations and insoluble metal hydroxides in water using sacrificial metal anodes. These cations and hydroxides interact with pollutants through several mechanisms, including charge neutralization, adsorption, coprecipitation and enmeshment. Pollutants can also be removed from water by electroflotation, caused by micrometer-sized hydrogen bubbles (15–23 μm diameter) which are produced on the cathode surface. This electroflotation process can occur simultaneously with sedimentation, but solid particles can also be removed using filtration [9]. The reactions that take place at electrodes in EC are as follows. For aluminum electrodes, oxidation reaction takes place at the anode:

$$Al_{(s)} \rightarrow Al_{(aq)}^{3+} + 3e^{-} \quad (1)$$

Reduction reaction takes place at the cathode:

$$3H_2O + 3e^{-} \rightarrow (3/2)H_2 + 3OH^{-} \quad (2)$$

Overall reaction during electrolysis can be summarized as [10]:

$$Al^{3+} \rightarrow Al(OH)_n^{(3-n)} \rightarrow Al_2(OH)_2^{4+} \rightarrow Al_3(OH)_4^{5+} \rightarrow Al_{13}\ \text{complex} \rightarrow Al(OH)_3 \quad (3)$$

Electrocoagulation has successfully been used for the treatment of wastewaters, including dairy wastewater [11], alcohol distillery wastewater [12] and textile wastewater [13]. Meanwhile, EC process has been widely used to treat wastewater, including a high quantity of oil grease, COD and toxic substances, such as olive oil mill wastewater [14]. Moreover, even if electrocoagulation of dairy wastewater has been carried out by some researchers, only

Guven et al. [15] and Un et al. [4] have studied electrocoagulation of cheese whey wastewater in the literature. However, concerning electrocoagulation of proteins, only Robić and Miranda [16] studied the recovery of bovine serum albumin and a phenolic compound, catechin, by EC. As far as the authors know, the literature describing the effect of electrocoagulation on whey proteins remains scarce.

In this study, the objective is, therefore, to investigate the elimination of whey proteins from water by electrocoagulation in the batch mode using aluminum electrodes as a function of current density. For this purpose, synthetic wastewater with various properties was prepared, so that the influence of initial whey proteins concentration, initial pH and electrolyte concentration could be studied on the efficiency of whey proteins removal. The results were used to better understand the mechanisms governing protein removal and to establish a model able to describe quantitatively the evolution of protein concentration vs. electrolysis time.

2. MATERIALS AND METHODS

2.1. WHEY PROTEINS SOLUTION PREPARATION

The solution was prepared by dissolving whey protein isolate (PROMILK 852 FB1, 85% proteins in which nitrogen represents about 15.92%) with ultra-pure water by the help of a magnetic stirrer at a speed of 500 rpm for two hours accompanied by gentle heating (40°C) to ensure a complete dissolution. Several initial concentrations were used (0.75 g/L, 1.5 g/L and 3.0 g/L). Initial pH (pH_i) was adjusted by a minute addition of 0.1 M HCl or KOH solution (pH_i 4, 7 or 9) in such a way that it did not modify significantly water conductivity (κ), knowing that the original pH of the solution is 6.7. Conductivity was modified by the addition of electrolyte (KCl) with various concentrations (1.25 g/L, 3.75 g/L and 6.25 g/L).

2.2. EXPERIMENTAL SETUP

In this study, electrocoagulation was applied to synthetic whey proteins solution. Electrocoagulation was carried out in a 4-L cylindrical tank, and agitation was performed by a Rushton turbine at a constant rate of 240 rpm. This rate was chosen since higher tested rotation speed up to 800 rpm consumes more energy and, at the same time, does not increase the efficiency of the process. EC was conducted in the galvanostatic mode using a 30 V-10 A power supply (ELC, France), while the cell voltage (U) was recorded to derive the electric

power input. Current, which is the key parameter of EC, was also varied between 1.5 A and 4.5 A. The experimental setup is depicted in **Figure 1**. Planar rectangular aluminum electrodes of identical dimensions (8.0 cm × 6.5 cm) were used as anode and cathode. Electrodes were rinsed with acetone and a 0.01 N HCl solution to remove organic and inorganic deposits, and then, weighed before and after each use to calculate the faradaic yield. For all the runs, the inter-electrode gap was maintained at 1 cm. Electrolysis time (t) was 60 min. Experiments were carried out at room temperature and atmospheric pressure and each experiment was repeated twice for assessing reproducibility of data. During EC, samples were taken out at different time intervals and filtered by 0.45 μm filters (Macherey-Nagel GmbH, Germany); the filtrates were then used for subsequent chemical analysis.

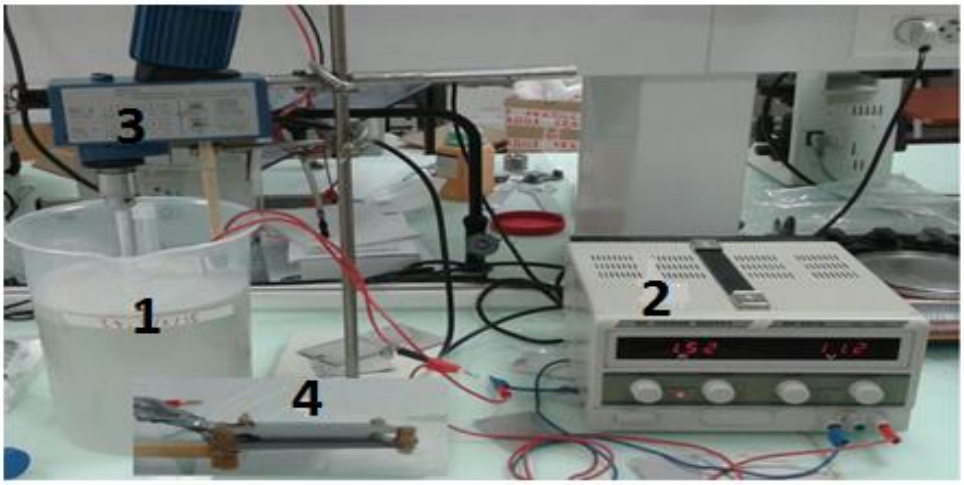

Fig. 1. Experimental setup (1: EC tank; 2: DC power supply; 3: Agitator; 4: Aluminum electrodes).

2.3. ANALYSES

To test for the elimination of whey proteins, total nitrogen was measured in each liquid sample using a TNM-1 analyzer (Shimadzu, Japan). The pH and the conductivity of water were monitored over time using a SevenEasy pH meter (Mettler-Toledo, Switzerland) and a CDM210 conductimeter (Radiometer Analytical, France), respectively.

Flocs recovered by sedimentation/flotation were filtered, washed and dried at 120ºC overnight before being weighed to quantify the mass of dry sludge. To test for the fate of the eliminated species, the solids were dissolved in HCl (0.1 M) to confirm the adsorption of whey proteins on the flocs during EC. The TNM-1 total nitrogen analyzer was used to estimate the amount of nitrogen in the dissolved solid phase. The solid phase was also characterized by

nitrogen BET surface area analysis based on nitrogen adsorption at 77 K (Tristar II, Micromeritics Instr., USA).

2.4. EXPERIMENTAL STRATEGY

The final objective is to develop a model based on a physical understanding of protein removal and robust against scale-up, which excludes for example design of experiments and response surface methodologies. The influence of wastewater properties on protein removal yield vs. electrolysis time will be investigated first: this study covers the initial pH to account for acid and neutral whey, respectively, and the effect of the initial concentration of whey proteins. Then, the operating parameter of electrocoagulation, current, will be investigated. Finally, the opportunity to enhance protein removal by changing water conductivity will be explored. These experimental results will be used to establish successively an economic analysis of the process, a better understanding of the mechanisms of protein removal and, lastly, a predictive model.

3. RESULTS AND DISCUSSION

3.1. INFLUENCE OF INITIAL PH

In chemical or electrochemical separation processes, pH is a key parameter and has a significant effect on the formation of hydroxide metal types and the mechanism of ion and pollutant removal [17]. The experimental data from the TNM-1 analyzer showed that, whatever the pH_i value, the protein removal yield reached about 99.5% after 40 minutes of treatment **(Figure 2a)**. However, the removal rate was the fastest at pH_i 4 where the removal reached about 95% after only 10 minutes of treatment, which corresponded to 39% removal at pH_i 7 and only 10% removal at pH_i 9. This could be explained by the fact that usually, at pH 4–8, Al^{3+} and OH^- ions generated by electrodes react to form various monomeric and polymeric species that finally transform into insoluble amorphous $Al(OH)_3(s)$ through complex polymerization [18]. In this case, the highest rate of elimination at pH_i 4 would be explained by the adsorption of whey proteins on the solids during electrocoagulation. The removal that was enhanced at pH_i 4 is contradictory with almost all the literature data [11], and this can be explained by the fact that pH is increasing with time during EC **(Figure 2b)**. More precisely, and after 10 minutes of treatment, pH reached 6.1 when pH_i was 4 and the recovery was 95%; this is expected since solubility of $Al(OH)_3$ is minimum at pH 6–7 for very

low Al^{3+} concentrations [14]. Conversely, pH reached 8.4 when pH_i was 7, which corresponded to 39% removal, since soluble anionic aluminum hydroxides start forming at this specific pH. Moreover, pH 4 is lower than the isoelectric point of the whey proteins. The isoelectric point of these proteins is 5.2 for β-Lg, from 4.2 to 4.5 for α-La, from 4.7 to 4.9 for BSA and between 5.5 and 6.8 for Ig [5]. This makes them less soluble when pH is close to 5 and, consequently, more easily captured by the solid flocs. On the other hand, at high pH, the concentration of the highly soluble monomeric anion $Al(OH)_4^-$ increases at the expense of $Al(OH)_{3(s)}$ [18]. Thus, floc formation is inhibited and, consequently, a lower efficiency of floc formation at higher pH_i values was proved experimentally, as only 1.1 g of solid was formed at pH_i 9 compared to about 1.5 g at pH_i 4 and 7. In addition, at pH higher than 8.5, all the aluminum hydroxides formed have lost their positive charge and; therefore, the adsorption of protein is reduced, since the gel and the proteins no longer have opposite charges under this condition [16]. Our results contradict, however; those of Robić and Miranda [16] who found that the maximal removal of BSA was at pH 8, but it must be reminded that BSA represents only a small fraction of whey proteins (~5.5%).

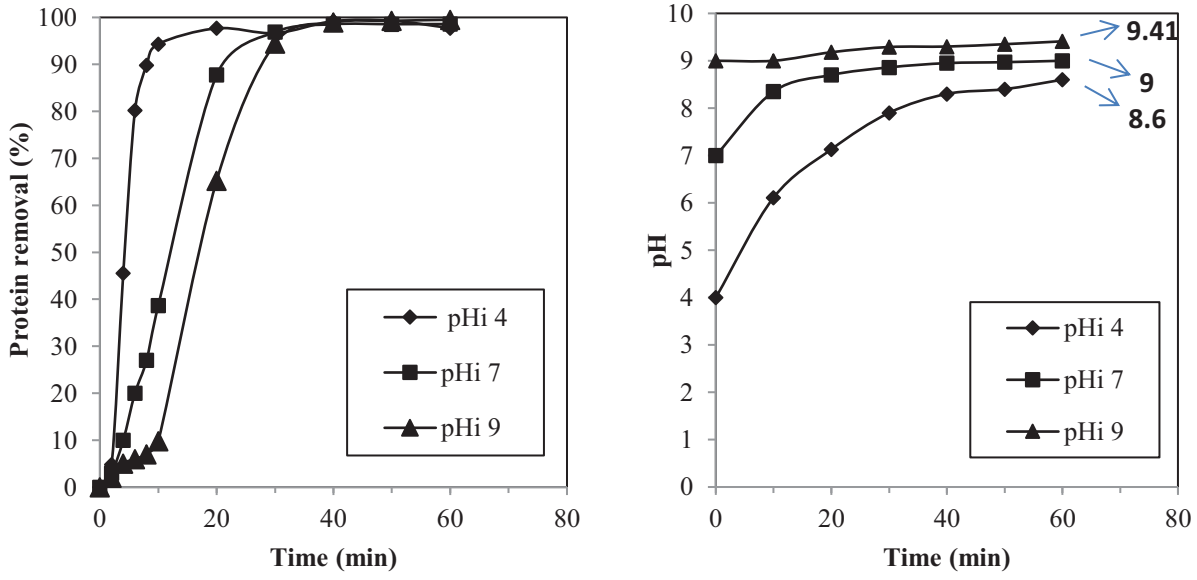

Fig. 2. Effect of initial pH (pH_i) on whey proteins removal (a) and on pH evolution (b) during electrocoagulation. Experimental conditions: Initial concentration of whey proteins 0.75 g/L, Current 1.5 A, KCl concentration 6.25 g/L, electrolysis time 60 minutes.

3.2. INFLUENCE OF THE INITIAL CONCENTRATION OF WHEY PROTEINS

A new set of experiments was dedicated to the study of the influence of the initial concentration of whey proteins on their removal efficiency. As shown in **Figure 3**, after the end of treatment, about 100% of proteins were removed for both initial concentrations 0.75 g/L and 1.5 g/L; however, only 96% were removed when the initial concentration was 3.0 g/L. In addition, removal rate depended clearly on the initial concentration; this means that the evolution of the removal rate was faster with lower concentrations, as it reached 85%, 55% and 50% for the initial concentrations 0.75 g/L, 1.5 g/L, and 3.0 g/L, respectively, after only 10 minutes of treatment, even though the quantity of proteins removed at time t increased with their initial concentration. So, as a rule of thumb, we can say that the removal efficiency of whey proteins decreases with an increase in the initial concentration of whey proteins for a constant current density. This results from the fact that the number of metal hydroxide flocs formed is insufficient to coagulate the greater number of protein molecules at higher initial concentration [10]. At the industrial scale, one must increase the surface of electrodes used, while keeping a constant current density to achieve the same removal efficiency as in our study.

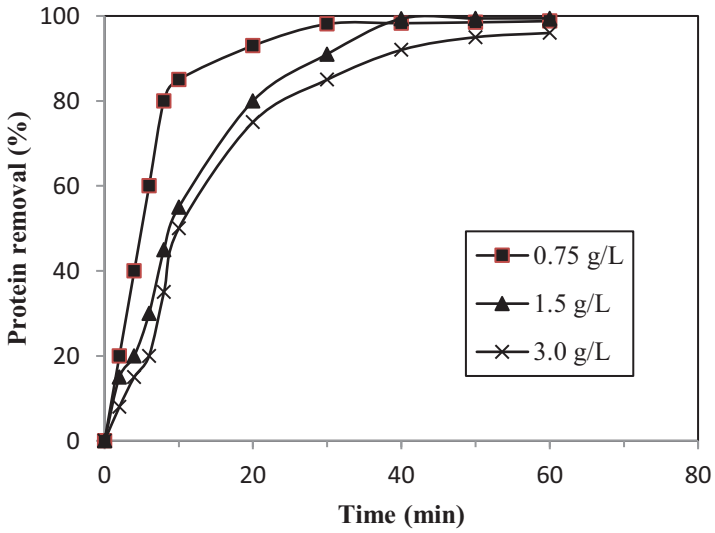

Fig. 3. Effect of initial concentration on whey proteins removal. Experimental conditions: Current 1.5 A, KCl concentration 6.25 g/L, initial pH 6.7, electrolysis time 60 minutes.

3.3. INFLUENCE OF CURRENT

In all the electrochemical processes, current density is the most important operating parameter for controlling the reaction rate inside the electrochemical reactor. It has been well shown that current can determine the production rate of coagulant, the production rate of bubbles, their size and distribution, and the rate of floc growth in electrocoagulation reaction with different electrodes [19]. This new set of experimental runs was dedicated to the study of the influence of the current (I) on whey proteins elimination using EC with Al electrodes. Three current values were tested (1.5 A, 3.0 A, and 4.5 A). In our results, complete elimination was obtained after 30 minutes of treatment with the three currents **(Figure 4a)**. However, the rate of removal was much faster with current 4.5 A where it was about 97% after 10 minutes of treatment, compared to only 30% and 72% with 1.5 A and 3.0 A, respectively, after the same time interval. This could be explained by the fact that at high current, the amount of aluminum oxidized increased, resulting in a greater quantity of precipitation [20].

To further investigate the relation between I and pH, and its influence on whey proteins elimination, pH change rate was investigated at different currents. It was found that the pH change rate depended strongly on the current applied to the EC unit. The highest current used led to the fastest rate of pH change during EC **(Figure 4b)**. It was also found that when current was 4.5 A, pH varied after 8 minutes of treatment between 7.0 and 8.2, which is the most suitable pH for floc formation. This results from the fact that during electrocoagulation, higher currents lead to a faster cathodic reduction and, thus, a faster production of OH^- anions. Moreover, the fastest elimination of whey proteins at the highest current is due to the highest dissolution rate of the sacrificial aluminum anode, which in turn contributes to the release of more Al^{3+} cations and, consequently, faster floc formation over time.

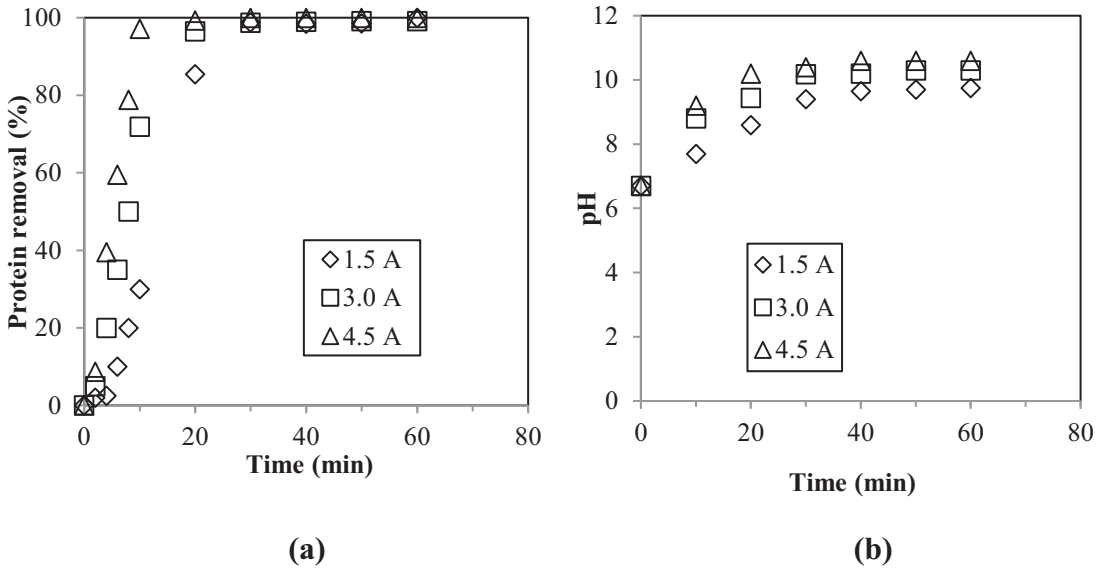

(a) **(b)**

Fig. 4. Effect of current: (a) on whey proteins removal, and (b) on pH evolution during EC. Experimental conditions: initial whey proteins concentration 0.75 g/L, KCl concentration 6.25 g/L, pH_i 6.7, electrolysis time 60 minutes.

3.4. INFLUENCE OF ELECTROLYTE (KCL) CONCENTRATION

The effect of supporting electrolyte (KCl) concentration (1.25 g/L, 3.75 g/L and 6.25 g/L) on the removal efficiency of whey proteins was investigated, so as to modify water conductivity. These concentrations correspond to conductivity values of 1.36 mS/cm, 3.79 mS/cm and 6.80 mS/cm, respectively. Our results show (**Figure 5)** that KCl concentration did not have any significant effect on the final removal yield of proteins, as this was about 99.2% after 30 minutes for the three KCl concentrations used. However, the rate of elimination was much faster when KCl concentration was 6.25 g/L, as removal yield reached about 78.5% for KCl concentration of 6.25 g/L after 20 minutes of treatment, while this was only 66.3% and 39.9% for KCl concentrations of 3.75 g/L and 1.25 g/L, respectively. This could be explained by the higher amount of Cl^- anions which could enhance the dissolution of the aluminum anode by pitting corrosion [21]. Enhanced dissolution, in turn, leads to higher amounts of Al^{3+} ions that increase the production of $Al(OH)_3$, causing higher elimination of whey proteins. These results might also be explained by the fact that the increase of the conductivity of the solution induces a higher screening for the electrostatic interactions, which could improve protein capture by aluminum hydroxides. Another reason is that the increase of water conductivity reduces the ohmic drop (IR) which is described by equation (4):

$$IR = \frac{I.d}{A.\kappa} \quad (4)$$

where I is the current (A), d is the inter-electrode distance (m), A is the active anode surface (m^2), κ is the specific conductivity (S/m). At higher conductivity, the applied potential needed to maintain a constant current decreases. This means that the power requirements of EC also decrease. But in this work, it was also observed that the faradaic yield increased with water conductivity, which means that the rate of anodic oxidation also increased. As the faradaic yield becomes higher, the number of cations released at the anode also increases, and thus, removal efficiency increases.

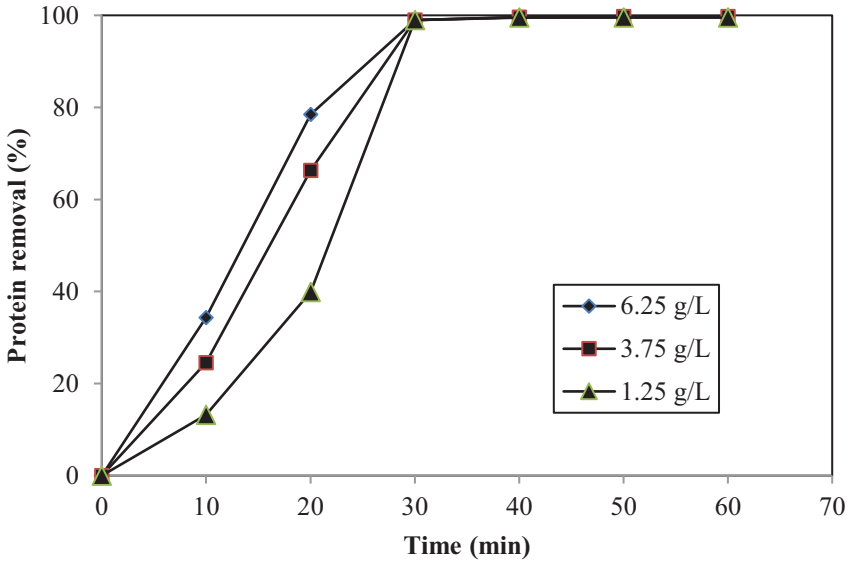

Fig. 5. Effect of electrolyte concentration on whey proteins removal. Experimental conditions: Initial concentration of whey proteins 0.75 g/L, Current 1.5 A, pH_i 6.7, electrolysis time 60 minutes.

3.5. EC COST ANALYSIS

One of the most important parameters that greatly influences the practical applicability of any technology of treatment is the cost of the applied process. The operating cost of EEC ($/m) was calculated as the sum of the costs of consumed material, electrical energy consumption and salt consumption. The price of electrical power used was considered 0.13 $/kWh, the price of the electrode material used was estimated as 1.5 $/kg Al, and the price of potassium chloride (KCl) was considered 0.30 $/kg. EC is the electrical energy consumption (kWh/m^3 water) after

60 minutes of whey proteins solution treatment. The electrical energy consumption was calculated in terms of kWh per m^3 of treated effluent using equation (5):

$$\mathrm{EEC(kWh/m^3)} = \frac{\mathrm{U.I.t}}{\mathrm{V}} \quad (5)$$

where U is the cell voltage (V), I the current (A), t the electrolysis time (h) and V the volume (L) of effluent to be treated. In parallel, EMC (kg/m^3) is the electrode material consumed at the same time t considered for EEC above. The amount of material dissolved from the anode is calculated by measuring electrode mass before and after electrocoagulation. Finally, SC is the salt consumption expressed in kg/m^3 and the EC cost was evaluated in terms of current, KCl concentration and pH_i, as follows:

$$\mathrm{EC\ Cost\ (\$/m^3)} = 0.13 \cdot \mathrm{EEC} + 1.5 \cdot \mathrm{EMC} + 0.3 \cdot \mathrm{SC} \quad (6)$$

First, it is clear from **Figure 6** that increasing KCl concentration always increases EC cost within the range studied. This increased from 1.11 $/m^3$ at KCl concentration of 1.25 g/L to 2.26 $/m^3$ at KCl concentration of 6.25 g/L. However, increasing KCl concentration decreased EEC cost due to conductivity increase, which decreased the total resistance (ohmic drop) of the solution; so, the needed voltage to maintain a given current decreased and, thus, electrical energy consumption decreased. However, this cost decrease was not enough to reduce the overall cost of the process, since at higher KCl concentration, SC increased from 0.375 $/m^3$ at KCl concentration of 1.25 g/L to 1.875 $/m^3$ at KCl concentration of 6.25 g/L. Moreover, faradaic yield increased from 105% at KCl concentration of 1.25 g/L to 120% at KCl concentration of 6.25 g/L, which also increased EMC from 0.198 $/m^3$ to 0.226 $/m^3$.

Then, **Figure 7** describes the influence of current on EC cost. A general observation that can be inferred is that higher current always leads to higher EC cost within the range investigated: increasing current from 1.5 A to 4.5 A increased EC cost from 2.31 $/m^3$ to 3.87 $/m^3$. In this figure, most of the costs at the three tested currents was due to SC, but this cost was identical for all the currents used. The difference in the total cost was due primarily to EEC. As current increased from 1.5 A to 3.0 A and 4.5 A, EEC contribution to EC cost increased, as it contributed to ~20% and ~33% from the total EC cost at current 3.0 A and 4.5 A, respectively, compared to the ~8% at 1.5 A. Higher energy expenditure at higher current could be easily explained by equation (4), as this is linearly related to IR×I contribution.

Another factor contributing to the difference in total cost of the process is EMC, as EMC increased from 0.23 $/m^3 at current of 1.5 A to 0.69 $/m^3 at current of 4.5 A.

Concerning the effect of pH_i on EC cost, we can say, as shown in **Figure 8**, that cost was slightly higher at pH_i 9 than at pH_i 4 and pH_i 7; more precisely, at pH_i 9, EC cost was 3.05 $/m^3 compared to 2.94 $/m^3 at pH_i 4 and 2.99 $/m^3 at pH_i 7. The difference in costs at different pH_i values was almost negligible and was due to more energy expenditure at pH_i 9, and higher EMC at higher pH_i values, as faradaic yield increased from 116% to 128% as pH_i increased from 4 to 9. Higher energy consumption at pH_i 9 could be explained by the fact that, at higher pH values, deposits on the anode surface lead to an increasing ohmic drop (because of the inert, little conducting layer formed) and to an increase in the electrical consumption [22]. Lower pH values are, thus, preferable both from efficiency and maintenance point of view.

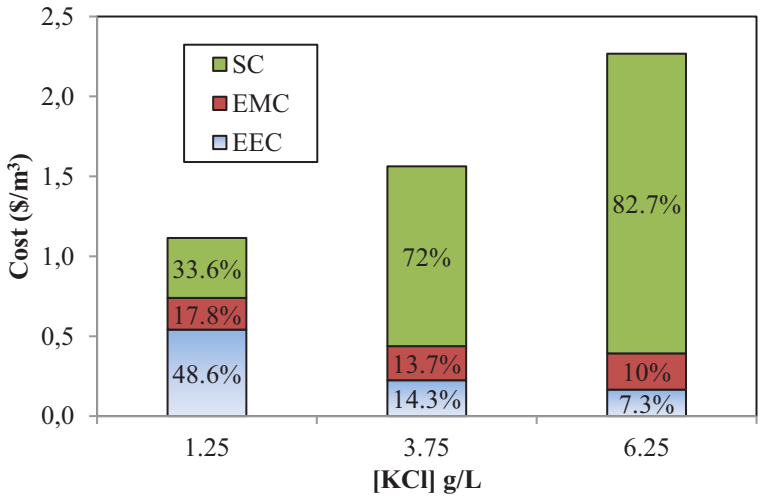

Fig. 6. Effect of electrolyte (KCl) concentration on EC cost. SC: Salt Consumption, EMC: Electrode Material Consumption, EEC: Electrical Energy Consumption. Experimental conditions: Initial concentration of whey proteins 0.75 g/L, pH_i 6.7, Current 1.5 A, electrolysis time 60 minutes.

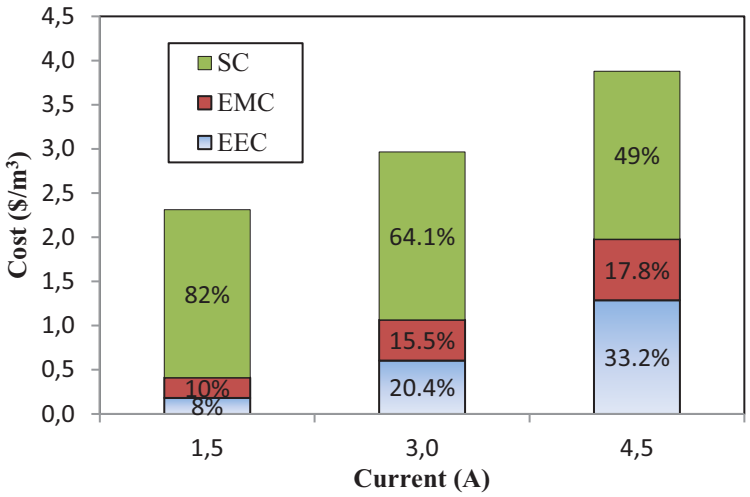

Fig. 7. Effect of current on EC cost. SC: Salt Consumption EMC: Electrode Material Consumption, EEC: Electrical Energy Consumption. Experimental conditions: Initial concentration of whey proteins 0.75 g/L, pH_i 6.7, KCl concentration 6.25g/L, electrolysis time 60 minutes.

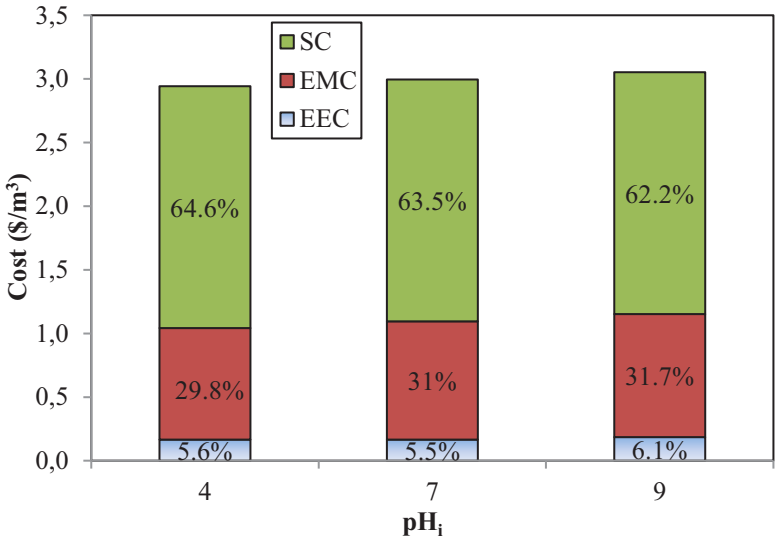

Fig. 8. Effect of pH_i on EC cost. SC: Salt Consumption, EMC: Electrode Material consumption, EEC: Electrical Energy Consumption. Experimental conditions: Initial concentration of whey proteins 0.75 g/L, Current 1.5 A, KCl concentration 6.25 g/L, electrolysis time 60 minutes.

3.6. ANALYSIS OF THE LIQUID AND THE SOLID PHASES

The analysis of liquid samples after 60 min electrolysis time, for I = 4.5 A and pH_i 4 using the TNM-1 analyzer showed that almost 100% of whey proteins were removed from water. If there was no adsorption on the solid phase (flocs) or no gas release, that is to say only protein

oxidation in the liquid phase, total nitrogen should have been constant over time in the liquid phase. However, experimental data (100% removal) highlight that proteins were preferentially adsorbed on the solid phase and that no CO_2 was produced. In fact, proteins with a low internal stability, the so-called "soft" proteins, such as bovine serum albumin (BSA), immunoglobulin (IgG) or α-lactalbumin generally tend to adsorb on all surfaces, irrespective of electrostatic interactions, owing to a gain in conformational entropy resulting from adsorption. Thus, the soft proteins do adsorb even on an electrostatically repelling surface [23], increasing adsorption on the solid at different operating conditions. This assumption is reinforced by Norde and Haynes [24] who studied the adsorption of α-lactalbumin on negatively charged polystyrene (PS) latex beads and on variably charged hematite. α-lactalbumin denatured on both PS, which has a hydrophobic surface, and on the hydrophilic surface of hematite. Here, we can say that the primary factor which determines the adsorption behavior of proteins to a sorbent is their structural stability. Whey proteins in which many soft proteins can be found exhibit therefore a weak internal stability, and are prone to adsorb on the surface of aluminum hydroxide. Moreover, the analysis of the dried flocs (solid phase) by nitrogen adsorption isotherm has shown that they exhibit a BET specific surface area that ranges between 30 and 50 m^2/g, which enhances the possibility of protein adsorption.

To investigate the fate of proteins during EC, the flocs were dissolved with 0.1 M HCl. The analysis done by TNM-1 analyzer ensured the presence of nitrogen entities in all tested conditions. The amount of these nitrogen entities is almost 98% of the initial nitrogen amount. To be sure that adsorption was responsible for whey proteins removal from the liquid, the same solid was produced by EC without the addition of proteins at current of 4.5 A, pH_i 6.7 and KCl concentration of 6.25 g/L. Four grams from the produced solid were added to whey proteins solutions of different concentrations (0.75 g/L, 1.5 g/L and 3.0 g/L). The solids were set in contact with the same initial concentrations of whey proteins used during EC for 24 hours to reach equilibrium in order to test for adsorption. Analyzing the liquid phase using the TNM-1 analyzer showed an average of 95.2% decrease of the whey proteins initial concentration. This ensures definitely that during electrocoagulation, adsorption is the main mechanism responsible for the removal of whey proteins.

For comparison purpose, adsorption data are illustrated by **Figure 9**. This compares the adsorption isotherms of whey proteins on preformed flocs and on flocs forming during EC. Results show that whey proteins are significantly adsorbed on preformed flocs at all tested

initial concentrations. Equilibrium concentrations of 5.85 mg N/L, 15.98 mg N/L and 62 mg N/L were found at initial concentrations of 0.75 g/L, 1.5 g/L and 3.0 g/L, respectively. These equilibrium concentrations correspond to 95%, 93.2% and 86.8% removal efficiency at initial concentrations of 0.75 g/L, 1.5 g/L and 3.0 g/L, respectively. As formed flocs and whey proteins are not oppositely charged at pH 6.7, electrostatic attraction is not a possible mechanism for protein adsorption which is mainly driven by hydrophobic interactions. The effect of surface hydrophobicity on the adsorption of β-Lg (the main whey protein), was tested by Krisdhasima et al. [25]: they found that increasing hydrophobicity of silicon leads to increasing adsorbed amounts of β-Lg. Usually, an interaction with a hydrophobic surface is energetically more favored than with a hydrophilic surface because water molecules are released from the surface and from the protein, which leads to a large entropy gain.

The adsorption behavior of whey proteins on preformed flocs in our case seems to be best fitted by Langmuir adsorption model, as shown in **Figure 9**. However, this model ignores the problem of reversibility, the fact that adsorption does not occur on fixed sites, that the spatial conformation of molecules usually changes upon adsorption and that lateral interaction may take place. This means that Langmuir assumptions are not necessarily correct for whey proteins, despite the good quantitative agreement in **Figure 9**. Our experiments ensured the adsorption of whey proteins into flocs, but the comparison of adsorption of whey proteins into already formed flocs to adsorption of these proteins on flocs being formed continuously during EC at the same initial concentration of 0.75 g/L displayed better adsorption during EC at all tested current values **(Figure 9)**. Experimental data showed that equilibrium concentration was always close to zero when the quantity of nitrogen adsorbed was 78.0 mg N/g solid, 61.57 mg N/g solid, and 53.18 mg N/g solid at current of 1.5 A, 3 A, and 4.5 A, respectively, compared with a maximum of 27.78 mg N/g solid for the quantity adsorbed on preformed flocs at the same initial protein concentration (0.75 g/L). This highlights that flocs formed during EC can contain far more proteins than preformed flocs, but also that protein removal is irreversible only during EC. This better adsorption performance with EC may be explained first by the enhanced mixing and mass transfer conditions near the anode: very small solid particles are formed in this region during EC, which leads to a very high interfacial area, while hydrogen bubbles strongly contribute to the reduction of mass transfer limitation, which is known to be the main limiting step of protein adsorption due to the molecular weight of whey proteins. In addition, proteins adsorbed on very small flocs can be progressively imprisoned by the growth and the aggregation of solid particles during electrolysis; this makes adsorption irreversible

and clearly differs from conventional adsorption in which interfacial area is constant. However, if current increases, more $Al(OH)_3$ is formed: so, the mass ratio of proteins to flocs decreases at constant protein concentration, leading to lower quantity of nitrogen adsorbed per gram of solid. As a result, higher adsorption at lower current during EC is due to the slower formation of flocs, so that a smaller amount of solid is more rapidly saturated by adsorbed proteins. Further work is still necessary to validate this analysis.

As a conclusion, our results demonstrate clearly that electrocoagulation is more efficient than conventional adsorption for the removal of whey proteins and that the in situ production of flocs is probably responsible for the enhanced effectiveness of EC.

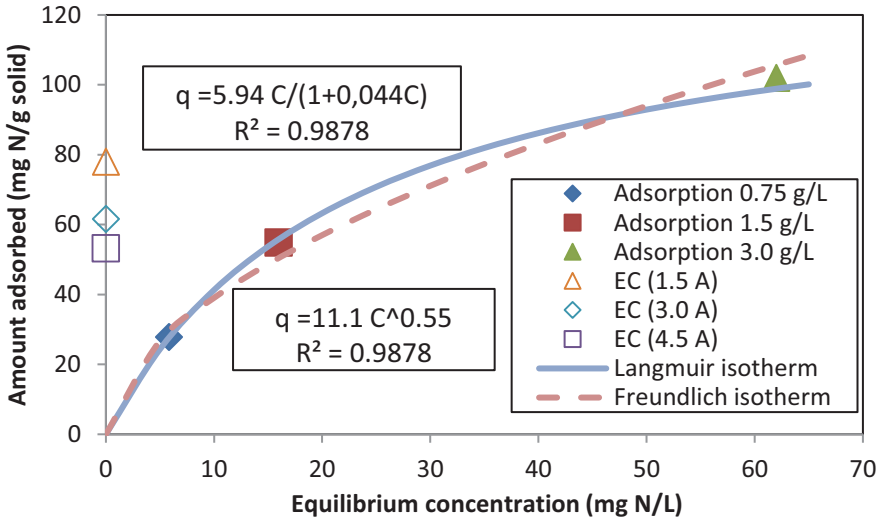

Fig. 9. Isotherms of whey proteins adsorption on preformed flocs at different initial concentrations without EC (filled symbols) and on flocs being formed during EC using a volume of water V=1 L to standardize with adsorption experiments at different current (empty symbols). Conditions of floc formation: Current 4.5 A, pH_i 6.7, KCl concentration 6.25 g/L, electrolysis time 60 minutes. Conditions of EC: Initial concentration 0.75 g/L, pH_i 6.7, KCl concentration 6.25 g/L, electrolysis time 60 minutes.

3.7. MODELING OF WHEY PROTEIN REMOVAL USING EC

Contributions to process modeling based on EC are quite rare in the literature. Typical examples can be found on solid particles and Chemical Oxygen Demand (COD) abatement [26] and fluoride anions removal [27]. EC is known as a process difficult to simulate because of the various mechanisms that contribute in parallel to pollution abatement, such as adsorption, coprecipitation, physical enmeshment and oxidoreduction in the bulk or on the electrodes. In this work, a simple model has been established from the mass balance on proteins using the following assumptions:

- Adsorption is the governing mechanism of protein removal;
- The mass of floc, *i.e.* adsorbent, changes with time and is proportional to the mass of aluminum m released by electrodes, which can be deduced from Faraday's law using a constant faradaic yield over time ϕ_{Al} =120%, the molar mass of Al (M_{Al}) and Faraday's constant (F):

$$m = M_{Al} \cdot \phi_{Al} \frac{I}{3F} t \tag{7}$$

- Adsorption is thermodynamically driven, without mass transfer limitation, and can be described using Langmuir isotherm that relates the amount of proteins adsorbed (q, expressed in g proteins/g Al) to their concentration in the liquid phase (*C*, g proteins/L) using the monolayer capacity q_m (g/g) and the affinity constant *K* (L/g Al):

$$q = q_m \frac{KC}{1+KC} \tag{8}$$

Consequently, the mass balance can be derived as follows:

$$V \frac{dC}{dt} = -q \frac{dm}{dt} - m \frac{dq}{dt} \tag{9}$$

Considering the derivatives of *m* and *q* as a function of time,

$$\frac{dm}{dt} = M_{Al} \cdot \phi_{Al} \frac{I}{3F} \quad \text{and} \quad \frac{dq}{dt} = q_m \frac{K}{(1+KC)^2} \frac{dC}{dt} \tag{10}$$

one finally gets the following ordinary differential equation that can be solved mathematically using a free (GNU Octave) or a commercial (Matlab®, The MathWorks) equation solver:

$$\frac{dC}{dt} = -q_m \frac{dm}{dt} \frac{KC}{1+KC} \left[\frac{(1+KC)^2}{V \cdot (1+KC)^2 + m q_m \cdot K} \right] \tag{11}$$

K and q_m are the only adjustable parameters that can be deduced by fitting experimental data. This model differs from those described previously that neglect the transient concentration term *dC/dt* [25], or the *dq/dt* term [26].

The model was used, first, to investigate the influence of current. Using current loading, $I \cdot t$, as a unique variable able to describe data for current between 1.5 and 4.5 A at constant initial concentration and pH_i, the fair agreement between experimental and predicted data is presented in **Figure 10a**. An empirical model can also be adjusted on pH evolution as a function of current loading, which follows an exponential trend, *i.e.* a first-order trend **(Figure 10b)**. Finally, **Figure 10** validates the assumptions of the model and highlights that protein removal can be easily predicted as a function of current and electrolysis time using equation (11). The comparison between the data from **Figure 9** and **Figure 10** is not straightforward, but using K=15 L/g Al and q_m=15 g proteins/g Al, one can estimate, for instance, that when 99% proteins are removed from water with an initial concentration of 0.75 g/L, q should be 1.5 g/g. Taking into account the 6.28 factor between nitrogen and proteins and the fact that Al content in flocs is between 25% and 33% w/w, one finally deduces that it corresponds to 60–80 mg N/g solid, which is in agreement with the experimental data extracted from **Figure 9**.

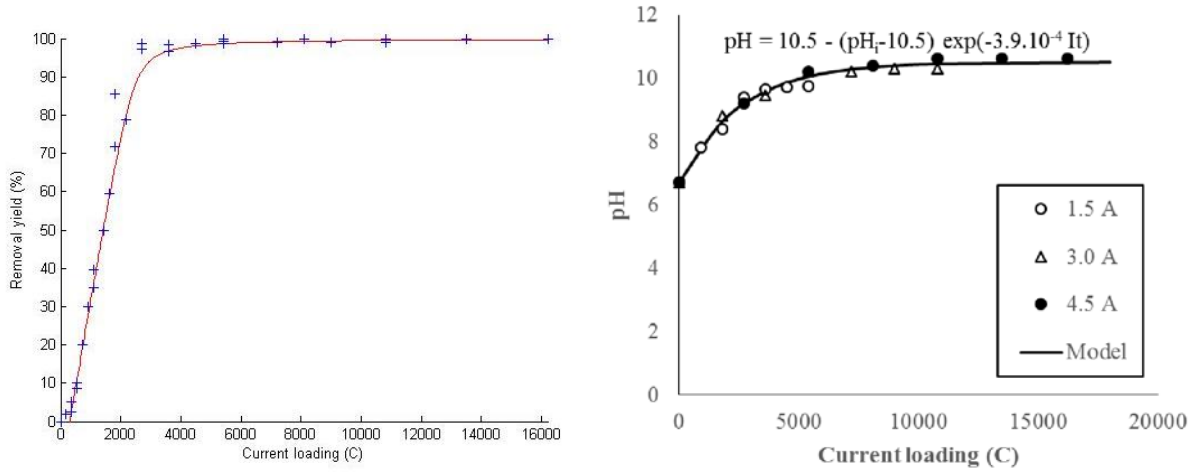

(a) **(b)**

Fig. 10. Comparison of predicted (q_m=15 g proteins/g Al and K=15 L/g Al) and experimental data as a function of current loading: (a) protein removal yield; (b) pH. Experimental conditions: Initial whey proteins concentration 0.75 g/L, KCl concentration 6.25 g/L, pH_i 6.7, electrolysis time 60 minutes.

Then, the effect of initial concentration was analyzed using the same model. Fitting the data was, however, more complex as far as the initial content of whey protein increases, as shown in **Figure 11**. While the model fits perfectly the initial concentration 0.75 g/L for which it has

been established with the same q_m and K values as in **Figure 10**, it agrees reasonably with experimental data for 1.5 g/L and it deviates between 2500 and 7500 C when the initial content is 3.0 g/L. But contrary to expectations, this deviation does not correspond to an overestimation of the removal rate due to a mass transfer limitation, but to an acceleration of protein removal. A parametric analysis of the model showed that only an increase of q_m from 15 to 20 g proteins/g Al can better fit the data when the initial protein concentration is 3 g/L, while the effect of K remains weak. This highlights an increase of the adsorption capacity of the flocs.

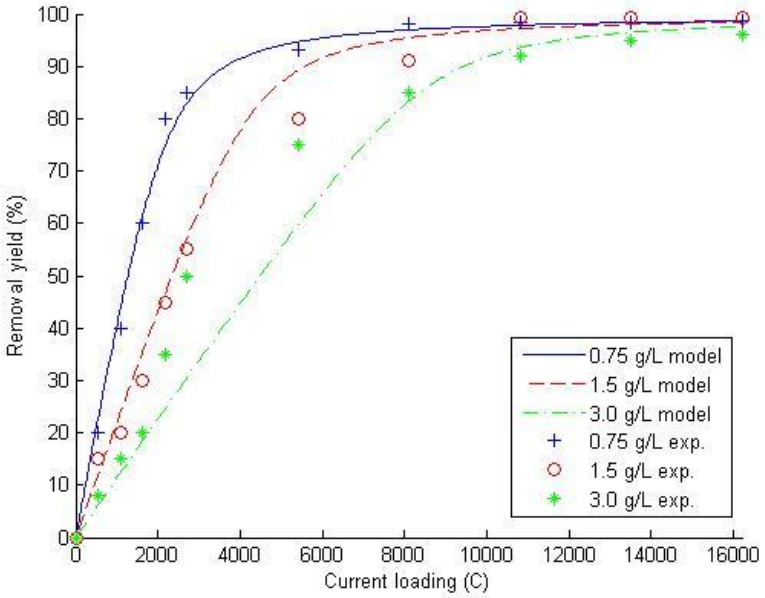

Fig. 11. Comparison of predicted (q_m=15 g/g and K=15 L/g) and experimental protein removal yield as a function of initial concentration. Experimental conditions: I = 4.5 A, KCl concentration 6.25 g/L, pH_i 6.7, electrolysis time 60 minutes.

Several reasons can explain this trend, among which a self-aggregation mechanism of proteins in the liquid phase seems the most probable. This could be due to the electric field at high protein content when the initial protein concentration is high. The consequence would be to enhance protein removal, as this could lead to the adsorption of aggregates. This corresponds to an "apparent" multilayer adsorption that contradicts the assumption of Langmuir isotherm and cannot be predicted by the present model. In the literature, multilayer adsorption of whey proteins has already been reported [28], which reinforces this assumption, even though the detailed mechanism has not been studied in the presence of an electric field.

As a conclusion, the model described by equations (7–11) can predict quantitatively protein removal for current between 1.5 A and 4.5 A, and for initial concentrations between 0.75 and

1.5 g/L, and to estimate the time needed for a complete removal at higher initial concentration up to 3 g/L. It requires only two adjustable parameters that must be readjusted only as a function of initial pH and conductivity. Even though it can still be improved to account for higher concentrations, the robustness of the parameters estimated at constant pH_i and conductivity when simulations are carried out as a function of current and initial concentration outperforms other models from the literature that usually require to adjust parameters for each new set of operating conditions. This model constitutes, therefore, a valuable tool for the design of EC process in the future.

4. CONCLUSION AND PERSPECTIVES

The treatment of water containing whey proteins by electrocoagulation using aluminum electrodes was studied in a batch reactor. Elimination of whey proteins has been investigated as a function of the following parameters: initial concentration, initial pH (pH_i), current and electrolyte concentration. Experimental results showed that the fastest removal of whey proteins occurred at pH_i 4, current 4.5 A, and electrolyte concentration of 6.25 g/L. Moreover, increasing the initial concentration of whey proteins decreased the rate of removal. Adsorption was found to be the main mechanism responsible for whey proteins elimination. Adsorption of whey proteins on flocs forming during EC at all tested currents (78.0 mg N/g solid, 61.57 mg N/g solid, and 53.18 mg N/g solid at current of 1.5 A, 3 A, and 4.5 A, respectively) was shown to be more efficient than adsorption of these whey proteins on preformed flocs (27.78 mg N/g solid) at the same initial concentration of 0.75 g/L. In addition, experimental data showed that a reduction of EC cost could be achieved by working at the lowest pH_i (4), where EC cost was 2.94 \$/m^3, at the lowest current 1.5 A which resulted in EC cost of 2.31 \$/m^3, and at the lowest KCl concentration (1.25 g/L), where EC cost was 1.11 \$/m^3. An unexpected result is the high cost of salt consumption that must also be minimized using cheaper salts, such as NaCl (0.065 \$/kg). Finally, a robust predictive model based on mass balance equations, Faraday's law and Langmuir isotherm was also established to describe protein removal using EC; this is not only able to fit experimental data, but it is also promising for other applications involving EC process.

Now, testing real dairy wastewater is the priority for further work so as to estimate the interaction between proteins and other matrix components on their removal. In addition,

further work should be carried out to investigate whether adsorption may be reversible and if proteins refold to their native conformation after desorption.

REFERENCES

1. W.K.M.B Salameh, H. Ahmad and M. Al-Shannag, Treatment of olive mill wastewater by electrocoagulation processes and water resources management, W.A.S.T., 9 (2015) 288–292.

2. A. García-García, V. Martínez-Miranda, I.G. Martínez-Cienfuegos, P.T. Almazán-Sánchez, M. Castañeda-Juárez and I. Linares-Hernández, Industrial wastewater treatment by electrocoagulation–electrooxidation processes powered by solar cells, Fuel, 149 (2015) 46–54.

3. S. Tchamango, C.P. Nanseu-Njiki, E. Ngameni, D. Hadjiev and A. Darchen, Treatment of dairy effluents by electrocoagulation using aluminum electrodes, Sci. Total Environ., 408 (2010) 947–952.

4. U.T. Un, A. Kandemir, N. Erginel and S.E. Ocal, Continuous electrocoagulation of cheese whey wastewater: An application of Response Surface Methodology, J. Environ. Manage., 146 (2015) 245–250.

5. A.L.F. Cavallieri, A.P. Costa-Netto, M. Menossi and R.L. Da Cunha, Whey protein interactions in acidic cold-set gels at different pH values, Lait, 87 (2007) 535–554.

6. A. Kandemir, Electrocoagulation of Cheese Whey Wastewater, MSc thesis, Anadolu University, Graduate School of Science, Turkey 2011.

7. E. Bazrafshan, H. Moein, F.K. Mostafapour and S. Nakhaie, Application of electrocoagulation process for dairy wastewater treatment, J. Chem., Article ID 640139 (2013) 8 pages.

8. M. Bayramoglu, M. Kobya, M. Eyvaz and E. Senturk, Technical and economic analysis of electrocoagulation for the treatment of poultry slaughterhouse wastewater, Sep. Purif. Technol., 51 (2006) 404–408.

9. M. Vepsäläinen, M. Pulliainenc and M. Sillanpääb, Effect of electrochemical cell structure on natural organic matter (NOM) removal from surface water through electrocoagulation (EC), Sep. Purif. Technol., 99 (2006) 20–27.

10. V. Khandegar, A.K. Saroha, Electrocoagulation for the treatment of textile industry effluent – A review, J. Environ. Manage., 128 (2013) 949–963.

11. I.A. Şengil, M. Özacar, Treatment of dairy wastewaters by electrocoagulation using mild steel electrodes, J. Hazard. Mater., 137 (2006) 1197–1205.

12. Y. Yavuz, EC and EF processes for the treatment of alcohol distillery wastewater, Sep. Purif. Technol., 53 (2007) 135–140.

13. O.T. Can, M. Kobya, E. Demirbas and M. Bayramoglu, Treatment of the textile wastewater by combined electrocoagulation, Chemosphere., 62 (2006), 181–187.

14. U.T. Un, A.S. Koparal and U.B. Ogutveren, Electrocoagulation of vegetable oil refinery wastewater using aluminum electrodes, J. Environ. Manage., 90 (2009) 428–433.

15. G. Guven, A. Perendeci and A. Tanyolac, Electrochemical treatment of deproteinated whey wastewater and optimization of treatment conditions with response surface methodology, J. Hazard. Mater., 15 (2008) 69–78.

16. G. Robić, E. A. Miranda, Modeling of Protein and Phenolic Compound Removal from Aqueous Solutions by Electrocoagulation, Biotechnol. Prog., 26 (2010) 186–191.

17. C. Ricordel, A. Darchen and D. Hadjiev, Electrocoagulation–electroflotation as a surface water treatment for industrial uses, Sep. Purif. Technol., 74 (2010) 342–347.

18. M.H. Isa, E.H. Ezechi, Z. Ahmed, S.F. Magram and S.R. Kutty, Boron removal by electrocoagulation and recovery, Water Res., 51 (2014) 113–123.

19. H.J. Mansoorian, A.H. Mahvi and A.J. Jafari, Removal of lead and zinc from battery industry wastewater using electrocoagulation process: Influence of direct and alternating current by using iron and stainless steel rod electrodes, Sep. Purif. Technol., 135 (2014) 165–175.

20. M. Uğurlu, A. Gürses, C. Doğar and M. Yalçin, The removal of lignin and phenol from paper mill effluents by electrocoagulation, J. Environ. Manage., 87 (2008) 420–428.

21. M.G. Arroyo, V. Pérez-Herranz, M.T. Montañés, J. García-Antón, J.L. Guiñón, Effect of pH and chloride concentration on the removal of hexavalent chromium in a batch electrocoagulation reactor, J Hazard Mater., 169 (2009) 1127–1133.

22. A. Attour, M. Touati, M. Tlili, M. Ben Amor, F. Lapicque and J-P. Leclerc, Influence of operating parameters on phosphate removal from water by electrocoagulation using aluminum electrodes, Sep. Purif. Technol., 123 (2014) 124–129.

23. K. Nakanishi, T. Sakiyama and K. Imamura, On the adsorption of proteins on solid surfaces, a common but very complicated phenomenon, J. Biosci. Bioeng., 91 (2001) 233–244.

24. W. Norde, F.G. Gonzalez and C.A. Haynes, Protein adsorption on polystyrene latex particles, Polym. Adv. Technol., 6 (1995) 518-525.

25. V. Krisdhasima, J. McGuire and R. Sproull, Surface hydrophobic influence on β-lactoglobulin adsorption kinetics, J. Colloid Interf. Sci., 154 (1992) 337–350.

26. M. Khemis, J-P. Leclerc, G. Tanguy, G. Valentin and F. Lapicque, Treatment of industrial liquid wastes by electrocoagulation: Experimental investigations and an overall interpretation model, Chem. Eng. Sci., 61 (2006) 3602–3609.

27. A.H. Essadki, B. Gourich, M. Azzi, C. Vial and H. Delmas, Kinetic study of defluoridation of drinking water by electrocoagulation/electroflotation in a stirred tank reactor and in an external-loop airlift reactor, Chem. Eng. J., 164 (2010) 106–114.

28. A. Addesso and B. Lundj, Influence of solid surface energy on protein adsorption, J. Food Process. Preserv., 21 (1997) 319–323.

CHAPTER 4: PRELIMINARY PURIFICATION OF VOLATILE FATTY ACIDS IN A DIGESTATE FROM ACIDOGENIC FERMENTATION BY ELECTROCOAGULATION

This article is published online on April 2017 in Separation and Purification Technology. Consequently, it follows the guidelines of this journal.

Nidal Fayad, Tania Yehya, Fabrice Audonnet, Christophe Vial.

Preliminary purification of volatile fatty acids in a digestate from acidogenic fermentation by electrocoagulation

Separation and Purification Technology, volume 184, pages 220–230.

ABSTRACT

This study investigated for the first time the use of electrocoagulation (EC) in the batch mode with aluminum or iron electrodes for the preliminary purification of volatile fatty acids (VFA) in a digestate from acidogenic fermentation. The respective influences of electrolysis time, electrode material, current density, inter-electrode distance and initial pH (pH_i) on the efficiency of the process were investigated. Experimental results showed that VFA were totally found in the liquid phase at the end of EC in all cases, while EC removed efficiently (> 80%) solids and other soluble compounds including nitrogenous and phosphorous species. Reduction of EC operating cost was achieved by working at the lowest current density (9.3 mA/cm^2) and at the lowest inter-electrode distance (1.0 cm), independently from pH_i. Operating costs were evaluated to be 0.26 ± 0.03 and 1.07 ± 0.04 US $/m^3$ with or aluminum electrodes, respectively.

Keywords: Electrocoagulation; digestate; preliminary purification; volatile fatty acids; soluble or solid compounds

1. INTRODUCTION

Volatile fatty acids (VFA) are versatile carboxylic acids, which are widely used in the food, pharmaceutical, petrochemical, cosmetic and leather (tanning) industries [1]. Moreover, VFA are used as a raw material in various industrial processes, carbon source in biological nitrogen/phosphorus elimination processes, carbon source in bio-electrochemical or bio-H_2 processes, and intermediates in the production of bulk commodities [2]. Additional innovative

applications for VFA include their thermal conversion to ketones and subsequent hydrogenation to alcohol fuels, or even their use as electron donors in microbial fuel cells [3]. Acidogenic fermentation and anaerobic digestion of organic wastes are favorable technologies for VFA production by eliminating the methane forming phase [4]. Harvesting the produced VFA from the digestate stays a major challenge due to the complex physicochemical nature of fermented effluents and the low concentration of VFA in fermentation broth. Among the newly developed technologies used for VFA recovery from the digestate, membrane based processes such as nanofiltration and water electrodialysis are considered attractive and efficient methods for VFA recovery [5]. However, these processes require either high pressure or high electric energy input which render them uneconomic, without forgetting the obstacle of fouling which limits the use of membranes if the concerned solution was not pre-treated. Other techniques such as reactive distillation [6] and extractive distillation [7] were proposed to recover VFA from aqueous solutions; however, these processes are more expensive for water removal than membrane technology [8, 9].

Electrocoagulation (EC) which is an electrochemical process mainly used to treat wastewaters in terms of both organic matter and nutrient removal [10], may be used as an alternative process for the preliminary purification of VFA in the digestate from acidogenic fermentation. EC has been successfully implemented for the treatment of different types of wastewater including alcohol distillery wastewater [11], olive mill wastewater [12] and tannery wastewater [13]. In addition to that, EC was successfully used as a preliminary purification process. For example, it was used for the pretreatment of produced water prior to reverse osmosis [14] and pretreatment of seawater prior to desalination by reverse osmosis [15].

EC has gained much attention due to its attractive advantages as: simplicity, reliability and cost efficiency. The process is based on the use of sacrificial electrodes such as aluminum, iron that are oxidized to produce metal ions that can be used to coagulate and react with organic matter and nutrients in the wastewater. When current is applied, the metal ions that are produced react with primary hydroxides and produce polyhydroxides and polyhydroxy-metallic flocs [16].

The reactions that occur at the electrodes in EC are as follows. For aluminum electrodes [17]:

Oxidation reaction takes place at the anode:

$$Al \rightarrow Al^{3+} + 3e^{-} \quad (1)$$

Reduction reaction takes place at the cathode:

$$3H_2O + 3e^- \rightarrow (3/2)H_2 + 3OH^- \quad (2)$$

At high pH values, both anode and cathode may be chemically attacked by OH^- ions according to the following reaction [18]:

$$2Al + 6H_2O + 2OH^- \rightarrow 2Al(OH)_4^- + 3H_2 \quad (3)$$

Then, the produced Al^{3+} and OH^- ions react to form monomeric and polymeric species which transform finally into $Al(OH)_3$.

For iron electrodes, two mechanisms have been suggested to explain the production of iron hydroxides [19].

Mechanism 1:

$$4Fe + 10H_2O + O_2 \rightarrow 4Fe(OH)_3 + 4H_2 \quad (4)$$

Mechanism 2:

$$Fe + 2H_2O \rightarrow Fe(OH)_2 + H_2 \quad (5)$$

Therefore, flocs are produced from either $Fe(OH)_2$ or $Fe(OH)_3$ precipitation.

The aim of this study was, therefore, to investigate the possibility of using EC for the preliminary purification of VFA in digestate from acidogenic fermentation using the coagulation and the co-precipitation of other species as purification mechanisms. The influence of the most important operating parameters (time, electrode material, current density, inter-electrode distance and initial pH (pH_i) on the efficiency of the process was studied. Moreover, the process operating cost was evaluated.

2. MATERIALS AND METHODS

2.1. DIGESTATE PREPARATION AND EC EXPERIMENTS

EC was applied to a digestate issued from acidogenic fermentation of glucose. Acidogenic fermentation was carried out at pH 6, temperature 35°C, and stirring speed of 100 rpm, but the pH of the digestate was 6.3. The composition and characteristics of this digestate are presented in **Table 1**. The digestate was preserved at 4°C throughout this study before experiments and analyses. EC was carried out in a 500-mL cylindrical tank, while agitation was performed by a magnetic stirrer. EC was conducted in the galvanostatic mode by the help of a generator (Voltcaraft HPS - 13015, Germany), while the cell voltage (U) was recorded in order to derive the electric energy consumption. The experimental setup is shown in **Figure 1**. Monopolar

rectangular aluminum or iron electrodes of identical dimensions (4.0 cm×6.5 cm) were used as anode and cathode.

Before each experiment, both electrodes were rinsed with acetone and a 0.01 N HCl solution to eliminate organic and inorganic deposits. These electrodes were weighed before and after each experiment to calculate the faradaic yield derived from Faraday's law. According to Faraday's law, the theoretical mass of dissolved iron or aluminum from the sacrificial anode at a specific electrical current during EC process is calculated according to the following mathematical expression:

$$m = M_r.I.t/z.F \quad (6)$$

where m is the amount of the dissolved anode material (g), M_r is the specific molecular weight of the anode (aluminum or iron) (g/mol), I is the applied current (A), t is the electrolysis time (s), z is the number of electrons involved in the reaction and F is the Faraday's constant (96485.3 C/mol).

Experiments were carried out at room temperature (20±1)°C and atmospheric pressure. During EC, samples were taken out with an interval time of 10 minutes and were left to settle for 90 minutes before analysis. Stirring speed during EC was always fixed at 100 rpm. This was chosen since preliminary results highlighted that higher tested rotation speeds up to 300 rpm consumed more energy and, at the same time, never changed significantly the removal yield of total solids, nitrogenous species, phosphorous compounds and chemical oxygen demand.

Table 1. Composition and properties of the digestate.

Parameter	**Value**

pH	6.3±0.1
Conductivity (μS/cm)	18700±200
TN (mg/L)	350±5
NH_4^+-N (mg/L)	200±5
TP (mg/L)	750±20
COD (mg/L)	19500±500
Turbidity (NTU)	3500±50
TSS (g/L)	8.0±0.5
Total VFA (g/L)	9.0±1.0
Butyric acid (g/L)	6.3±0.5
Acetic acid (g/L)	1.5±0.5
Ethanol (g/L)	0.4±0.1
Glycerol (g/L)	0.9±0.1

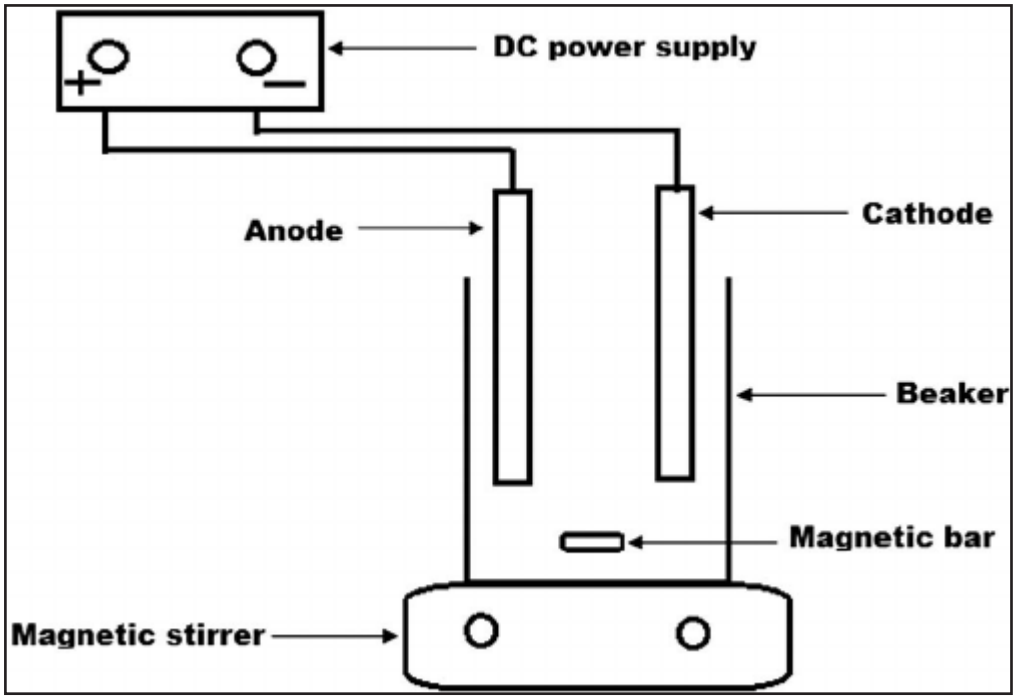

Figure 1. Schematic diagram of the experimental set-up.

2.2. ANALYSES

All analyses were conducted in triplicate. pH and conductivity of the solution were monitored over time using a Seven Easy pH meter (Mettler-Toledo, Switzerland) and a Seven Excellence multimeter (Mettler-Toledo, Switzerland), respectively. The concentration of VFA was measured using a high-performance liquid chromatography (HPLC) device. Before analysis, each sample was de-proteinized to prevent clogging of the column. For this, 250 µL of barium hydroxide solution ($Ba(OH)_2$; 0.3 M) and 250 µL of zinc sulphate solution ($ZnSO_4$, $7H_2O$; 5% w/v) were added to 2 mL of the sample. These compounds cause precipitation of the proteins present in the medium. After centrifugation (Beckman Coulter, USA) for 5 minutes at 10000 rpm, the supernatant was filtered using a cellulose acetate syringe filter 0.45 µm (CHROMAFIL, Germany) and placed in vials. The used apparatus was HPLC 1260 Infinity Quaternary LC system (Agilent Technology, USA). The used chain consisted of two columns of ion exclusion connected in series (Rezex ROA 300 × 7.8 mm, Phenomenex, USA). The mobile phase was a solution of 2 mM sulfuric acid diluted in ultrapure water (Millipore, MilliQmore) continuously degassed with a degasser (Ney Ultrasonik 300) integrated to the apparatus. The flow rate was fixed at 0.7 mL/min using a pump (HP 100 Series, Agilent Technologies, USA). The device was equipped with an automatic injector fixed loop (Rheodyne valve Agilent) that delivers 10 µL. VFA detection was done by a refractometer (HP 1100 series, Agilent Technologies, USA). The signals delivered by the sensor were processed by an integrator (HP 1100 series). The acquisition and integration of data were achieved through a software (HP Chem, Agilent Technologies, USA). Turbidity was measured using a colorimeter DR/890 (Hach Lange GmbH, Germany) containing an infrared diode of 890 nm and a light reflection detector. The concentration of total suspended solids (TSS) was determined according to the standard method 2540 D by filtering a defined water volume through a membrane filter (cellulose nitrate 0.45 µm) and weighing the dried residues. Chemical oxygen demand (COD) measurement was performed using a thermoreactor COD meter and a spectrophotometer DR/890 (Hach Lange GmbH, Germany). Total nitrogen (TN) was measured using a TNM-1 analyzer (Shimadzu, Japan). Ammonium nitrogen (NH_4^+-N) was measured using Berthelot method. Total phosphorus (TP) was measured using the acid persulfate digestion method.

The removal efficiency of each soluble or solid compound was calculated using the following equation:

$$R\ \% = (C_0 - C_t)/C_0 \quad (7)$$

where R is the removal efficiency of the soluble or solid compound, C_0 is the initial concentration of the soluble or solid compound and C_t is its concentration at time t. The concentration of dissolved aluminum in the effluent at the end of the EC treatment was determined using a spectrophotometric analysis based on the aluminum(III)-Eriochrome Cyanine R complex [20].

3. RESULTS AND DISCUSSION

3.1. PRELIMINARY SETTLING EXPERIMENTS

Before exposing the digestate to EC and to investigate the effect of settling on digestate components, this digestate was left to settle for 24 hours. These results showed that settling did not affect VFA concentration in the digestate. However, settling resulted in low removal efficiency of 31.5 ± 2.0 %, 35.6 ± 1.0 %, 2.6 ± 0.2%, 3.8 ± 0.5 % and 3.5 ± 0.4% for turbidity, TSS, COD, TN and TP, respectively. Due to the inefficiency of settling alone to separate VFA from other digestate components, EC was applied to the digestate before leaving it to settle.

3.2. EC EXPERIMENTS

As settling was not efficient in separating the VFA from the other components of the digestate, EC was carried out to assess its effect on the digestate components. The effects of electrolysis time, electrode material current density, inter-electrode distance and initial pH were investigated.

3.2.1. INFLUENCE OF EC ELECTROLYSIS TIME

The first series of experiments aimed to study the influence of EC time on the digestate components. For this, EC was performed at current density 9.3 mA/cm^2 for 90 min., pH_i 6.3, a stirring speed of 100 rpm and 1 cm inter-electrode distance with aluminum electrodes. Experimental results showed that the concentrations of the main VFA (butyric acid and acetic acid) were constant during EC, regardless of EC time (**Table 2**). VFA were not removed, as it seems that they were neither oxidized by EC, nor adsorbed on flocs formed during EC, due on the one hand to the incompatibility of sizes between the small low molecular weight VFA and the large pores in flocs and, on the other hand, to the electrostatic properties of the flocs and the VFA. Moreover, VFA did not precipitate as they are very soluble in water, and at the same time, it is probable that the compounds which may precipitate the VFA do not exist or exist in

negligible concentrations in the digestate. Results also showed that turbidity, TSS, COD, TN and TP were effectively removed by EC (**Table 3**). The observed low COD removal efficiency could be explained by the inefficiency of EC in removing the VFA and the low efficiency of EC in removing glycerol and ethanol, the other two main organics in the digestate. Also, this might be due to the low removal efficiency of some other organic compounds found in very low amounts which were not taken into consideration. This low efficiency of EC in removing glycerol and alcohol was also reported by Zhao et al. [14]. In fact, the increase of removal efficiency as time proceeds was also reported by Sadeddin at al. [21]. This result could be easily explained according to Faraday's law which implies that aluminum ions that are at the origin of aluminum hydroxides formation (responsible for soluble or solid compounds removal) increase with time [22].

As seen in **Table 3**, 60 min. of EC was enough for the insoluble and soluble organic compounds, or N and P species (Turbidity, TSS, COD, TN and TP), as the removal efficiency of all these tested parameters did not increase significantly after 60 min. of electrolysis. Based on these results, the subsequent experiments were performed for 60 min to save energy.

Table 2. Influence of time on VFA (butyric and acetic acid). Conditions: Al electrodes, current density 9.3 mA/cm^2, pH_i 6.3, inter-electrode distance 1 cm, stirring speed 100 rpm.

Time (min)	Butyric acid concentration (g/L)	Acetic acid concentration (g/L)
0	6.34 ± 0.02	1.36 ± 0.01
10	6.35 ± 0.03	1.36 ± 0.02
20	6.33 ± 0.01	1.35 ± 0.02
30	6.34 ± 0.02	1.34 ± 0.01
40	6.34 ± 0.04	1.33 ± 0.02
50	6.33 ± 0.04	1.34 ± 0.03
60	6.34 ± 0.03	1.34 ± 0.02
70	6.33 ± 0.03	1.33 ± 0.02
80	6.34 ± 0.02	1.35 ± 0.01
90	6.35 ± 0.02	1.36 ± 0.02

Table 3. Influence of time on the removal efficiency of turbidity, TSS, TN, COD and TP. Conditions: Al electrodes, current density 9.3 mA/cm^2, pH$_i$ 6.3, inter-electrode distance 1 cm, stirring speed 100 rpm.

Time (min)	Turbidity removal efficiency (%)	TSS removal efficiency (%)	TN removal efficiency (%)	COD removal efficiency (%)	TP removal efficiency (%)
10	15.5 ± 0.5	18.1 ± 1.0	20.5 ± 0.5	2.3 ± 0.5	25.5 ± 1.0
20	29.5 ± 0.5	31.5 ± 1.5	32.3 ± 1.0	6.8 ± 0.5	39.9 ± 2.0
30	40.5 ± 1.5	43.5 ± 0.5	45.5 ± 1.5	10.2 ± 1.0	55.7 ± 1.5
40	59.6 ± 1.0	63.5 ± 2.0	52.3 ± 1.0	13.2 ± 0.5	68.5 ± 1.0
50	61.5 ± 1.5	66.7 ± 1.5	55.3 ± 0.5	14.5 ± 1.5	72.5 ± 0.5
60	63.2 ± 2.0	68.5 ± 1.0	56.4 ± 1.0	15.6 ± 1.0	75.4 ± 1.0
70	64.3 ± 1.0	69.1 ± 1.0	57.2 ± 1.0	16.2 ± 0.5	78.2 ± 1.5
80	65.1 ± 1.0	69.2 ± 1.0	57.4 ± 1.0	16.5 ± 0.5	79.1 ± 1.0
90	65.9 ± 1.0	70.1 ± 1.5	58.3 ± 0.5	17.1 ± 1.0	80.1 ± 1.0

3.2.2. INFLUENCE OF THE ELECTRODE MATERIAL: ALUMINUM AND IRON

Electrode material is essential in the EC process. Therefore, this material should be chosen carefully. The most common electrode materials used for electrocoagulation are aluminum and iron, as they are cheap, readily available and effective [23, 24]. In this series of experimental runs, the effect of EC on the digestate was investigated with both electrode materials (aluminum and iron) at current density 9.3 mA/cm^2, pH$_i$ 6.3, stirring speed of 100 rpm and inter-electrode distance 1 cm for 60 min. Experimental data showed that EC with both electrode materials did not have any significant influence on the removal of the VFA which remained in the digestate (**Figure 2a**). However, as shown in **Figure 2b**, aluminum electrodes were more efficient than iron electrodes in the removal of insoluble and soluble organic compounds, or N and P species (turbidity, TSS, COD, TN and TP). The removal efficiency of turbidity, TSS, TN, TP, and COD increased from 45.3 ± 1.0%, 61.2 ± 2.0%, 51.2 ± 1.0%, 63.5 ± 1.0% and 7.5 ± 1.0% with iron electrodes to 63.2 ± 1.0%, 68.5 ± 2.0%, 56.4 ± 1.0%, 75.4 ± 1.0% and 15.6 ± 1.0% with aluminum, respectively. The better performance of aluminum electrodes in comparison to iron ones is because iron hydroxides are relatively inefficient coagulants compared to aluminum hydroxides [25] coupled to ahigher faradaic yield with aluminum electrodes [26]. Higher efficiency of aluminum electrodes was also reported by Govindan et al. [27] who worked on the removal of fluoride ions. The weak decrease of COD is mainly due to VFA which are not removed. TN abatement is also limited by the fact that EC is not able to remove NH_4^+ cations. Even though the faradaic yield increased from 97 ± 3% to 157 ± 6% when switching from iron

to aluminium electrodes, the mass of dissolved metal at constant current density was higher with Fe electrodes than with Al electrodes, the mass of dissolved metal at constant current density was higher with iron electrodes than with aluminium electrodes (**Figure 2c**). This is due to the fact that the dissolution of 1 mol Al needs 3 mol electrons, whereas 1 mol Fe needs only 2 mol electrons at constant current; moreover, the molar mass of Fe is much higher (55.85 g/mol) than that of Al (26.98 g/mol). The high faradaic yield (>100%) with aluminum electrodes may be explained by the chemical oxidation of aluminum electrodes [28]. This oxidation is not taken into consideration by Faraday's law. The lower faradaic yield with iron electrodes (<100%) is due to the fact that iron corrosion occurs only in acidic media and in much lower extent than that for aluminium [29]. Moreover, in this case, pH reached more than 8 after 40 min. of electrolysis. At this alkaline pH value, iron oxidation leads to Fe (III) species formation as oxides or hydroxides. This decreases the iron concentration produced, because Fe (III) species formation requires 3 electrons instead of 2 and so, a higher current is needed for achieving the same iron concentration.

Experimental results also showed that pH increased more with iron electrodes, as illustrated by **Figure 2d**. Actually, pH reached 8.6 ± 0.1 and 7.3 ± 0.1 with iron and aluminum electrodes, respectively after 60 min. of electrolysis. This difference may be due to the different buffering properties of the two metal hydroxides. After settling, it was observed that the effluent treated with aluminum electrodes was very clear; however, in the case of iron electrodes, a yellow color was observed in the effluent which is due to the presence of $FeCl_3$. Usually at the beginning of EC with iron electrodes, a green color appears due to $FeCl_2$. Later, Fe (II) is oxidized to Fe (III) that combines with Cl^- ions to form $FeCl_3$ which turns color yellow and turbid. However, in this study, the green color was not observed at the beginning of EC as the solution was highly turbid.

From these results that highlight a better performance of aluminum electrodes, subsequent experiments were performed only with aluminum electrodes.

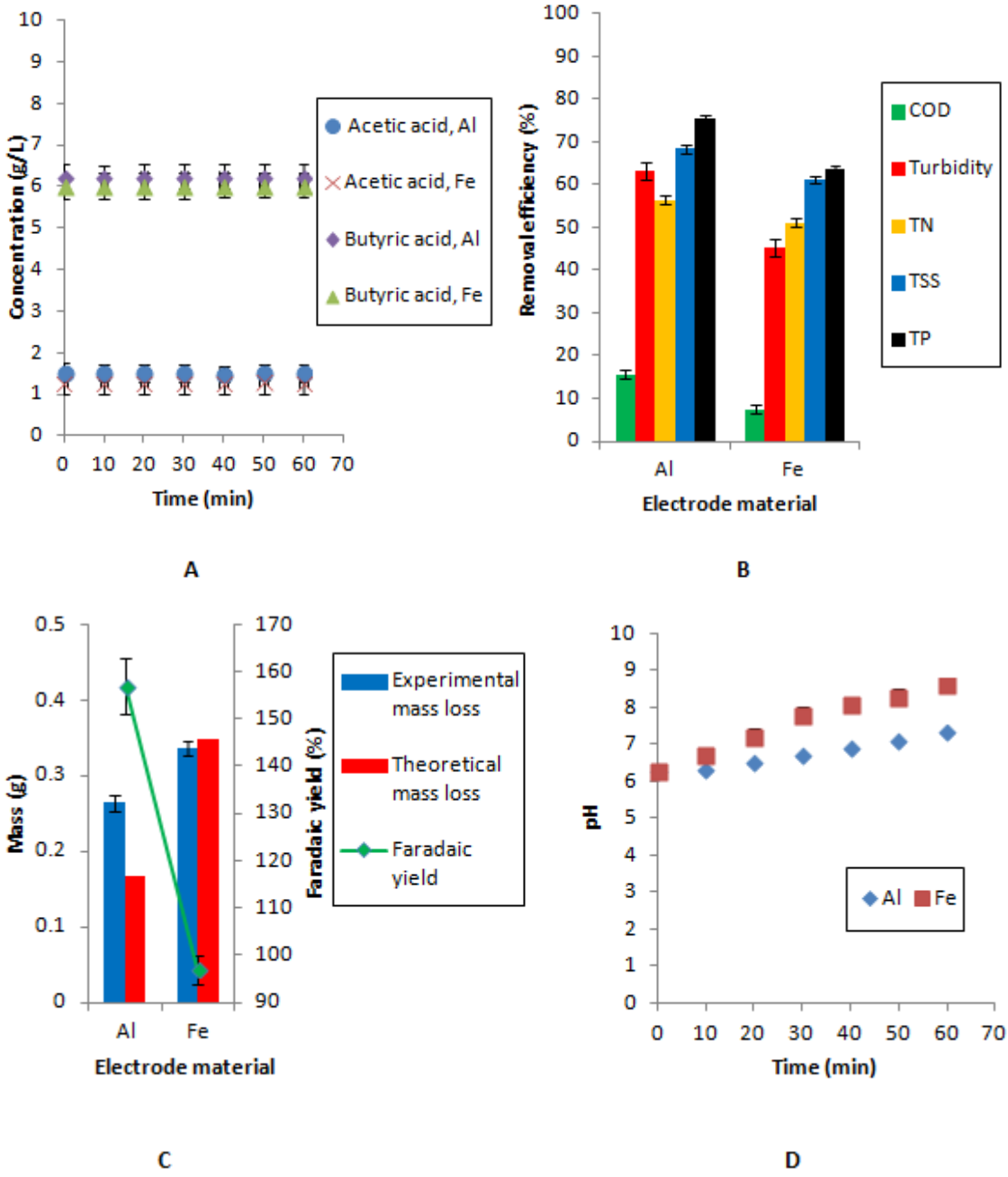

Figure 2. Influence of electrode material on: A) VFA (butyric and acetic acid) concentration, B) Removal efficiency of COD, turbidity, TN, TSS and TP, C) Experimental mass loss and faradaic yield, and D) pH evolution. Conditions: current density 9.3 mA/cm^2, pH_i 6.3, stirring speed 100 rpm, inter-electrode distance 1 cm, electrolysis time 60 min. Error bars represent standard deviations.

3.2.3 INFLUENCE OF CURRENT DENSITY

Current density is the most important parameter in all electrochemical processes as it determines the rate of the coagulant release, bubble production and growth of flocs [30]. In this series of runs, three current densities were tested (9.3 mA/cm^2, 18.5 mA/cm^2 and 27.8 mA/cm^2) at pH_i 6.3, stirring speed of 100 rpm and inter-electrode distance 1.0 cm.

Experimental results showed that current density did not affect the concentration of VFA in the digestate, as this concentration remained invariable during EC **(Figure 3a)**. **Figure 3b** shows the influence of EC on soluble or solid compounds in the digestate. It is clear that the removal efficiency of all these compounds was higher as current density increased. For example, the removal efficiency of turbidity, TSS, TN, TP and COD increased from 75.3 ± 1.0%, 80.5% ± 2.0, 70.3 ± 2.0%, 85.6 ± 2.0% and 19.6 ± 1.0% to 85.3 ± 2.0%, 88.3 ± 1.0%, 80.5 ± 1.0%, 92.3 ± 1.0% and 23.3 ± 1.0% as current density increased from 18.5 mA/cm2 to 27.8 mA/cm2, respectively. This result is consistent with those of Zeboudji et al. [31] and Palahouane et al. [32], who found that the removal efficiency of boron and fluoride ions by EC, respectively, increased with the increase of current density. This result is due to the enhanced aluminum dissolution at higher current density values which results in the formation of more aluminum hydroxide flocs [33]. This was proved experimentally in this study, as the mass of flocs formed increased from 0.90 ± 0.02 g (corresponds to 1.80 ± 0.04 kg/m^3) to 2.30 ± 0.01 g (corresponds to 4.60 ± 0.02 kg/m^3) when current density increased from 9.3 mA/cm^2 to 27.8 mA/cm^2. The produced flocs adsorb or neutralize insoluble and soluble organic compounds, or N and P species and consequently result in better removal efficiency. Concerning sludge disposal costs, at the lowest current density of 9.3 mA/cm^2, it is 0.108 ± 0.002 US \$/m^3, assuming that this cost (excluding drying costs and including transportation) is 0.06 US \$/kg.

The final conductivity of the digestate decreased slightly from 18700 ± 500 µS/cm to 17500 ± 200 µS/cm and the final pH increased from 7.3 ± 0.1 to 8.2 ± 0.1 as current density increased from 9.3 (mA/cm^2) to 27.8 (mA/cm^2). The conductivity decrease may be attributed to the adsorption of ions (cations and anions) on the formed aluminum hydroxide flocs. Lower conductivity values at higher current density values can be explained by the higher final pH at higher current density. pH increased at all the current densities tested, and it reached higher values with higher current density **(Figure 3c)**. The reason behind pH increase during EC is due to OH^- ions production at the cathode [34]. More OH^- ions are produced at higher current densities resulting in higher pH values. In this case, the extent of OH- ions production was more

important than OH^- consuming phenomena. However, there is still a debate on the cause of pH increase with aluminum electrodes. Several authors [35] attributed the pH increase to hydrogen evolution at the cathode (accompanied by OH^- ions production). However, according to Chen et al. [36], this pH increase can result from the transfer of CO_2 or from the existence of some anions such as Cl^- and SO_4^{2-}, they can exchange partly with OH^- in $Al(OH)_3$ to free OH^-, which also causes pH increase.

Faradaic yield was always higher than 100%, but decreased when current density increased with Al electrodes **(Figure 3d)**, which resulted from an increase of the cathodic protection of the cathode against chemical corrosion when current increased and secondary reactions as water oxidation (equation 8) that compete with aluminum oxidation especially at high current density values [29].

$$2H_2O \rightarrow O_2 + 4H^+ + 4e^- \quad (8)$$

In fact, if the experimental mass loss from the cathode is disregarded and only the experimental mass loss from the anode is taken into account, faradaic yield would decrease and get closer to 100% than when the experimental mass loss is measured from both electrodes. Actually, faradaic yield values would become 123 ± 4%, 115 ± 1% and 109 ± 1% for current densities of 9.3 mA/cm^2, 18.5 mA/cm^2 and 27.8 mA/cm^2, respectively. This means that in all cases, the majority of excess aluminum dissolved is due to pitting corrosion (due to Cl^- in the digestate) on the one hand and chemical attack of the cathode on the other hand due to the alkalinity at its vicinity according to the equation (9):

$$2Al + 6H_2O \rightarrow 2[Al(OH)_4]^- + 3H_2 \quad (9)$$

Excess aluminum from the anode that was less than that from the cathode is due on the one hand to pitting corrosion and on the other hand to chemical attack due to acidity at the proximity of the anode according to equation (10):

$$2Al + 6H^+ \rightarrow 2Al^{3+} + 3H_2 \quad (10)$$

These results also showed that the concentration of residual aluminum was higher at higher current densities. This concentration was 1.3 ± 0.1 mg/L, 1.9 ± 0.2 mg/L and 2.5 ± 0.2 mg/L at current densities of 9.3 mA/cm^2, 18.5 mA/cm^2 and 27.8 mA/cm^2, respectively. Due to this residual aluminium, attention must be paid for the further valorisation of the VFA, especially if microorganisms will be used, as they maybe would not survive. As soluble or solid compounds

were best removed at the highest current density (27.8 mA/cm^2), subsequent experiments were carried out at this current density.

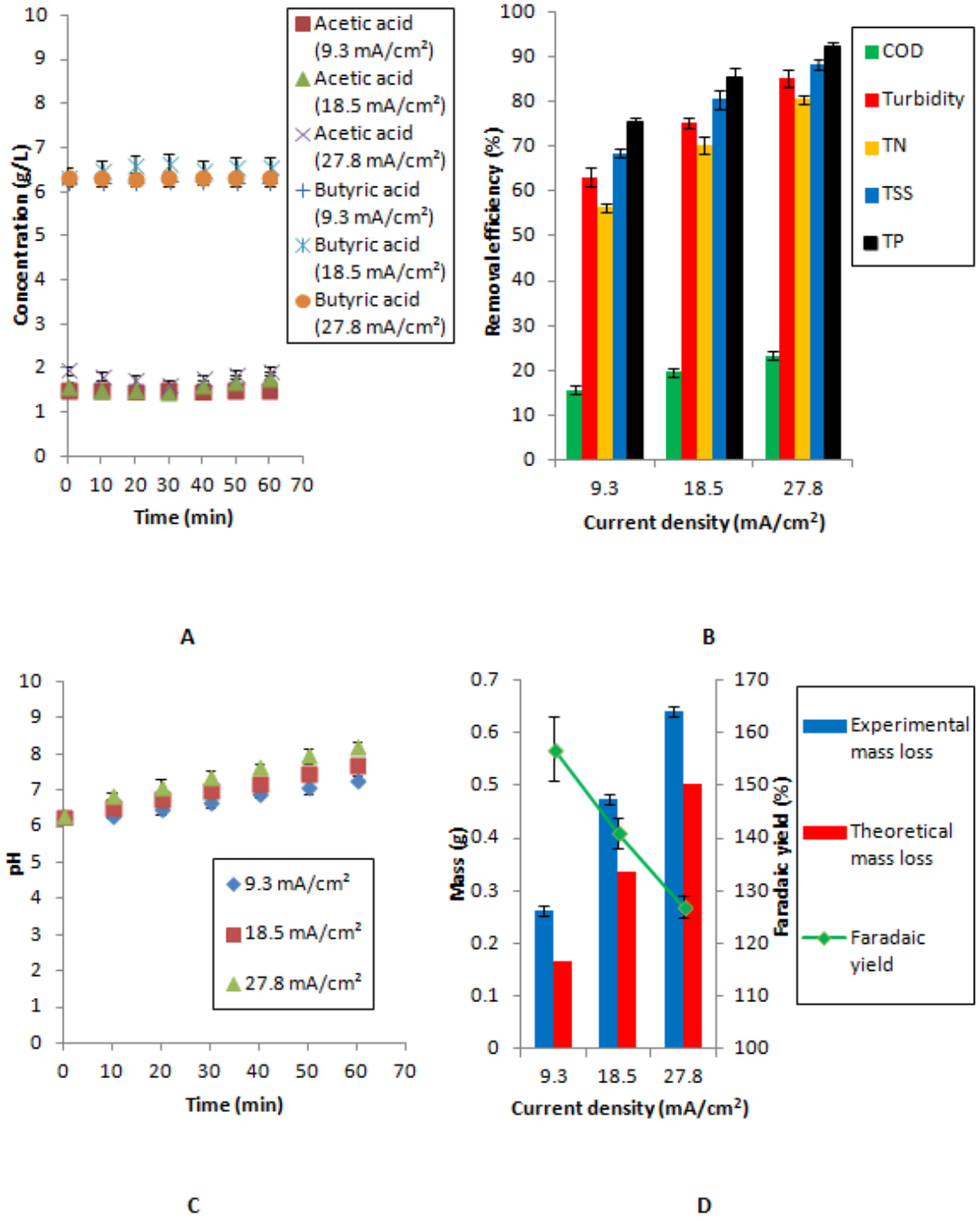

Figure 3. Influence of current density on: A) VFA (butyric and acetic acid) concentration, B) Removal efficiency of COD, turbidity, TN, TSS and TP, C) pH evolution, and D) Experimental mass loss and faradaic yield. Conditions: Al electrodes, pH_i 6.3, stirring speed 100 rpm, inter-electrode distance 1 cm, electrolysis time 60 min. Error bars represent standard deviations.

3.2.4. INFLUENCE OF INTER-ELECTRODE DISTANCE

This new set of experimental runs was dedicated to study the influence of the inter-electrode distance during EC on the digestate components. Three inter-electrode distances were tested (1.0 cm, 1.5 cm and 2.0 cm) at pH_i 6.3, current density 27.8 mA/cm^2 and stirring speed of 100 rpm with aluminum electrodes. As **Figure 4a** shows, VFA concentration was not affected by the inter-electrode distance. These results also showed that, increasing the inter-electrode distance from 1.0 cm to 2.0 cm decreased the removal efficiency of turbidity, TSS, TN, TP, and COD from 85.3 ± 0.2%, 88.3 ± 0.2%, 80.5 ± 0.1%, 92.3 ± 0.1% and 23.3 ± 0.1% to 70.5 ± 0.1%, 76.3 ± 0.2%, 60.3 ± 0.1%, 74.2 ± 0.1% and 8.5 ± 0.1% after 60 min. of electrolysis (**Figure 4b**), respectively. Similar results on the effect of inter-electrode distance were reported by Ghosh et al. [37] who worked on the removal of Fe(II) from tap water by EC.

This better removal efficiency of insoluble and soluble organic compounds, or N and P species at lower inter-electrode distances could be explained by the fact that at this inter-electrode distance, the faradaic yield increases, so that the amount of coagulant released with time is increased [38]. Another possible explanation is that low inter-electrode distances result in an electric field with high potential gradient and low resistance to motion of ions. This results in a faster formation of aluminum hydroxide species and in faster collision of precipitate particles with pollutants and nutrients and H_2 bubbles [15].

Moreover, as the inter-electrode distance increased from 1.0 cm to 2.0 cm, faradaic yield decreased from 127 ± 2% to 96 ± 2%. Experimental aluminum mass loss was 0.48 ± 0.01 g, 0.55 ± 0.01 g and 0.64 ± 0.01 g at inter-electrode distances of 2.0 cm, 1.5 cm and 1.0 cm, respectively (**Figure 4c**). The amount of produced sludge was nearly proportional to the quantity of dissolved aluminum, as the mass of sludge was 1.70 ± 0.02 g (corresponds to 3.40 ± 0.04 kg/m^3), 1.90 ± 0.01 g (corresponds to 3.80 ± 0.02 kg/m^3), and 2.30 ± 0.01 g (corresponds to 4.60 ± 0.02 kg/m^3) at inter-electrode distances of 2.0 cm, 1.5 cm and 1.0 cm, respectively. Considering the amount of sludge produced, the sludge disposal cost is 0.277 ± 0.001 kg/m^3 at inter-electrode distance 1.0 cm. In addition, as aluminum dissolution increased at lower inter-electrode distance, the concentration of residual aluminum also increased. For example, Al concentration in water increased from 1.2 ± 0.1 mg/L to 2.5 ± 0.1 mg/L as the distance decreased from 2.0 cm to 1.0 cm at the same current density (**Figure 4d**), showing an increased effect of the rear faces of the electrodes.

Based on the results in this part, a last set of experiments was carried out at the inter-electrode distance 1.0 cm.

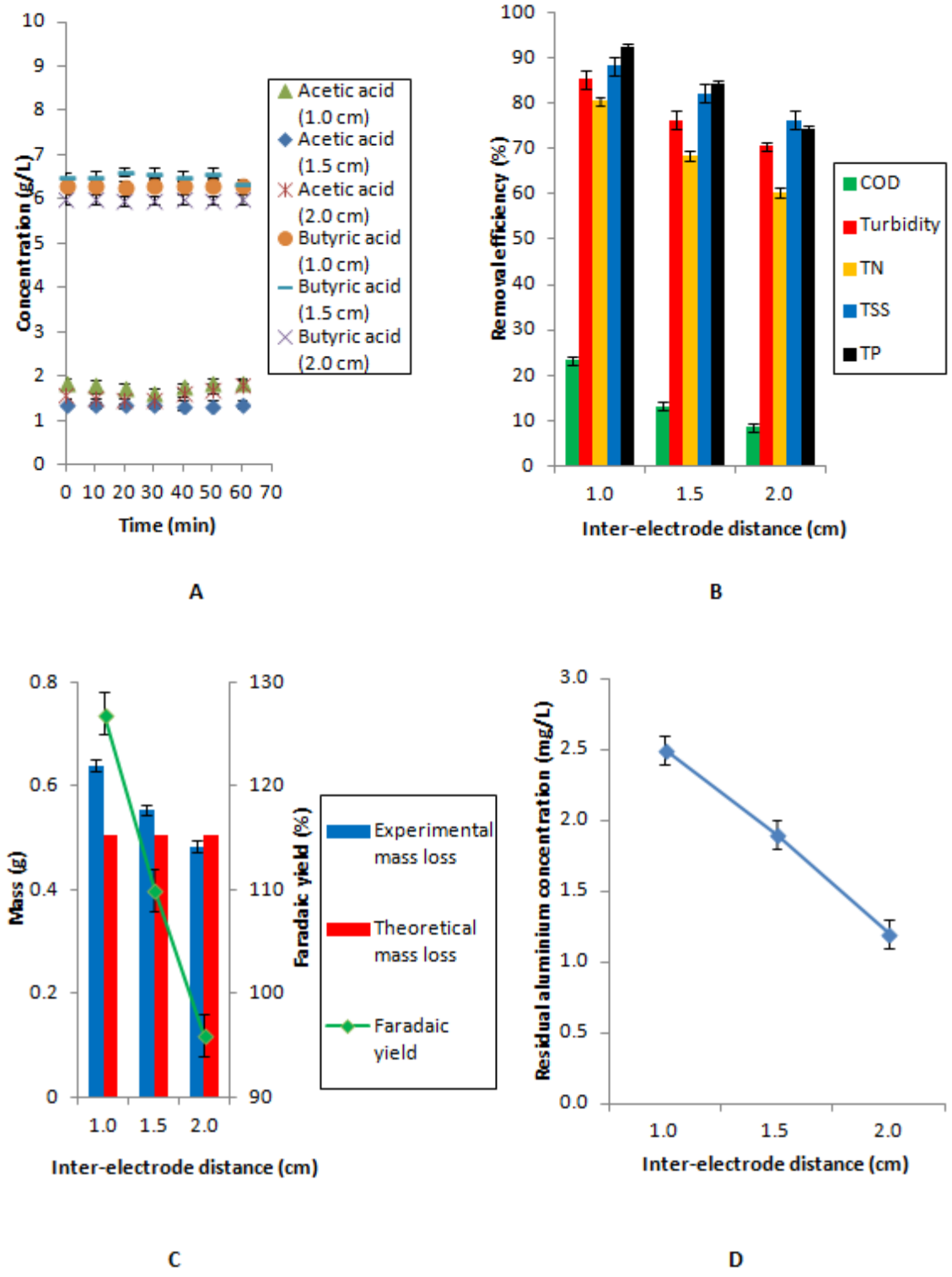

Figure 4. Influence of inter-electrode distance on: A) VFA (butyric and acetic acid) concentration, B) Removal efficiency of COD, Turbidity, TN, TSS and TP, C) Experimental mass loss and faradaic yield, and D) Concentration of residual aluminum. Conditions: Al electrodes, current density 27.8 cm/cm^2, pH_i 6.3, stirring speed 100 rpm, electrolysis time 60 min. Error bars represent standard deviations.

3.2.5. INFLUENCE OF INITIAL pH

Initial pH (pH_i) of the solution is considered as one of the most important parameters influencing strongly the overall EC process as it determines aluminum speciation that results from a spontaneous hydrolysis of electrochemically generated metal cations [31]. This new set of experimental runs was dedicated for the investigation of the influence of pH_i on the removal efficiency of the digestate components during EC. In practice, the pH of digestate should vary only between 5.5 and 6.5. The objectives are to estimate the influence of pH_i and to check whether the adjustment of the initial pH is necessary. Thus, three pH_i values of 4.0, 6.3 (natural pH of the digestate) and 9.0 were tested at current density 27.8 mA/cm^2, stirring speed 100 rpm and inter-electrode distance 1.0 cm with aluminum electrodes. Experimental data showed, as in the previous experiments, that VFA were not removed when pH_i value of the digestate was changed **(Figure 5a)**.

Figure 5b demonstrates that the highest removal efficiency of all insoluble and soluble organic compounds, or N and P species was achieved at pH_i 4.0. But while an alkaline pH_i as 9.0 strongly impaired all the removal efficiencies, the differences between the results at pH_i 4.0 and pH_i 6.3 were slighter: COD, turbidity and TSS removal yields did not vary significantly, whereas only TN and TP removal yields decreased. This constitutes an attractive result because the initial pH of digestate remains between 5.5 and 6.5, in which EC is known to be a robust process. Conversely, lower removal efficiency at pH_i 9.0 is due to the predominance of an ineffecient adsorbant (monomeric $Al(OH)_4^-$ anion) under alkaline conditions [39]. For TN, the decrease of the removal yield when pH increases is probably due a reduced adsorption of charged nitrogenous species (such as proteins) which strongly depends on pH. In the case of TP, this better removal efficiency at more acidic pH_i values may be related to the dominance of $AlPO_4$ at more acidic conditions [38] where phosphate elimination takes place mainly by precipitation. Moreover, at acidic conditions, the oxide surfaces have a net positive charge, and adsorption of anionic phosphate is enhanced by columbic attraction. At higher pH values, the oxide surface has a net negative charge and would tend to repulse the anionic phosphate in solution [40]. This result on phosphate removal is in agreement with the previous works of İrdemez et al. [41] and Attour at al. [38] who found that the most effective phosphate removal is at pH_i 3.0.

Figure 5c shows the influence of pH_i on experimental mass loss and consequently faradaic yield. These results showed that pH_i value did not have a significant influence on aluminum

dissolution. Faradaic yield values were 129 ± 2%, 127 ± 2% and 126 ± 2% at pH_i of 4.0, 6.3 and 9.0, respectively. Concerning pH evolution, and as **Figure 5d** shows, pH increased gradually to reach 6.8 ± 0.1 and 8.2 ± 0.1 at the end of EC at pH_i 4.0 and 6.3, respectively. However, pH decreased slightly down to 8.6 ± 0.1 at pH_i 9.0. This highlights the buffering effect of EC when Al electrodes are involved. This trend is, indeed, attributed to the formation of aluminum hydroxide $[Al(OH)_4]^-$ which is an alkalinity consumer [36, 42]. Finally, the initial pH of the digestate appeared to have no signficant effect on the residual VFA concentration, on the electrode dissolution and, therefore, on the residual aluminum concentration, that was (2.50 mg/L at all pH_i values.). The negligible effect of pH_i on the extent of aluminum dissolution is consistent with the results of Mouedhen et al. [43] who found that there was no significant effect of pH_i on aluminum dissolution above pH_i 3.0 and confirms the previous explanation that removal efficiency was not related to the amount of dissolved aluminum or formed flocs but to the nature of aluminum hydroxides at each pH_i value. The conclusion is, therefore, that no pH adjustment of the disgestate is necessary before EC treatment.

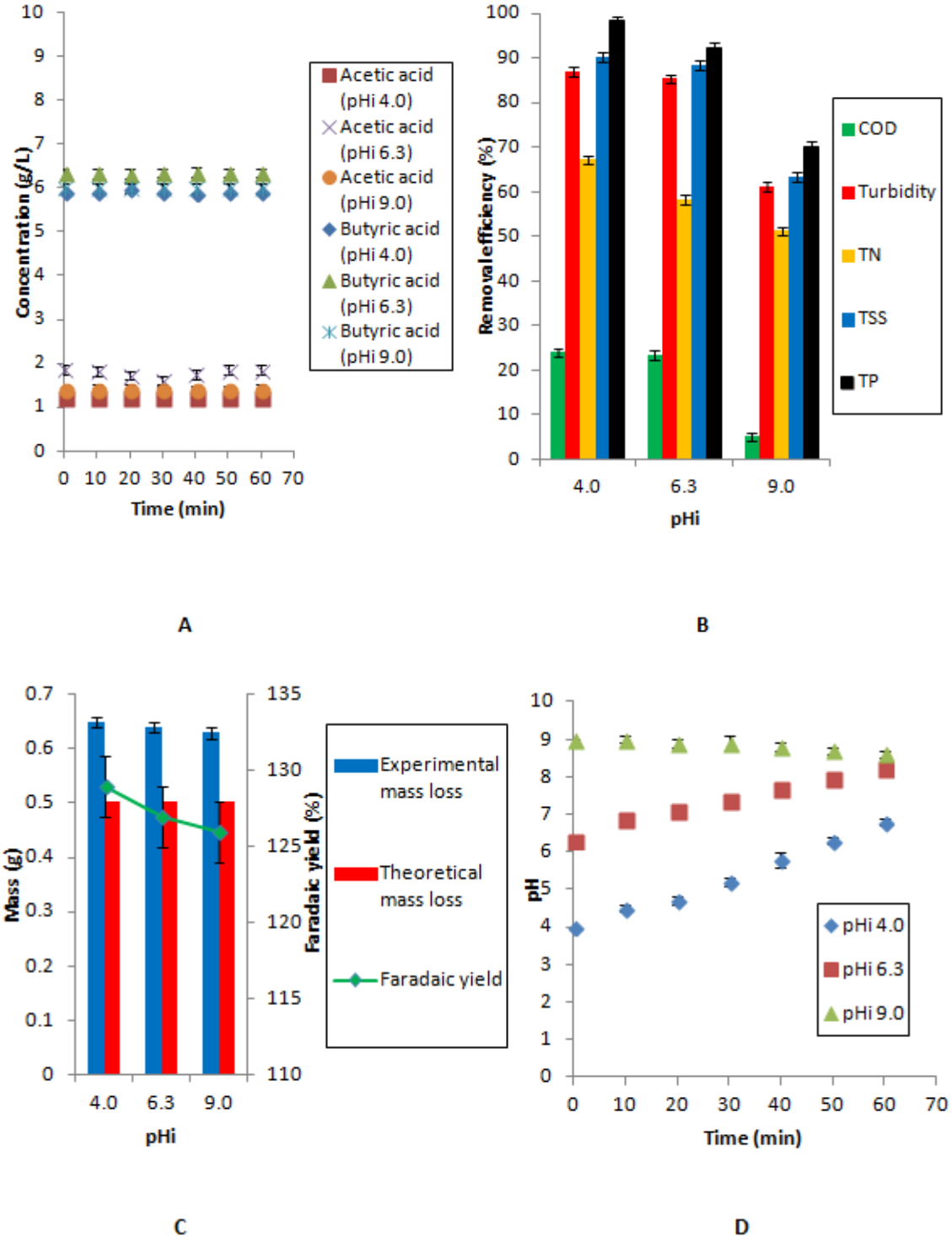

Figure 5. Influence of initial pH (pH_i) on: A) VFA (butyric and acetic acid) concentration, B) Removal efficiency of COD, Turbidity, TN, TSS and TP, C) Experimental mass loss and Faradaic yield, and D) pH evolution. Conditions: Al electrodes, current density 27.8 cm/cm^2, stirring speed 100 rpm, inter-electrode distance 1 cm, electrolysis time 60 min. Error bars represent standard deviations.

3.3. EC COST ANALYSIS

EC showed its efficiency in the preliminary purification of VFA in the digestate from acidogenic fermentation, as VFA remained in the liquid phase at all tested conditions, while the other components were removed at different percentages. EC was proven to be an efficient process; however, its practical applicability is related to its operating cost. In this study, EC operating cost (US $/m^3) was calculated as the total sum of the costs of electrode material consumption (EMC) and electrical energy consumption (EEC). The price of the electrode material used was estimated at 1.5 US $/kg Al and 0.08 US $/kg Fe and the price of electrical power was considered at 0.13 US $/kWh. The mass of electrode material consumed (g) after 60-minute electrolysis time is estimated from electrodes mass difference before and after electrocoagulation.

EEC (kWh/m^3 water) after 60 minutes of digestate solution treatment was calculated using equation (11):

$$EEC\ (kWh/m^3) = U.I.t/V \quad (11)$$

where U is the cell voltage (V), I is the current (A), t is the electrolysis time (h) and V is the volume (L) of effluent to be treated. EC cost was calculated in terms of electrode material, current density, inter-electrode distance and pH_i. The consequence of Eq. (10) and (11) is that EC cost is nearly proportional to time; so, only the results at 60 min. of electrolysis will be presented.

Experimental results showed that EC cost was higher with aluminum electrodes than with iron electrodes. In fact, EC cost increased from 0.26 ± 0.03 US $/m^3 to 1.07 ± 0.04 US $/m^3, switching from iron to aluminum when current density was 9.3 mA/cm^2 **(Figure 6a)**. This difference in operating cost is due to the much higher EMC with aluminum electrodes, as EEC was only slightly higher with iron electrodes (between 1.5 and 2.0 kWh/m^3). Although the amount of experimental electrode mass loss is higher in the case of iron (0.34 ± 0.01 g compared to 0.26 ± 0.01 g in the case of aluminum electrodes); however, EMC is 0.8 US $/m^3 and 0.05 US $/m^3 with aluminum and iron electrodes, respectively. This is due to the much higher price of aluminum.

Then, **Figure 6b** describes the influence of current density with aluminum electrodes on EC operating cost. As shown in this figure, higher current density led to higher EC cost in the range investigated: increasing current density from 9.3 mA/cm^2 to 27.8 mA/cm^2 increased EC cost from 1.07 ± 0.04 US $/m^3 to 3.75 ± 0.04 US $/m^3. At all current densities tested, EMC

contribution to the total EC cost was higher than the contribution of EEC. However, at current density 27.8 mA/cm^2, EMC contribution to the total EC cost was just slightly higher than the contribution of EEC. EMC and EEC both increased as current density increased.

Figure 6c shows the effect of inter-electrode distance at current density of 27.8 mA/cm^2 with aluminum electrodes for 60 min. of electrolysis time on EC operating cost. In fact, as the inter-electrode distance increased from 1.0 cm to 2.0 cm, EC cost increased from 3.75 ± 0.04 US \$/m^3 to 4.92 ± 0.04 US \$/m^3. This higher cost at higher inter-electrode distance is due to higher EEC at higher inter-electrode distance, as EMC was higher at lower inter-electrode distance where metal dissolution was higher. However, the difference in EMC between the three tested inter-electrode distances was low and was not sufficient to balance the greater difference in EEC. In fact, EEC contribution to the total EC cost increased from 1.83 ± 0.01 US \$/m^3 (14 kWh/m^3) to 3.47 ± 0.01 US \$/m^3 (27 kWh/m^3) as inter-electrode distance increased from 1.0 cm to 2.0 cm, but EMC contribution cost decreased from 1.92 ± 0.03 US \$/m^3 to 1.45 ± 0.03 US \$/m^3 with the same increase in inter-electrode distance.

The influence of initial pH (pH_i) on EC operating cost is shown in **Figure 6d**. It is clear that EC cost was not affected by initial pH as the difference in EEC and EMC between the three tested pH_i values was negligible. This resulted in EC operating cost of 3.76 ± 0.05 US \$/m^3 at all pH_i values of 4.0, 6.3 and 9.0.

As a conclusion, it can be said that working at the lowest current density of 9.3 mA/cm^2 and the lowest inter-electrode of 1.0 cm, could reduce EC cost to 0.26 ± 0.03 US \$/m^3 and 1.07 ± 0.04 US \$/m^3 when working with iron and aluminum electrodes, respectively, whereas, pH_i had no significant effect on cost. EC cost was much lower when working with iron electrodes, mainly due to metal price and EMC, while energy consumption remained between 1.5 and 2.0 kWh/m^3 for both metals; however, aluminum electrodes were more efficient for the preliminary purification of VFA as shown before. These operating costs of EC, which correspond to 0.026 US \$/kg and 0.107 US \$/kg of purified organic acids with iron and aluminum electrodes, respectively (as the concentration of volatile fatty acids in the digestate is around 10 g/L) are more economic than the values of 3.92–22.84 kWh/kg acids recovered required by electrodialysis for the recovery of a mixture of organic acids [44] and also more cost-effective than the value of 0.111 \$/kg acetate needed by two stages of nanofiltration preceded by microfiltration for the recovery of acetic acid from fermentation broth [45]. In practice, the comparison is more complex because EC constitutes only a preliminary treatment for VFA

purification, so that concentration, *e.g.* using nanofiltration, must still be carried out. These results demonstrate that EC will not increase significantly the concentration cost and will probably decrease membrane fouling and, therefore, cleaning and maintenance requirements.

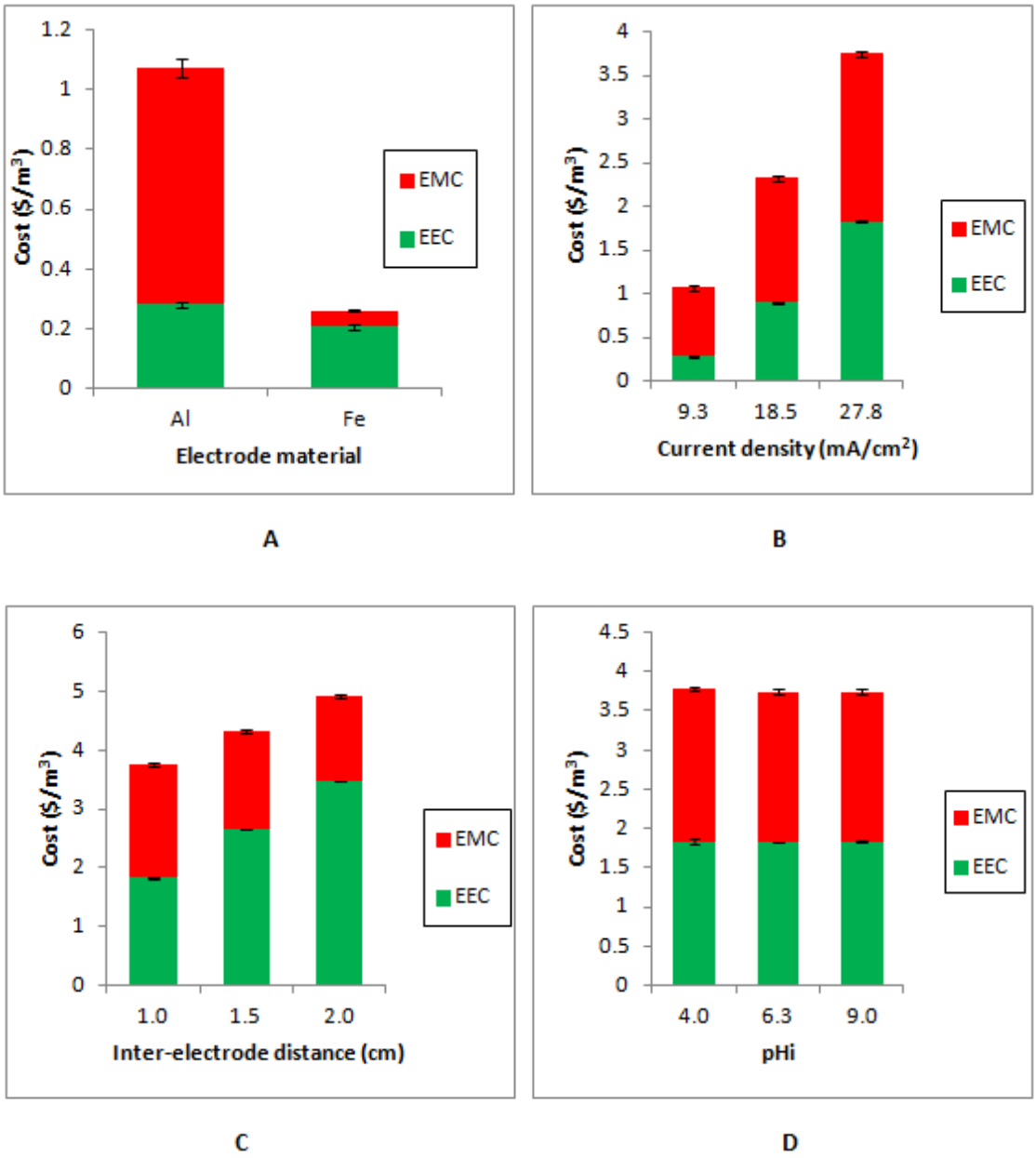

Figure 6. EC cost after 60 min. of electrolysis as a function of: A) electrode material (1.0 cm electrode distance; pH_i 6.3; 9.3 mA/cm^2), B) current density (Al electrodes; 1.0 cm electrode distance; pH_i 6.3), C) inter-electrode distance (Al electrodes; pH_i 6.3; 27.8 mA/cm^2), and D) initial pH (Al electrodes; 1.0 cm electrode distance; 27.8 mA/cm^2). Error bars represent standard deviations.

4. CONCLUSION

As a conclusion, electrocoagulation (EC) in the batch mode has been shown to be efficient for the preliminary purification of volatile fatty acids (VFA) in a digestate from acidogenic fermentation. The mechanism of VFA purification occurred by the coagulation and the co-precipitation of other species in the digestate, while the VFA stayed totally in the liquid phase. Highest removal efficiencies of 85.3 ± 1.0 %, 88.3 ± 1.0 %, 80.5 ± 2.0% and 92.3 ± 1.0% for turbidity, TSS, TN and TP, respectively were obtained with aluminum electrodes at the highest current density 27.8 mA/cm^2, natural pH of the digestate 6.3, and at the lowest inter-electrode distance 1.0 cm. EC operating cost depended on electrode material, current density, and inter-electrode distance, whereas initial pH did not have any significant effect on EC cost. The lowest EC operating cost with aluminum and iron electrodes was 1.07 ± 0.04 US \$/m^3 and 0.26 ± 0.03 US \$/m^3, respectively, when working at the lowest current density 9.3 mA/cm^2 and the lowest inter-electrode distance 1.0 cm.

REFERENCES

[1] R.R. Singhania, A.K. Patel, G. Christophe, P. Fontanille, C. Larroche, Biological upgrading of volatile fatty acids, key intermediates for the valorization of biowaste through dark anaerobic fermentation, Bioresource Technology. 145 (2013) 166–174.

[2] A.E. Tugtas, Recovery of volatile fatty acids via membrane contactor using flat membranes: Experimental and theoretical analysis, Waste Management. 34 (2014) 1171–1178.

[3] S. Freguia, E.H. Teh, N. Boon, K.M. Leung, J. Keller, K. Rabaey, Microbial fuel cells operating on mixed fatty acids, Bioresource Technology. 101 (2010) 1233–1238.

[4] M. Gryta, M. Barancewicz, Separation of volatile compounds from fermentation broth by membrane distillation, Polish Journal of Chemical Technology. 13 (2011) 56–60.

[5] L. Masse, D.I. Massé, Y. Pellerin, The effect of pH on the separation of manure nutrients with reverse osmosis membranes, Journal of Membrane Science. 325 (2008) 914–919.

[6] B. Saha, S. Chopade, S. Mahajani, Recovery of dilute acetic acid through esterification in a reactive distillation column, Catalysis Today. 60 (2000) 147–157.

[7] Z. Lei, C. Li, Y. Li, B. Chen, Separation of acetic acid and water by complex extractive distillation, Separation and Purification Technology. 36 (2004) 131–138.

[8] H.N. Chang, N. Kim, C. Joeng Jongwon Kang, H. Choi, Biofuel Production from biomass-derived volatile fatty acid platform in "Bioenergy - II: Fuels and Chemicals from Renewable Resources" (C. Briens, F. Berruti, M. Al-Dahhan, Eds.), ECI Symposium Series (2009) http://dc.engconfintl.org/bioenergy_ii/15.

[9] R. Kleerebezem, B. Joosse, Rene RozendalMark C.M. Van Loosdrecht, Anaerobic digestion without biogas?, Reviews in Environmental Science and Bio/Technology. 14 (2015) 787–801.

[10] Y. Tian, W. He, X. Zhu, W. Yang, N. Ren, B.E. Logan, Energy efficient electrocoagulation using an air-breathing cathode to remove nutrients from wastewater, Chemical Engineering Journal. 292 (2016) 308–314.

[11] Y. Yavuz, EC and EF processes for the treatment of alcohol distillery wastewater, Separation and Purification Technology. 53 (2007) 135–140.

[12] N. Adhoum, L. Monser, Decolourization and removal of phenolic compounds from olive mill wastewater by electrocoagulation, Chemical Engineering and Processing: Process Intensification. 43 (2004) 1281–1287.

[13] Ö. Apaydin, U. Kurt, M.T. Gonullu, An investigation on the treatment of tannery wastewater by electrocoagulation, Global NEST Journal. 11 (2009) 546–555

[14] S. Zhao, G. Huang, G. Cheng, Y. Wang, H. Fu, Hardness, COD and turbidity removals from produced water by electrocoagulation pretreatment prior to reverse osmosis membranes, Desalination. 344 (2014) 454–462.

[15] J.N. Hakizimana, B. Gourich, C. Vial, P. Drogui, A. Oumani, J. Naja, L. Hilali, Assessment of hardness, microorganism and organic matter removal from seawater by electrocoagulation as a pretreatment of desalination by reverse osmosis, Desalination. 393 (2016) 90-101.

[16] S. Pulkka, M. Martikainen, A. Bhatnagar, M. Sillanpää, Electrochemical methods for the removal of anionic contaminants from water–A review, Separation and Purification Technology. 132 (2014) 252–271.

[17] A.E. Yilmaz, R. Boncukcuoğlu, M.M. Kocakerim, B. Keskinler, The investigation of parameters affecting boron removal by electrocoagulation method, Journal of Hazardous Materials. 125 (2005) 160–165.

[18] C.P. Nanseu-Njiki, S.R. Tchamango, P.C. Ngom, A. Darchen, E. Ngameni, Mercury (II) removal from water by electrocoagulation using aluminium and iron electrodes, Journal of Hazardous Materials. 168 (2009) 1430–1436.

[19] M. Bayramoglu, M. Kobya, O.T. Can, M. Sozbir, Operating cost analysis of electrocoagulation of textile dye wastewater, Separation and Purification Technology. 37 (2004) 117–125.

[20] W. Siriangkhawut, S. Tontrong, P. Chantiratiku, Quantitation of Aluminum Content in Waters and Soft Drinks by Spectrophotometry Using Eriochrome Cyanine R'Research, Journal of Pharmaceutical, Biological and Chemical Sciences. 4 (2013) 1156–1161.

[21] K. Sadeddin, A. Naser, A. Firas, Removal of turbidity and suspended solids by electro-coagulation to improve feed water quality of reverse osmosis plant, Desalination. 268 (2011) 204–207.

[22] F. Akbal, S. Camcı, Copper, chromium and nickel removal from metal plating wastewater by electrocoagulation, Desalination. 269 (2011) 214–222.

[23] M. Zaied, N. Bellakhal, Electrocoagulation treatment of black liquor from paper industry, Journal of Hazardous Materials. 163 (2009) 995–1000.

[24] K. Cheballah, A. Sahmoune, K. Messaoudi, N. Drouiche, H. Lounici, Simultaneous removal of hexavalent chromium and CODfrom industrial wastewater by bipolar electrocoagulation, Chemical Engineering and Processing: Process Intensification. 96 (2015) 94–99.

[25] M.M. Emamjomeh, M. Sivakumar, Fluoride removal by a continuous flow electrocoagulation reactor, Journal of Environmental Management. 90 (2009) 1204–1212.

[26] P. Cañizares, F. Martínez, C. Jiménez, J. Lobato, M.A. Rodrigo, Coagulation and electrocoagulation of wastes polluted with dyes, Environmental Science and Technology. 40 (2006) 6418–6424.

[27] K. Govindan, M. Raja, S.U. Maheshwari, M. Noel, Y. Oren, Comparison and understanding of fluoride removal mechanism in Ca^{2+}, Mg^{2+} and Al^{3+} ion assisted electrocoagulation process using Fe and Al electrodes, Journal of Environmental Chemical Engineering. 3 (2015) 1784–1793.

[28] M. Chafi, B. Gourich, A.H. Essadki, C. Vial, A. Fabregat, Comparison of electrocoagulation using iron and aluminium electrodes with chemical coagulation for the removal of a highly soluble acid dye, Desalination. 281 (2011) 285–292.

[29] C. Jiménez, C. Sáez, F. Martínez, P. Cañizares, M.A. Rodrigo, Electrochemical dosing of iron and aluminum in continuous processes: A key step to explain electro-coagulation processes, Separation and Purification Technology. 98 (2012) 102–108.

[30] S. Barışçı, O. Turkay, Domestic greywater treatment by electrocoagulation using hybrid electrode combinations, Journal of Water Process Engineering. 10 (2016) 56–66.

[31] B. Zeboudji, N. Drouiche, H. Lounici, N. Mameri, N. Ghaffour, The influence of parameters affecting boron removal by electrocoagulation process, Separation Science and Technology. 48 (2013) 1280–1288.

[32] B. Palahouane, N. Drouiche, S. Aoudj, K. Bensadok, Cost-effective electrocoagulation process for the remediation of fluoride from pretreated photovoltaic wastewater, Journal of Industrial and Engineering Chemistry. 22 (2015) 127–131.

[33] M. Uğurlu, A. Gürses, C. Doğar, M. Yalçin, The removal of lignin and phenol from paper mill effluents by electrocoagulation, Journal of Environmental Management. 87 (2008) 420–428.

[34] M. Vlachou, J. Hahladakis, E. Gidarakos, Effect of various parameters in removing Cr and Ni from model wastewater by using electrocoagulation, Global NEST Journal. 15 (2013) 494–503.

[35] N. Adhoum, L. Monser, N. Bellakhal, J.-E. Belgaied, Treatment of electroplating wastewater containing Cu^{2+}, Zn^{2+} and Cr (VI) by electrocoagulation, Journal of Hazardous Materials. 112 (2004) 207–213.

[36] X. Chen, G. Chen, P.L. Yue, Separation of pollutants from restaurant wastewater by electrocoagulation, Separation and Purification Technology. 19 (2000) 65–76.

[37] D. Ghosh, H. Solanki, M.K. Purkait, Removal of Fe (II) from tap water by electrocoagulation technique, Journal of Hazardous Materials. 155 (2008) 135–143.

[38] A. Attour, M. Touati, M. Tlili, M.B. Amor, F. Lapicque, J.-P. Leclerc, Influence of operating parameters on phosphate removal from water by electrocoagulation using aluminum electrodes, Separation and Purification Technology. 123 (2014) 124–129.

[39] M. Behloul, H. Grib, N. Drouiche, N. Abdi, H. Lounici, N. Mameri, Removal of Malathion Pesticide from Polluted Solutions by Electrocoagulation: Modeling of Experimental Results using Response Surface Methodology, Separation Science and Technology. 48 (2013) 664–672.

[40] S. Vasudevan, G. Sozhan, S. Ravichandran, J. Jayaraj, J. Lakshmi, M. Sheela, Studies on the removal of phosphate from drinking water by electrocoagulation process, Industrial & Engineering Chemistry Research. 47 (2008) 2018–2023.

[41] Ş. İrdemez, N. Demircioğlu, Y.Ş. Yıldız, Z. Bingül, The effects of current density and phosphate concentration on phosphate removal from wastewater by electrocoagulation using aluminum and iron plate electrodes, Separation and Purification Technology. 52 (2006) 218–223.

[42] M. Kobya, H. Hiz, E. Senturk, C. Aydiner, E. Demirbas, Treatment of potato chips manufacturing wastewater by electrocoagulation, Desalination. 190 (2006) 201–211.

[43] G. Mouedhen, M. Feki, M.D.P. Wery, H.F. Ayedi, Behavior of aluminum electrodes in electrocoagulation process, Journal of Hazardous Materials. 150 (2008) 124–135.

[44] Z.X. Wang, Y.B. Luo, P. Yu, Recovery of organic acids from waste salt solutions derived from the manufacture of cyclohexanone by electrodialysis, Journal of Membrane Science. 280 (2006) 134–137.

[45] P. Pal, J. Nayak, Acetic Acid Production and Purification: Critical Review Towards Process Intensification, Separation & Purification Reviews. 46 (2017) 44–61.

CHAPTER 5: THE USE OF RESPONSE SURFACE METHODOLOGY FOR EVALUATING THE RECOVERY OF THE MICROALGAE *CHLAMYDOMONAS REINHARDTII* BY ELECTRO-COAGULATION-FLOCCULATION

This article is submitted to Algal Research. Consequently, it follows the guidelines of this journal.

FAYAD Nidal, YEHYA Tania, DE BAYNAST Hélène, LAROCHE Céline, AUDONNET Fabrice, VIAL Christophe.

ABSTRACT

For the first time, response surface methodology (RSM) was used to investigate the effect of the most influential variables including initial pH, current density and operating time on the recovery efficiency of the microalgal species *Chlamydomonas reinhardtii* from the culture medium by electro-coagulation-flocculation (ECF) in the batch mode using aluminum electrodes, while estimating the relative operating costs. Experimental results showed that the maximum recovery efficiency of 90% was obtained at operating time 60 minutes, current density 14.4 mA/cm^2 and initial pH 6. Data also showed that the effect of initial pH was insignificant on ECF operating cost, which ranged from 0.13 to 1.8 US \$/m^3. Two models for predicting recovery efficiency and ECF operating cost were developed. Microalgae recovery followed a second-order kinetics, with charge neutralization being the mechanism responsible for recovery, as shown by the increase of zeta potential value with time. Moreover, ECF was shown to be more efficient than chemical flocculation with chitosan.

Keywords: microalgae recovery, *Chlamydomonas reinhardtii*, electro-coagulation-flocculation, response surface methodology

1. INTRODUCTION

Microalgae have a great potential in diverse applications [1]. However, for challenging societal pressure such as carbon sequestration, wastewater treatment, and biofuel production, microalgae cultivation at a very high scale is compulsory [2]. Microalgae as the 3rd generation source of biofuels have major advantages, such as short life cycle and varied cultivation conditions. As well, microalgae cultivation does not take up the agricultural land [3], and in

marked contrast to soybean, sugarcane and canola, microalgae are not edible; their production is less expensive, allow higher yield and do not need clean water to grow [4]. In spite of these interesting advantages, there are many obstacles that render microalgae commercialization difficult. The major limitation is the separation of microalgae from their culture media, which is expensive due to the dilute nature of the microalgae in their cultivation media [5]. Moreover, the microalgal cells, with a size range between 5 and 50 μm, form a stable colloidal suspension because of their negatively charged cellular surfaces [6]. An efficient microalgae dewatering process should be suitable for all microalgae strains, provide a product with a high microalgal concentration and require the minimum possible costs of energy, operation and maintenance. Microalgae dewatering is a two-step concentration method which concentrates the microalgae from 0.02-0.06 % total dissolved solids (TDS) to 15–25% TDS or more, depending on the intended future utilisation of microalgae [7]. Industrial techniques employed for the separation of microalgal biomass from the culture media include flocculation [8], flotation [9], centrifugation [10] or filtration [11]; these techniques may be used separately or in combination. Centrifugation is the most widely used harvesting process. However, for low added-value products like biodiesel and feed, conventional centrifugation and filtration methods are deemed energy intensive and costly [12].

Electrochemical technologies, such as electrocoagulation (EC), which had been already implemented successfully in many industrial and environmental applications [13-16] represent a promising alternative for microalgae recovery. In EC, controlled current is applied between two metal electrodes immersed in an aqueous solution. The electrical current causes the dissolution of anodes often made of iron or aluminum into the solution. The metal species released in solution, at an appropriate pH, can form vast species of solid flocs that destabilize and aggregate the suspended particles or precipitate, and adsorb dissolved substances [17]. The reactions that occur at electrodes in EC are as follows [18]. For aluminum electrodes, oxidation reaction takes place at the anode:

$$Al_{(s)} \rightarrow Al_{(aq)}^{3+} + 3e^{-} \qquad \text{(eq. 1)}$$

Reduction reaction takes place at the cathode:

$3H_2O + 3e^- \rightarrow (3/2)\ H_2 + 3OH^-$ (eq. 2)

Overall reaction can be summarized as:

$Al^{3+} \rightarrow Al(OH)_n^{(3-n)} \rightarrow Al_2(OH)_2^{4+} \rightarrow Al_3(OH)_4^{5+} \rightarrow Al_{13}$ complex $\rightarrow Al(OH)_3$ (eq. 3)

EC presents various advantages, such as low energy dissipation, versatility, environment compatibility, safety, selectivity and cost effectiveness [11].

EC has been already used for algae removal for water treatment purposes [19-21]; however, the studies on microalgae recovery by EC for biorefinery purposes are scarce in the literature, without, to the best of our knowledge, any study reported on the recovery of any *Chlamydomonas* species.

In order to fill this gap in the literature, the aim of this study was to investigate the harvesting of the microalgae *Chlamydomonas reinhardtii* from its culture medium using electro–coagulation–flocculation (ECF). The effects of current density, initial pH, and operating time on microalgae recovery efficiency and ECF operating cost have been evaluated using the response surface methodology. Models for predicting recovery efficiency and ECF operating cost have been developed. Moreover, the kinetics and mechanism of recovery have been explained. In addition to that, ECF has been compared to chemical flocculation chitosan, which is intensively studied in the literature.

2. MATERIALS AND METHODS

2.1. MICROALGAE SPECIES (*CHLAMYDOMONAS REINHARDTII*)

All experiments were carried out with the fresh-water microalgae *Chlamydomonas reinhardtii* **(Figure 1)**, a unicellular biflagellate green microalgae [22]. *Chlamydomonas* species are widely distributed in soil and fresh water. *C. reinhardtii* is a widely studied biological model organism, due to its ease of cultivation, rapid growth, and its ability to manipulate its genetics [23]. Its whole genome sequencing has been completed in 2007 [24]. It is very interesting commercially, as it produces metabolites with industrial/pharmaceutical interest [25], biofuels [26] and hydrogen [24].

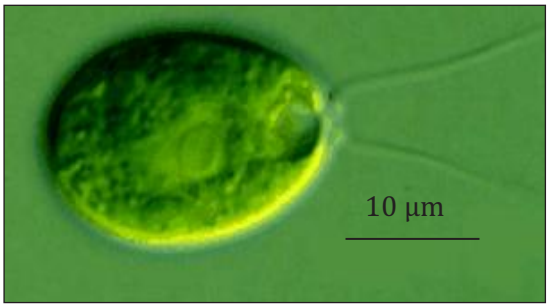

Figure 1. Microscopic image of the microalgal species, *Chlamydomonas reinhardtii*.

2.2. MICROALGAE CULTIVATION

The culture medium used for pre-cultures preparation was prepared and pH was adjusted to 7. This culture medium contained: 3.15 g/L CH_3COOH, 1.38 g/L NH_4Cl, 0.27 g/L $MgSO_4$, $7H_2O$, 0.74 g/L K_2HPO_4 and 0.05 g/L $CaCl_2$, $2H_2O$. Hunter's solution, a trace elements solution, was also prepared (pH adjusted at 6.5 – 6.8) and autoclaved separately to avoid any precipitation of elements. The components of Hunter's solution per 100 mL of distilled water are: 5 g Na_2EDTA, 2.2 g $ZnSO_4.7H_2O$, 1.14 g H_3BO_3, 0.506 g $MnCl_2.4H_2O$, 0.499 g $FeSO_4.7H_2O$, 0.161 g $CoCl_2.6H_2O$, 0.157g $CuSO_4.5H_2O$ and 0.11 g $(NH_4)_6Mo_7O_{24}.4H_2O$. After that, 250 mL of the culture medium were poured in two separate 500 mL erlenmeyer flasks; these flasks were then autoclaved at 120°C for 20 minutes. After autoclaving, the flasks were aseptically inoculated with 30 mL of the microalgal suspension. Then, 0.5 mL of Hunter's solution were added. These erlenmeyer flasks were placed in an incubator for 7 days to allow microalgae grow reasonably dense under controlled light (intensity of 150 µmol photon/m^2/s, the day and night pattern was 16 hrs. day – 8 hrs. night, using fluorescent lamps (*Osram*, Italy)) and temperature (24 ± 1) °C. The erlenmeyer flasks were stirred at 130 rpm by an agitating plate (*Dragon Lab*, China).

After reaching the stationary phase of growth, the microalgae (pre-cultures) were used as starter cultures to inoculate a 5 L cylindrical, radially illuminated photobioreactor of radius 0.08 m **(Figure 2)**. A continuous artificial illumination was supplied by 55 halogen lamps (*Sylvania professional 25*, BAB 38°, 12 V, 20 W) surrounding the culture and allowing control of irradiance up to 8000 µmol photons/m^2/s. Illumination of the culture was controlled by adjusting the power supplied to the lamps. Light incident fluxes were calibrated using a method described elsewhere [27]. Agitation speed was fixed at 300 rpm and temperature at 24°C. The photosynthetic activity of microalgae was monitored using pO_2 sensor and pH was maintained

at around 7 by varying the CO_2 content (between 0.5 to 2%) in the continuously injected air (100 mL/min).

Figure 2. The photobioreactor used for *Chlamydomonas reinhardtii* culture.

2.3. MICROALGAE GROWTH MONITORING

To evaluate the growth profile of microalgae, samples were collected daily and quantification of cells' number per mL was carried out by cell counting using a Malassez hemocytometer (Tiefe depth, 0.200 mm) and a microscope (*Olympus BX41TF*, Japan) at a magnification ×100 (oil immersion lens). The same collected samples were analyzed by a spectrophotometer UV/Visible Biomate 3S (*Thermo Fisher Scientific*, USA) at a wavelength of 750 nm. A correlation curve between the number of cells per mL and the optical density at 750 nm was generated **(Figure 3)**. The stationary phase started after 12 days of culture and the culture was interrupted after 14 days before the beginning of the death phase.

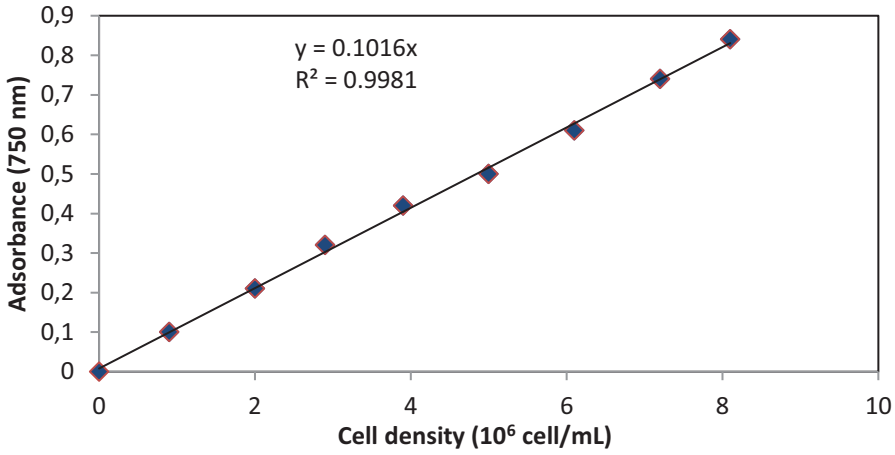

Figure 3. Correlation curve between absorbance at 750 nm and cell density of *Chlamydomonas reinhardtii*.

2.4. ELECTRO-COAGULATION-FLOCCULATION (ECF) EXPERIMENTS

All ECF experiments were carried out at room temperature in a 1 L transparent plexiglass vessel. The cultures were agitated using a magnetic stirrer at a constant rate of 250 rpm. ECF was conducted in the galvanostatic mode using a DC generator (Voltcraft HPS-13015, Germany). Two planar monopolar aluminum electrodes of 52 cm^2 surface area were used as anode and cathode and were separated in the beaker by an inter-electrode distance of 1 cm. The experimental setup is shown in **Figure 4**. The electrodes were rinsed with acetone and a 0.01 N HCl solution after each use to remove the impurities. To determine the mass of dissolved aluminum, electrodes were weighed before and after each run. pH was measured by using a pH meter (Mettler Toledo, Switzerland). In order to investigate the microalgal recovery efficiency, the optical density of the microalgal suspension of the samples was measured at 750 nm using a spectrophotometer UV/Visible Biomate 3S (Thermo Fisher Scientific, USA). Microalgal recovery efficiency (ηa (t)) was calculated as follows (equation 4):

$$\eta_a(t) = (OD_{t=0} - OD_t)/\ OD_{t=0} \qquad \text{(eq. 4)}$$

where $OD_{t=0}$ is the optical density of the suspension before exposing it to ECF, and OD_t is the optical density of the microalgal suspension at time *t*.

2.5. ZETA POTENTIAL MEASUREMENT

ζ-potential manifests the stability of colloidal dispersions. A high ζ-potential accords stability, i.e. the microalgal suspension becomes resistant to coagulation. However, when the potential is low, attractive forces outpace repulsion forces and the dispersion flocculates. So, colloids with high ζ- potential (negative or positive) are electrically stabilized, while colloids with low ζ-potential values are apt to coagulate or flocculate. In this study, ζ-potential was measured during the culture and during ECF using a Zetasizer Nano ZS (*Malvern*, UK) to evaluate the stability of the microlalgal suspension and determine the mechanism responsible for microalgae recovery.

2.6. CHEMICAL FLOCCULATION EXPERIMENTS

Chemical flocculation experiments were carried out with chitosan. This bioflocculant was selected, as it is intensively reported in the literature. For these experiments, the pH of the microalgal suspension (1 L) was adjusted at 6 using 0.1 M HCl. Then, the suspension was stirred at 250 rpm. After adding 150 mg of chitosan, stirring was continued for 2 minutes [28]. Finally, the suspension was left to settle for 20 minutes and a sample of the supernatant was taken to measure its optical density. Each assay was carried out in triplicate.

2.7. RESIDUAL ALUMINUM ANALYSIS

To investigate the extent of microalgal suspension contamination by aluminum cations during ECF, residual aluminum in the supernatant was measured using a spectrophotometric analysis based on the aluminum (III)-eriochrome cyanine R complex [29].

2.8. ECF OPERATING COST EVALUATION

ECF operating cost (US \$/m^3) was calculated as the sum of the costs of consumed electrode material (CEM) and electrical energy consumption (EEC). CEM was determined as mentioned before by weighing the electrodes before and after ECF. EEC was calculated in terms of kWh/m^3 using equation 5.

$$\text{EEC (kWh/m}^3) = \text{U.I.t/V} \quad \text{(eq. 5)}$$

where U is the voltage (V), I the electric current (A), t the operating time (h) and V the volume (L) of microalgal suspension.

The price of the aluminum electrode material was estimated at 1.7 US $/kg Al, and the price of electrical power was considered 0.13 US $/kWh. ECF cost was evaluated as follows (equation 6):

$$\text{ECF cost (US \$/m}^3) = 0.13 \cdot \text{EEC} + 1.7 \cdot \text{CEM} \quad \text{(eq. 6)}$$

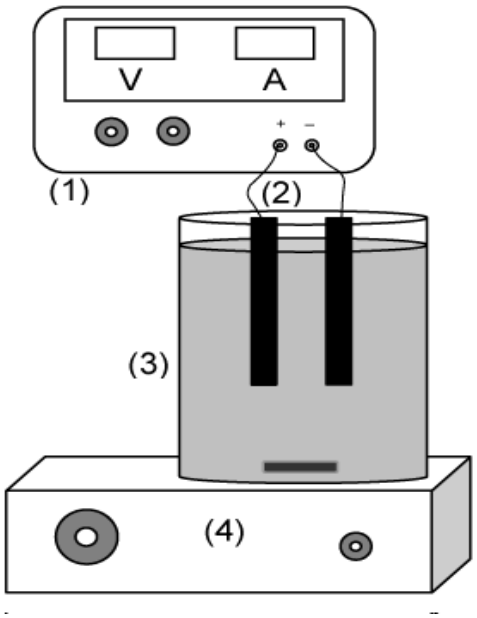

Figure 4. Experimental set-up, 1: DC generator; 2: Electrode pair; 3: Electrolytic cell; 4: Magnetic stirrer.

2.9. RESPONSE SURFACE METHODOLOGY (RSM)

RSM is a combination of mathematical and statistical techniques employed to enhance and optimize different processes [30]. In this study, RSM was used to design the experiments and evaluate the microalgal recovery efficiency and ECF operating cost by investigating the influence of three factors at three levels and three center points. Fifteen experiments were carried out randomly according to Box-Behnken design (BBD), which is a category of rotatable or nearly rotatable second-order designs based on three-level incomplete factorial designs. In this method, appropriate estimation of the first and second-order coefficients of the model has been carried out by picking out certain points of three level factorial arrangement [31]. The factors investigated in RSM were initial pH (X_1), current density (X_2) and ECF operating time (X_3). The coded and real values of these factors are shown in Table 1.

The general equation of the second order mathematical model used for predicting recovery efficiency (Y_1, %,) and ECF operating cost (Y_2, US \$/m^3) as a function of the factors in **Table 1** is presented in equation 7.

$$Y = a_0+\sum a_iX_i+\sum a_{ij}X_iX_j+\sum a_{ii}X_i^2 \quad \text{(eq. 7)}$$

In equation 7, a_0 is the constant coefficient, a_i is the linear coefficient, a_{ij} is the interaction coefficient and a_{ii} is the quadratic coefficient.

Table 1: Coded and actual values of the variables of the experimental design

Factor	Variable	Coded levels of variables		
		-1	0	+1
X_1	Initial pH	3	6	9
X_2	Current density (mA/cm^2)	4.8	9.6	14.4
X_3	Time (minutes)	20	40	60

3. RESULTS AND DISCUSSION

3.1. MICROALGAE GROWTH

Monitoring the microalgal growth showed that the microalgal cell concentration reached 1.5×10^7 cells/mL from an initial cell density of 2.7×10^4 cells/mL after 14 days of culture. The evolution of microalgal growth is shown in **Figure 5**. The curve usually has 5 phases: an induction or lag phase, an exponential phase, a phase of reduced growth, a stationary phase and a death phase. In our case, the lag (adaptation) phase in which the microalgal cells were adapting to their culture medium lasted till the 2nd day of culture, the time where the exponential (log) phase began. The exponential phase in which the microalgal cells increase rapidly, as they are now adapted to their new culture, lasted from the 2nd day till the 11th day of culture, where the log phase started to slow down, due to the decrease of nutrients available for the microalgal cells at this stage. The stationary phase where the growth of microalgae stabilized started in the 12th day. The culture was interrupted after 14 days to avoid passing into the death phase, which consequently was not observed in the curve.

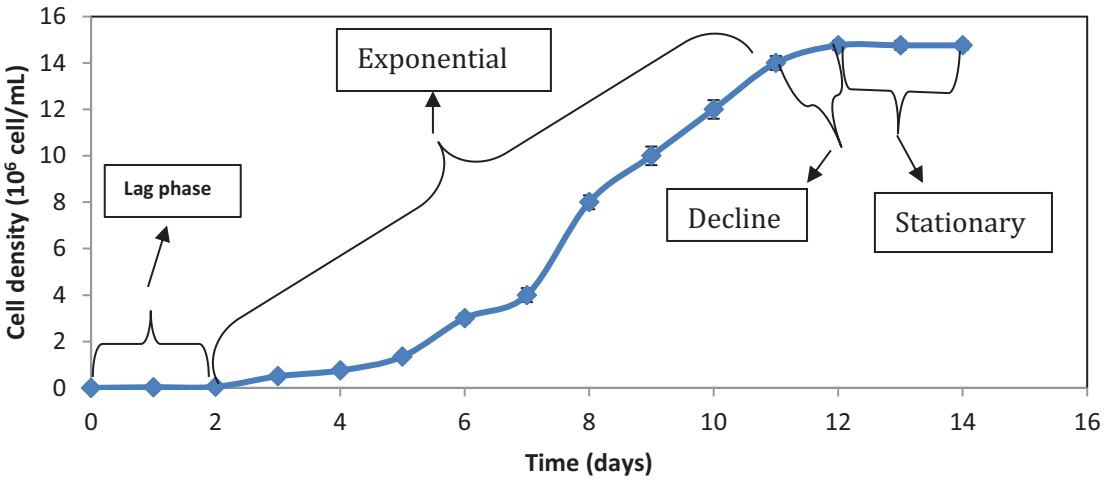

Figure 5. Growth profile of the microalgae *Chlamydomonas reinhardtii.* Error bars represent standard deviations.

3.2. Z-POTENTIAL EVOLUTION DURING MICROALGAL GROWTH

ζ-potential of the microalgal cells was analyzed during the culture. As shown in **Figure 6**, ζ-potential decreased at the onset of the log phase probably due to the increase of the extracellular organic matter concentration (generated from the photosynthetic activity of the microalgal cells) [32]. Then, ζ-potential remained almost constant till the 11th day of culture (where the growth of cells started slowing down to enter the stationary phase), where ζ negativity started decreasing, to reach a value of (-9±1) mV at the end of culture. As ζ-potential value is essential for keeping the cells stabilized in the suspension, reduced ζ-potential negativity in the stationary phase facilitates microalgae recovery.

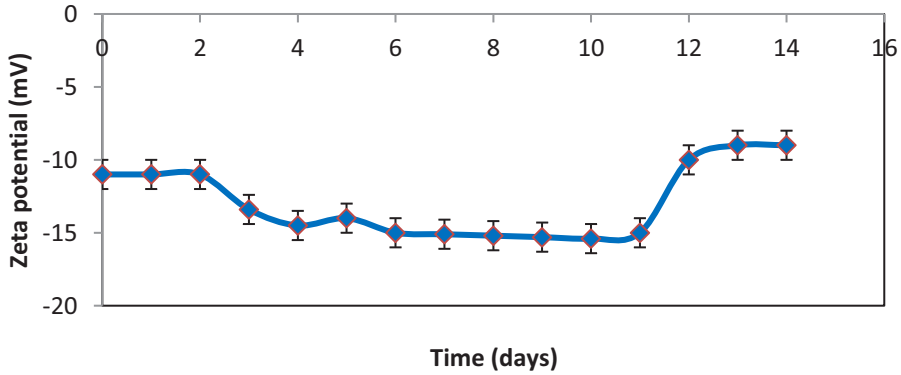

Figure 6. ζ-potential variation during the culture of *Chlamydomonas reinhardtii.* Error bars represent standard deviations.

3.3. ECF PROCESS

3.3.1. ANALYSIS OF BOX-BEHNKEN DESIGN

In this study, ECF was employed to recover the microalgal cells (*Chlamydomonas reinhardtii*) from their culture medium. The initial concentration of microalgae was fixed at 1.5×10^6 cell/mL in all experimental runs by diluting the cultures with distilled water. The investigated operating conditions were: initial pH (3 to 9), current density (4.8 to 14.4 mA/cm^2) and ECF operating time (20 to 60 minutes). Three factors at three levels each were tested with Box-Behnken response surface to investigate the influence of the independent variables on microalgae recovery efficiency and ECF operating cost. **Table 2** shows the arrangements of the experiments with the results obtained.

Figure 7 displays the pareto charts of recovery efficiency and ECF operating cost. **Figure 8a** shows that the coefficient X_2X_3 was not significant on recovery efficiency, so it was disregarded in the corresponding model. Moreover, **Figure 8b** shows that the coefficients X_1, X_1X_2, X_1X_3, X_1^2, and X_3^2 were not significant on ECF operating cost, so they were not included in the ECF operating cost model.

The response functions with the determined coefficients for both microalgae recovery efficiency and ECF operating cost are reported in equations 8 and 9, respectively.

Y_1 (Recovery efficiency, %) = $48.5 + 7.2X_1 + 1.6X_2 + 0.7X_3 + 0.2X_1X_2 - 0.02\ X_1X_3 - 0.8X_1^2 - 0.09X_2^2 - 0.005X_3^2$ (eq. 8)

Y_2 (ECF operating cost, US \$/m^3) = $0.1 - 0.03X_2 - 0.004X_3 + 0.002X_2X_3 + 0.002X_2^2$ (eq. 9)

Table 2. Results of experiments performed by Box-Behnken design with three factors. Minimum and maximum values are shown in bold.

Run	Initial pH	Current density (mA/cm^2)	Time (minutes)	Recovery efficiency (%)	Electrode consumed (kg/m^3)	Energy consumed (kWh/m^3)	ECF cost (US $/$m^3$)
1	6	9.6	40	87.0	0.22	2.41	0.69
2	6	4.8	60	82.6	0.17	1.19	0.44
3	9	9.6	60	73.4	0.33	3.66	1.04
4	3	4.8	40	83.3	0.11	0.78	0.29
5	6	4.8	20	75.1	0.05	0.39	0.13
6	6	14.4	20	85.5	0.18	2.40	0.62
7	3	9.6	60	89.0	0.33	3.60	1.03
8	3	14.4	40	84.3	0.35	4.81	1.22
9	9	4.8	40	66.6	0.11	0.82	0.29
10	3	9.6	20	80.2	0.13	1.21	0.38
11	9	14.4	40	76.5	0.33	4.93	1.20
12	6	9.6	40	87.8	0.24	2.41	0.72
13	9	9.6	20	68.8	0.11	1.26	0.35
14	6	9.6	40	87.5	0.25	2.41	0.74
15	6	14.4	60	90.0	0.50	7.28	1.80

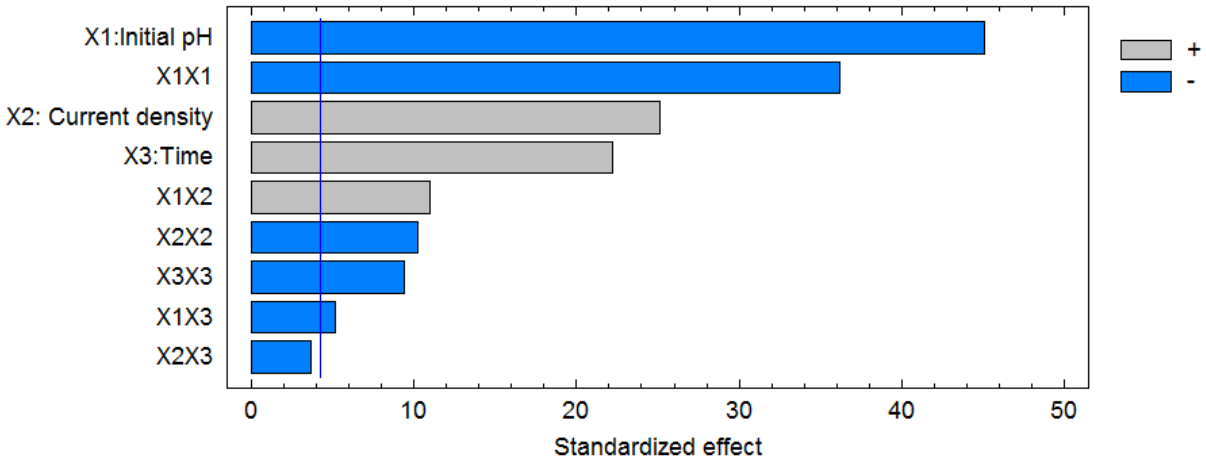

a)

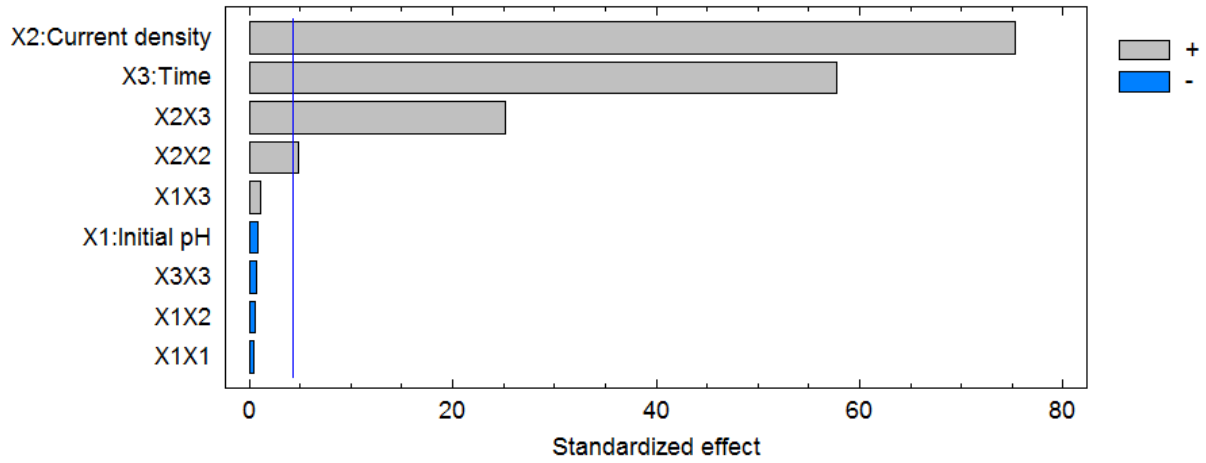

b)

Figure 7. Pareto charts of a) microalgae recovery efficiency and b) ECF operating cost.

The predicted values of the responses were obtained by quadratic model fitting techniques for recovery efficiency and ECF operating cost. The quadratic model fits well, as the experimental and predicted responses of both recovery efficiency (R^2 = 98.77 %) and ECF operating cost (R^2 = 99.85 %) are close **(Figure 8)**.

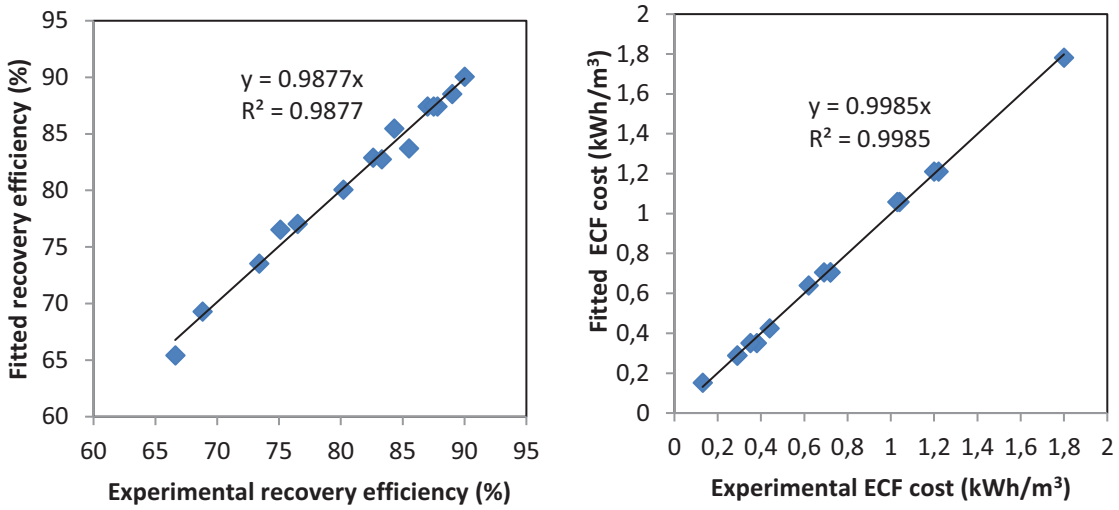

a) b)

Figure 8. Experimental *vs.* predicted values of a) recovery efficiency and b) ECF cost.

The obtained results were then analyzed by ANOVA to assess the "goodness-of-fit". The results of ANOVA of the fitting model for microalgae recovery efficiency and ECF operating cost are shown in **Tables 3** and **4**, respectively. **Table 3** shows that the coefficients of determination (R^2) and adjusted R^2 (a modified version of R^2 that has been adjusted for the number of predictors in the model) were 98.77 % and 97.13 %, respectively. Moreover, it shows that the P-value for lack of fit was more than 0.05. This indicates that the quadratic model is able to describe successfully microalgae recovery efficiency. **Table 3** also shows that the linear coefficients (X_1, X_2, and X_3), the interaction coefficients (X_1X_2, X_1X_3), and the quadratic coefficients (X_1^2, X_2^2, and X_3^2) had significant effects on microalgae recovery, with low P-values ($P < 0.05$). **Table 4** shows that the coefficients of determination (R^2) and adjusted R^2 were 99.85% and 99.79%, respectively, and P-value for lack-of-fit was more than 0.05. This confirms that the quadratic model is able to describe successfully ECF operating cost. **Table 4** also shows that the linear coefficients (X_2 and X_3), the interaction coefficient (X_2X_3) and the quadratic coefficient (X_2^2) had significant effects on ECF operating cost, with low P-values ($P < 0.05$).

Table 3. Analysis of variance for recovery efficiency.

Source	Sum of Squares	Df	Mean Square	F-Ratio	P-Value
X_1: Initial pH	331.5	1	331.5	2029.8	0.0005
X_2: Current density	103.0	1	103.0	630.4	0.002
X_3: Time	80.6	1	80.6	493.7	0.0020
X_1^2	213.5	1	213.5	1307.2	0.0008
X_1X_2	19.8	1	19.80	121.2	0.008
X_1X_3	4.4	1	4.4	27.0	0.04
X_2^2	17.1	1	17.1	104.9	0.009
X_3^2	14.5	1	14.5	88.6	0.01
Lack-of-fit	9.2	4	2.3	14.1	0.07
Pure error	0.3	2	0.2		
Total (corr.)	777.7	14			
R^2 = 98.77% adjusted R^2 = 97.13%					

Table 4. Analysis of variance for ECF operating cost.

Source	Sum of Squares	Df	Mean Square	F-Ratio	P-Value
X_2: Current density	1.70	1	1.70	7855.4	0.0000
X_3: Time	1.0	1	1.0	4620.5	0.0000
X_2X_3	0.2	1	0.2	873.4	0.0000
X_2^2	0.007	1	0.007	34.1	0.001
Lack-of-fit	0.003	4	0.0008	3.7	0.09
Pure error	0.001	6	0.0002		
Total (corr.)	2.90	14			
R^2 = 99.85 % adjusted R^2 = 99.79 %					

3.3.2. ASSESSMENT OF MODELS' VALIDITY

Residuals were used to investigate graphically the adequacy of the models used to describe recovery efficiency and operating cost. Residuals are unexplained variations by model and they

are normally distributed, if the model is a suitable predictor. **Figures 9a** and **9b** show normal probability plots of residuals for recovery efficiency and EC cost. As shown in these figures, the points in normal plot of residuals fit well a straight line, so the residuals are nearly normally distributed. **Figures 10a** and **10b** show residuals versus fit plots for recovery efficiency and ECF operating cost. The residuals, as shown, are randomly distributed and do not follow any specific pattern. Therefore, the two models are valid.

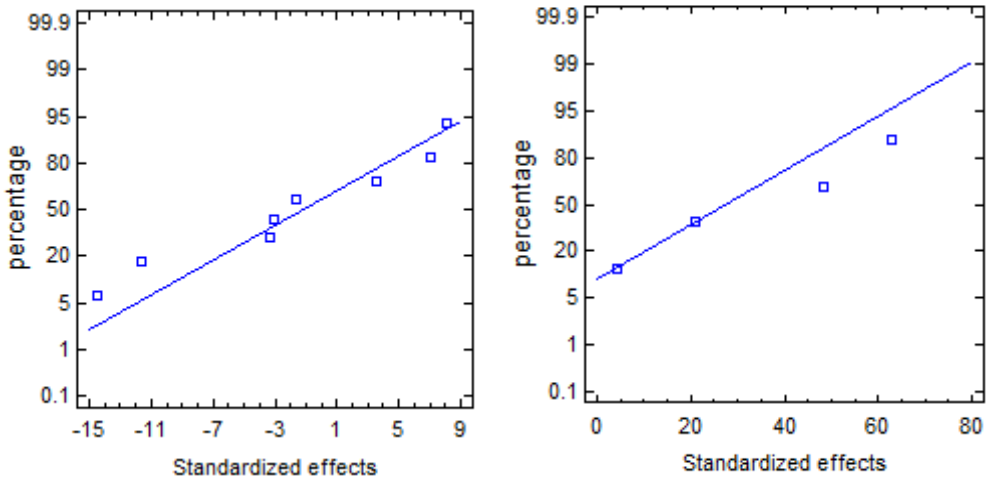

a) b)

Figure 9. Normal probability plots of residuals for: a) Recovery efficiency and b) ECF operating cost.

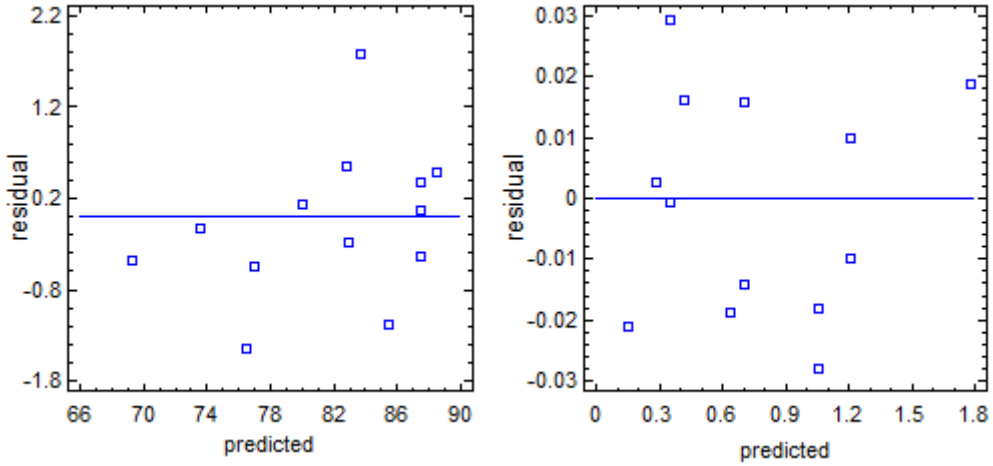

a) b)

Figure 10. Residuals vs. fit plots for: a) Recovery efficiency, b) ECF operating cost.

3.3.3. INFLUENCE OF INDEPENDENT VARIABLES ON RECOVERY EFFICIENCY AND ECF OPERATING COST

3.3.3.1. THE INTERACTION EFFECT OF CURRENT DENSITY AND ECF OPERATING TIME

Figure 11a shows the effect of current density and ECF operating time on recovery efficiency of microalgae at pH_i 6. As seen in this figure, recovery efficiency increased with the increase of both current density and operating time. The same result was also found at different values of the operating parameters. For example, at constant ECF operating time and initial pH (t = 40 minutes, pH_i 9), the recovery efficiency increased from 66.6% to 76.5% as current density increased from 4.8 mA/cm^2 to 14.4 mA/cm^2, and at constant current density and initial pH (current density 9.6 mA/cm^2, pH_i 9), increasing operating time from 20 minutes to 60 minutes increased recovery efficiency from 68.8% to 73.4%. Higher harvesting efficiency at higher current density can be explained based on Faraday's law which implies that the amount of metal dissolved is nearly proportional to current density, but not exactly proportional, as the faradaic yield measured at the end of each run on the basis of electrode mass loss slightly decreases as current increases. Therefore, current density has a direct influence on the anode dissolution rate and on Al dosage, which strongly influences the performance of the ECF process [33]. Moreover, current density governs the speed and the amount of hydrogen gas produced at the cathode [34]. As the amount of hydrogen gas released increases, the recovery efficiency of microalgae by flotation increases. Higher recovery efficiency at longer ECF operating time is also explained by Faraday's law which implies that increasing operating time increases the mass of aluminum oxidized [35], and thus, recovery efficiency increases. Our results are consistent with those of Tak et al. [36], who found that the maximum removal of color and COD from livestock wastewater was at the highest current density of 30 mA/cm^2 and longest operating time of 30 minutes.

Figure 11b shows the effect of current density and time on ECF operating cost at pH_i 6. As shown in this figure, ECF cost increased with the increase of both current density and time. The same result was also found at different levels of the operating parameters. For example, at constant ECF operating time and initial pH (t = 60 minutes, pH_i 6), increasing current density from 4.8 mA/cm^2 to 14.4 mA/cm^2 increased EC cost from 0.13 US \$/m^3 to 1.8 US \$/m^3.

According to **Table 4**, the linear and quadratic effects of current density, the linear effect of operating time as well as the effect of interaction between time and current density are significant on ECF operating cost ($p<0.05$). ECF cost increase at higher current densities and longer operation time is due to higher electrical energy consumption and higher electrode consumption under such conditions.

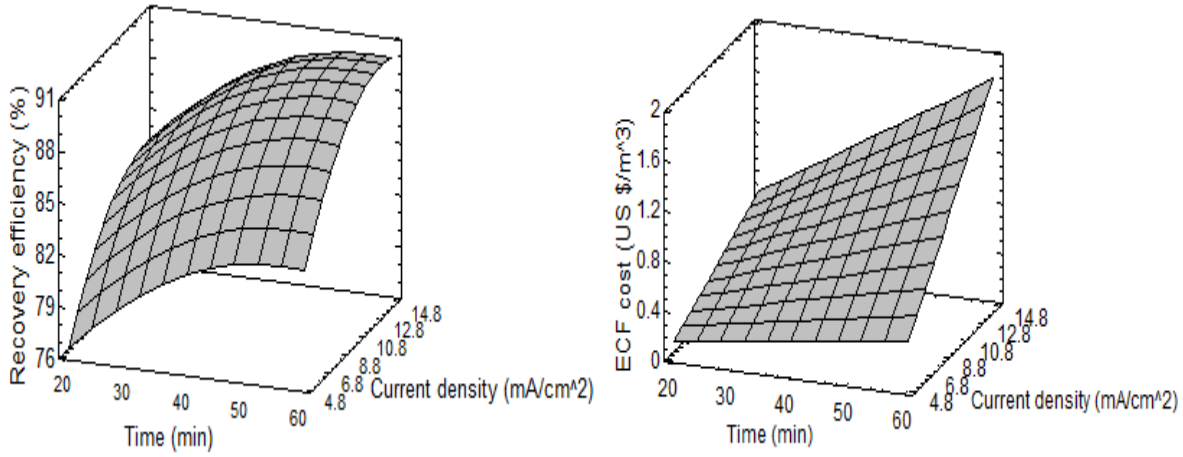

a) b)

Figure 11. Three dimensional representations of the effects of time and current density on a) recovery efficiency and b) ECF cost, at initial pH 6.

3.3.3.2. THE INTERACTION EFFECT OF INITIAL pH AND CURRENT DENSITY

Figure 12a depicts the effect of initial pH and current density on recovery efficiency of microalgae at 40 minutes operating time. The recovery efficiency decreased at high and low pH_i values and with the decrease of current density at alkaline pH values. **Table 3** shows that the linear effect of current density and time, their interaction effect, and the quadratic effect of each is significant on recovery efficiency ($P<0.05$). The highest and lowest recovery efficiency obtained at pH_i 6 and pH_i 9, respectively is due to the fact that different aluminum species are formed at different pH values. In fact, at pH<4, $Al(H_2O)_6^{3+}$ species dominate. As pH increases, polymeric aluminum hydroxide cations such as $Al_6(OH)_{15}^{3+}$, $Al_7(OH)_{17}^{4+}$, $Al_8(OH)_{20}^{4+}$, $Al_{13}O_4(OH)_{34}^{7+}$, and $Al_{13}(OH)_{34}^{5+}$ become the dominant species [37]. At slightly acidic to neutral pH values, insoluble $Al(OH)_{3(s)}$ species which are strong adsorbents prevail, and microalgae separation takes place mainly by adsorption and neutralization. However, in alkaline media, $Al(OH)_4^-$ species which are weak coagulants prevail and microalgae separation in this case is accomplished by sweeping flocculation [5].

Figure 12b shows the effect of initial pH and current density on ECF operating cost at 40 minutes operating time. It is clear from this figure that ECF operating cost increased with the increase of current density regardless of pH_i value.

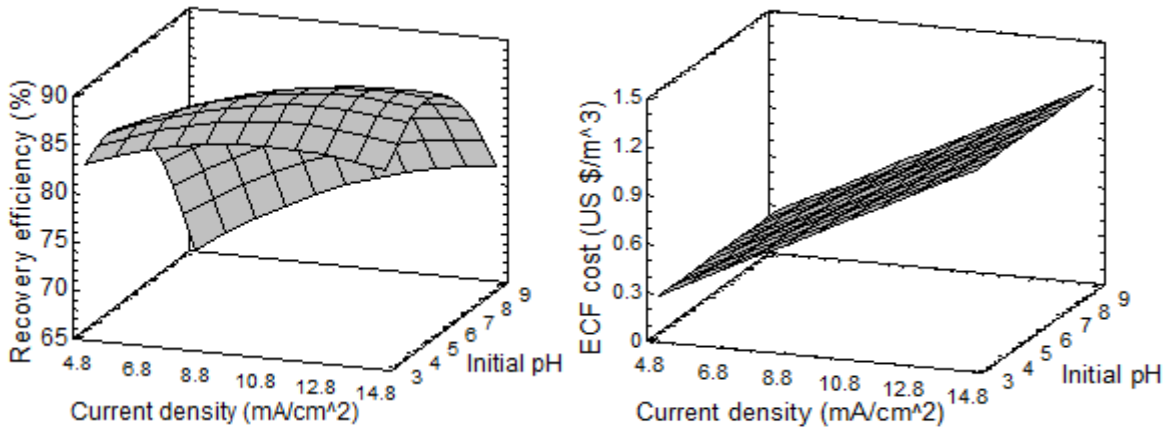

a) b)

Figure 12. Three dimensional representations of the effects of current density and initial pH on a) recovery efficiency and b) ECF cost, at time 40 minutes.

3.3.3.3. THE INTERACTION EFFECT OF TIME AND INITIAL pH

Figure 13a displays the effect of ECF operating time and initial pH on the recovery efficiency of microalgae at current density 9.6 mA/cm^2. Recovery efficiency increased with the increase of operating time; however, it decreased drastically at the alkaline pH_i of 9, where it reached 68.8% at current density 9.6 mA/cm^2 and 20 minutes operating time. In addition to that, **Table 3** shows that the linear effects of time and initial pH, in addition to their interaction and quadratic effects are significant on microalgae recovery efficiency ($P<0.05$).

Figure 13b depicts the effect of initial pH and operating time on ECF operating cost at current density 9.6 mA/cm^2. In fact, ECF operating cost increased with the increase of operating time whereas pH_i did not have any significant effect on ECF cost. Higher ECF operating cost at longer operation time is due to higher electrical energy consumption and higher electrode consumption, according to equation 10.

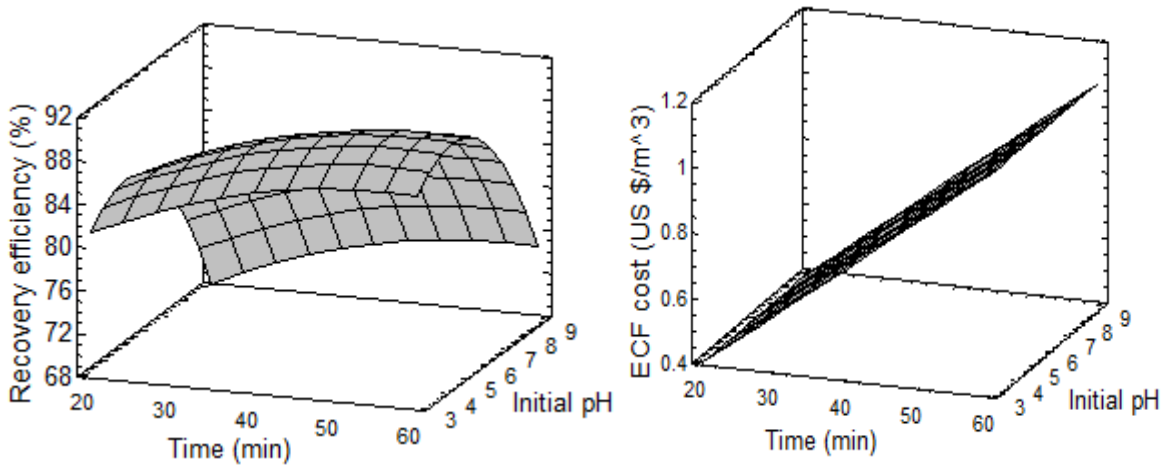

a) b)

Figure 13. Three dimensional representations of the effects of operating time and initial pH on a) recovery efficiency and b) ECF cost at current density 9.6 mA/cm^2.

3.3.4. RECOVERY KINETICS AND Z-POTENTIAL EVOLUTION DURING ECF

To investigate the kinetics of *Chlorella vulgaris* recovery, first-order (equation 10) and second order (equation 11) kinetic models were fitted to experimental results at current densities 4.8 mA/cm^2, 9.6 mA/cm^2 and 14.4 mA/cm^2. Experimental data fit better second-order kinetics (with higher R^2 values), as shown in **Figure 14**.

$$\ln(C_0/C) = k(t - t_0) \quad \text{(eq. 10)}$$

$$\frac{1}{C_t} - \frac{1}{C_0} = k(t - t_0) \quad \text{(eq. 11)}$$

ζ-potential was measured at the conditions which resulted in maximum recovery efficiency of *C. Reinhardtii* (pH_i 6, current density 14.4 mA/cm^2 and operating time 60 minutes) to assess the mechanism of recovery at these conditions. **Figure 15** shows ζ-potential evolution with time during ECF. As shown in the figure, ζ-potential increased with time to reach zero after 60 minutes. operating time. This result indicates that the mechanism responsible for microalgae recovery at pH_i 6 is charge neutralization.

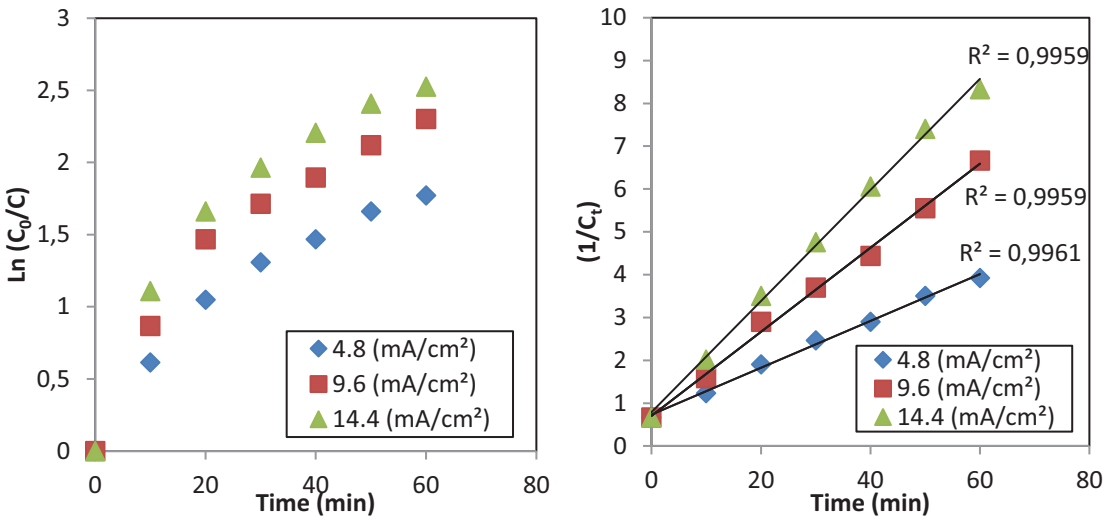

a) b)

Figure 14. Fitting of a) first-order kinetic models and b) second-order kinetic models to experimental data at different current densities. Initial pH 6, operating time 60 minutes.

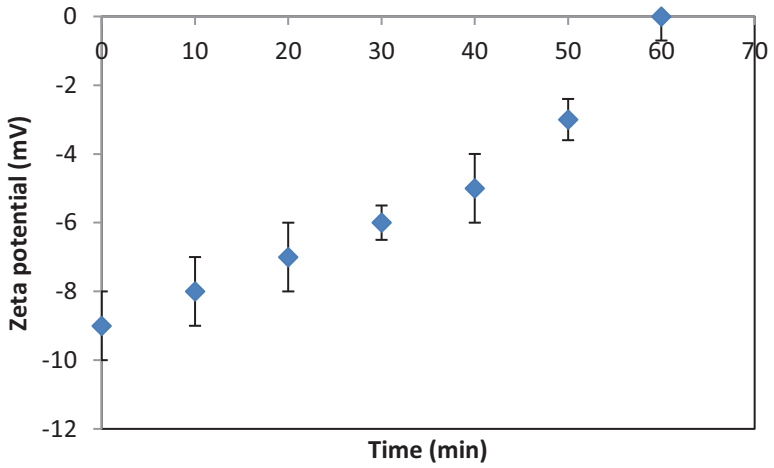

Figure 15. ζ-potential evolution with time. Current density 14.4 mA/cm^2, initial pH, time 60 minutes.

3.3.5. COMPARISON OF ECF WITH CHEMICAL FLOCCULATION

Chemical flocculation experiments using chitosan were conducted and the results were compared to those obtained with ECF. As **Figure 16** shows, the recovery efficiency was higher (90±1)% with ECF at pH_i 6, current density 14.4 mA/cm^2 and operating time 60 minutes) than with chitosan (85±1)%. In addition to the better recovery efficiency of *C. reinhartii* with ECF in this study, it should be noted that only 4.7 mg/L residual aluminum existed at the end of ECF,

which corresponds to less than 1% of the aluminum that should have dissolved under the studied conditions. This result is interesting and displays that ECF is more appropriate than chemical coagulation in order to avoid culture contamination, as inorganic coagulants, including alum and iron chloride, contaminate growth media with high levels of aluminum or iron [38]. The contaminated growth medium could not be used again, leading to an environmental problem and a considerable water loss. Organic polymer/polyelectrolyte flocculants, such as cationic starch and chitosan, are not toxic and do not contaminate growth media. However, they are expensive of about 10 US $ per kilogram for chitosan [39]. In our study, recovery cost ranged from 0.13 to 1.8 US $/m^3, which is much less than a cost of 15 US $/m^3 estimated with chitosan flocculation.

As a conclusion, we can say that ECF is a preferred microalgae recovery technique, as it does not cost much and contaminates less the growth medium.

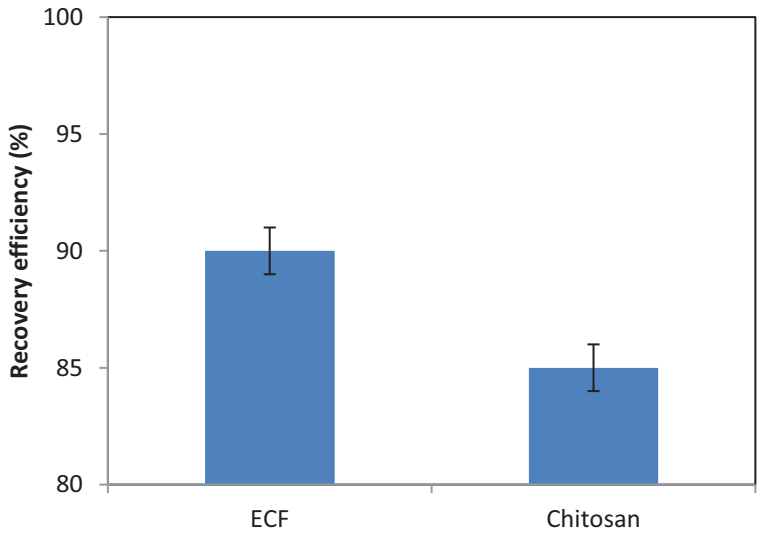

Figure 16. Comparison between ECF and flocculation with chitosan for *Chlamydomonas reinhardtii* recovery. Error bars represent standard deviations.

4. CONCLUSION

In the present study, response surface methodology (RSM) was employed as an experimental design tool to explain the effect of the main operating parameters and their interactions on the recovery efficiency of *Chlamydomonas reinhardtii* from the culture medium by ECF and estimate the operating costs. For this purpose, the effects of three major variables including initial pH, current density and ECF operating time were evaluated. The results showed that the

recovery efficiency, which reached 90.0% at pH_i 6, current density 14.4 mA/cm^2 and operating time 60 minutes, was significantly affected by all the investigated variables, whereas ECF operating cost, that ranged from 0.13 to 1.8 US \$/m^3, was only significantly influenced by current density and operating time. Two statistically significant models were developed for predicting recovery efficiency and ECF operating cost from RSM methodology.

Zeta potential increase with time depicts that charge neutralization is the mechanism responsible for microalgae recovery, with a rate following the second-order kinetics. Finally, ECF was proven to be more efficient than chemical flocculation with chitosan.

REFERENCES

1. A.I. Barros, A.L. Gonçalves, M. Simões, J.C.M. Pires, Harvesting techniques applied to microalgae: A review, Renewable and Sustainable Energy Reviews. 41 (2015) 1489–1500.

2. P. Das, M.I. Thaher, M.A.Q.M. Abdul Hakim, H.M.S.J. Al-Jabri, G.S.H.S. Alghasal, Microalgae harvesting by pH adjusted coagulation-flocculation, recycling of the coagulant and the growth media, Bioresource Technology. 216 (2016) 824–829.

3. S. Wang, J. Zhu, L. Dai, X. Zhao, D. Liu, W. Du, A novel process on lipid extraction from microalgae for biodiesel production, Energy. 115, Part 1 (2016) 963–968.

4. H.M.-G. Maleki, M. Almassi, M. Hejazi, S. Minaei, Harvesting of microalgae by electro-coagulation-flocculation for biodiesel production: an investigation of the effect of operational parameters and forecast model using response surface methodology, Journal of Biosciences. 4 (2014) 258–269.

5. A. Golzary, S. Imanian, M.A. Abdoli, A. Khodadadi, A. Karbassi, A cost-effective strategy for marine microalgae separation by electro-coagulation–flotation process aimed at bio-crude oil production: Optimization and evaluation study, Separation and Purification Technology. 147 (2015) 156–165.

6. T. Ndikubwimana, X. Zeng, N. He, Z. Xiao, Y. Xie, J.-S. Chang, L. Lin, Y. Lu, Microalgae biomass harvesting by bioflocculation-interpretation by classical DLVO theory, Biochemical Engineering Journal. 101 (2015) 160–167.

7. N. Uduman, V. Bourniquel, M.K. Danquah, A.F.A. Hoadley, A parametric study of electrocoagulation as a recovery process of marine microalgae for biodiesel production, Chemical Engineering Journal. 174 (2011) 249–257.

8. S. Lama, K. Muylaert, T.B. Karki, I. Foubert, R.K. Henderson, D. Vandamme, Flocculation properties of several microalgae and a cyanobacterium species during ferric chloride, chitosan and alkaline flocculation, Bioresource Technology. 220 (2016) 464–470.

9. S. Garg, L. Wang, P.M. Schenk, Flotation separation of marine microalgae from aqueous medium, Separation and Purification Technology. 156, Part 2 (2015) 636–641.

10. A.J. Dassey, C.S. Theegala, Harvesting economics and strategies using centrifugation for cost effective separation of microalgae cells for biodiesel applications, Bioresource Technology. 128 (2013) 241–245.

11. C. Nurra, E. Clavero, J. Salvadó, C. Torras, Vibrating membrane filtration as improved technology for microalgae dewatering, Bioresource Technology. 157 (2014) 247–253.

12. A. Guldhe, R. Misra, P. Singh, I. Rawat, F. Bux, An innovative electrochemical process to alleviate the challenges for harvesting of small size microalgae by using non-sacrificial carbon electrodes, Algal Research. 19 (2016) 292–298.

13. N.R. Neti, R. Misra, Efficient degradation of Reactive Blue 4 in carbon bed electrochemical reactor, Chemical Engineering Journal. 184 (2012) 23–32.

14. M.K. Mbacké, C. Kane, N.O. Diallo, C.M. Diop, F. Chauvet, M. Comtat, T. Tzedakis, Electrocoagulation process applied on pollutants treatment- experimental optimization and fundamental investigation of the crystal violet dye removal, Journal of Environmental Chemical Engineering. 4 (2016) 4001–4011.

15. M. Kobya, E. Demirbas, F. Ulu, Evaluation of operating parameters with respect to charge loading on the removal efficiency of arsenic from potable water by electrocoagulation, Journal of Environmental Chemical Engineering. 4 (2016) 1484–1494.

16. B. Palahouane, N. Drouiche, S. Aoudj, K. Bensadok, Cost-effective electrocoagulation process for the remediation of fluoride from pretreated photovoltaic wastewater, Journal of Industrial and Engineering Chemistry. 22 (2015) 127–131.

17. S. Elabbas, N. Ouazzani, L. Mandi, F. Berrekhis, M. Perdicakis, S. Pontvianne, M.-N. Pons, F. Lapicque, J.-P. Leclerc, Treatment of highly concentrated tannery wastewater using electrocoagulation: Influence of the quality of aluminum used for the electrode, Journal of Hazardous Materials. 319 (2016) 69–77.

18. V. Khandegar, A.K. Saroha, Electrocoagulation for the treatment of textile industry effluent – A review, Journal of Environmental Management. 128 (2013) 949–963.

19. S. Gao, J. Yang, J. Tian, F. Ma, G. Tu, M. Du, Electro-coagulation–flotation process for algae removal, Journal of Hazardous Materials. 177 (2010) 336–343.

20. C.G. Alfafara, K. Nakano, N. Nomura, T. Igarashi, M. Matsumura, Operating and scale-up factors for the electrolytic removal of algae from eutrophied lakewater, Journal of Chemical Technology and Biotechnology. 77 (2002) 871–876.

21. G. Azarian, A. Mesdaghinia, F. Vaezi, R. Nabizadeh, D. Nematollahi, Algae removal by electro-coagulation process, application for treatment of the effluent from an industrial wastewater treatment plant, Iranian Journal of Public Health. 36 (2007) 57–64.

22. K. Küçük, R. Tevatia, E. Sorgüven, Y. Demirel, M. Özilgen, Bioenergetics of growth and lipid production in *Chlamydomonas reinhardtii*, Energy. 83 (2015) 503–510.

23. M. Erculiani, R. Claudi, L. Cocola, E. Giro, N. La Rocca, T. Morosinotto, L. Poletto, D. Barbisan, D. Billi, M. Bonato, Atmospheres in a test tube: state of the art at the Astronomical Observatory of Padova, Memorie Della Societa Astronomica Italiana. 87 (2016) 112.

24. Z.-Z. He, H. Qi, M.-J. He, L.-M. Ruan, Experimental research on the photobiological hydrogen production kinetics of *Chlamydomonas reinhardtii* GY-D55, International Journal of Hydrogen Energy. 41 (2016) 15651–15660.

25. K. Skjånes, C. Rebours, P. Lindblad, Potential for green microalgae to produce hydrogen, pharmaceuticals and other high value products in a combined process, Critical Reviews in Biotechnology. 33 (2013) 172–215.

26. M.A. Scranton, J.T. Ostrand, F.J. Fields, S.P. Mayfield, *Chlamydomonas* as a model for biofuels and bio-products production, The Plant Journal. 82 (2015) 523–531.

27. J.-F. Cornet, A. Marty, J.-B. Gros, Revised technique for the determination of mean incident light fluxes on photobioreactors, Biotechnology Progress. 13 (1997) 408–415.

28. T. Chatsungnoen, Y. Chisti, Harvesting microalgae by flocculation–sedimentation, Algal Research. 13 (2016) 271–283.

29. W. Siriangkhawut, S. Tontrong, P. Chantiratiku, Quantitation of Aluminum Content in Waters and Soft Drinks by Spectrophotometry Using Eriochrome Cyanine R, Research, Journal of Pharmaceutical, Biological and Chemical Sciences. 4 (2013) 1156–1161.

30. E. Gengec, M. Kobya, E. Demirbas, A. Akyol, K. Oktor, Optimization of baker's yeast wastewater using response surface methodology by electrocoagulation, Desalination. 286 (2012) 200–209.

31. H. Rubí-Juárez, C. Barrera-Díaz, I. Linares-Hernández, C. Fall, B. Bilyeu, A Combined Electrocoagulation-Electrooxidation Process for Carwash Wastewater Reclamation, International Journal of Electrochemical Science. 10 (2015) 6754–6767.

32. H. Konno, Settling and Coagulation of Slender Type Diatoms, Water Science & Technology. 27 (1993) 231–24.

33. M. Kumar, F.I.A. Ponselvan, J.R. Malviya, V.C. Srivastava, I.D. Mall, Treatment of bio-digester effluent by electrocoagulation using iron electrodes, Journal of Hazardous Materials. 165 (2009) 345–352.

34. C.P. Nanseu-Njiki, S.R. Tchamango, P.C. Ngom, A. Darchen, E. Ngameni, Mercury(II) removal from water by electrocoagulation using aluminum and iron electrodes, Journal of Hazardous Materials. 168 (2009) 1430–1436.

35. F. Akbal, S. Camcı, Copper, chromium and nickel removal from metal plating wastewater by electrocoagulation, Desalination. 269 (2011) 214–222.

36. B. Tak, B. Tak, Y. Kim, Y. Park, Y. Yoon, G. Min, Optimization of color and COD removal from livestock wastewater by electrocoagulation process: Application of Box–Behnken design (BBD), Journal of Industrial and Engineering Chemistry. 28 (2015) 307–315.

37. P. Cañizares, F. Martínez, C. Jiménez, J. Lobato, M.A. Rodrigo, Coagulation and electrocoagulation of wastes polluted with dyes, Environmental Science & Technology. 40 (2006) 6418–6424.

38. H.-M. Oh, S.J. Lee, M.-H. Park, H.-S. Kim, H.-C. Kim, J.-H. Yoon, G.-S. Kwon, B.-D. Yoon, Harvesting of *Chlorella vulgaris* using a bioflocculant from *Paenibacillus sp. AM49*, Biotechnology Letters. 23 (2001) 1229–1234.

39. D. Vandamme, I. Foubert, B. Meesschaert, K. Muylaert, Flocculation of microalgae using cationic starch, Journal of Applied Phycology. 22 (2010) 525–530.

CHAPTER 6: HARVESTING OF MICROALGAE *CHLORELLA VULGARIS* USING ELECTRO-COAGULATION-FLOCCULATION IN THE BATCH MODE

This article is published in Algal Research. Consequently, it follows the guidelines of this journal.

FAYAD Nidal, YEHYA Tania, AUDONNET Fabrice, VIAL Christophe.
Harvesting of microalgae *Chlorella vulgaris* using electro-coagulation, volume 25, pages 1-11.

ABSTRACT

The aim of this study was to evaluate the harvesting of microalgae *Chlorella vulgaris* by electro-coagulation-flocculation (ECF) using aluminum and iron electrodes, assess the mechanisms responsible for microalgae recovery, quantify the metal contamination in the effluent and biomass, analyze power requirements, and investigate the effect of ECF on lipid and pigment content in the biomass. The influence of six operating parameters (electrode material, sedimentation time, current density, stirring speed, initial pH (pH_i) and inter-electrode distance) on the harvesting efficiency was tested. A specific strategy involving flotation and pH-controlled ECF experiments was developed to identify the prevailing mechanism of harvesting: adhesion on flocs was shown to be negligible; flotation contributed to a maximum of 36.6% of microalgae recovery; zeta potential highlighted that the main mechanism responsible for microalgae recovery was charge neutralization at pH_i 4.0 and 6.0, and sweep flocculation at pH_i 8.0. The most energy saving conditions for the harvesting of *Chlorella vulgaris* involved aluminum electrodes, and 60 min. electrolysis with a current density of 2.9 mA/cm^2, pH_i 4.0, stirring speed 250 rpm and an inter-electrode distance of 1.0 cm. Economic and competitive energy input (1.0 kWh/kg microalgae) could be achieved by adding 1.5 g/L NaCl. In addition, ECF did not affect significantly the amount of microalgal lipids and pigments.

Keywords: microalgae harvesting, electro-coagulation-flocculation, batch mode, microalgal pigments, microalgal lipids

1. INTRODUCTION

Microalgae are promising resources for bio-fuel production, as they are not exposed to many of the inconveniences of 1st and 2nd generation bio-fuels [1]. These microorganisms produce oils by photosynthesis and are approved worldwide as a source of biodiesel that can satisfy the global need for renewable and green fuels [2]. They can also play a key role in alleviating the effects of anthropic pollution. For example, they can capture CO_2 to reduce atmospheric pollution and reduce the effects of global warming and climate change. In addition to lipids as an energy source, microalgae are also able generate coproducts of great pertinence to the food, pharmaceutical, and the chemical industries, such as proteins, pigments and polysaccharides [3].

One the challenges of 3rd generation bio-fuels based on microalgal biomass is to effectively recover the tiny microalgal cells from highly dilute solutions [4]. Regarding the small size of these cells (5-30 μm), their physical separation from the culture medium using filtration techniques is difficult. Many separation processes have been proposed for recovering microalgae, such as centrifugation [5], flocculation [6, 7], filtration [8], flotation [9, 10], ultrasound [11], pH adjustment (at high pH about 11.0 [12]), and electrolysis [4]. Centrifugation is a typical method that is widely used for harvesting microalgae, but it is time consuming, complex and expensive [13]. Concentrating microalgae 30–50 times by coagulation-flocculation and gravity sedimentation before applying centrifugation, strongly lowers the energy demand for harvesting [14, 15]. In filtration process, filter clogging is the most common issue in harvesting of microalgae; clogging considerably raises head loss and needs frequent maintenance [16]. Alternatively, coagulation-flocculation requires flocculating agents, but these may have associated environmental impacts, as these flocculating agents in excess may directly cause secondary pollution, or act indirectly through the formation of by-products. Another disadvantage is the possibility of changing the profile of biomass fatty acids, in this case the type of flocculating agent determines the extent of this change [3].

Some new studies have proposed economic techniques for the recovery of microalgae as substitutes to flocculation and centrifugation, which are the conventional methods of recovery, but are too energy intensive. For example, Xu et al. [17] worked on the harvesting of two microalgae species using Fe_3O_4 and found that it is possible to regenerate and use these nanoparticles. Vandamme et al. [18] also worked on a pre-concentration method, called auto-flocculation, in which increasing pH till 11.0 caused flocculation as a result of magnesium

precipitation. Other research studies investigated the implementation of microbial flocculants as substitutes for the known conventional chemicals [19, 20].

An alternative technique consisted in recovering marine microalgae using electrolysis-based coagulation and flotation methods that markedly decreased the electric energy consumption [21]. Actually, several studies investigated the use of electro-coagulation-flocculation (ECF) for the elimination of microalgae from drinking and wastewater [22-24]. In fact, the use of ECF for recovering microalgal biomass has been intensively evaluated in these papers; however, microalgal densities were much lower than those found in microalgal production systems [4]. Even though ECF has been reported to be adequate for harvesting microalgae cultivated for bio-fuel production, another key issue is that the mechanisms of microalgae harvesting by ECF are less precisely established than in centrifugation. Compared to coagulation-flocculation with Fe^{3+} or Al^{3+} salts, ECF has the advantage that no counter anions, such as chlorides and sulfates, are added to water. The drawback is that ECF requires the electrolytic dissolution of the sacrificial anode, which requires electric power. As a result, electrolytic reactions occur both at the anode and the cathode during ECF [4]. Using an aluminum anode, one gets:

$Al \rightarrow Al^{3+} + 3e^-$

$xAl^{3+} + yOH^- \rightarrow Al_x(OH)_y^{z+}$

The speciation of the aluminum hydroxides formed during ECF is extremely variable and is greatly affected by pH [4], but $Al(OH)_3$ and AlOOH precipitates dominate when pH is between 4.0 and 10.0. Using an iron anode, the same behaviour can be observed, with the particularity that Fe (II) and Fe (III) species can be obtained [25]:

$Fe \rightarrow Fe^{2+} + 2e^-$

$Fe^{2+} + 2OH^- \rightarrow Fe(OH)_{2(s)}$

or

$Fe \rightarrow Fe^{3+} + 3e^-$

$Fe^{3+} + 3OH^- \rightarrow Fe(OH)_{3(s)}$

The precipitation of metal hydroxide plays the same role as in conventional coagulation: first, *charge neutralisation* by cations, and then *sweep coagulation* due to precipitation and floc formation (which means an enmeshment in the precipitate). But another major advantage of ECF is that water reduction at the cathode prevents pH decrease and releases H_2 in the form of tiny microbubbles, which promotes the flotation of the flocs formed by precipitated hydroxides, leading to a combined coagulation-flotation mechanism for harvesting microalgae.

Finally, the purpose of this work is to investigate the applicability and the pros and cons of the harvesting of microalgae *Chlorella vulgaris* from its culture medium using electro-coagulation-flocculation. For this purpose, the influence of the most important operating variables of the ECF process on the harvesting efficiency will be evaluated and power requirements will be estimated. The respective effects of the various mechanisms able to favor microalgae harvesting in ECF will assessed, while the impact of ECF on microalgal lipid and pigment contents will be measured. Finally, the pollution of microalgal biomass and process water by metal cations dissolved from the sacrificial anode will also be estimated.

2. MATERIALS AND METHODS

2.1. MICROALGAL SPECIES *(CHLORELLA VULGARIS)*

All the experiments were performed with the freshwater chlorophyte *Chlorella vulgaris* **(Figure 1)**, which is a spherical microscopic cell of 2–10 μm diameter. *C. vulgaris* is an interesting species for the production of microalgal biomass for food, pharmaceuticals, cosmetics or bio-fuel, and is presently thoroughly studied. *Chlorella vulgaris* biomass was kindly provided by *Algosource Technologies* (France). Experiments were performed using a modified Bold Basal Medium with 3-fold nitrogen and vitamins (3N-BBM+V) prepared from pure chemicals dissolved in distilled water to simulate culture conditions of *Chlorella vulgaris*. For 1.0 L medium, the following components were added: 0.75 g $NaNO_3$, 0.025 g $CaCl_2.2H_2O$, 0.075 g $MgSO_4.7H_2O$, 0.075 g $K_2HPO_4.3H_2O$, 0.175 g KH_2PO_4, 0.025 g NaCl, 6.0 mL of trace elements solution, 1.0 mL of both vitamin B1 and vitamin B12.

The trace elements solution was prepared by adding to 1000 mL distilled water, 0.75 g Na_2EDTA and the minerals in exactly the following sequence: $FeCl_3$ $6H_2O$ (97.0 mg), $MnCl_2$ $4H_2O$ (41.0 mg), $ZnCl_2$ (5.0 mg), $CoCl_2$ $6H_2O$ (2.0 mg) and Na_2MoO_4 $2H_2O$ (4.0 mg). Vitamin B1 was prepared by dissolving 0.12 g thiaminhydrochloride in 100.0 mL distilled water and, then, filtered sterilely. Vitamin B12 was prepared by dissolving 0.1 g cyanocobalamin in 100.0 mL distilled water; then, 1.0 mL was taken from this solution and added to 99.0 mL distilled water and, finally, the solution was filtered sterilely. The ECF experiments were carried out at a microalgal concentration of approximately 0.5 g/L.

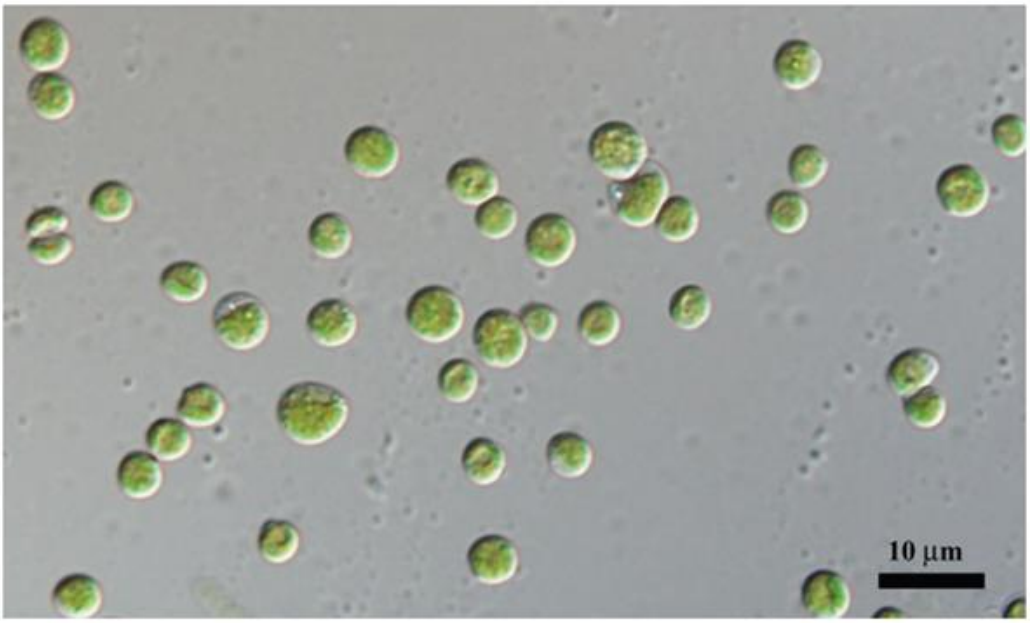

Figure 1. Microscope image of the microalgae species, *Chlorella vulgaris* at ×100 magnification.

2.2. ECF EXPERIMENTS

All ECF experiments were carried out at room temperature in a vessel filled with 1.0 L microalgal broth, and agitation was carried out by a magnetic stirrer at a constant agitation speed of 250 rpm. ECF was conducted in the galvanostatic mode by the help of a 30.0 V-10.0 A generator (ELC, France), while the cell voltage (U) was recorded (it ranged from 14.0 V to 29.5 V depending on the operating conditions) in order to calculate the electric energy consumption. The experimental setup is shown in **Figure 2**. Monopolar aluminum or iron rectangular electrodes of identical dimensions (8.0 cm×6.5 cm), were used as anode and cathode material. Electrodes were rinsed with acetone and a 0.01 N HCl aqueous solution to eliminate deposits, and then weighed before and after each experimental run. pH was measured by using a pHmeter (*Mettler Toledo*, Switzerland). Flotation of the flocs containing microalgae appears as the main mechanism of harvesting in **Figure 2**. This originated from the release of H_2 gas at the cathode and, to a lesser extent, O_2 gas at the anode.

To evaluate the harvesting efficiency of microalgal biomass, 10.0 mL samples were taken at different time (t) during the ECF process below the froth layer enriched in inorganic flocs and microalgae. These samples contained, however, solid particles and microalgae that could either settle to the bottom or float to the surface of the sample tube. The efficiency of microalgae recovery (η_a) was determined after settling based on the reduction in optical density OD of the

microalgal suspension measured at 550 nm with a UV–Vis spectrophotometer (*Jenway*, UK), as follows:

$$\eta_a(t) = \frac{OD_{t=0} - OD_t}{OD_{t=0}}$$

where $OD_{t=0}$ is the optical density of the suspension before ECF, and OD_t is the optical density of the suspension at time t.

To analyze the mechanism of microalgal recovery, zeta potential was measured using a Zetasizer Nano ZS (*Malvern*, UK), as this parameter estimates the electrostatic repulsion between colloids. To assess the role of flocculation, similar experiments were conducted using indissoluble titanium electrodes that only release H_2 by water reduction at the cathode and O_2 by water oxidation at the anode.

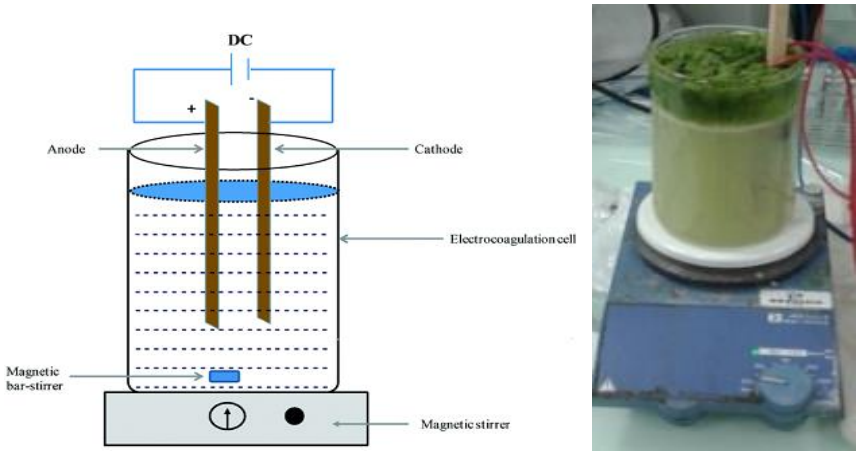

Figure 2. Sketch of experimental set-up and picture illustrating microalgae flotation during ECF experiments.

2.3. ALUMINUM ANALYSIS IN THE RECOVERED MICROALGAE AND IN WATER

To evaluate the extent of pollution of the microalgal biomass and of water by aluminum cations liberated from the sacrificial anode, the content of soluble metal both in harvested microalgae, and in the supernatant recovered after ECF was determined. For example, Al content was measured using a spectrophtometric analysis based on the aluminum (III)-eriochrome cyanine R complex [26]. For microalgal biomass, the procedure consisted first in calcinating the sample in a furnace at 550°C during 20.0 hrs. until ash was formed before analyzing ash. These ashes were then dissolved in 1.0 mL concentrated nitric acid and transferred to 25.0 mL volumetric flask, then made up the volume with distilled water. After that, samples were transferred into

polyethylene bottles and stored at 4.0°C until further analysis. The metal content in these samples were, then, analyzed, as previously described.

2.4. EXTRACTION AND QUANTIFICATION OF TOTAL LIPIDS

Microalgal biomass was gathered, first, by skimming the surface of the beaker after the end of ECF; this was freeze-dried for dewatering. For experimental control, microalgal biomass that was not subjected to ECF experiments was harvested by centrifugation and freeze-dried. For ECF and control samples, lipid extraction was performed by Bligh and Dyer method [27]. Hemolysis tubes were dried at 60.0°C for 2.0 hrs.; these tubes were, then, successively labelled, weighed using a precision balance and placed in a dessicator. In each tube, the subsequent addition of 0.5 g of grinded sample, 4.0 mL chloroform, 2.0 mL methanol and 1.0 mL distilled water was carried out for extracting lipids. Three phases appeared:

- a light phase consisting of methanol on the top, which contained the water-soluble products (carbohydrates and phenolic components);
- an intermediate phase containing the powder;
- a heavy phase consisting of chloroform which contained the lipids.

Then, vortexing and subsequent centrifugation at 2000*g* for 10 min. were applied. The heavy phase was collected and concentrated in a vacuum concentrator (*Thermo Fisher Scientific*, USA) for at least 2.5 hrs. at 40.0°C. Finally, the final product was weighed, the mass corresponding to the lipid fraction. As a result, the percentage of lipids in the biomass was determined per gram of dried biomass.

2.5. EXTRACTION AND QUANTIFICATION OF PIGMENTS

Pigments were extracted from ground microalgae (50.0 mg) using 4.0 mL of 80% acetone and sonication. After extraction, the supernatant was gathered by centrifugation. The process was repeated until the supernatant showed no color. Pigments content was quantified by spectrophotometry using a Biomate 3S spectrophotometer (*Thermo Fisher Scientific*, USA). The following equations involving the absorbance A_x measured at wavelength x (in nm) were used to estimate the concentrations of three pigments, namely, chlorophyll A (C_a), chlorophyll B (C_b), and carotenoids (C_c) [28], as follows:

$$C_a = 12.21 \cdot A_{663} - 2.81 \cdot A_{646}$$

$$C_b = 20.13 \cdot A_{646} - 5.03 \cdot A_{663}$$

$$C_c = \left(1000 \cdot A_{470} - 3.27 \cdot C_a - 104 \cdot C_b\right) / 198$$

Control and ECF samples were treated similarly.

2.6. STATISTICAL ANALYSIS

All experiments were carried out in triplicate. The results are expressed as the mean of three independent replicates with error bars representing the standard deviation for each set of conditions. For the analysis of the influence of the factors, either t-test or one-way ANOVA were used, depending on the number of means to be compared. For statistical hypothesis testing, the significance level was 0.05.

3. RESULTS AND DISCUSSION

3.1. INFLUENCE OF STIRRING SPEED AND OF SEDIMENTATION TIME

Mixing may improve the recovery efficiency of microalgae harvesting by improving contact rates between the coagulants and the microalgal cells in ECF process [29]. In this work, three stirring speeds were tested (100 rpm, 250 rpm and 400 rpm). Experimental data displayed in **Figure 3** shows that the highest recovery efficiency (99 ± 1)% after 60 min. of electrolysis was achieved at the stirring speed 250 rpm when pH_i 8.0, current density is 6.7 mA/cm^2, and inter-electrode distance is 1.0 cm, using aluminum electrodes. However, after the same electrolysis time, (93 ± 1)% and (96 ± 1)% recovery efficiencies were obtained for stirring speeds of 400 rpm and 100 rpm, respectively. ANOVA analysis shows that there is a significant recovery efficiency difference when using different stirring speeds ($p<0.05$). These results could be explained by the fact that increasing stirring speed increases the contact probability between coagulants and microalgae and, hence, increases microalgae recovery. However, when the stirring speed becomes higher than a certain threshold, this causes the break-up of microalgal flocs due to the high shear forces applied, and thus, recovery efficiency decreases again [4]. The data in **Figure 3** are consistent with Maleki et al. [30], who found that by increasing stirring speed from 0 to 200 rpm, the recovery efficiency increased from 91% to 97%, but when further increasing the speed from 200 to 400 rpm, the recovery efficiency decreased from 97 to 94%. These results also agree with those from Vandamme et al. [4], who showed that for an increase in stirring speed from 0 to 60, and finally to 150 rpm, the time required to destabilize the

microalgal suspension decreased by almost a factor of two, but that at the maximum stirring speed of 200 rpm, destabilization was delayed.

As the same conclusion was made using iron electrodes and various current density values, a stirring speed of 250 rpm was used in the subsequent experiments.

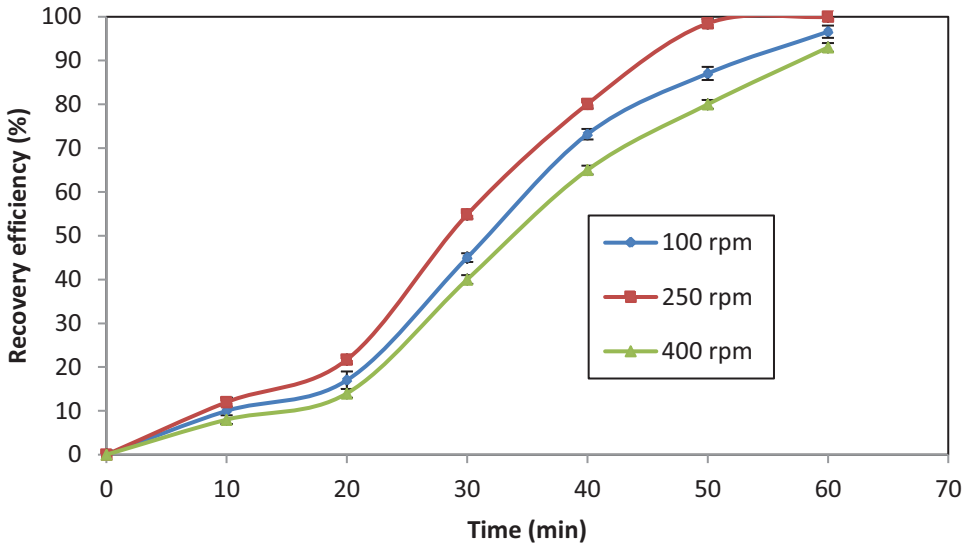

Figure 3. Microalgae recovery efficiency as a function of stirring speed. Conditions: Al electrodes, pH_i 8.0, current density 6.7 mA/cm^2, inter-electrode distance 1.0 cm, electrolysis time 60 minutes. Error bars represent standard deviations.

In **Figure 3**, the efficiency values correspond to measurements carried out after 45 min settling. Actually, when the samples were collected, the destabilization of the microalgal suspension continued after sampling. Contrary to the ECF cell in which flotation was the main mechanism of harvesting, settling prevailed in the collected water samples. The influence of settling time is illustrated in **Table 1**, both for iron and aluminum electrodes. A significant effect was evidenced for both metals ($p<0.05$); ongoing destabilization after sampling caused a significant increase in recovery efficiency, as η_a increased with settling time both with aluminum and iron electrodes. This could be explained by the fact that the contact between dissolved metal hydroxides and microalgal cells continues after sampling and also because more time is required for the smaller flocs to sediment [4]. As a conclusion, **Table 1** justifies why 45 min. settling were always applied after ECF process.

Table 1. Microalgae recovery efficiency as a function of settling time using Al and Fe electrodes. Conditions: Current density 6.7 mA/cm^2, pH_i 8.0, stirring speed 250 rpm, inter-electrode distance 1.0 cm, electrolysis time 60 minutes.

Electrode material	Settling time (min)	Recovery efficiency (%)
Aluminum	0	81 ± 1
	15	92 ± 1
	30	96 ± 1
	45	99 ± 1
Iron	0	45 ± 1
	15	53 ± 1
	30	59 ± 1
	45	64 ± 1

3.2. INFLUENCE OF ELECTRODE MATERIAL

It is well established in the literature on ECF that the electrode material plays a significant role on the process efficiency. Aluminum and iron are the most common sacrificial electrode materials and their respective efficiency has already been compared for example for the harvesting of *Dunaliella salina* microalgae [30]. In this work, ECF experiments have been carried out with both metals under the same conditions to select the best electrode material for the process optimization. As shown in **Figure 4**, *Chlorella vulgaris* recovery was always higher with Al electrodes than with Fe electrodes for all the values of electrolysis time. This confirms the data of **Table 1** for various settling time. For example, the recovery was nearly complete using aluminum electrodes ((99 ± 1)% efficiency) and was far higher than using iron electrodes ((64 ± 1)% efficiency) for 60 min. electrolysis time at the same current density ($p<0.05$). The lower efficiency of iron electrodes may be due, first, to the lower faradaic yield with iron in comparison to aluminum electrodes [31], (97 ± 1)% in this work for Fe, while it achieved up to (133 ± 3)% with Al due to the chemical corrosion of the electrodes superimposed on the electrodissolution of the anode. In addition, iron hydroxides are reported to be relatively poor coagulants compared to aluminum hydroxides [32]. These results are consistent with those of Baierle et al. [3], Vandamme et al. [4], Maleki et al. [30], and Gao et al. [23] who also advocated that aluminum is more efficient than iron as electrode material for the recovery of microalgae. However, the curves exhibit the same S-shaped curve for both metals, which means that

harvesting probably proceeds through similar mechanisms. A comparison of literature data is summarized in **Table 2**. The experimental results of **Figure 4** show a higher efficiency on *C. vulgaris* than in [4], especially with iron electrodes, but it must be pointed out that ECF was carried out at higher current in this work. Based on these results, aluminum electrodes will be used in the subsequent experiments and the influence of current will be analyzed.

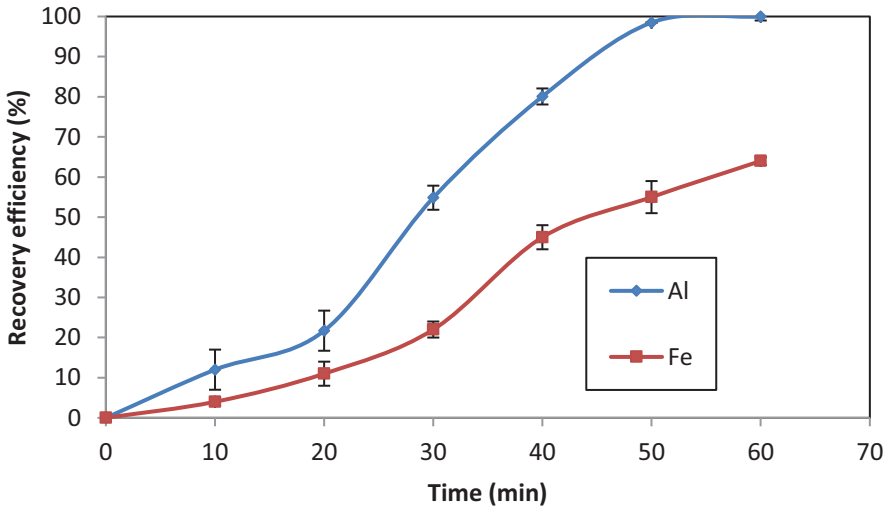

Figure 4. Microalgae recovery efficiency as a function of ECF time using different electrode materials. Conditions: Current density 6.7 mA/cm^2, pH$_i$ 8.0, stirring speed 250 rpm, inter-electrode distance 1.0 cm, electrolysis time 60 minutes. Error bars represent standard deviations.

Table 2. Comparison of aluminum and iron as sacrificial electrode material for microalgae recovery based on literature data: pH$_i$: initial pH, c_i: initial concentration, I: current, d_s: inter-electrode distance, N: stirring speed, j: current density, t: time.

Microalgae	Process	Operating conditions	Electrode material	Recovery efficiency (%)	References
Desmodesmus subspicatus	Electroflotation in batch	pH_i 5.70 ± 0.15 c_i = 1.84×10^7 cells/ml I = 3.0 A t = 20 min	Aluminum	95.4	[3]
			Iron	64.7	
Dunaliella salina	Electro-coagulation-flocculation in batch	I = 1.0 A d_s = 1.0 cm N = 200 rpm t = 5 min	Aluminum	86	[30]
			Iron	75	
Microcystis aeruginosa	Electro-coagulation–flotation in batch	pH_i 7.0 c_i =1.2×10^9-1.4×10^9 cells/mL j = 1.0 mA/cm^2 t = 45 min	Aluminum	100	[23]
			Iron	78.9	
Chlorella vulgaris	Electro-coagulation-flocculation in batch	pH_i 8.0 c_i = 0.3-0.6 g/L j = 3.0 mA/cm^2 t = 30 min	Aluminum	~80	[4]
			Iron	~0	

3.3. INFLUENCE OF CURRENT DENSITY

In all the electrolytic harvesting processes, current density is a critical parameter which governs not only the efficiency, but also power consumption, coagulant dosage and microbubble density [2]. In this work, current density values were 2.9 mA/cm^2, 4.8 mA/cm^2 and 6.7 mA/cm^2, respectively. These were tested for an initial pH of 8.0. Only aluminum was used as the electrode material, as this is far more efficient than iron. Experimental results are displayed in **Figure 5a**; these show that the recovery efficiency was (40 ± 1)%, (72 ± 2)% and (99 ± 1)% at current density 2.9 mA/cm^2, 4.8 mA/cm^2 and 6.7 mA/cm^2 after 60 min. electrolysis, respectively ($p<0.05$). The increase of recovery efficiency with the increase of current density is consistent with the results of Aragón et al. [33]. The highest recovery efficiency of (99 ± 1)%

reached in this study was higher than the highest recovery efficiency of 95% and 94.9% reached in the studies of Vandamme et al. [4] and Matos et al. [34] who worked on the same microalgal species *(Chlorella vulgaris).* All the curves were S-shaped, with a steep rise after 20 min. electrolysis at 6.7 mA/cm^2, while this was delayed after 30 min at 4.8 mA/cm^2. As a result, while the difference in harvesting efficiency was less than 5% between the three current density values after 20 min electrolysis, η_a reached (80 ± 3)%, (37 ± 2)% and (24 ± 2)% at current density 6.7, 4.8, and 2.9 mA/cm^2 after 40 min. treatment, respectively.

The higher harvesting efficiency at higher current density can be explained from Faraday's law:

$$W = \Phi \cdot \frac{I \cdot t \cdot M}{n \cdot F}$$

In this equation, F is Faraday's constant (F = 96487 C/mol), M is the molecular weight of a given metal (g/mol), n the number of electrons exchanged in the electrode surface (n=3 for aluminum), I the current (A), t the electrolysis time (s), Φ is faradaic yield, and W estimates the mass of dissolved metal (g). Based on Faraday's law, the amount of coagulant released is nearly proportionally to current density, but not exactly proportional, as the faradaic yield measured at the end of each run on the basis of electrode weight loss slightly decreases when current increases. Therefore, current density has a direct effect on the anode dissolution rate and on Al dosage, which strongly affects the performance of the ECF process. The consequence is an enhanced microalgae separation rate, in agreement with literature data [35]. To investigate the effect of the amount of coagulant released on η_a, this was plotted as a function of volumetric charge loading in **Figure 5b**, even though this neglects the influence of the faradaic yield. Volumetric charge loading (q) is calculated as

$$q = I.t/V$$

where I is the current (A), t is the operating time (s) and V is the cell volume (L). In this figure, the curves for the three current density values follow the same trend, even though they do not perfectly superimpose at high volumetric charge loading. This may be partially due to the difference in faradaic yield, but there are many other phenomena that can explain this point. For example, current density also determines the rate of production of hydrogen gas, again on the basis of Faraday's law [36], and thus, the propensity of microalgae to be harvested by flotation. **Figure 5c** also compares our results to those of Vandamme et al. [4] in terms of volumetric charge loading required for achieving the highest microalgal recovery efficiency.

This figure highlights the strong differences observed in this work as a function of initial pH, but also with Vandamme et al. data; these differences demonstrate the strong influence of pH and water composition on microalgae harvesting at constant volumetric charge loading. This figure also shows that the present results outperform those of Vandamme et al. [4], especially under acidic pH values: In this study, only 840 C/L volumetric charge loading is needed to reach almost complete microalgal recovery at current density 6.7 mA/cm^2 and fixed pH 4.0 while 1440 C/L were needed by Vandamme et al. to reach the highest recovery efficiency of only 92% obtained in their work. In addition, pH changes during the ECF treatment, and its evolution also depends on current. As shown in **Figure 6**, there is a gradual increase in pH with electrolysis time, whatever the current density, but the rate of pH increase is enhanced by the increase in current density. For example, when initial pH was 8.0, the final pH was 9.6 ± 0.1 when the current density was 2.9 mA/cm^2, 9.9 ± 0.1 when it was 4.8 mA/cm^2, and 10.4 ± 0.1 when it was 6.7 mA/cm^2. A similar behavior was observed for all the values of pH_i between 4.0 and 8.0, which was attributed to the continuous production of OH^- ions at the cathode with the generation of Al^{3+} at anode [23].

As a conclusion, current density is the key operating parameter of the ECF process, as expected. However, it plays a complex role as it governs at the same time the rate of coagulant dosage, the evolution of pH, and the amount of microbubbles able to collect microalgae and solid flocs. Based on the results of **Figure 5**, 6.7 mA/cm^2 was chosen as the current density to be used in the subsequent experiments, since 100% recovery could be reached only when this value was applied in the ECF process within less than 60 minutes.

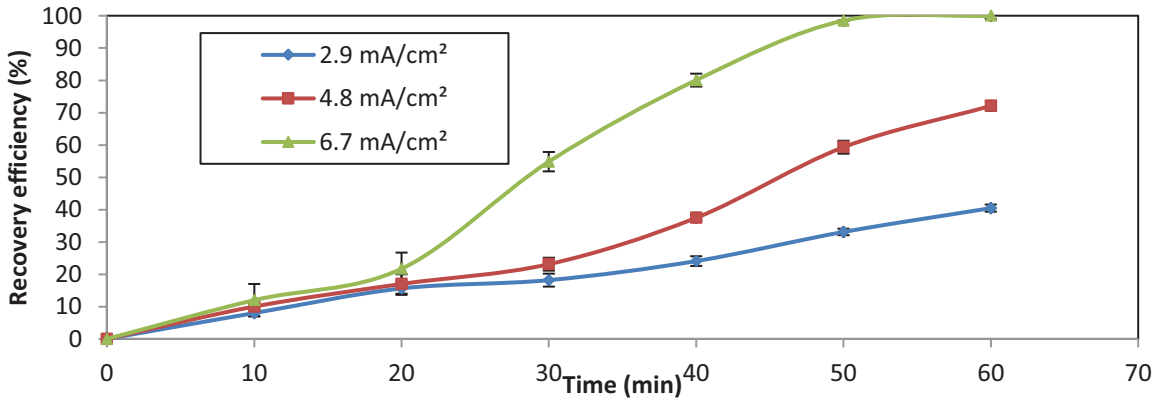

(a)

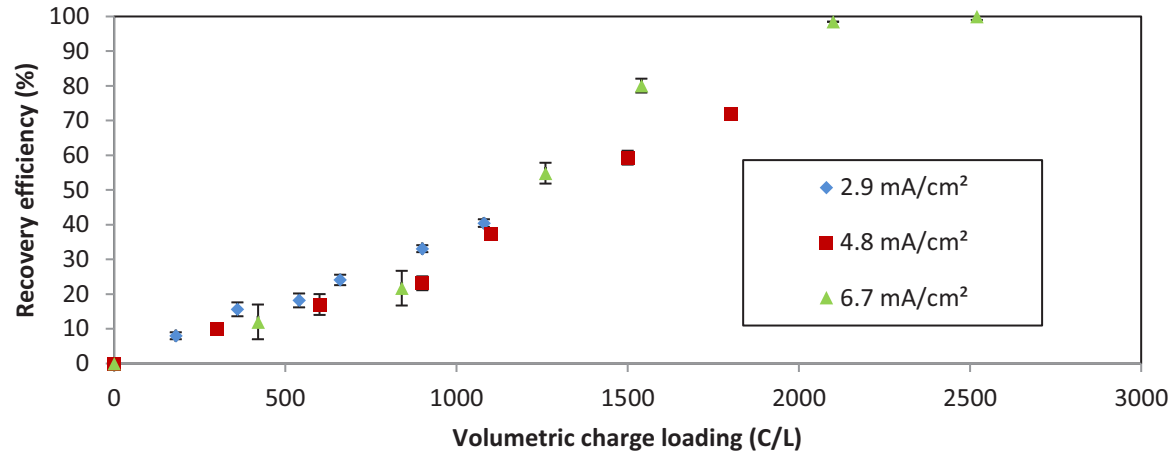

(b)

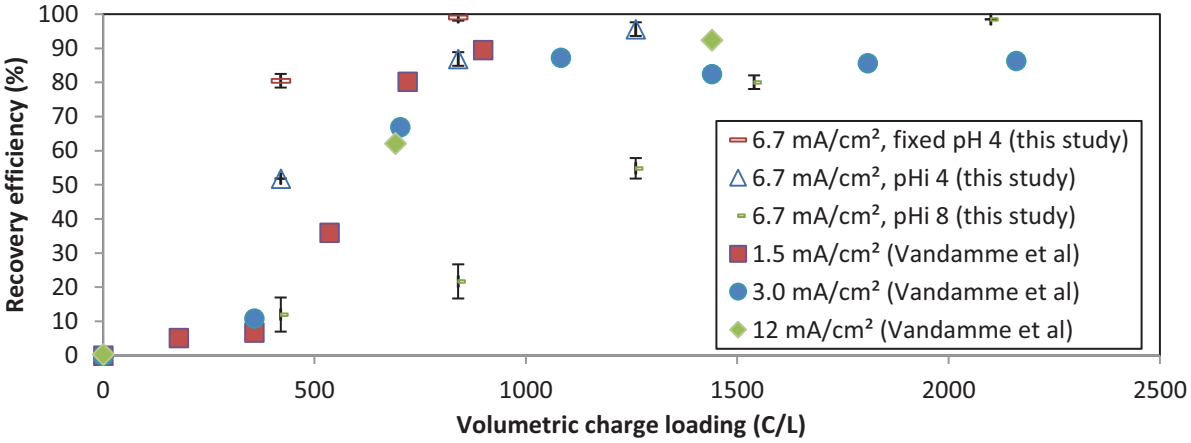

(c)

Figure 5. Microalgae recovery efficiency: (a) vs. ECF time (in our study); (b) vs. volumetric charge loading as a function of current density; (c) vs. volumetric charge loading in comparison with results from Vandamme et al. [4]. Conditions of this study: stirring speed 250 rpm, inter-electrode distance 1.0 cm. Error bars represent standard deviations.

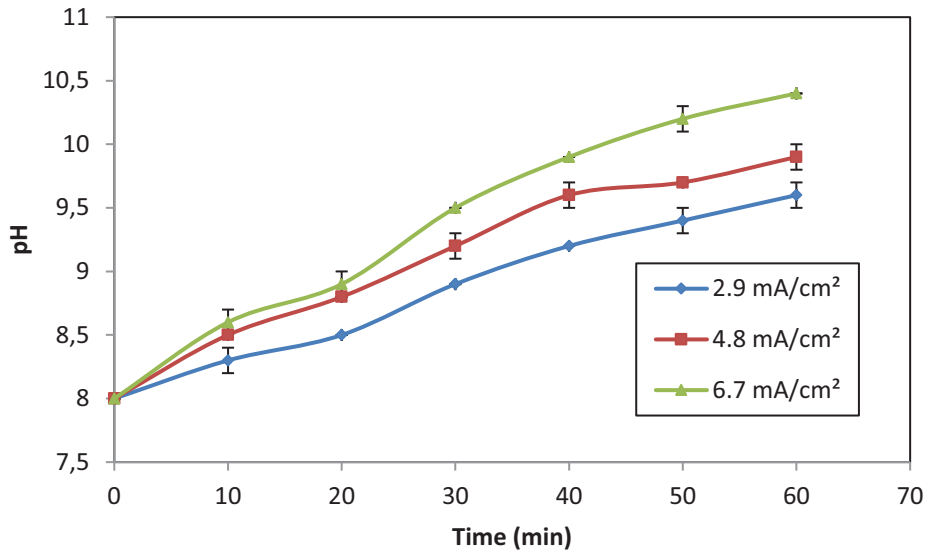

Figure 6. pH change as a function of current density. Conditions: pH_i 8.0, stirring speed 250 rpm, inter-electrode distance 1.0 cm, electrolysis time 60 minutes. Error bars represent standard deviations.

3.4. INFLUENCE OF INITIAL pH AND MECHANISMS OF HARVESTING

pH is a key water property influencing the performance of ECF process [37], as it determines the speciation of metal hydroxides in the solution. For aluminum, the net charge of Al species is positive at acidic pH and negative at alkaline pH [32]. In this work, three initial pH values were compared (4.0, 6.0 and 8.0). As shown by experimental data **(Figure 7)**, the recovery efficiency decreased with the increase of pH_i: this reached about (87 ± 2)% after only 20 minutes at pH_i 4.0, while it was (45 ± 1)% and (22 ± 5)% at pH_i 6.0 and 8.0 after the same electrolysis time, respectively ($p<0.05$). These results are consistent with those of Vandamme et al. [4] who also found that recovery efficiency decreased with the increase of pH_i. **Figure 7** also highlights that the main effect of pH_i is to change the kinetics of microalgae recovery: this followed a S-shaped curve at pH_i 8.0 (as already observed in **Figure 5**), while the initial period in which recovery rate is slow tended to vanish when pH_i was decreased.

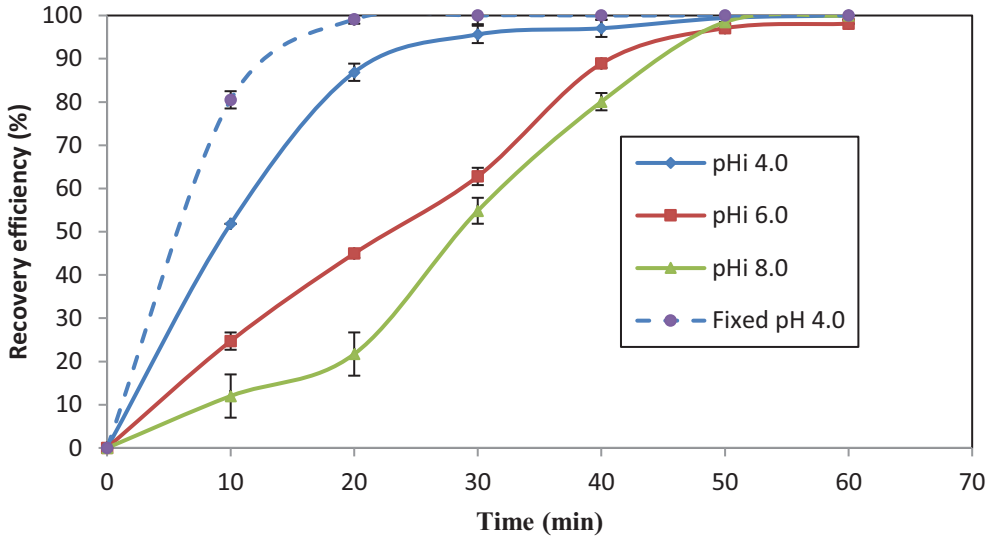

Figure 7. Microalgae recovery efficiency as a function of initial pH and fixed pH 4.0. Conditions: current 6.7 mA/cm^2, stirring speed 250 rpm, inter-electrode distance 1.0 cm, electrolysis time 60 minutes. Error bars represent standard deviations.

These results might be explained by the aluminum speciation, which relies both on the actual pH and Al concentration on the basis of the concentration Pourbaix diagram of aluminum. Under acidic conditions, aluminum hydroxide precipitates and monomeric hydroxoaluminum cations, as well as polymeric species (such as $Al_{13}O_4(OH)_{24}^{7+}$) dominate in water. Consequently, positively charged precipitates are formed (i.e. aluminum hydroxide together with the adsorbed hydroxoaluminum cations). Therefore, the negatively charged microalgae would be neutralized, which facilitates microalgae recovery [23]. This result also agrees with the high rate of harvesting when ECF begins in **Figure 7** and highlights that charge neutralization plays a key role on microalgae recovery at acidic pH_i, while only sweep coagulation acts on harvesting at alkaline pH_i. pH_i value did not affect the faradaic yield that was (134 ± 2)% at the three tested pH_i values.

To ascertain the analysis of the effect of pH, another series of ECF experiments under controlled pH conditions (pH 4.0) was carried out. This was achieved using a pH control system constituted by a pHmeter and a dosing pump BL7-2 (Black Stone, Romania) connected to a PID controller (*Ero Electronic*, Italy), the pump being fed by a 0.1 HCl solution. The results showed that almost complete recovery was reached after 20 min. electrolysis time **(Figure 7)**. Data also showed that the faradaic yield at fixed pH 4.0 which was (136 ± 2)% (which corresponds to (0.080 ± 0.001) g electrode mass loss after 20 min. electrolysis time) did not

increase significantly compared to the faradaic yield of (134 ± 2)% obtained at pH_i 4.0, 6.0 and 8.0. The results of this section confirm that the recovery mechanism is charge neutralization, as mainly cationic species are formed at this fixed acidic pH. Faster recovery at fixed pH 4.0 than at pH_i 4.0 is due to pH increase when experiments are carried out without pH control, as already shown in **Figure 6**. Consequently, a change of harvesting mechanism occurs progressively when pH becomes more alkaline in conventional ECF experiments, corresponding to a decrease of the effect of charge neutralization, as this seems to have a higher ability the separation of microalgae than other mechanisms, such as sweep flocculation, adhesion, or enmeshment. When alkaline conditions prevail, charge neutralization and adhesion of the negatively charged microalgae on flocs are unlikely to occur, as $Al(OH)_4^-$ anions and insoluble $Al(OH)_3$ are the dominant species, and these are obviously less efficient for the separation of negatively charged microalgae [38]. In ECF, as a large amount of aluminum has to be released to achieve high pH, sweep flocculation is the most probable mechanism of microalgae separation in this case; this agrees with S-shaped curves with a significant break of slope when sweep flocculation starts. Based on this conclusion, further experiments will be performed at pH_i 4.0.

3.5. ASSESSMENT OF HARVESTING MECHANISM

In order to compare the respective effects of charge neutralization, adhesion on flocs, direct flotation on microbubbles, and sweep coagulation, several series of experiments were carried out. First, to check whether adhesion of microalgae proceeds on preformed flocs under acidic, neutral or alkaline conditions, these were mixed with microalgal cells for 24.0 hrs. at pH values 4.0, 6.0 and 8.0. Experimental results showed that there was no adhesion of microalgae on the flocs at the three tested pH values.

Similarly, to get a better insight in the influence of charge neutralization, the evolution of zeta potential during ECF was investigated at the same three different pH_i (4.0, 6.0 and 8.0). Zeta potential is a physicochemical parameter that describes the electrokinetic potential of a colloidal system. It is an important index of the stability of colloidal dispersions: zeta potential magnitude measures the extent of electrostatic repulsion between adjacent, similarly charged, particles in a dispersion. For macromolecules and colloidal particles, a high zeta potential provides stability, *i.e.* the solution or dispersion resists aggregation. When the potential is low, attractive forces surpass the electrostatic repulsion and the dispersion may flocculate or aggregate [39, 40].

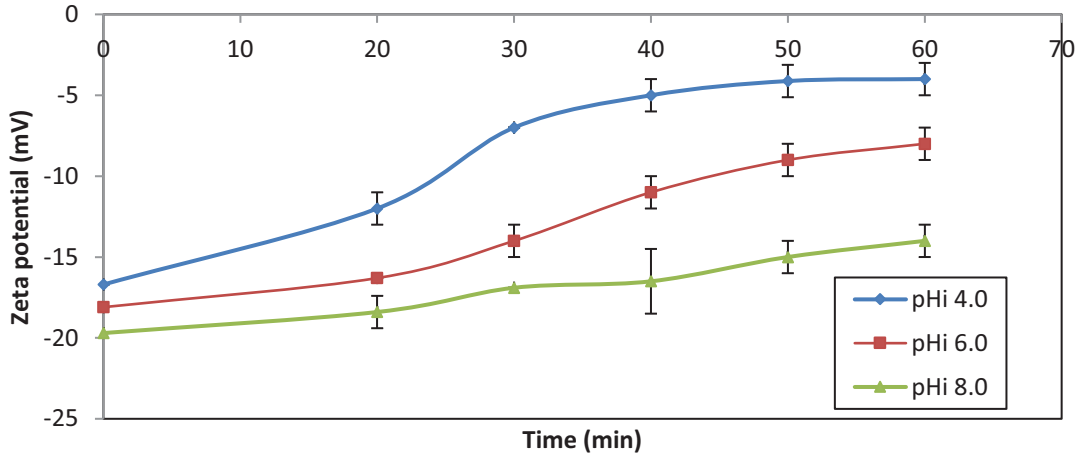

Figure 8. Zeta potential change during ECF. Conditions: Current density 6.7 mA/cm^2, stirring speed 250 rpm, inter-electrode distance 1.0 cm, electrolysis time 60 minutes. Error bars represent standard deviations.

Before the onset of electrocoagulation, zeta potential was shown to be more electronegative at higher pH_i values, *i.e.* -19.7 mV at pH_i 8.0, -18.1 mV at pH_i 6.0 and -16.7 mV at pH_i 4.0. This is due to negative charge of microalgal cells, in agreement with literature data; the electrostatic repulsion decreases when pH is decreased, which means that zeta potential is closer to zero at lower pH values. **Figure 8** shows that during ECF, zeta potential values increased with time at all the pH_i values, even though they always remained negative. This trend was less prominent for pH_i 8.0, for which zeta potential just increased from -19.7 mV into (-14.0 ± 1.0) mV after 60 min. electrolysis time. This result highlights the enhanced role of charge neutralization due to Al release when pH_i is decreased. During ECF, it can be assumed that the zeta potential which is initially imposed by microalgal cells evolves progressively to that of the colloidal solid particles when the amount of aluminum released increases. Under alkaline conditions, the values of the zeta potential indicate that the mechanism responsible for microalgae harvesting is sweep flocculation, rather than charge neutralization. Conversely, at pH_i 6.0, almost complete recovery was reached after 50 min. electrolysis time, when zeta potential value reached (-9.0 ± 1.0) mV, while the same result was achieved after 40 min. at pH_i 4.0 when zeta potential was (-5.0 ± 1.0) mV, highlighting the enhanced role of charge neutralization.

Finally, to assess the role of Al dosage and verify the necessity of floc formation during ECF, electroflotation experiments without floc formation were carried out using titanium electrodes at-pH_i 4.0, 6.0 and 8.0. This gives access to the contribution of microalgae adhesion on microbubbles in the absence of coagulant. Experimental data revealed a lower recovery

efficiency in the three cases: (33.2 ± 0.2)%, (36.6 ± 0.3)% and (35.2 ± 0.3)% at pH_i 4.0, 6.0 and 8.0, respectively. These results ensure the importance of coagulant release and floc formation on the recovery efficiency.

As a conclusion, the direct adhesion of microalgae on flocs plays only a weak role on microalgal recovery when flocs are stabilized; flotation directly onto bubbles contributes to a maximum of 36.6% of harvesting yield, but floc formation is compulsory to complete the operation. Conversely, sweep flocculation is a key process of ECF, but this requires a minimum amount of coagulant to process, which explains the S-shaped curves. So, the effectiveness of the microalgal recovery can be enhanced when initial pH is acidic, so that removal starts immediately, combining charge neutralization coagulation at the beginning of ECF to sweep coagulation at longer electrolysis time. This is consistent with the results of Gao et al. [23] and Vandamme et al. [4].

3.6. INFLUENCE OF INTER-ELECTRODE DISTANCE

In this work, three different inter-electrode distances were studied; 1.0 cm, 1.5 cm and 2.0 cm, respectively. As **Figure 9** shows, the efficiency of microalgae harvesting decreased when the inter-electrode distance increased. Almost complete recovery was obtained with the inter-electrode distance of 1.0 cm after 60 min. electrolysis, while only 95% and 90% recovery efficiency were obtained with the inter-electrode distance of 1.5 cm and 2.0 cm, respectively, after the same electrolysis time ($p<0.05$). The main reason is that the recovery was faster at lower inter-electrode distance, as it reached about (87 ± 2)% with the inter-electrode distance 1.0 cm after 20 min. electrolysis, while it was only (75 ± 1)% and (70 ± 1)% with the inter-electrode distance of 1.5 cm and 2.0 cm, respectively, after the same time interval.

This result could be explained by the fact that when the distance increases, the faradaic yield Φ decreases, so that the amount of coagulant released with time is reduced [38]. This was proved experimentally in this work, as the faradaic yield was (134 ± 2)%, (123 ± 1)% and (115 ± 1)% at inter-electrode distance of 1.0 cm, 1.5 cm and 2.0 cm, respectively. Experimental results are also consistent with those of Valero et al. [41] who found that electrode distance of 5.5 cm was about 3% more effective than with an electrode distance of 7.0 cm.

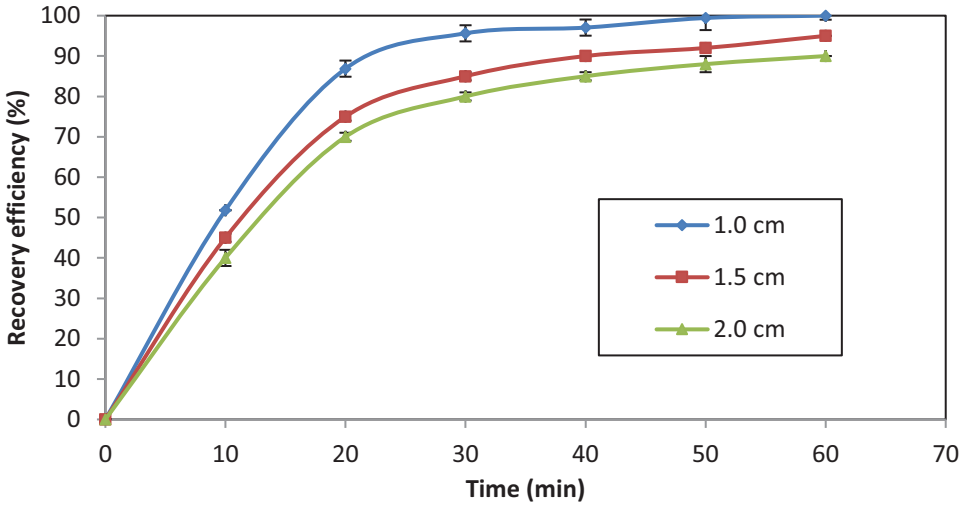

Figure 9. Microalgae recovery efficiency as a function of inter-electrode distance. Conditions: pH_i 4.0, current density 6.7 mA/cm^2, stirring speed 250 rpm, electrolysis time 60 minutes. Error bars represent standard deviation.

4. ELECTRIC ENERGY CONSUMPTION

The electric energy consumption (EEC) in kWh/kg of recovered microalgae was deduced from the following equation:

$$EEC = \frac{U \cdot I \cdot t}{1000 \cdot V \cdot \eta_a \cdot c_i}$$

where U is the cell voltage (V) (it ranged from 14.0 V to 29.5 V), I is the current (A), t is the time of ECF treatment (h) needed for complete microalgae recovery, V is the volume of the microalgal solution (m^3), η_a is the microalgae recovery efficiency, and c_i is the initial microalgae biomass concentration (kg/m^3).

Experiments performed at pH_i 4.0 at all current density values showed that complete microalgal recovery could be achieved in the three cases, but at longer electrolysis time with lower current density, as expected. For power input, it was found that using lower current density for longer time was less energy consuming because U also increased with I, while EEC was only proportional to electrolysis time. For completing microalgae recovery, EEC increased therefore from (5.3 ± 0.2) kWh/kg to (9.4 ± 0.3) kWh/kg with the increase of current density from 2.9 to 6.7 mA/cm^2 when electrode distance was 1.0 cm (**Figure 10**), in agreement with Kim et al. [2]. EEC at current density 2.9 mA/cm^2 (5.3 ± 0.2 kWh/kg) in this work is also lower than EEC obtained for the recovery of *Tetraselmis sp.* (9.16 kWh/kg), but higher than that of *Chlorococcum sp.* (4.44 kWh/kg) [21]. As a conclusion, the most energy saving conditions for

the harvesting of microalgae corresponds to 2.9 mA/cm^2, *i.e.* the smallest value used in this work. **Figure 10** also shows the evolution of EEC as a function of inter-electrode distance at three current densities. In all cases, EEC increased with the increase of inter-electrode distance, as electrical conductance is inversely proportional to electrode distance. For example, at current density 2.9 mA/cm^2, increasing the inter-electrode distance from 1.0 cm to 2.0 cm, increased EEC from (5.3 ± 0.2) kWh/kg to (8.1 ± 0.1) kWh/kg. Similar results were reported by Zenouzi et al. [16]. In an attempt to further reduce EEC, another possibility is to increase the electrical conductance by acting on water conductivity. The simplest and most cost-effective way is the addition of NaCl salt. Different concentrations of this cheap salt were added to the microalgal solution (0.5 g/L, 1.0 g/L and 1.5 g/L). As shown in **Table 3**, increasing NaCl concentration always decreased EEC. The lowest EEC value, about 1.0 kWh/kg, was achieved at current density 2.9 mA/cm^2 when 1.5 g/L NaCl was added.

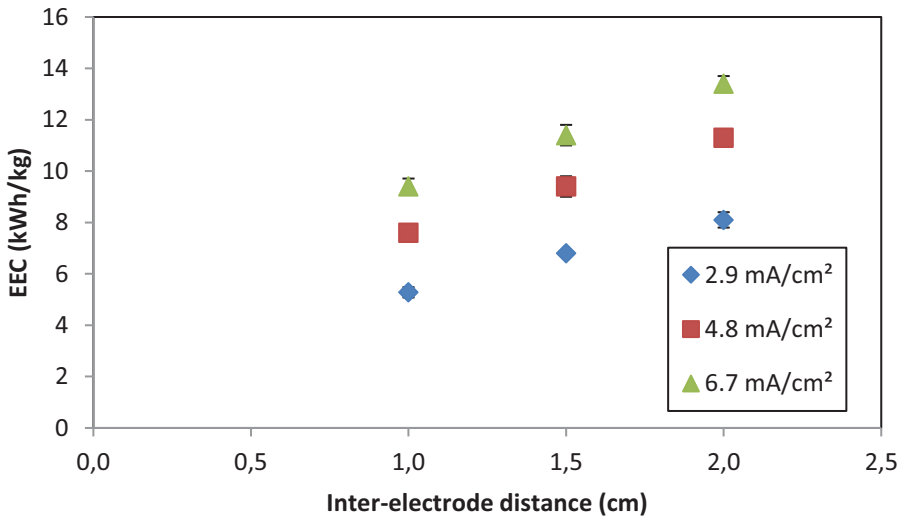

Figure 10. Electric energy consumption as a function of current density and inter-electrode distance for complete microalgae recovery. Conditions: pH_i 4.0, stirring speed 250 rpm. Error bars represent standard deviations.

Table 3. Electric energy consumption as a function of current density and NaCl concentration for complete microalgae recovery. Conditions: pH_i 4.0, stirring speed 250 rpm, inter-electrode distance 1.0 cm.

Current density (mA/cm^2)	EEC (kWh/kg)		
	0.5 g/L NaCl	1.0 g/L NaCl	1.5 g/L NaCl
2.9	2.8 ± 0.1	1.7 ± 0.2	1.0 ± 0.1
4.8	4.9 ± 0.2	2.6 ± 0.3	1.5 ± 0.1
6.7	5.7 ± 0.1	2.9 ± 0.2	1.6 ± 0.2

This EEC value needed for complete microalgae recovery is lower than most values reported in literature for microalgae recovery by electrochemical techniques; for example, 1.3 kWh/kg energy consumption was reported in the study carried out by Vandamme et al. for the recovery of *Chlorella vulgaris* [4]. This seems also more economic than EEC values obtained when using other techniques for microalgae harvesting. **Table 4** compares EEC in our study to EEC in other microalgae harvesting techniques. Even though the cost of NaCl addition must be accounted for, NaCl is a cheap salt, and further optimization of the amount of salt added can be driven from an economic point of view.

Table 4. Recovery efficiency and energy consumption of different microalgae harvesting techniques.

Harvesting technique	Recovery efficiency (%)	Energy input (kWh/kg)	Reference
Electro-coagulation-flocculation	100	1.0	This work
Tangential flow filtration	89	3.6	[8]
Electrochemical harvesting (ECH) with non-sacrificial electrodes	94.5	1.6	[42]
Vacuum filters	99	1.2	[43]
Polymer flocculation	80	36.8	[8]
Centrifugation	99	16.0	[44]

As a conclusion, EEC can be minimized usually by reducing current, while maintaining a complete microalgae harvesting at the expense of longer electrolysis time, provided pH_i is decreased to 4.0 and salt is added. A techno-economic optimization is, however, compulsory

because longer time requires larger equipment and higher equipment cost under continuous process.

5. INFLUENCE OF ECF ON LIPID AND PIGMENT CONTENT

Microalgal lipid content results from cultivation conditions [42]. The used microalgae harvesting technique must not affect lipid yield and should not restrict lipid extraction process. For this reason, the influence of ECF as the harvesting method on lipid content of microalgae was investigated at different current densities (2.9 mA/cm^2, 4.8 mA/cm^2 and 6.7 mA/cm^2).

Experimental results (data not shown) display that ECF at different current density values had no significant effect on the lipid content of *Chlorella vulgaris* ($p>0.05$). More precisely, lipid content was always (18 ± 1)% (in the control sample and in the samples exposed to ECF at all current density values (2.9 mA/cm^2, 4.8 mA/cm^2 and 6.7 mA/cm^2). This result is interesting, as microalgal lipids are highly oxidizable in certain conditions, such as high temperature and presence of light and oxygen (mainly due to the presence of unsaturated fatty acids which are preferably oxidized) [45]. This invariability in lipid content in samples exposed to ECF was also reported by Misra et al. [42] who investigated the harvesting of *Chlorella sorokiniana* and *Scenedesmus obliquus*; however, in their work lipid content of both microalgae tested was lower than in our case (12% and 15% dry cell weight for *C. sorokiniana* and *S. obliquus*, respectively). As no additional chemicals except salt are added during ECF process, nothing interferes with the organic solvent extraction of lipids. Consequently, the application of ECF at the commercial scale biodiesel production plant is possible.

Microalgal pigment content was also analyzed after ECF and compared with the results obtained from the control sample. As **Figure 11** shows, there was no significant decrease ($p>0.05$) in total pigment content in samples exposed to ECF, in which the percentage of pigments in the biomass was (2.1 ± 0.2)%, (2.0 ± 0.2)%, (1.9 ± 0.2)% and (2.2 ± 0.2)% in samples exposed to ECF at current density 2.9 mA/cm^2, 4.8 mA/cm^2, 6.7 mA/cm^2, and in the control sample, respectively. Our results disagree with those of Matos et al. who found a significant decrease of pigments content in samples exposed to electrocoagulation [46]. These variations in pigment content could be explained by oxidation of the pigments and their conversion to esters [46]. Performing ECF more rapidly even at higher current may reduce the reduction in pigment content and microalgae may avoid the effect of other oxidative agents, such as oxygen, pH and light. It seems that ECF experimental conditions of this work are

suitable for conserving the biological identity of the microalgal lipids, contrary to Matos et al. [46].

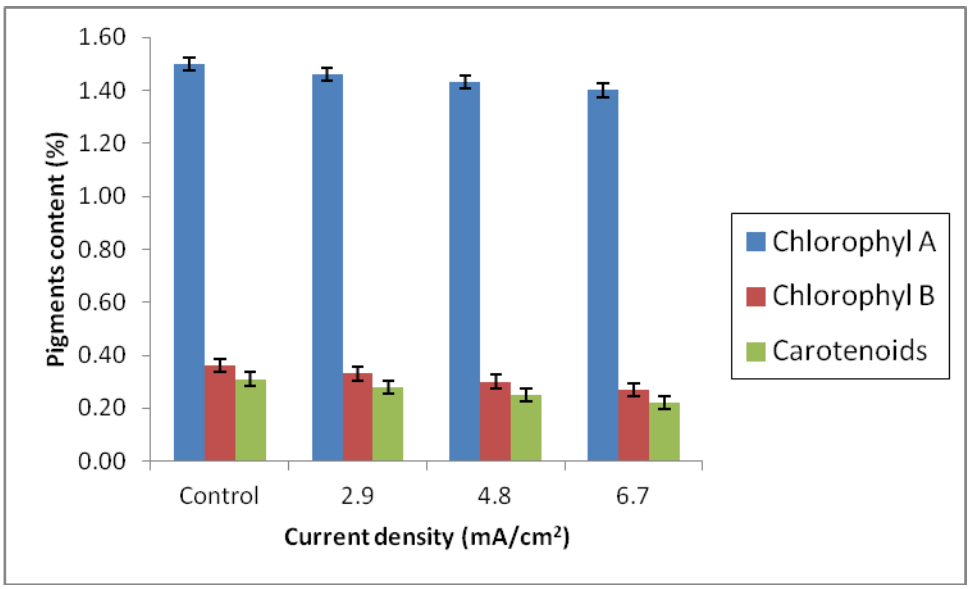

Figure 11. Effect of ECF at different current density values on pigment content. Conditions: pH_i 4.0, stirring speed 250 rpm, inter-electrode distance 1.0 cm, electrolysis time 60 minutes. Error bars represent standard deviations.

6. ALUMINUM ACCUMULATION DURING ECF

Aluminum concentration in the process water must be minimized because of its harmful effects on human health [3]. In a study conducted by Arain et al. [47], a relationship was established between the amount of aluminum cations in scalp hair samples and Alzheimer's disease in patients. Other researchers reported deficiency in learning and weakness in memory following oral administration of small doses of aluminum sulfate to rats [48]. In addition, aluminum may also be harmful to the environment. Due to these harmful effects, it is of utmost importance to reach the lowest possible concentration of aluminum ions in the liquid after biomass separation. However, it was found that the Al^{3+} content in the biomass recovered after electroflotation is higher than in centrifuged samples (0.08 mg/g) [3].

In this study, aluminum accumulation in the harvested microalgae and in the liquid phase was investigated with two different current density values. As shown in **Figure 12a** and **Figure 12b** and as expected by Faraday's law, aluminum concentration in the microalgal biomass and in water increased as time and current density increased, but a plateau emerged in the curves of both figures. The increase of Al content in water with current is in agreement with Vandamme

et al. who also reported higher aluminum content in the liquid phase at higher current density [4]. Similarly, higher Al concentrations in the biomass at higher current density are in agreement with Vandamme et al. [4] who found that aluminum content in the recovered microalgal biomass (*Chlorella vulgaris*) was about twice as high at 3.0 mA/cm^2 than at 1.5 mA/cm^2, and also with Matos et al. [46]. Vandamme et al. [4] found 1.5% of Al in the biomass for 10 min. ECF at 3.0 mA/cm^2, while Matos et al. found 1.4% at current density 8.3 mA/cm^2 [46], which means that current is not the only parameter to account for. In order to prevent Al concentration in water from increasing above 2.0 mg/L and keep Al percentage in microalgal biomass less than 1%, ECF should be applied with shorter electrolysis time and at lower current. In this case, recovery efficiency may decrease, so that a compromise must be found to maintain an acceptable level of recovery and a low amount of aluminum in process water and in recovered microalgal biomass at the same time.

In this work, complete removal may be achieved within 30 minutes treatment when pH_i is 4.0 and current density 6.7 mA/cm^2. In this case, Al concentration in the liquid phase was reduced to (1.2 ± 0.1) mg/L and the Al content in microalgal biomass was only (0.9 ± 0.1)%, which substantially reduces liquid and biomass contamination with aluminum. This takes benefits from the plateau region of **Figure 12** and from the fact that low pH_i prevents reaching pH values at which soluble aluminate anions prevail. Working at lower current needed longer electrolysis time, so that the final Al content in biomass and water were similar. It emerges that if it is possible to reduce aluminum release in the biomass and the effluents, a minimum value cannot be avoided to complete the harvesting of microalgae. Similarly, it appears that electrolysis time and current must also be optimized and controlled during ECF for environmental reasons.

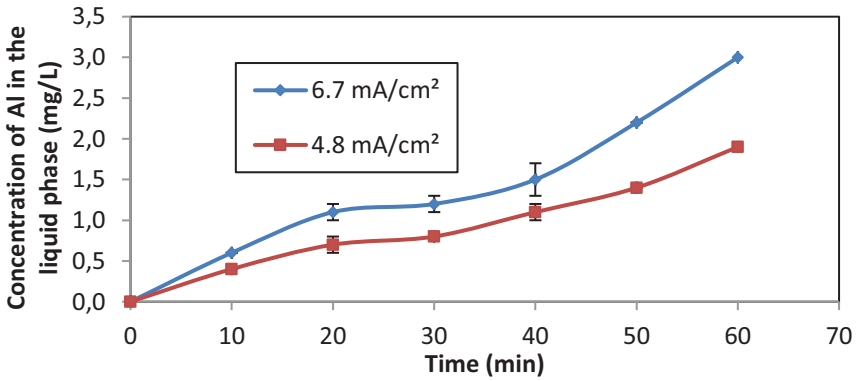

(a)

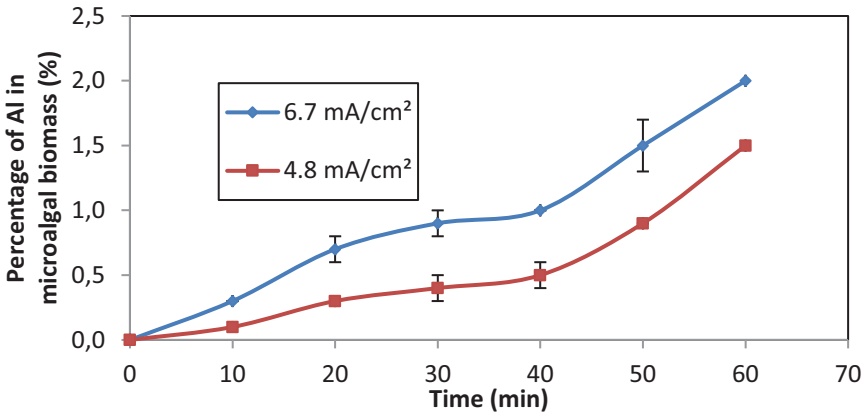

(b)

Figure 12. Aluminum content in (a) liquid phase and in (b) microalgal biomass measured as a function of current density. Conditions: pH_i 4.0, stirring speed 250 rpm, inter-electrode distance 1.0 cm, electrolysis time 60 minutes. Error bars represent standard deviations.

7. CONCLUSIONS AND PERSPECTIVE

In this study, ECF for harvesting the microalgae *Chlorella vulgaris* was investigated. Microalgae recovery was studied as a function of stirring speed, electrode material, current density, initial pH and inter-electrode distance. Experimental results showed that aluminum electrodes were far more efficient than iron electrodes for *Chlorella vulgaris* recovery. The mechanisms of microalgae harvesting were elucidated: zeta potential analysis showed that the mechanism responsible for microalgae recovery was charge neutralization at pH_i 4.0 and 6.0 and sweep flocculation at pH_i 8.0, while flotation only on bubbles could contribute to a maximum of 36.6% of harvesting efficiency. Moreover, experimental data showed that ECF did not affect microalgal biomass lipid and pigment content. In addition, these showed that a reduction of ECF cost could be achieved by working at the lowest current density and lowest inter-electrode distance to achieve complete recovery. The amount of aluminum in water and biomass could also be minimized by optimizing electrolysis time and current. However, water conductivity and inter-electrode distance were the key factors to save energy, so that a minimum value about 1.0 kWh/kg microalgae recovered could be achieved using the addition of 1.5 g/L NaCl. Now, testing ECF of *Chlorella vulgaris* in the continuous mode is the priority for further work before process optimization.

REFERENCES

[1] J. Kim, B.-G. Ryu, K. Kim, B.-K. Kim, J.-I. Han, J.-W. Yang, Continuous microalgae recovery using electrolysis: effect of different electrode pairs and timing of polarity exchange, Bioresource Technology. 123 (2012) 164–170.

[2] J. Kim, B.-G. Ryu, B.-K. Kim, J.-I. Han, J.-W. Yang, Continuous microalgae recovery using electrolysis with polarity exchange, Bioresource Technology. 111 (2012) 268–275.

[3] F. Baierle, D.K. John, M.P. Souza, T.R. Bjerk, M.S. Moraes, M. Hoeltz, A.L. Rohlfes, M.E. Camargo, V.A. Corbellini, R.C. Schneider, Biomass from microalgae separation by electroflotation with iron and aluminum spiral electrodes, Chemical Engineering Journal. 267 (2015) 274–281.

[4] D. Vandamme, S.C.V. Pontes, K. Goiris, I. Foubert, L.J.J. Pinoy, K. Muylaert, Evaluation of electro-coagulation–flocculation for harvesting marine and freshwater microalgae, Biotechnology and Bioengineering. 108 (2011) 2320–2329.

[5] L. Rodolfi, G.C. Zittelli, L. Barsanti, G. Rosati, M.R. Tredici, Growth medium recycling in *Nannochloropsis sp*. mass cultivation, Biomolecular Engineering. 20 (2003) 243–248.

[6] D. Bilanovic, G. Shelef, A. Sukenik, Flocculation of microalgae with cationic polymers—effects of medium salinity, Biomass. 17 (1988) 65–76.

[7] D. Vandamme, I. Foubert, B. Meesschaert, K. Muylaert, Flocculation of microalgae using cationic starch, Journal of Applied Phycology. 22 (2010) 525–530.

[8] M.K. Danquah, L. Ang, N. Uduman, N. Moheimani, G.M. Forde, Dewatering of microalgal culture for biodiesel production: exploring polymer flocculation and tangential flow filtration, Journal of Chemical Technology and Biotechnology. 84 (2009) 1078–1083.

[9] Y.M. Chen, J.C. Liu, Y.-H. Ju, Flotation removal of algae from water, Colloids and Surfaces B: Biointerfaces. 12 (1998) 49–55.

[10] N. Uduman, Y. Qi, M.K. Danquah, G.M. Forde, A. Hoadley, Dewatering of microalgal cultures: a major bottleneck to algae-based fuels, Journal of Renewable and Sustainable Energy. 2 (2010) 12701.

[11] R. Bosma, W.A. van Spronsen, J. Tramper, R.H. Wijffels, Ultrasound, a new separation technique to harvest microalgae, Journal of Applied Phycology. 15 (2003) 143–153.

[12] S.J. Lee, S.B. Kim, J.E. Kim, G.S. Kwon, B.D. Yoon, H.M. Oh, Effects of harvesting method and growth stage on the flocculation of the green alga *Botryococcus braunii*, Letters in Applied Microbiology. 27 (1998) 14–18.

[13] C.A. Price, L.R. Mendiola-Morgenthaler, M. Goldstein, E.N. Breden, R.R.L. Guillard, Harvest of planktonic marine algae by centrifugation into gradients of silica in the CF-6 continuous-flow zonal rotor, Biological Bulletin. 147 (1974) 136–145.

[14] R. Harun, M. Singh, G.M. Forde, M.K. Danquah, Bioprocess engineering of microalgae to produce a variety of consumer products, Renewable and Sustainable Energy Reviews. 14 (2010) 1037–1047.

[15] M.R. Tredici, Photobiology of microalgae mass cultures: understanding the tools for the next green revolution, Biofuels. 1 (2010) 143–162.

[16] A. Zenouzi, B. Ghobadian, M.A. Hejazi, P. Rahnemoon, Harvesting of microalgae *Dunaliella salina* using electroflocculation, Journal of Agricultural Science and Technology. 15 (2013) 879–887.

[17] L. Xu, C. Guo, F. Wang, S. Zheng, C.-Z. Liu, A simple and rapid harvesting method for microalgae by in situ magnetic separation, Bioresource Technology. 102 (2011) 10047–10051.

[18] D. Vandamme, I. Foubert, I. Fraeye, B. Meesschaert, K. Muylaert, Flocculation of *Chlorella vulgaris* induced by high pH: role of magnesium and calcium and practical implications, Bioresource Technology. 105 (2012) 114–119.

[19] A.K. Lee, D.M. Lewis, P.J. Ashman, Microbial flocculation, a potentially low-cost harvesting technique for marine microalgae for the production of biodiesel, Journal of Applied Phycology. 21 (2009) 559–567.

[20] H. Zheng, Z. Gao, J. Yin, X. Tang, X. Ji, H. Huang, Harvesting of microalgae by flocculation with poly (γ-glutamic acid), Bioresource Technology. 112 (2012) 212–220.

[21] N. Uduman, Y. Qi, M.K. Danquah, G.M. Forde, A. Hoadley, Dewatering of microalgal cultures: a major bottleneck to algae-based fuels, Journal of Renewable and Sustainable Energy. 2 (2010) 12701.

[22] C.G. Alfafara, K. Nakano, N. Nomura, T. Igarashi, M. Matsumura, Operating and scale-up factors for the electrolytic removal of algae from eutrophied lakewater, Journal of Chemical Technology and Biotechnology. 77 (2002) 871–876.

[23] S. Gao, J. Yang, J. Tian, F. Ma, G. Tu, M. Du, Electro-coagulation–flotation process for algae removal, Journal of Hazardous Materials. 177 (2010) 336–343.

[24] E. Poelman, N. De Pauw, B. Jeurissen, Potential of electrolytic flocculation for recovery of micro-algae, Resources, Conservation and Recycling. 19 (1997) 1–10.

[25] M. Bayramoglu, M. Kobya, O.T. Can, M. Sozbir, Operating cost analysis of electrocoagulation of textile dye wastewater. Separation and Purification Technology. 37 (2004) 117–125.

[26] W. Siriangkhawut, S. Tontrong, P. Chantiratiku, Quantitation of Aluminum Content in Waters and Soft Drinks by Spectrophotometry Using Eriochrome Cyanine R, Research, Journal of Pharmaceutical, Biological and Chemical Sciences. 4 (2013) 1156–1161.

[27] E.G. Bligh, W.J. Dyer, A rapid method of total lipid extraction and purification, Canadian Journal of Biochemistry and Physiology. 37 (1959) 911–917.

[28] A.R. Wellburn, The spectral determination of chlorophylls a and b, as well as total carotenoids, using various solvents with spectrophotometers of different resolution, Journal of Plant Physiology. 144 (1994) 307–313.

[29] M.Y. Mollah, P. Morkovsky, J.A. Gomes, M. Kesmez, J. Parga, D.L. Cocke, Fundamentals, present and future perspectives of electrocoagulation, Journal of Hazardous Materials. 114 (2004) 199–210.

[30] H.M.-G. Maleki, M. Almassi, M.A. Hejazi, S. Minaei, others, Harvesting of microalgae by electro-coagulation-flocculation for biodiesel production: an investigation of the effect of operational parameters and forecast model using response surface methodology, Journal of Biosciences. 4 (2014) 258–269.

[31] P. Cañizares, F. Martínez, C. Jiménez, J. Lobato, M.A. Rodrigo, Coagulation and electrocoagulation of wastes polluted with dyes, Environmental Science & Technology. 40 (2006) 6418–6424.

[32] M.M. Emamjomeh, M. Sivakumar, Fluoride removal by a continuous flow electrocoagulation reactor, Journal of Environmental Management. 90 (2009) 1204–1212.

[33] A.B. Aragón, R.B. Padilla, J.A.F.R. de Ursinos, Experimental study of the recovery of algae cultured in effluents from the anaerobic biological treatment of urban wastewaters, Resources, Conservation and Recycling. 6 (1992) 293–302.

[34] C.T. Matos, M. Santos, B.P. Nobre, L. Gouveia, Microalgae biomass harvesting by electrocoagulation, in proceedings: Energy for Sustainability 2013; Sustainable Cities: Designing for People and the Planet Coimbra, 8 to 10 September 2013; (2013) 1–6.

[35] M. Kumar, F.I.A. Ponselvan, J.R. Malviya, V.C. Srivastava, I.D. Mall, Treatment of bio-digester effluent by electrocoagulation using iron electrodes, Journal of Hazardous Materials. 165 (2009) 345–352.

[36] C.P. Nanseu-Njiki, S.R. Tchamango, P.C. Ngom, A. Darchen, E. Ngameni, Mercury (II) removal from water by electrocoagulation using aluminium and iron electrodes, Journal of Hazardous Materials. 168 (2009) 1430–1436.

[37] S. Vasudevan, G. Sozhan, S. Ravichandran, J. Jayaraj, J. Lakshmi, M. Sheela, Studies on the removal of phosphate from drinking water by electrocoagulation process, Industrial & Engineering Chemistry Research. 47 (2008) 2018–2023.

[38] A. Attour, M. Touati, M. Tlili, M.B. Amor, F. Lapicque, J.-P. Leclerc, Influence of operating parameters on phosphate removal from water by electrocoagulation using aluminum electrodes, Separation and Purification Technology. 123 (2014) 124–129.

[39] R. Greenwood, K. Kendall, Electroacoustic studies of moderately concentrated colloidal suspensions, Journal of the European Ceramic Society. 19 (1999) 479–488.

[40] D.A.H. Hanaor, M. Michelazzi, C. Leonelli, C.C. Sorrell, The effects of carboxylic acids on the aqueous dispersion and electrophoretic deposition of ZrO2, Journal of the European Ceramic Society. 32 (2012) 235–244.

[41] E. Valero, X. Álvarez, Á. Cancela, Á. Sánchez, Harvesting green algae from eutrophic reservoir by electroflocculation and post-use for biodiesel production, Bioresource Technology. 187 (2015) 255–262.

[42] R. Misra, A. Guldhe, P. Singh, I. Rawat, F. Bux, Electrochemical harvesting process for microalgae by using nonsacrificial carbon electrode: A sustainable approach for biodiesel production, Chemical Engineering Journal. 255 (2014) 327–333.

[43] E.M. Grima, E.-H. Belarbi, F.A. Fernández, A.R. Medina, Y. Chisti, Recovery of microalgal biomass and metabolites: process options and economics, Biotechnology Advances. 20 (2003) 491–515.

[44] D. Vandamme, I. Foubert, K. Muylaert, Flocculation as a low-cost method for harvesting microalgae for bulk biomass production, Trends in Biotechnology. 31 (2013) 233–239.

[45] L. Balduyck, K. Goiris, C. Bruneel, K. Muylaert, I. Foubert, Stability of Valuable Components during Wet and Dry storage, In: Kim S. (Eds.), Handbook of Marine Microalgae, Chap. 7. London: Elsevier, (2015) 81–89.

[46] C.T. Matos, M. Santos, B.P. Nobre, L. Gouveia, *Nannochloropsis sp*. biomass recovery by Electro-Coagulation for biodiesel and pigment production, Bioresource Technology. 134 (2013) 219–226.

[47] M.S. Arain, S.A. Arain, T.G. Kazi, H.I. Afridi, J. Ali, S.S. Arain, K.D. Brahman, M.A. Mughal, others, Temperature controlled ionic liquid-based dispersive micro-extraction using two ligands, for determination of aluminium in scalp hair samples of Alzheimer's patients: A multivariate study, Spectrochimica Acta Part A: Molecular and Biomolecular Spectroscopy. 137 (2015) 877–885.

[48] S.C. Bondy, The neurotoxicity of environmental aluminum is still an issue, Neurotoxicology. 31 (2010) 575–581.

CHAPTER 7: HARVESTING OF MICROALGAE *CHLORELLA VULGARIS* USING CONTINUOUS ELECTRO-COAGULATION-FLOCCULATION WITH POLARITY EXCHANGE (PE)

This article is submitted to Algal Research. Consequently, it follows the guidelines of this journal.

FAYAD Nidal, YEHYA Tania, AUDONNET Fabrice, VIAL Christophe.

ABSTRACT

Response surface methodology (RSM) was employed to evaluate the influence of current density and inlet flow rate (retention time) on the recovery efficiency of the microalgae *Chlorella vulgaris* from the culture medium by electro-coagulation-flocculation (ECF) in the

continuous mode using aluminum electrodes. Experimental data showed that almost complete microalgal recovery was obtained at current density 1.4 mA/cm^2 and inlet flow rate 40 mL/min. A model for predicting recovery efficiency cost was developed. In the transient period, microalgae recovery followed a first-order kinetics with time. The steady state conditions were attained after 80 min at inlet flow rate 40 mL/min. Under these conditions, almost complete microalgal recovery required only 1100 C/L charge loading in continuous mode with electrode polarity exchange (PE) every 2 minutes, while 1650 C/L was needed in continuous mode without PE. Moreover, Electrical energy consumption (EEC) was reduced from 10.6 kWh/kg to 5.2 kWh/kg, when switching from ECF without PE to ECF with PE. Further, ECF with PE was also more economic than ECF in the batch mode, which consumed 6.8 kWh/kg and required up to 1800 C/L charge loading for complete microalgal recovery.

Keywords: microalgae recovery, *Chlorella vulgaris*, electro-coagulation-flocculation, continuous mode, response surface methodology

1. INTRODUCTION

Biofuels production is nowadays a controversial issue, as terrestrially-derived biofuels are linked to reduced biodiversity, deforestation, farmland shortage, rise of food prices and increase in the emissions of CO_2 and N_2O [1]. Therefore, it is of utmost importance to develop a renewable, clean and sustainable energy source and technologies worldwide [2, 3]. The European Commission is also aware of this problem, and has an objective of increasing the share of renewable energy to at least 27% of the European Union (EU) energy consumption by 2030 [4].

Microalgae, as a renewable energy source, constitute a potential feedstock for the generation of transportation fuels. These microorganisms are so advantageous, as they may be cultivated on barren land, have a high growth rate and higher lipid content compared to other feedstocks [5, 6]. In addition, they accumulate high-value substances such as omega-3 fatty acids, antibiotics and vitamins as well as antioxidants, pharmaceuticals and animal feed [7, 8].

There are several steps for the production of microalgal products. The first step constitutes of cultivating the microalgal strain. Then, and once the microalgae grow sufficiently, they are harvested from the culture medium. After that, the harvested microalgae are subject to thickening, dewatering and drying, and post-processing (may include oil extraction and fractionation) [9]. Among the previously mentioned steps, the harvesting step constitutes the

greatest challenge due to the small size of microalgae (few micrometers), their density (similar to water) and their low concentration in the culture medium [10]. This step consumes more than 30% of the overall biodiesel production costs [11].

The most common harvesting methods include flocculation [12], gravity sedimentation [13], centrifugation [14], filtration [15] and flotation [16]. However, most of these methods are costly, have low harvesting efficiencies and sometimes, result in an unacceptable biomass quality [17]. The selection of the harvesting technique depends on the density and the size of the microalgae as well as the nature and value of the desired products [18].

Electrochemical techniques such as electrocoagulation is a suitable economic alternative for harvesting microalgae. Electrocoagulation (EC) is a cheap technique and requires very little addition of chemicals [19]. During EC, the metal ions which are released by electrolytic oxidation of the anode act as coagulant agents for the formation of microalgal flocs [20]. At the same time, hydrogen microbubbles are generated at the cathode, [21]. These bubbles help the generated flocs rise to the surface by electroflotation [18].

Most studies in the literature on microalgal recovery using electrochemical techniques concern batch studies. These works are interesting to understand the involved phenomena but at the industrial scale, batch processes are more expensive and time consuming. To fill this gap in the literature, this study describes a continuous electrolytic microalgae recovery system for harvesting the microalgal species *Chlorella vulgaris*. The study was carried out with electrodes polarity exchange (PE) to conserve the electrodes for longer time and to prevent passivation.

The aim of the study was to investigate the efficiency of harvesting the microalgal species *Chlorella vulgaris* by electro-coagulation-flocculation (ECF) in the continuous mode with electrode PE every 2 minutes. The effects of current density and inlet flow rate (retention time) on microalgae recovery efficiency were evaluated using the response surface methodology, with the objective to develop a model for predicting recovery efficiency. Moreover, ECF performance in continuous mode with PE and without PE modes could be compared to ECF in the batch mode reported in a previous work [22].

2. MATERIALS AND METHODS

2.1. MICROALGAL SPECIES *(CHLORELLA VULGARIS)*

Chlorella vulgaris **(Figure 1)** was kindly supplied by *Algosource Technologies* (France). All the experiments were performed using a modified Bold Basal Medium with 3-fold nitrogen

and vitamins (3N-BBM+V). This medium was prepared from pure chemicals dissolved in distilled water for simulating real *Chlorella vulgaris* culture conditions. For preparing 1.0 L medium, the addition of the following components was carried out: 0.75 g $NaNO_3$, 0.025 g $CaCl_2.2H_2O$, 0.075 g $MgSO_4.7H_2O$, 0.075 g $K_2HPO_4.3H_2O$, 0.175 g KH_2PO_4, 0.025 g NaCl, 6.0 mL of trace elements solution, 1.0 mL of both vitamin B1 and vitamin B12.

The trace elements solution was prepared by adding to 1.0 L distilled water, 0.75 g Na_2EDTA and the minerals in the following order: $FeCl_3$ $6H_2O$ (97.0 mg), $MnCl_2$ $4H_2O$ (41.0 mg), $ZnCl_2$ (5.0 mg), $CoCl_2$ $6H_2O$ (2.0 mg) and Na_2MoO_4 $2H_2O$ (4.0 mg). Vitamin B1 was prepared by dissolving 0.12 g thiaminhydrochloride in 100.0 mL distilled water and, then, filtered sterilely. Vitamin B12 was prepared by dissolving 0.1 g cyanocobalamin in 100.0 mL distilled water; then, 1.0 mL was taken from this solution and added to 99.0 mL distilled water and, finally, the solution was filtered sterilely.

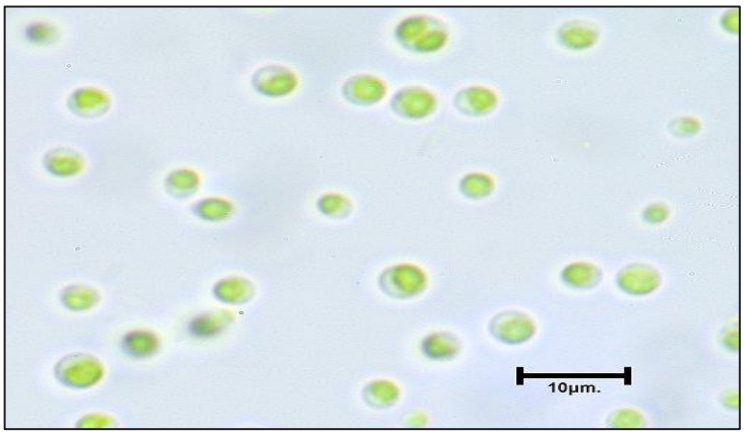

Figure 1. Microscopic image of the microalgae species, *Chlorella vulgaris* at ×100 magnification.

2.2. CONTINUOUS ECF EXPERIMENTS

A continuous flow electrocoagulation system made up of a feed tank, a piston pump, an EC cell and a sedimentation tank was used **(Figure 2)**. The used EC cell is a container made up of transparent polyvinyl chloride and can hold up to 2.5 L of microalgal suspension (the experiments were started after filling this cell with microalgal suspension). The electrodes are placed in the grooves embedded in the wall of the cell to remain motionless during the experiment. They are staggered to act as baffles. The suspension is obliged to follow a zigzag path in the cell **(Figure 3)** to improve mixing. This zigzag path forces the suspension to pass

between all the electrodes. This process maximizes the active surfaces, and as the path followed by the suspension is longer, therefore the residence time of the suspension in the reactor becomes higher.

ECF was carried out in the galvanostatic mode using a direct current (DC) generator (*Voltcaraft HPS - 13015*, Germany), with current direction inversion (polarity exchange (PE)) by the help of a current inverter. The chosen PE time interval was 2 minutes. Nine planar aluminum electrodes of identical dimensions (12 cm × 9 cm) were used as anode and cathode material. The inter-electrode distance was kept at 1.5 cm. Before each experiment, electrodes were rinsed with acetone and a 0.01 N HCl solution to remove organic and inorganic deposits. pH, voltage and current were recorded online. To determine the microalgal recovery efficiency as a function of the time, $\eta_a(t)$, samples were collected at the outlet of the reactor until the steady phase regime was attained. The microalgal recovery efficiency was determined based on the decrease in optical density of the microalgal suspension measured at 550 nm with a UV–VIS spectrophotometer (*Jenway*, UK). Microalgal recovery efficiency was calculated using (eq. 1):

$$\eta_a(t) = (OD_{t=0} - OD_t)/\, OD_{t=0} \qquad \text{(eq.1)}$$

where $OD_{t=0}$ is the optical density of the suspension before the beginning of ECF, and OD_t is the optical density of the suspension at time *t*.

The electric energy consumption (EEC) in kWh/kg of harvested microalgae was deduced

$$EEC = \frac{UI}{1000\eta_a Q c_i} \qquad \text{(eq. 2)}$$

where *U* is the cell voltage (V), *I* is the current (A), η_a is the microalgae recovery efficiency, *Q* is the inlet flow rate (m^3/h) and c_i is the inlet microalgae biomass concentration (kg/m^3).

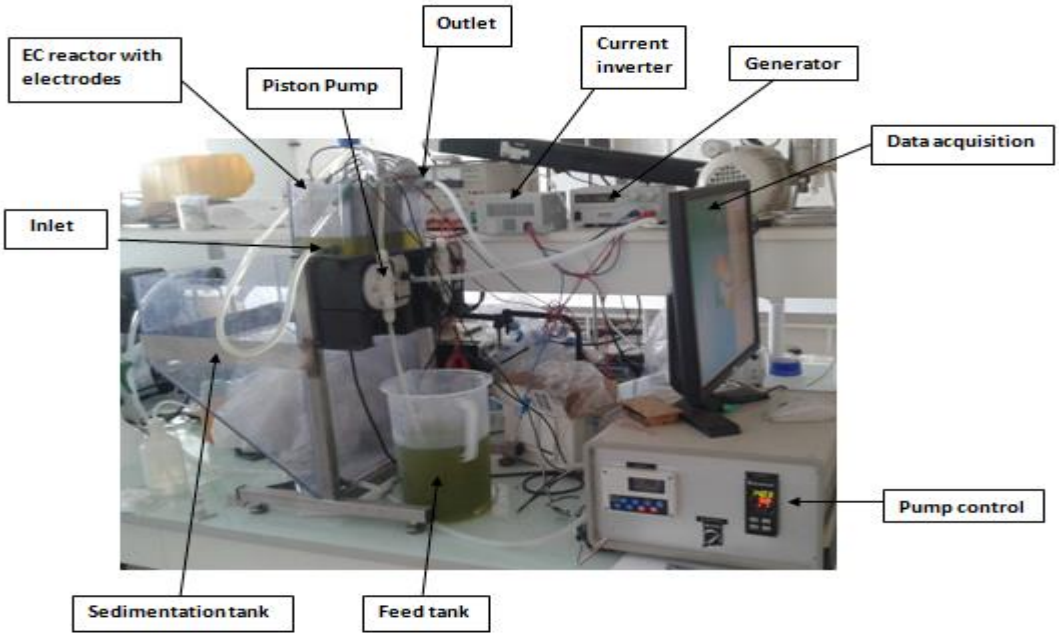

Figure 2. Scheme of the experimental set-up.

Figure 3. Scheme of the circulation of the microalgal suspension in the reactor. The black vertical segments reprensent the electrodes, and the arrows represent the zigzag path.

2.3. EXPERIMENTAL DESIGN AND DATA ANALYSIS

A three-level full factorial design (in addition to three replicates of the center point) with response surface methodology (RSM) was used to investigate the influence of two factors namely, current density and inlet flow rate. The number of experimental runs carried out was: 3^2 (full factorial design for two variables at three levels) + 3 replicates of the center point = 12 experimental runs. Before designing the experimental runs, preliminary experiments were conducted to select a narrower range of the studied independent variables based on one-factor-

at-a-time concept. **Table 1** shows the real and coded values of the variables studied in RSM. The investigated inlet flow rates of 40 mL/min, 60 mL/min and 80 mL/min correspond to retention times in ECF cell of 62.5 min, 41.7 min and 31.3 min, respectively.

Table 1. Experimental range with the coded and real values of the studied variables.

Factor	Variable	Coded levels of variables		
		-1	0	+1
X_1	Current density (mA/cm^2)	0.4	0.9	1.4
X_2	Inlet flow rate (mL/min)	40	60	80

Experimental data were analysed and fitted to the following second-order polynomial model (eq. 3):

$$Y = a_0 + \sum a_i x_i + \sum a_{ij} x_{ij} + \sum a_{ii} x_i^2 \quad \text{(eq. 3)}$$

where Y is the response (recovery efficiency, %), a_0 is the constant coefficient, a_i is a linear coefficient, a_{ij} is an interaction coefficient, a_{ii} is a quadratic coefficient, and x_i and x_{ij} are the independent factors.

3. RESULTS AND DISCUSSION

3.1. PRELIMINARY EXPERIMENTS ON THE EFFECTS OF CURRENT DENSITY AND INLET FLOW RATE

In the RSM study, the effects of two factors, namely current density and inlet flow rate were evaluated. Preliminary experiments were carried out with PE every 2 minutes to prevent passivation of electrodes and to conserve them for longer time, at inlet pH 4 (as this pH value was shown to be the most efficient than the other initial pH values in our previous batch study on the same microalgal species [22]) in order to select the range of values to be used in the RSM design for these variables.

In most electrochemical processes, current density is the most important parameter affecting the performance of the process, as it determines the coagulant production rate, bubble production rate, size and growth of flocs [23]. In this study, experimental runs were conducted at two current densities of 0.2 mA/cm^2 and 0.4 mA/cm^2 at an inlet flow rate of 80 mL/min. As shown in Figure 4, *Chlorella vulgaris* recovery efficiency increased at both current densities till the stationary state was reached. Recovery efficiency reached 78% at current density 0.4

mA/cm^2, while it was only 71% at current density 0.2 mA/cm^2 under steady state conditions. This result is ascribed to the fact that increasing current density increases both coagulant production rate and the amount of aluminum hydroxide available in the solution to form complexes and precipitate microalgae [23]. As recovery efficiency was less than 75% at current density 0.2 mA/cm^2, a range of 0.4–1.4 mA/cm^2 was used for current density in the RSM design.

The effect of inlet flow rate on the recovery efficiency of *Chlorella vulgaris* was studied by varying the inlet flow rate in the range of 40 mL/min - 120 mL/min for a current density of 0.4 mA/cm^2. As **Figure 5** shows, recovery efficiency decreased with the increase of inlet flow rate. In fact, recovery efficiency under steady state conditions was 86%, 78% and 73% at inlet flow rates of 40 mL/min, 80 and 120 mL/min, respectively. This result is due to the fact that the amount of dissolved aluminum per unit of time and volume becomes lower and that there is a lower contact time between microalgal cells and coagulants at higher inlet flow rates [24]. These results are consistent with those of Benhadji et al. who worked on COD and turbidity removal from industrial wastewater [25] and with those of El-Ashtoukhy et al. who worked on the removal of acid green dye 50 from wastewater [26].

As the recovery efficiency was less than 75% at inlet flow rate of 120 mL/min, the range of 40 -80 mL/min was chosen in the RSM design.

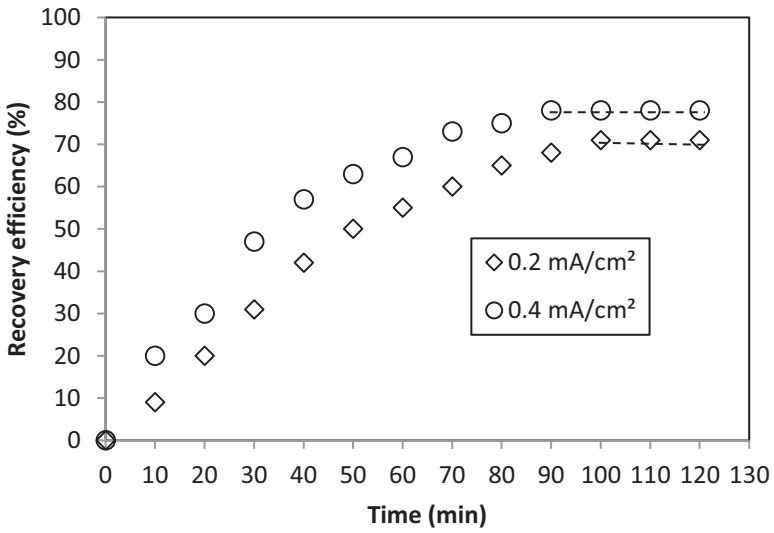

Figure 4. Effect of current density on the recovery efficiency of *Chlorella vulgaris* in a continuous flow electrocoagulation reactor. Experimental conditions: pH_i 4, inter-electrode distance 1.5 cm, initial concentration 0.5 g/L, inlet flow rate 80 mL/min.

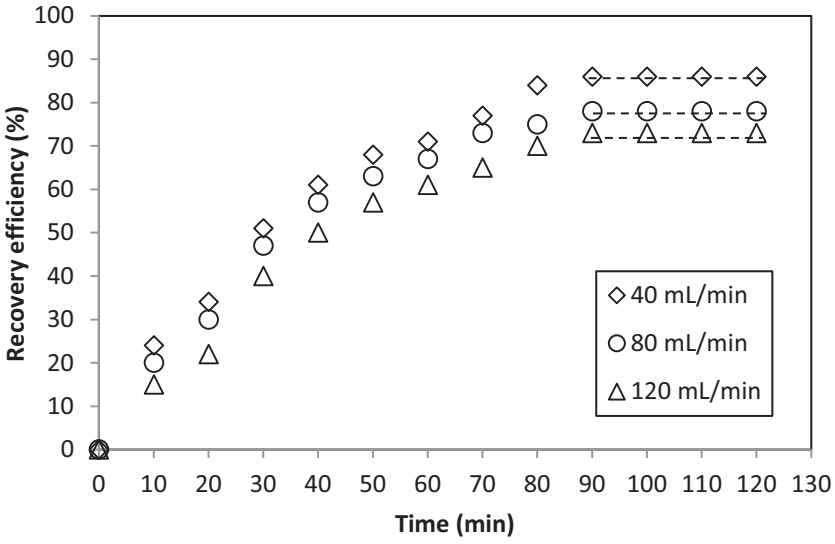

Figure 5. Effect of inlet flow rate on the recovery efficiency of *Chlorella vulgaris* in a continuous flow electrocoagulation reactor. Experimental conditions: pH_i 4, current density 0.4 mA/cm^2, inter-electrode distance 1.5 cm, initial concentration 0.5 g/L.

3.2. MODEL DEVELOPMENT AND VALIDATION

Based on the experimental design, twelve experimental runs with four central points were conducted. Experimental results of recovery efficiency are summarized in **Table 2**. The observed recovery efficiency values were used to develop the model based on the following second order polynomial (eq. 4):

$$Y = a_0 + a_1 X_1 + a_2 X_2 + a_{11} X_1^2 + a_{22} X_2^2 + a_{12} X_1X_2 \quad \text{(eq. 4)}$$

ANOVA analysis presented in **Table 3** shows that the coefficients of determination (R^2) and adjusted R^2 were 99.5% and 99.1%, respectively. This indicates that the quadratic model is able to describe successfully microalgae recovery. ANOVA analysis also shows that the effects of the quadratic term X_2^2 is insignificant on the recovery efficiency ($p<0.05$). The insignificance of this term is also shown in the pareto chart **(Figure 6)**. Therefore, the previous model was developed by eliminating the statistically insignificant term X_2^2, and there, in terms of coded factors, it was determined by (eq. 5):

$$Y \text{ (Recovery efficiency, \%)} = 96.9 - 0.2 X_1 - 0.3 X_2 + 5.1 X_1^2 + 0.06 X_1X_2 \quad \text{(eq. 5)}$$

Table 2. Design matrix along with observed responses; the extremal values of the recovery efficiency were noted in bold.

Run	Current density (mA/cm^2)	Inlet flow rate (mL/min)	Recovery efficiency (%)
1	0.9	60	88.2
2	0.4	80	**78.3**
3	0.9	60	88.6
4	1.4	60	95.4
5	0.9	80	83.3
6	0.9	60	88.0
7	0.4	60	84.2
8	0.4	40	87.4
9	1.4	40	**99.0**
10	0.9	40	92.6
11	1.4	80	92.1
12	0.9	60	88.1

Table 3. Analysis of variance (ANOVA) for recovery efficiency.

Source	Sum of Squares	Df	Mean Square	F-Ratio	P-Value
X_1: Current density	223.3	1	223.3	3227.9	0.0000
X_2: Inlet flow rate	106.7	1	106.7	1542.4	0.0000
X_1^2	5.3	1	5.3	76.9	0.0031
X_1X_2	1.2	1	1.2	17.5	0.02
X_2^2	0.5	1	0.5	7.4	0.07
Lack-of-fit	1.4	3	0.5	6.7	0.08
Pure error	0.2	3	0.07		
Total (corr.)	338.1	11			
R^2 = 99.5 % Adjusted R^2= 99.1 %					

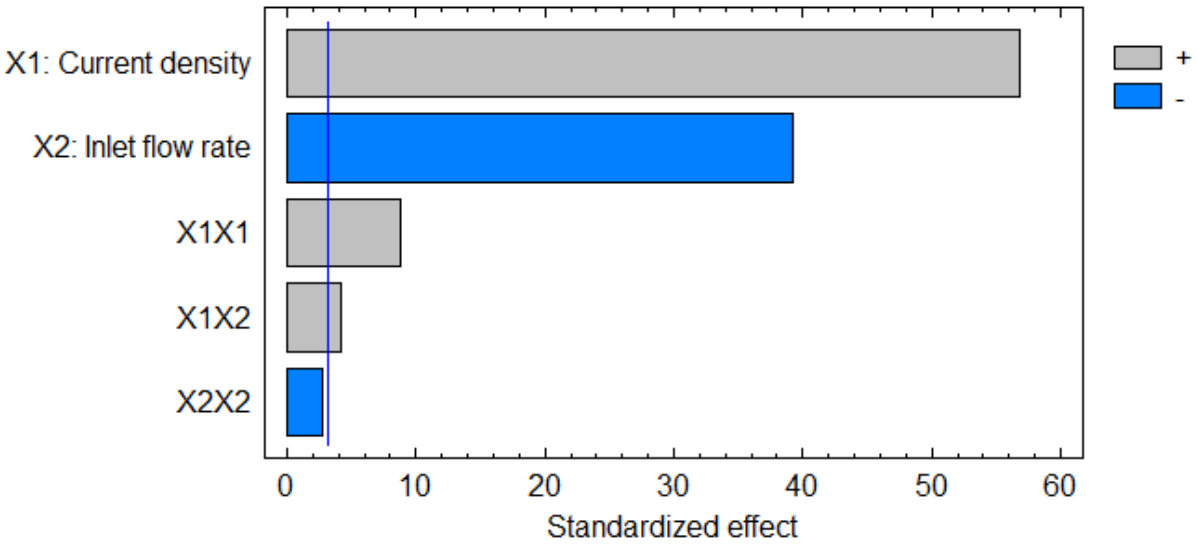

Figure 6. Pareto chart of recovery efficiency.

The plot of actual and fitted values of microalgae recovery efficiency shows a very good agreement between observed and fitted values with R^2 of 0.99 **(Figure 7)**. Consequently, the model developed in this work could be successfully used to predict *Chlorella vulgaris* recovery efficiency under the investigated experimental conditions.

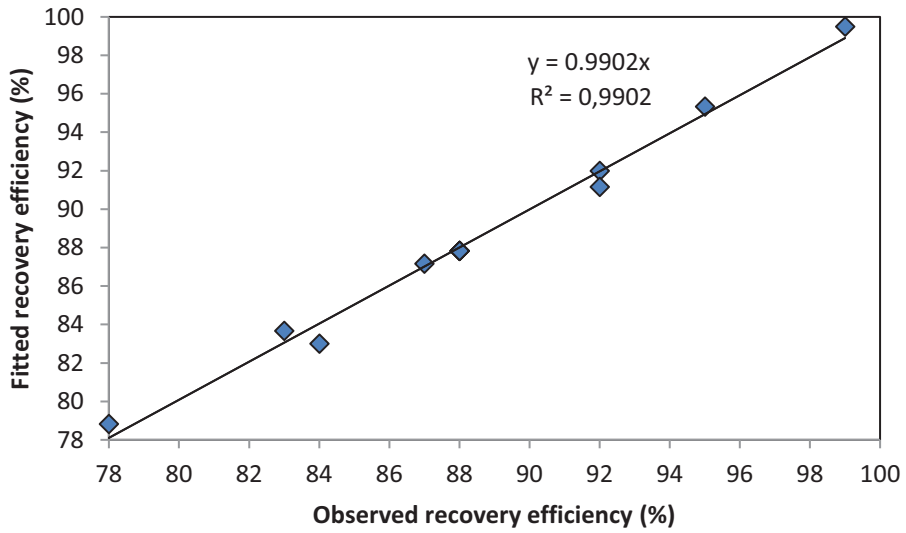

Figure 7. Fitted *vs* observed values for *Chlorella vulgaris* recovery efficiency.

3.3. THE INTERACTION EFFECT OF CURRENT DENSITY AND INLET FLOW RATE

Figure 8 shows a 3-D surface plot for the interaction effect of current density and inlet flow rate on microalgae recovery efficiency. As this figure shows, recovery efficiency increased with the increase of current density and the decrease of inlet flow rate. Highest recovery efficiency of 99% was reached at current density of 1.4 mA/cm^2 and inlet flow rate of 40 mL/min.

The highest recovery efficiency at the highest current density is explained by Faraday's law, which implies that the amount of metal dissolved is nearly proportionally to current density. Consequently, as current density increases, more aluminum is available in the microalgal suspension for neutralizing or precipitating microalgae [23].

Higher (total) recovery efficiency at lower inlet flow rates is expected, as such rates lead to higher retention time, and hence, the microalgal cells have more contact time with aluminum species in the reactor [27].

Table 3 shows that the linear effects of current density and inlet flow rate (X_1 and X_2), their interaction effect as well as the quadratic effect of current density (X_1^2) have a significant effect on microalgae recovery efficiency ($P<0.05$); however, the quadratic effect of inlet flow rate (X_2^2) is insignificant ($P>0.05$).
However, equipment cost increases when Q decreases and operating cost increases with current.

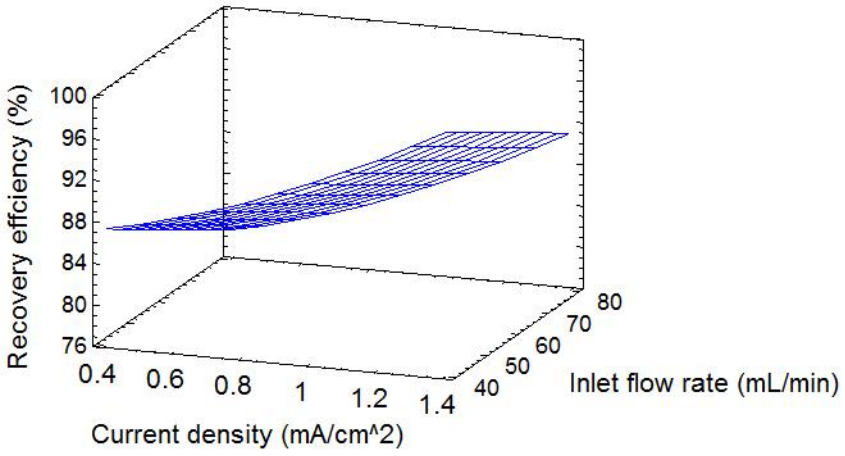

Figure 8. 3-D surface plot for the interaction effect of current density and inlet flow rate on the recovery efficiency of *Chlorella vulgaris*.

3.4. KINETICS OF RECOVERY DURING THE TRANSIENT PERIOD

As the cell has been filled with microalgal suspension prior to the beginning of ECF, the transient period (time needed to achieve steady state conditions) was poorly dependant on the inlet flow rate. *Chlorella vulgaris* recovery kinetics during the transient phase was investigated at different current densities (0.4 mA/cm^2, 0.9 mA/cm^2 and 1.4 mA/cm^2) with PE. Two of the most used kinetic models, first-order (eq. 6) and second-order (eq. 7) were fitted to our experimental results.

$$\text{Ln } C_t = \text{Ln } C_0 - K_1 t \qquad \text{(eq. 6)}$$

$$1/C_t = K_2 t + 1/C_0 \qquad \text{(eq. 7)}$$

where C_0 is the initial microalgae concentration and C_t is the microalgae concentration at time t; K_1 and K_2 are the first and second-order kinetic constants, respectively.

As **Figure 9** shows, the first-order model fitted better our experimental data with higher R^2 values at all tested current densities. **Table 4** displays R^2 values and the corresponding kinetic constants at all current densities.

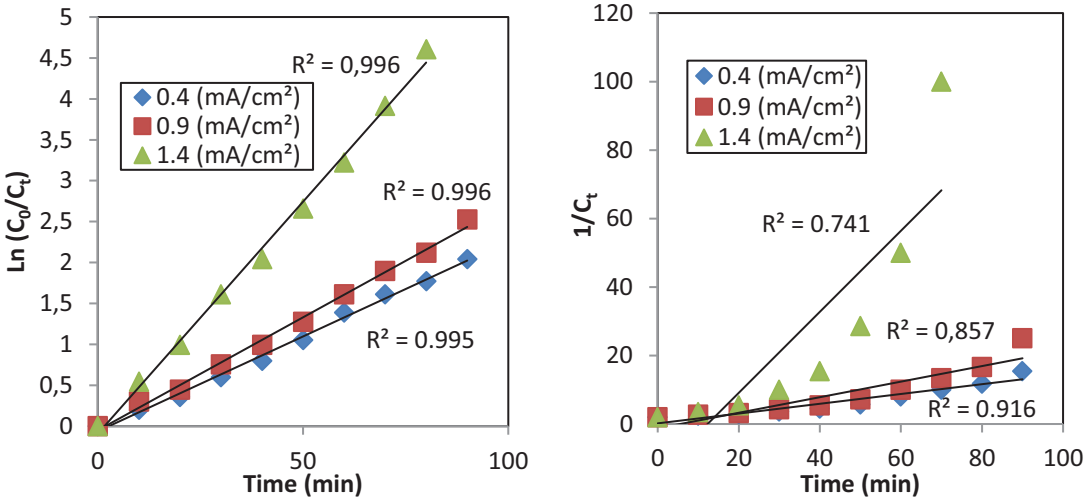

a) b)

Figure 9. Fitting of a) first-order models and b) second-order models to our experimental data at different current densities.

Table 4. Kinetic constants corresponding to first-order and second-order kinetics at different current densities.

Current density	First-order kinetics		Second-order kinetics	
	R^2	K_1 / min^{-1}	R^2	K_2 / L.g^{-1}.min^{-1}
0.4 mA/cm^2	0.995	0.021	0.916	0.14
0.9 mA/cm^2	0.996	0.032	0.857	0.23
1.4 mA/cm^2	0.996	0.064	0.741	1.18

3.5. COMPARISON OF CONTINUOUS ECF WITH POLARITY EXCHANGE (PE) AND WITHOUT PE TO ECF IN BATCH MODE IN OUR PREVIOUS STUDY

All the compared results were obtained at the same inlet pH 4 and inter-electrode distance of 1.5 cm. The steady state conditions with recovery efficiency of 99% and 95% obtained with ECF with and without PE, respectively, was reached after 80 minutes of operation time, whereas 100 minutes time was required to reach a complete recovery in the batch mode [22]. Higher recovery efficiency in ECF with PE mode is due to the uniform dissolution of anode and cathode during electrocoagulation with PE [28].

Figure 10a shows that a volumetric charge loading value of 1800 C/L was required to reach almost complete microalgae recovery in batch mode, compared to 1100 C/L and 1650 C/L in the continuous mode with and without PE, respectively. As a result, we can say that the continuous mode is more efficient than the batch one, as it requires less charge loading for microalgae recovery. Figure 10b shows electrical energy consumption (EEC) in batch, continuous with PE and continuous without PE modes. Results show that 6.8 kWh/kg was needed in the batch mode, 5.2 kWh/kg in the continuous mode with PE, whereas, in continuous without PE mode, EEC reached 10.6 kWh/kg probably due to passivation, which increases the applied potential and thus EEC.

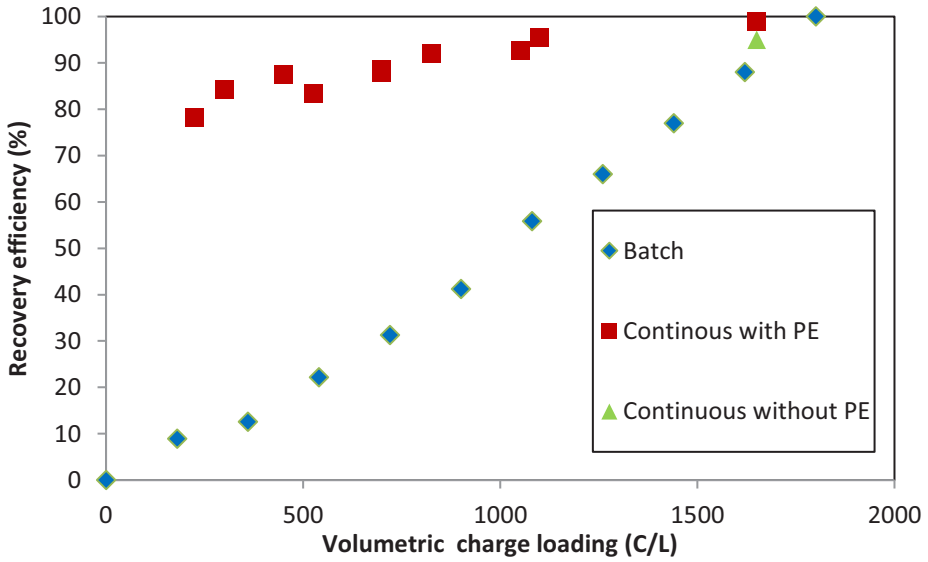

a)

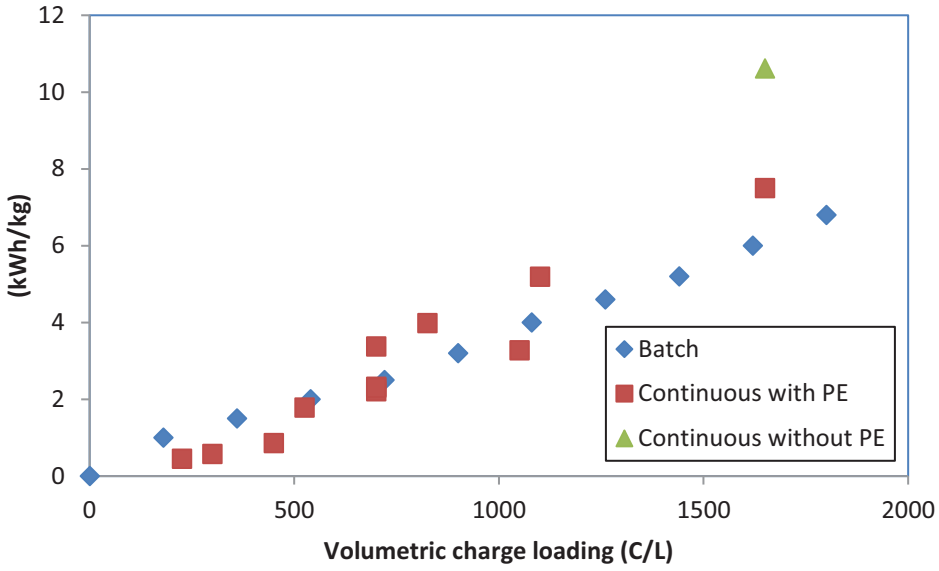

b)

Figure 10. Comparative performances of ECF in continuous mode with PE, continuous mode without PE and batch mode in terms of a) recovery efficiency and b) Electrical energy consumption (EEC). Experimental conditions: inlet pH 4, inter-electrode distance 1.5 cm, initial concentration 0.5 kg/m^3.

4. CONCLUSION

In this study, response surface methodology (RSM) was used as a tool to explain the effects of current density and inlet flow rate (retention time) and their interactions on the recovery efficiency of *Chlorella vulgaris* from the culture medium by electro-coagulation-flocculation (ECF) in the continuous mode. Experimental results showed that almost complete microalgal recovery (99.0 %) was obtained at current density 1.4 mA/cm^2 and inlet flow rate 40 mL/min. The linear effects of current density and inlet flow rate, their interaction effect as well as the quadratic effect of current density were significant on recovery efficiency. A statistically significant model was developed for predicting recovery efficiency from RSM methodology. The steady state conditions in the continuous mode were reached after 80 min at 40 mL/min inlet flow rate. At steady state conditions, comparing ECF in continuous mode with polarity exchange (PE) every 2 minutes to continuous ECF without PE, depicted that ECF in continuous mode with PE was more economic than ECF in continuous mode without PE. Moreover, ECF in continuous mode with PE was also more efficient and economic than ECF in the batch mode.

REFERENCES

1. M.L. Gerardo, S.V.D. Hende, H. Vervaeren, T. Coward, S.C. Skill, Harvesting of microalgae within a biorefinery approach: A review of the developments and case studies from pilot-plants, Algal Research. 11 (2015) 248–262.

2. B.K. Ndimba, R.J. Ndimba, T.S. Johnson, R. Waditee-Sirisattha, M. Baba, S. Sirisattha, Y. Shiraiwa, G.K. Agrawal, R. Rakwal, Biofuels as a sustainable energy source: An update of the applications of proteomics in bioenergy crops and algae, Journal of Proteomics. 93 (2013) 234–244.

3. G. Najafi, B. Ghobadian, T.F. Yusaf, Algae as a sustainable energy source for biofuel production in Iran: a case study, Renewable and Sustainable Energy Reviews. 15 (2011) 3870–3876.

4. N. Scarlat, J.-F. Dallemand, F. Monforti-Ferrario, M. Banja, V. Motola, Renewable energy policy framework and bioenergy contribution in the European Union – An overview from National Renewable Energy Action Plans and Progress Reports, Renewable and Sustainable Energy Reviews. 51 (2015) 969–985.

5. Y. Chisti, Biodiesel from microalgae beats bioethanol, Trends in Biotechnology. 26 (2008) 126–131.

6. T.M. Mata, A.A. Martins, N.S. Caetano, Microalgae for biodiesel production and other applications: A review, Renewable and Sustainable Energy Reviews. 14 (2010) 217–232.

7. R. Harun, M. Singh, G.M. Forde, M.K. Danquah, Bioprocess engineering of microalgae to produce a variety of consumer products, Renewable and Sustainable Energy Reviews. 14 (2010) 1037–1047.

8. S.-K. Wang, Y.-R. Hu, F. Wang, A.R. Stiles, C.-Z. Liu, Scale-up cultivation of *Chlorella ellipsoidea* from indoor to outdoor in bubble column bioreactors, Bioresource Technology. 156 (2014) 117–122.

9. C.-Y. Chen, K.-L. Yeh, R. Aisyah, D.-J. Lee, J.-S. Chang, Cultivation, photobioreactor design and harvesting of microalgae for biodiesel production: a critical review, Bioresource Technology. 102 (2011) 71–81.

10. L. Pérez, J.L. Salgueiro, R. Maceiras, Á. Cancela, Á. Sánchez, An effective method for harvesting of marine microalgae: pH induced flocculation, Biomass and Bioenergy. 97 (2017) 20–26.

11. M. Bilad, H.A. Arafat, I.F. Vankelecom, Membrane technology in microalgae cultivation and harvesting: a review, Biotechnology Advances. 32 (2014) 1283–1300

12. K.V. Gorin, Y.E. Sergeeva, V.V. Butylin, A.V. Komova, V.M. Pojidaev, G.U. Badranova, A.A. Shapovalova, I.A. Konova, P.M. Gotovtsev, Methods coagulation/flocculation and flocculation with ballast agent for effective harvesting of microalgae, Bioresource Technology. 193 (2015) 178–184.

13. S. Salim, L. Gilissen, A. Rinzema, M. Vermuë, R. Wijffels, Modeling microalgal flocculation and sedimentation, Bioresource Technology. 144 (2013) 602–607.

14. A.J. Dassey, C.S. Theegala, Harvesting economics and strategies using centrifugation for cost effective separation of microalgae cells for biodiesel applications, Bioresource Technology. 128 (2013) 241–245.

15. C. Nurra, E. Clavero, J. Salvadó, C. Torras, Vibrating membrane filtration as improved technology for microalgae dewatering, Bioresource Technology. 157 (2014) 247–253.

16. T. Ndikubwimana, J. Chang, Z. Xiao, W. Shao, X. Zeng, I. Ng, Y. Lu, Flotation: A promising microalgae harvesting and dewatering technology for biofuels production, Biotechnology Journal. 11 (2016) 315–326.

17. A. Guldhe, R. Misra, P. Singh, I. Rawat, F. Bux, An innovative electrochemical process to alleviate the challenges for harvesting of small size microalgae by using non-sacrificial carbon electrodes, Algal Research. 19 (2016) 292–298.

18. J.W. Richardson, M.D. Johnson, R. Lacey, J. Oyler, S. Capareda, Harvesting and extraction technology contributions to algae biofuels economic viability, Algal Research. 5 (2014) 70–78.

19. C.T. Matos, M. Santos, B.P. Nobre, L. Gouveia, Nannochloropsis sp. biomass recovery by Electro-Coagulation for biodiesel and pigment production, Bioresource Technology. 134 (2013) 219–226.

20. S. Gao, J. Yang, J. Tian, F. Ma, G. Tu, M. Du, Electro-coagulation–flotation process for algae removal, Journal of Hazardous Materials. 177 (2010) 336–343.

21. M. Majlesi, S.M. Mohseny, M. Sardar, S. Golmohammadi, A. Sheikhmohammadi, Improvement of aqueous nitrate removal by using continuous electrocoagulation/electroflotation unit with vertical monopolar electrodes, Sustainable Environment Research. 26 (2016) 287–290.

22. N. Fayad, T. Yehya, F. Audonnet, C. Vial, Harvesting of microalgae Chlorella vulgaris using electro-coagulation-flocculation in the batch mode, Algal Research. 25 (2017) 1–11.

23. M. Kobya, E. Gengec, E. Demirbas, Operating parameters and costs assessments of a real dyehouse wastewater effluent treated by a continuous electrocoagulation process, Chemical Engineering and Processing: Process Intensification. 101 (2016) 87–100.

24. S. Zodi, B. Merzouk, O. Potier, F. Lapicque, J.-P. Leclerc, Direct red 81 dye removal by a continuous flow electrocoagulation/flotation reactor, Separation and Purification Technology. 108 (2013) 215–222.

25. A. Benhadji, M.T. Ahmed, R. Maachi, Electrocoagulation and effect of cathode materials on the removal of pollutants from tannery wastewater of Rouïba, Desalination. 277 (2011) 128–134.

26. E.Z. El-Ashtoukhy, N. Amin, Removal of acid green dye 50 from wastewater by anodic oxidation and electrocoagulation - A comparative study, Journal of Hazardous Materials. 179 (2010) 113–119.

27. M.H. El-Naas, S. Al-Zuhair, A. Al-Lobaney, Treatment of petroleum refinery wastewater by continuous electrocoagulation, International Journal of Engineering Research and Technology. 2 (2013) 3387–3394.

28. S. Vasudevan, Effects of alternating current (AC) and direct current (DC) in electrocoagulation process for the removal of iron from water, The Canadian Journal of Chemical Engineering. 90 (2012) 1160–1169.

CONCLUSIONS AND PERSPECTIVES

This thesis comprises two submitted literature review articles and five articles; three of which are published and two are submitted. The main objective of this work was to develop a technically and economically reliable technique for wastewater treatment and for the separation and purification of biological media. In this context, electrocoagulation (EC) was first employed for the elimination of whey proteins from synthetic wastewater. Then, the efficiency of EC for separating and purifying volatile fatty acids in a digestate (first biological medium) from acidogenic fermentation was tested. Moreover, two microalgae species namely, *Chlamydomonas reinhardtii* and *Chlorella vulgaris* were recovered from their culture medium (second biological medium) using electro-coagulation-flocculation (ECF).

In more details, in chapter 3, EC was used to remove whey proteins (initial concentration ranged from 0.75 to 3.0 g/L) from synthetic wastewater using aluminum electrodes. EC has been shown to be able to completely eliminate whey proteins, with adsorption onto the flocs being the mechanism responsible for removal. This work also proved that whey proteins adsorption onto flocs forming during EC at all currents (78.0 mg N/g solid, 61.57 mg N/g solid, and 53.18 mg N/g solid at current of 1.5 A, 3.0 A, and 4.5 A, respectively) was more efficient than adsorption of these proteins on preformed flocs (27.78 mg N/g solid) at the same initial concentration of 0.75 g/L. It was also shown in this work that EC cost increased with increasing initial pH (pH_i), current and electrolyte concentration. This work was finalized by defining a model that can predict whey proteins removal quantitatively. This model which requires only two adjustable parameters that must be readjusted only as a function of initial pH and conductivity, outperforms other models from the literature that usually require to adjust parameters for each new set of operating conditions.

The second part of this work, detailed in chapter 4, was the implementation of EC process for the preliminary purification of volatile fatty acids (VFA) in a digestate issued from acidogenic fermentation. The collected experimental results have proved that EC is an efficient process for purifying VFA, as they completely remain in the solution, while the other soluble and insoluble compounds were eliminated efficiently. The purification costs were evaluated to be (0.26 ± 0.03) and (1.07 ± 0.04) US $/m^3 with iron or aluminum electrodes, respectively. Comparison of these costs to costs of other techniques used for VFA purification as electrodialysis and nanofiltration showed that EC is more economic.

The third study of this thesis (chapter 5), consisted of harvesting the microalgal species *Chlamydomonas reinhardtii* using electrocoagulation-flocculation (ECF) in batch mode with aluminum electrodes. Experimental data proved that these microalgae can be effectively recovered by ECF, as 90% recovery efficiency was attained at current density 14.4 mA/cm^2 and initial pH 6 for 60 min operating time. Data also showed that ECF cost which ranged from 0.13 to 1.8 US \$/m^3 was not influenced by initial pH (from 3 to 9). Moreover, in this study, two models able to predict recovery efficiency and ECF operating cost were established. When studying the kinetics of harvesting, it was demonstrated that *Chlamydomonas reinhardtii* recovery followed a second-order kinetics, with charge neutralization being the mechanism responsible for recovery, as depicted by the increase of zeta potential value with time. Lastly, it was shown that ECF is more efficient than chemical flocculation with chitosan for *Chlamydomonas reinhardtii* recovery.

The fourth study involved the use of ECF for the recovery of another interesting microalgal species (*Chlorella vulgaris*). Experimental data showed that aluminum electrodes were much more effective than iron electrodes for *Chlorella vulgaris* recovery. Zeta potential analysis demonstrated that the mechanism responsible for microalgae harvesting was charge neutralization at pH_i 4.0 and 6.0 and sweep flocculation at pH_i 8.0, while flotation on bubbles contributed to a maximum of 36.6% of harvesting efficiency. In addition, it was shown that ECF did not affect microalgal biomass lipid and pigment content.Moreover, it was possible to reduce ECF cost by working at the lowest current density and the lowest inter-electrode distance. A minimum value of about 1.0 kWh/kg microalgae recovered was achieved by adding of 1.5 g/L NaCl.

In the fifth and last study, as a continuation of the fourth study, *Chlorella vulgaris* was harvested in the continuous mode using ECF with aluminum electrodes. In this study, response surface methodology (RSM) was employed to explain the effects of current density and inlet flow rate and their interactions on the recovery efficiency of *Chlorella vulgaris.* Experimental data depicted that 99.0 % recovery efficiency was obtained at current density 1.4 mA/cm^2 and inlet flow rate 40 mL/min in a 2.5 L volume cell. The linear effects of current density and inlet flow rate, their interaction effect as well as the quadratic effect of current density were significant on harvesting efficiency. Moreover, in this work, a statistically significant model was developed for predicting recovery efficiency. The steady state conditions in the continuous mode were reached after 80 min at 40 mL/min inlet flow rate. At steady state conditions, ECF in the continuous mode with polarity exchange (PE) was more economic than ECF in the continuous

mode without PE. Moreover, ECF in the continuous mode with PE was also more efficient and economic than ECF in the batch mode. But a key result emerges from this study is that a simple transition from batch to continuous EC process is not straightforward, as it is not possible to deduce the removal yield of microalgae recovery or pollution removal under continuous conditions from batch experiments as a function of residence time or energy input. This poses a serious question in terms of EC design and scale-up that has not been solved yet. It is certain that hydrodynamic conditions strongly differ between the mechanically-stirred EC cell of chapter 5 and the continuous cell of chapter 6. However, the change in cell design not only modifies hydrodynamic conditions, but also the rates at which the coagulant is released and the pH varies locally. As pointed out by Hakizimana et al.[*], many mathematical approaches have been developed for EC modelling and simulation, but no general method has received a general acceptance. In particular, the molecular and microscopic processes are probably so highly non-linear that lack reliable scale-up models.

As a consequence, the perspectives of this work can be summarized as follows:

The main objective will be to develop a robust methodology able to use data from batch experiments in continuous EC cells, starting initially with model systems, for example the whey proteins solutions studied in chapter 3. This emerges undoubtedly as an essential prerequisite for the future developments of the EC technology. For whey proteins, this strategy implies to apply the EC treatment in the continuous mode in the laboratory and to deeply analyze the effect of electrode polarity. For microalgae, this also implies to complete the experimental study using batch and continuous experiments, not only for *Chlorella vulgaris*, but also for *Chlamydomonas reinhardtii* for which only batch experiments have been carried out. A key perspective could be to establish the adequate conditions of batch experiments for the definition and the a priori optimization of the operating conditions of continuous EC process. A second objective would be to further improve the design and scale-up of continuous EC cells. A last one would be to establish at least the basis of a scale-up methodology of continuous EC cells, which would be a major advance to make EC a popular technological solution for water or wastewater treatments, but also for recovery of valuable colloids from water.

[*] J.N. Hakizimana, B. Gourich, M. Chafi, Y. Stiriba, Ch. Vial, P. Drogui, A. Oumani, J. Naja (2017). Electrocoagulation process in water treatment: A review of electrocoagulation modeling approaches. *Desalination*, 393, 1–21.

Another objective will be to improve the design of the continuous EC cell of chapter 7. Several parameters can be modified, including the distance between electrodes and the electrode connection mode. In addition, the influence of the period of polarity exchange has not been investigated up to now. Similarly, several conventional designs of continuous EC cells can be found in the literature[†] which differ from that of the present study. The EC cell used in this work could also be compared to alternative designs, so that the pros and cons of each design could be assessed on a rational basis.

Specific objectives for the different media treated can also be considered. For whey proteins, EC should be applied to industrial dairy wastewater, to assess the cocktail effect on the removal efficiency of whey proteins in whey or white waters, particularly in the continuous mode. For VFA and microalgae recovery, EC must be coupled to a concentration process that further removes water prior to subsequent treatments. Membrane processes arises as a serious potential, and further developments in the coupling between EC and membrane processes emerge as an attractive solution for the future of EC, as already highlighted for seawater desalination[‡].

More generally, a significant perspective remains a better understanding of the interplay between the various electrochemical, chemical and physical mechanisms involved in the removal of soluble and colloidal species, including precipitated hydroxides, and particularly those involving electrogenerated microbubbles in the flotation process. This would constitute a key improvement in the definition of technological solutions involving the EC process, but it constitutes also a crucial step in the use of advanced modelling tools, such as CFD (Computational Fluid Dynamics), that requires an accurate description of these mechanisms at the microscopic scale.

Finally, these perspectives highlight that electrocoagulation remains a subject of high interest that deserves further research, not only because it remains not well understood even though it has been discovered more than one century ago, but also because it is an efficient and economic process for applications that are still to be discovered and in which fundamental understanding

[†]M.Y.A. Mollah, P. Morkovsky, J.A.G. Gomes, M. Kesmez, D.L. Cocke (2004). Fundamentals, present and future perspectives of electrocoagulation. *Journal of Hazardous Materials*, 114,199–210.

[‡]J.N. Hakizimana, B. Gourich, Ch. Vial, P. Drogui, A. Oumani, J. Naja, L. Hilali (2016). Assessment of hardness, microorganism and organic matter removal from seawater by electrocoagulation as a pretreatment of desalination by reverse osmosis. *Desalination*, 393, 90–101.

of technological solutions have still to be found, particularly at the process scale in the field of chemical engineering.

Abstract

Electrocoagulation (EC) is a non-specific electrochemical method usually used for water and wastewater treatment. In this work, EC is firstly investigated as a conventional wastewater treatment technique for the removal of whey proteins from water, where the mechanisms of removal are explained and a model on whey proteins elimination is developed. Then, EC use is extended for the separation and purification of volatile fatty acids issued from acidogenic fermentation. In this second study, the effects of operating parameters on EC efficiency and cost are discussed. Moreover, EC is used for the harvesting of two microalgae species from their culture medium. In the study that concerns recovering *Chlamydomonas reinhardtii,* response surface methodology (RSM) is employed and two models for predicting recovery efficiency and operating cost are developed. The harvesting of the other microalgae species *Chlorella vulgaris* is studied using EC in the batch and continuous modes. In the batch mode, the effects of the main operating parameters on the process effectiveness are explained along with discussing the mechanisms of recovery. In the continuous mode study, response surface methodology (RSM) is applied and a model for predicting microalgae recovery is developed. Finally, comparison of EC performance in continuous mode with and without polarity exchange (PE) to EC performance in batch mode is carried out.

***Keywords*:**

Electrocoagulation, Wastewater treatment, Whey proteins, Separation, Purification, Volatile fatty acids, Harvesting, Chlamydomonas reinhardtii, Chlorella vulgaris

Résumé

L'électrocoagulation (EC) est une méthode électrochimique non spécifique couramment utilisée pour le traitement de l'eau et des eaux usées. Dans ce travail, l'EC est d'abord étudiée comme une technique classique de traitement des eaux usées dédiée à l'élimination des protéines de lactosérum de l'eau pour laquelle les mécanismes d'élimination sont expliqués et un modèle est développé. Ensuite, l'utilisation de l'EC est étendue à la séparation et à la purification d'acides gras volatils issus de la fermentation acidogénique. Dans cette deuxième étude, les effets des paramètres opératoires sur l'efficacité et le coût de l'EC sont discutés. En outre, l'EC est utilisée pour la récolte de deux espèces de microalgues de leur milieu de culture. En ce qui concerne la récolte de *Chlamydomonas reinhardtii*, la méthodologie de la surface de réponse est utilisée et deux modèles permettant de prédire respectivement l'efficacité de la récupération et le coût opératoire sont développés. La récolte d'une autre espèce de microalgues, *Chlorella vulgaris*, est étudiée en utilisant l'EC respectivement en mode discontinu et continu. En mode discontinu, les effets des principaux paramètres de fonctionnement sur l'efficacité du processus sont expliqués et les mécanismes de récupération sont discutés. Dans l'étude en mode continu, la méthodologie de la surface de réponse est utilisée et un modèle permettant de prédire l'efficacité de récupération des microalgues est développé. Enfin, la comparaison des performances de l'EC en mode continu avec et sans échange de polarité aux performances de l'EC en mode discontinu est effectuée.

***Mots-clés* :**

Electrocoagulation, Traitement des eaux usées, Protéines de lactosérum, Séparation, Purification, Acides gras volatils, Récolte, Chlamydomonas reinhardtii, Chlorella vulgaris